# Dynamic Regulation of Apoptosis Signal-Regulating Kinase 1

By

Joel Davis Federspiel

Dissertation
Submitted to the Faculty of the
Graduate School of Vanderbilt University
in partial fulfillment of the requirements
for the degree of

DOCTOR OF PHILOSOPHY

in
Biochemistry
August, 2016
Nashville, Tennessee

Approved:

Daniel Liebler, Ph.D.

Bruce Carter, Ph.D.

BethAnn McLaughlin, Ph.D.

Kevin Schey, Ph.D.

Bing Zhang, Ph.D.

ACKNOWLEDGEMENTS

I wish to acknowledge my mentor, Dr. Daniel Liebler, for guiding me through the process of becoming a scientist. He gave me the freedom to grow as a researcher while still pushing me to be better than I ever thought I could be. I will be forever grateful for his insight, creativity, and eternal optimism.

I wish to thank all of the members of the laboratory, past and present, who helped make my stay there an enjoyable and educational experience. The helpful discussions and collaborative atmosphere made this lab a perfect place to learn.

I also wish to thank my dissertation committee members, Dr. Bruce Carter, Dr. BethAnn McLaughlin, Dr. Kevin Schey, and Dr. Bing Zhang. Your guidance and support throughout my project was instrumental for the completion of this work.

I wish to acknowledge the funding support from the NIEHS T32 training grant (T32ES007028) and the ASK1 R01 (R01ES022936).

I am grateful for the continual support of my friends and family. My parents instilled in me a love of learning and a strong work ethic that has greatly benefited me in the pursuit of my career and I would not be where I am today without them. Finally, I wish to thank my amazing wife, Ava. She has patiently supported me in all things and has given me the strength and encouragement I needed to complete my degree. This accomplishment belongs as much to her as to me.

TABLE OF CONTENTS

Page

## LIST OF TABLES



## LIST OF FIGURES

# CHAPTER I

# INTRODUCTION

## Overview

Appropriate response to a variety of intra- and extracellular stress signaling molecules is critical for maintenance of proper cellular function. As such, there exist many signaling pathways in the cell that are capable of sensing and responding to signals of varying chemotypes. A unifying feature of these pathways is the ability of sensor proteins to translate a non-specific chemical signal into a specific biological response. This is in direct contrast to receptor-ligand or antibody-antigen based signaling which relies on a specific signal to generate a specific response. The end result of signaling through stress response pathways typically is one of two phenotypes: adaptive stress response or programmed cell death. Understanding how the master regulatory proteins for these pathways sense chemical stress and are regulated is therefore of great interest and could potentially have an important impact on human health.

Apoptosis signal-regulating kinase 1 (ASK1 or MAP3K5) is one such regulatory switch that integrates a wide array of stress signals and transduces them into activation of the mitogen-activated protein kinase (MAPK) signaling cascade. Upon activation by these stimuli, ASK1 phosphorylates downstream kinases and initiates the P38 and JNK signaling cascades that ultimately result in apoptosis if the stress signal is severe enough. Because of its role as a key regulator of two important MAPK pathways, ASK1

is tightly regulated by both phosphorylation and protein-protein interactions. Understanding how these regulatory mechanisms function in response to diverse stress stimuli is important for predicting how ASK1 will function in various disease states where these stressors are present. Until now, most of the mechanistic work in the ASK1 field was performed using $H_2O_2$ as the activating stress molecule to trigger ASK1 signaling. $H_2O_2$ is a valid and interesting second messenger that plays a role in stress signaling in many contexts, but it is only one of many known ASK1 activating molecules. A deeper understanding of how ASK1 is regulated in response to other stressors of diverse chemotypes is needed and may provide valuable insight into how stress sensing proteins as a whole are able to transduce non-specific chemical signals into specific biological responses.

The work presented in this dissertation examines the regulatory mechanisms of ASK1 in response to 4-hydroxy-2-nonenal (HNE), an endogenously produced end product of lipid peroxidation that can activate the ASK1 MAPK pathway. I hypothesize that ASK1 or its regulatory protein partners are chemically modified by electrophiles (represented by HNE), resulting in ASK1 pathway activation and a change in the regulatory mechanisms of ASK1. These regulatory mechanism changes could manifest as a change in the protein-protein interactions of ASK1 and as a change in the phosphorylation pattern on ASK1. The following chapters present a series of studies using mass spectrometry to examine the dynamic changes in protein-protein interactions and phosphorylation for ASK1 as a result of HNE treatment. The remainder of chapter I will examine the importance of oxidative stress, discuss what is known about ASK1 and its regulation, introduce the mass spectrometry concepts that will be

used in the later chapters, and provide a rationale for the studies discussed in chapters 2 and 3.

## Oxidative Stress

Oxidative stress is acknowledged as an important component of many disease states, including cardiovascular disease, neurological disease, liver disease, and diabetes, and plays a principal role in disease processes involving inflammation (1-10). One interesting area of human health where oxidative stress plays a role is in neurodegenerative diseases, due to the large amount of oxygen, lipids, and reactive metals present in the brain (2, 3). Whether this oxidative stress is causative or symptomatic of neurodegeneration is unknown; but in either case, oxidative stress appears to be an important part of these disease states. Both Alzheimer's disease and Parkinson's disease are characterized by high concentrations of oxidized cellular components (proteins, lipids, and DNA) and reactive oxygen species (ROS) levels (11, 12). ROS exist in many forms in the cellular environment; commonly observed species include the superoxide anion, hydrogen peroxide ($H_2O_2$), and hydroxyl radical (13). Of these three, $H_2O_2$ is the least reactive and thus most diffusible molecule and has been recognized as a second messenger in many signaling pathways (14). Many of the endogenously generated ROS are created in the mitochondria through the process of oxidative respiration and, as such, these highly reactive species are present in areas with high lipid content (organelle membranes) which leads to the creation of reactive lipid electrophiles like HNE (15).

Lipid electrophiles are created through a series of radical-mediated polyunsaturated fatty acid peroxidation reactions that can propagate beyond the initial site of damage to result in the generation of many molecules of reactive peroxidation products for each molecule of initiating ROS (15, 16). One of the most well-studied end products of this chain reaction is the $\alpha,\beta$-unsaturated aldehyde HNE, which is considered the prototype for the whole class of lipid electrophiles (17, 18). HNE can diffuse far from the site of creation and is capable of damaging DNA and proteins (15, 17). The protein damage is typically in the form of Michael adducts on nucleophilic amino acids (Fig. I-1). The most commonly adducted sites in proteins are cysteine residues, but histidine and lysine adducts also occur (19). HNE can also produce Schiff base adducts with lysine residues, giving this molecule the ability to crosslink proteins (20, 21). Identification of the exact sites of HNE adduction in a protein can be accomplished via mass spectrometry techniques (22-25), which can greatly aid in understanding the functional consequences of this adduction.

It is interesting to note that cysteine residues are the recipients of most of the oxidative and alkylation damage to proteins. Initially, it was believed that the majority of this damage was non-specific, but recently it has become clear that the modification of proteins by reactive species is a highly specific phenomenon that controls many processes in the cell (26). The interplay between direct oxidation of proteins and the generation of reactive lipid electrophiles by ROS is even more interesting when one takes into account that the damage done to proteins is generally readily reversible in the former case and less so in the latter (16, 26). Understanding how a sensor protein like ASK1 is capable of responding to both types of stress is of considerable interest.

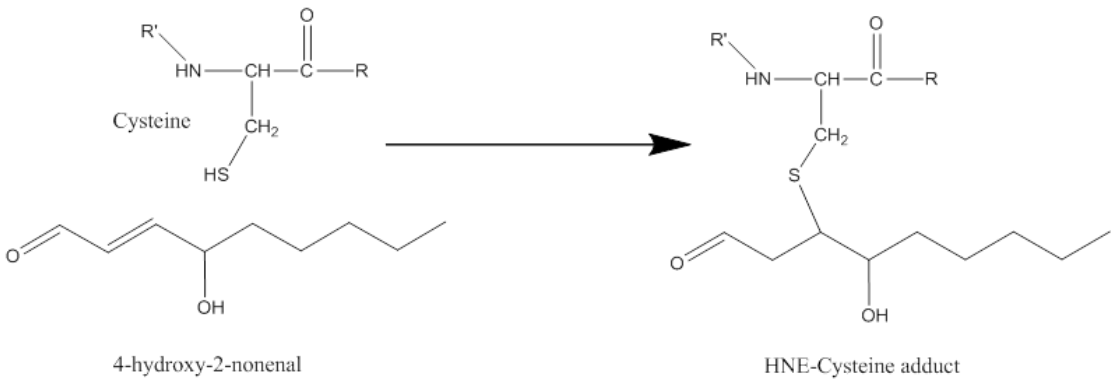


**Figure I-1. HNE Michael adduct on cysteine residue.**

## Apoptosis Signal-regulating Kinase 1

Apoptosis Signal-regulating Kinase 1 is a mitogen-activated protein kinase (MAPK) kinase kinase (MAP3K) which acts as a key stress sensor for the cell upstream of the P38 and JNK pathways (27). It was first described by Ichijo *et. al.* in 1997 as a 154 kDa MAP3K protein that was capable of directly phosphorylating MKK3, MKK4, and MKK6 and thereby activating the P38 and JNK pathways in response to treatment of cells with tumor necrosis factor alpha (TNF$\alpha$) (27).

### *ASK1 Protein Structure*

ASK1 consists of three large domains: an N-terminal coiled-coil domain, a serine/threonine kinase domain, and a C-terminal coiled-coil domain (28). In addition, ASK1 contains several smaller domains with specific binding recognition sequences, including a 14-3-3 binding motif and a deubiquitinase binding motif (Fig. I-2) (28, 29). ASK1 exists as a homodimer that is joined through both its c-terminal coiled-coil domain and its kinase domain and interacts with a number of other proteins, potentially in a large complex termed the ASK1 signalosome (28, 30, 31).

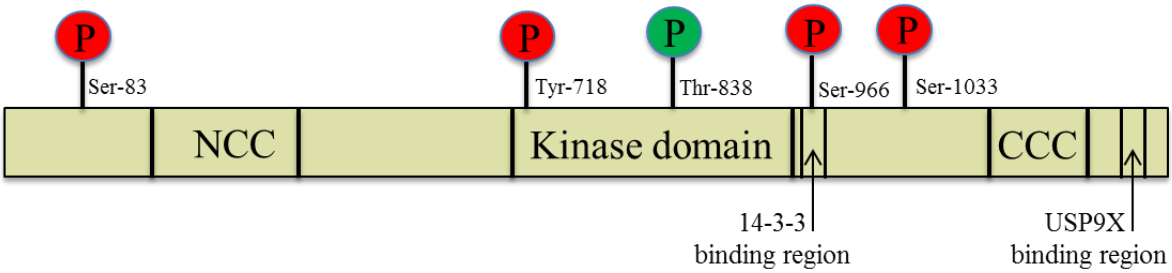


**Figure I-2. ASK1 domain structure with key phosphorylations highlighted**. Red circles indicate inactivating phosphosites while the green circle indicates the activating one. NCC/CCC = N/C-terminal coiled-coil domain.

*ASK1 Evolutionary Conservation*

The role of ASK1 in the MAPK pathway appears to be evolutionarily conserved as the *Drosophila* analogue (DASK1) and the *C. elegans* analogue (NSY-1) both activate their respective P38 and JNK pathways (32, 33). Additionally, the broad structural features of ASK are similar among these three organisms – the activation domain in particular is highly conserved (32). ASK1 also shares a great deal of similarity with 14 other members of the *homo sapiens* MAP3K family members. The kinase domain of ASK1 is fairly well conserved among all MAP3Ks, but especially when compared against ASK2 (80% similarity) and ASK3 (87% similarity) (34-36).

*Activation of the ASK1 MAPK pathway in response to stress*

Activation of ASK1 by stress signals results in autophosphorylation of a critical threonine residue (T838) and subsequent phosphorylation of MAP2Ks in the P38 and JNK pathways – specifically, MKK3/6 and MKK4/7 (27, 32). Upon phosphorylation by ASK1, the MAP2K proteins are activated and in turn can phosphorylate their MAPK targets: P38 and JNK(32). The end result of this signaling pathway is either adaptive stress response or apoptosis, depending on the severity of the stress. In the case of apoptosis, signaling through the ASK1 MAPK pathway results in release of cytochrome c from the mitochondria and activation of caspase 9 and caspase 3 in a canonical mitochondria-dependent apoptotic pathway (37).

Activation of ASK1 and subsequent apoptotic cell death can occur as a result of a number of stress insults. ASK1 is known to be activated in response to both

endogenously- and exogenously-generated stress signals (Fig. I-3). Endogenously, ASK1 is activated in response to oxidative stress, endoplasmic reticulum stress, calcium stress, and inflammatory signals (32, 38-41). Additionally, many chemical species are known to activate ASK1, including methylmercury, 1,2-naphthoquinone, denbinobin, acetaminophen, troglitazone, 2,3,7,8-tetrachlorodibenzo-*p*-dioxin, acrolein, capsaicin, 1-methyl-4-phenyl-1,2,3,6-tetrahydropyridine, 6-hydroxydopamine, and paraquat (42-52). While many molecules are known to activate ASK1, two in particular (TNF$\alpha$ and $H_2O_2$) have been used extensively to characterize the function of ASK1.

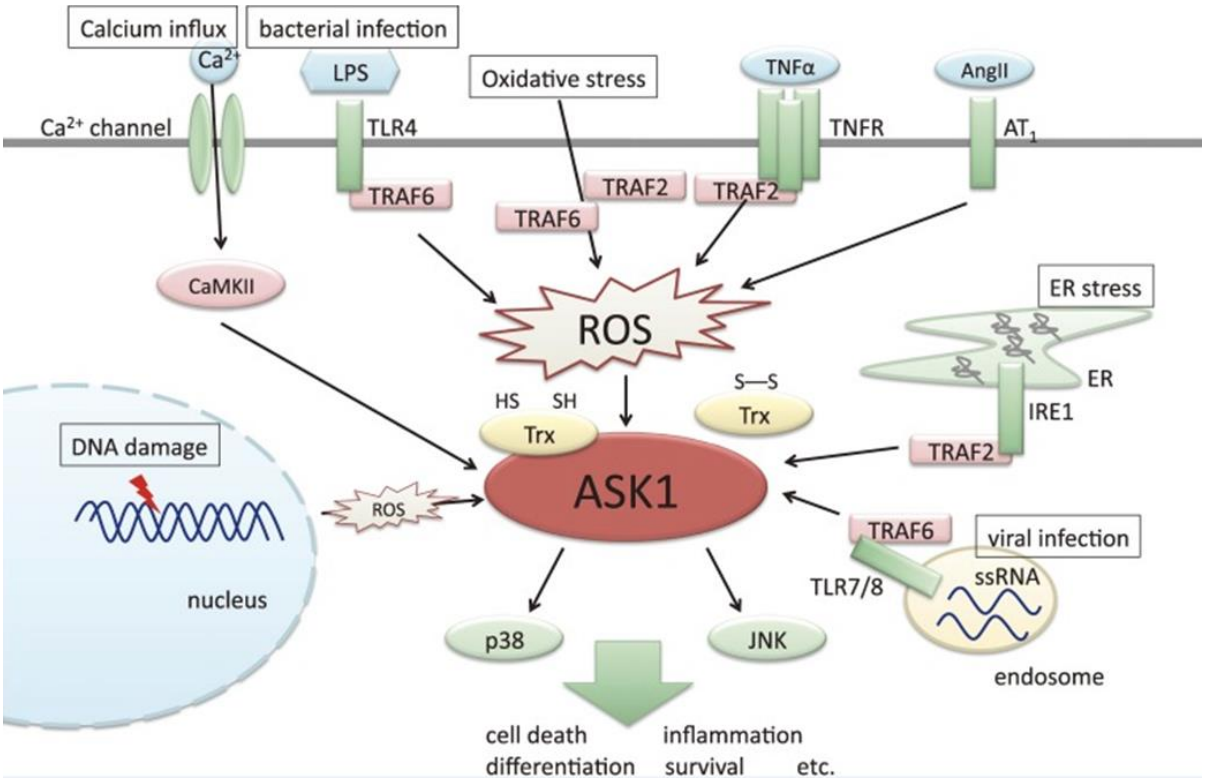


**Figure I-3. ASK1 is activated in response to many different stressors.** Reproduced with permission from Hayakawa et. al. Proc Jpn Acad Ser B Phys Biol Sci. 2012; 88(8):434-453.

*Activation of ASK1 by TNFα*

TNFα was the first stress signal defined as an ASK1 activator, as it was already known to activate the P38 and JNK pathways (27). It was further noted that ASK1 is required for TNFα–mediated sustained activation of these two pathways via use of a mouse knockout model (53). This experiment confirmed ASK1 as a TNFα-responsive protein and localized the induction of that signal to the MAP3K level of the P38 and JNK pathways. In another study, it was shown that TNF receptor-associated factor 2 (TRAF2) is also required for ASK1 activation by TNFα, which suggested that, while TNFα acted at the MAP3K level in the signaling pathway, it did not directly act on ASK1 (54).

Further evidence of the indirect action of TNFα on ASK1 came about after the discovery of the ASK1-interacting protein thioredoxin (TRX). TRX is a small (~12kDa) protein with a redox-active pair of Cys residues (Cys 32 and 35) that, upon oxidation, form a disulfide bond. It is this bond formation that was believed to cause TRX to dissociate from ASK1, thereby relieving ASK1 of its inhibitory influence (38). The link between the redox regulation of ASK1 and activation of ASK1 by TNFα was first made by Liu *et.al.* who observed that TNFα activation of this pathway was dependent on ASK1-TRAF2 association, which was in turn dependent on TRX-ASK1 dissociation (55). This study further noted that TNFα production or overexpression of TRAF2 causes an increase in ROS levels within the cell, which would allow for oxidation of TRX and activation of ASK1 (55).

*Activation of ASK1 by ROS and HNE*

Because activation of ASK1 via TNFα was redox-dependent, the focus in the literature shifted to using $H_2O_2$ to study ASK1 activation. One of the first studies to focus on $H_2O_2$ as an activator of ASK1 used ROS scavengers to show that TNFα-mediated activation of ASK1 was likely redox-dependent (56). As a consequence, the majority of the protein-protein interaction studies on ASK1 have been performed using $H_2O_2$ to stress the cell model systems. These experiments will be described in the protein-protein interaction section below.

Another known activator of ASK1 is HNE (57). As discussed above, HNE is an electrophilic end product of lipid peroxidation that is capable of diffusing throughout the cell and causing damage to macromolecules like DNA and proteins (16, 17). Adduction of proteins by HNE has been observed to alter intracellular signaling pathways (including activating the ASK1 pathway) and is therefore of considerable biological interest (16, 24, 57, 58). Specifically, HNE has been shown to be involved in the NF-κB and KEAP1/NRF2 pathways among others (58). In the NF-κB pathway, HNE was found to directly inhibit IκB kinase (IKK) which is responsible for phosphorylating the NF-κB inhibitory protein IκBα (59). By inhibiting IKK, HNE blocks the translocation of NF-κB to the nucleus and the subsequent gene regulation by this transcription factor (58, 59).

The KEAP1/NRF2 pathway works by a similar mechanism to the NFkB pathway – NRF2 is a transcription factor that promotes transcription of anti-oxidant genes (the anti-oxidant response element). NRF2 transactivation of its target genes is controlled

by KEAP1-mediated degradation of NRF2. Upon oxidative or electrophilic modification of KEAP1 sensor cysteine residues by HNE and other chemicals, NRF2 is released from its complex with KEAP1, translocates to the nucleus, and promotes target gene expression (58). It has been shown that HNE directly adducts KEAP1, which results in an increase in NRF2 target gene transcription and that decreased KEAP1 expression confers resistance to HNE stress (60-63).

As mentioned above, HNE has also been shown to activate ASK1 and the downstream MAPK pathway in PC12 cells (57). The mechanism of ASK1 activation by HNE was not examined in this study, but given the examples of HNE modulation of other pathways above, it is reasonable to hypothesize that the activation of ASK1 is accomplished through a similar means. Thus, it is possible that direct covalent modification of ASK1 by HNE may be the activating step for HNE-mediated MAPK signaling. In support of this hypothesis, we have shown that ASK1 can also be activated by HNE in HEK-293 cells and, furthermore, that ASK1 is covalently modified by HNE (see chapters II-III).

*Functional role and disease relevance of ASK1*

ASK1 has been most often studied for its role in apoptotic regulation and, as evidenced by their evolutionary conservation, the MAPK stress pathways that are controlled by ASK1 are quite important. Dysregulation of the P38 and JNK pathways has been implicated in several disease states, including cancer, heart disease, diabetes, polyglutamine repeat disorders, Parkinson's disease, Alzheimer's disease,

multiple sclerosis, and amyotrophic lateral sclerosis (64-70). As a key control step for the JNK and P38 MAPK pathways, ASK1 has been investigated in many of these disease contexts to see if the dysregulation of the pathway originated with a change in ASK1 signaling. Conflicting roles have been reported for ASK1 in cancer depending on the cellular context. Through an investigation of skin cancer in a murine model system, ASK1 was shown to work in concert with ASK2 to promote apoptosis of carcinogenic cells; however in the same study it was noted that in cells that had ASK2 knocked out, ASK1 promoted tumorigenesis (71). In the context of gastric cancer however, the results were clearer - ASK1 acted as a tumor promoter in conjunction with the protein cyclin D1 and inhibition of ASK1 with a small molecule retarded tumor growth (72, 73).

Despite the conflicting reports in the context of cancer, there has been more of an interest in the role of ASK1 in neurodegenerative diseases and in attempting to develop drugs to target ASK1 in this context (70, 74). In the case of Alzheimer's disease, ASK1 is believed to be activated in response to ROS caused by the buildup of amyloid beta plaques (75). Similarly, ROS-induced activation of ASK1 was found to be important in Parkinson's disease as well (50).

In the case of Huntington's disease, caused by expansion of polyglutamine repeats in key genes, ASK1 has been found to play a role in the subsequent neuronal cell death via endoplasmic reticulum (ER) stress activation of the JNK pathway that is abrogated in ASK1 knockout mice (41). Another neurological condition symptomatically linked to ASK1 activation by ER stress is familial amyotrophic lateral sclerosis (76). In this context, ER stress is caused by a mutant superoxide dismutase protein, which then results in ASK1 pathway activation and apoptotic cell death. This cell death was

mitigated in an ASK1 knockout model system (76). ASK1 is also believed to play a role in multiple sclerosis, whereby the inflammatory signaling pathways activate ASK1 (77). An ASK1 knockout mouse model of multiple sclerosis showed reduced cell death and neuroinflammation and an inhibitor of ASK1 applied to an ASK1 expressing multiple sclerosis model *in vivo* had a similar effect (77).

In addition to diseases where ASK1 signaling and subsequent MAPK pathway activation results in apoptosis and disease progression, ASK1 is also believed to play a role in the immune response to foreign pathogens (70, 78). ASK1 has been reported to be important for the defensive macrophage apoptotic response to *mycobacterium* infection (79). Additionally, ASK1 has been implicated as an activator in influenza virus-mediated apoptosis of infected cells as a host defense mechanism (80). This type of ASK1-regulated apoptotic antiviral response mechanism may be fairly ubiquitous, as it has also been demonstrated that the human immunodeficiency virus 1 (HIV-1) protein Nef inhibits the function of ASK1 to decrease apoptosis of infected cells (81). Interestingly, ASK1 has also been shown to interact with another HIV-1 protein called Vif and this interaction promotes the stabilization of another host protein called A3G which destroys viral RNA before it is reverse-transcribed (82). Thus, it seems that ASK1 plays both a direct and indirect role in innate immune response.

The wide variety of human pathologies described above where the ASK1 MAPK pathway is believed to play a critical role highlight the importance of understanding the ASK1 system. Better knowledge of the regulation of ASK1 and under what conditions it is activated could potentially reveal new therapeutic targets to ultimately improve human health.

Because of the key role that ASK1 plays in determining cell fate in response to a highly varied set of signals, careful regulation of its activity is extremely important. This regulation is achieved through two interrelated mechanisms: phosphorylation and dynamic changes in protein-protein interactions. Each of these will be discussed in detail below.

## ASK1 Phosphoregulation

Regulation of ASK1 function by differential phosphorylation is an important control mechanism employed by the cell. ASK1 is a large protein and has 114 serine, 77 threonine, and 40 tyrosine residues that could serve as potential regulatory sites. In practice, however, only 5 phosphorylated sites have thus far been identified as important for regulation (Fig. I-2). It is interesting to note that four of these are inhibitory, with only one phospho-residue serving an activating role (49).

The sole well-studied phospho-tyrosine residue in ASK1 is Tyr-718, which acts as a binding location for suppressor of cytokine signaling 1 (SOCS1). This residue is phosphorylated by Janus Kinase 2 (JAK2) to allow SOCS1 to bind and promote the degradation of ASK1 through recruitment of ubiquitin ligase proteins (83, 84). TNF$\alpha$ treatment promotes a decrease in phosphorylation at this site, which is accomplished via the protein tyrosine phosphatase SHP2 (83, 84).

One of the most well-studied inactivating phosphorylations on ASK1 is on Ser-83. It was first noted that pro-survival kinase AKT could phosphorylate ASK1 at Ser-83 and decrease the kinase activity of ASK1 in response to $H_2O_2$ (85). Later, PIM1 was also

identified as a kinase that can phosphorylate ASK1 at Ser-83 with a similar negative impact on ASK1 function (86). These two kinases act in different biological contexts to phosphorylate the same residue on ASK1, thereby keeping tight control over the activity of ASK1 (86).

Similarly, ASK1 is phosphorylated on Ser-966 by 3-phosphoinositide-dependent protein kinase 1 (PDK1), which serves as a negative regulator of ASK1 by acting as a binding site for 14-3-3 proteins (87, 88). Dephosphorylation of this site by protein phosphatase 2A (PP2A) results in decreased 14-3-3 binding to ASK1 and increased ASK1 activity (89, 90). One last known inactivating phosphorylation on ASK1 is on Ser-1033 which has been shown to be present on ASK1 and to correlate with decreased ASK1 activity (90). However, unlike the other residues, no kinase or phosphatase is known for this site.

As the sole known activating phosphorylation on ASK1, Thr-838 has been thoroughly investigated and is often used as a surrogate marker for ASK1 activity. This key phosphosite is autophosphorylated by N-terminal dimerization of ASK1 and possibly phosphorylated by ASK2 or another unidentified kinase (30, 36, 56). Two different phosphatases have been identified as capable of removing the phosphorylation from Thr-838, which highlights the importance of fine control over this site. The first phosphatase that targets Thr-838 was identified as protein phosphatase 5 (PPP5C), which was shown to act in response to ROS (91). Recently, Cho *et. al.* reported that cell division cycle 25C (CDC25C) was also capable of dephosphorylating Thr-838 of ASK1 and that it could do so in a cell cycle-dependent fashion by inhibiting ASK1 activity during interphase (92). Interestingly, cells that were halted in mitosis showed an

increase in ASK1 activity and a decreased association between CDC25C and ASK1, suggesting that, in addition to stress response, ASK1 may play an important role in normal cell cycle events (92).

In addition to pThr-838, two other threonine residues have been identified as potential autophosphorylation sites on ASK1. Thr-813 and Thr-842 have been shown to become autophosphorylated when the kinase domain of the protein is expressed by itself and mutation of either of these residues to alanine resulted in a decrease in reporter gene activity in a cell model of ASK1-JNK signaling (28). However, in an *in vitro* phosphorylation model, mutation of each threonine residue (813, 838, and 842) resulted in similar activity levels as the wild type protein, indicating that these residues may be more important for protein-protein interactions than for intrinsic kinase activity (28).

## ASK1 regulation by protein-protein interactions

### *Signalosome hypothesis*

Since ASK1 was first described, over 80 proteins have been reported as ASK1-interacting proteins. All of these proteins have been investigated for a positive or negative regulation on the function of ASK1 and, taken together, they form a highly nuanced regulatory mechanism that can exercise fine control over ASK1-mediated MAPK pathway signaling. In almost every case, the ASK1-interacting proteins have been examined as part of a binary interaction with ASK1. Thus, our understanding of

the protein-protein regulatory mechanism for ASK1 is limited to how these protein pairs dynamically associate or dissociate in response to stress.

However, in 2005 Noguchi *et. al.* performed a gel filtration experiment (Fig. I-4) in which they showed that ASK1 formed a constitutive high molecular mass complex that shifted to an even higher mass complex upon activation of ASK1 (93). This observation led to the hypothesis that ASK1 is actually regulated by a large multiprotein complex that they named the ASK1 signalosome. The exact membership of this proposed signalosome has never been investigated, but the potential members include all of the reported ASK1 interacting proteins. These proteins will be discussed in detail below in the context of the binary interaction between each protein and ASK1, and are further summarized in Table 1 at the end of this chapter.

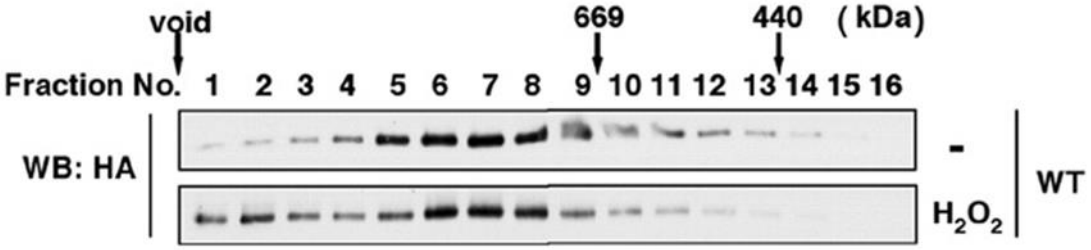


**Figure I-4. The ASK1 complex shifts to a higher molecular mass upon treatment with $H_2O_2$.** Reproduced with permission from Takuya Noguchi et al. J. Biol. Chem. 2005;280:37033-37040.

*ASK1 and its related kinase ASK2*

ASK2 is another MAP3K that shares a good deal of homology with ASK1 (~45% overall, ~80% in the kinase domain) and is also capable of activating the JNK and P38 MAPK pathways (94). While ASK1 has been the focus of a large research effort, the functional importance and regulation of ASK2 remains largely unknown. A pair of studies determined that ASK2 exists in a heteromeric complex with ASK1 and that these two kinases may directly affect each other (36, 95). One study found that ASK1 stabilized ASK2 by inhibiting the degradation of ASK2 and that, in turn, ASK2 was capable of phosphorylating ASK1 and promoting its activity (36). A second study also found that ASK2 supported and enhanced ASK1-mediated signaling (95). Interestingly, while these studies above would indicate a positive regulatory role of ASK2, a later report indicated that ASK2 enhanced 14-3-3 binding to ASK1 which negatively regulates ASK1 (96). However, in a mouse tumor model, ASK1 and ASK2 were observed to work cooperatively as tumor suppressors by triggering apoptosis, which would seem to support the idea of ASK2 as a positive regulator of ASK1 (71). Given the conflicting reports discussed above, more study of the role that ASK2 plays in ASK1 regulation is needed. Several other ASK1-interacting proteins also have conflicting roles reported in the literature (see below), thus it is possible that many of the protein-protein interactions that regulate ASK1 may possess varying roles depending on the stress and cellular context.

*ASK1 regulation by protein turnover*

The first reported protein-protein interaction for ASK1 was with TRX and was described shortly after the function of ASK1 was elucidated (38). The TRX-ASK1 interaction was detected using a yeast two-hybrid strategy, and it was further demonstrated with a series of ASK1 deletion mutants that TRX bound with the N-terminus of ASK1. This study also showed that TRX had an inhibitory effect on the function of ASK1 and that this inhibition was dependent on the redox status of TRX (38). The end result of this study was the first model of ASK1 regulation, which has largely remained unchanged (Fig. I-5). Later, it was shown that the repression of ASK1 activity by TRX was due to TRX blocking a homophilic interaction between the N-terminal regions of two ASK1 molecules (31). In addition to this mechanism of inhibition, TRX is also capable of promoting ubiquitination of ASK1 as a means of controlling its activity (97).

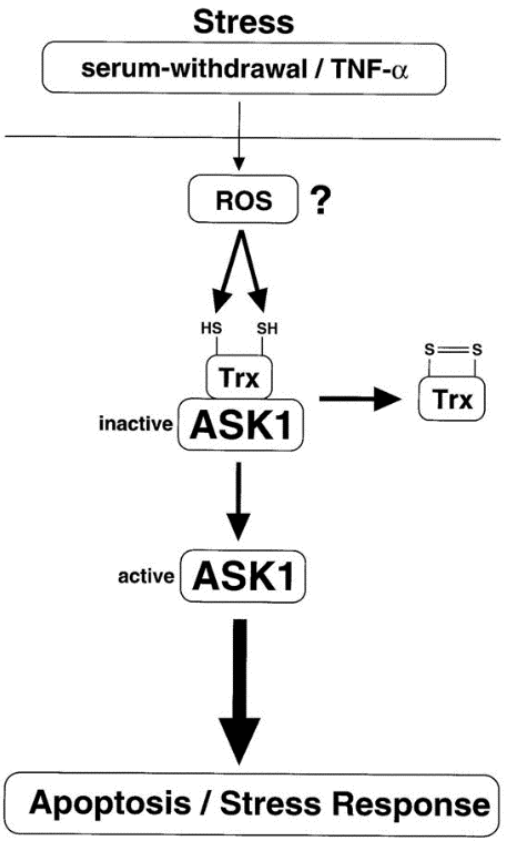


**Figure I-5. Initial model of ASK1 regulation by TRX.** Reproduced with permission from Saitoh et. al. The EMBO Journal. 1998; 2596-2606.

While TRX was the first protein reported to promote ubiquitination of ASK1, it is not the only one, as ubiquitination has been recognized to play an important role in ASK1 regulation. Ubiquitination is a post-translational modification, whereby ubiquitin (a small protein made of 76 amino acids) is attached via its C-terminal glycine to another protein at the epsilon amino group of a lysine. Additional ubiquitin molecules can be added to ubiquitin lysine residues to form polyubiquitin chains, which act as degradation signals and target the polyubiquitinated proteins to the proteasome for degradation (98). Ubiquitination (Fig. I-6) is a multi-step process that begins when an E1 enzyme (UBA1 or UBA6 in humans) transfers a bound ubiquitin molecule to an E2 enzyme (there are more than 30 encoded in the human genome) (98, 99). Once the ubiquitin is attached to the E2, it must be transferred to one of several hundred E3 enzymes prior to making the final transfer to the target substrate protein (99).

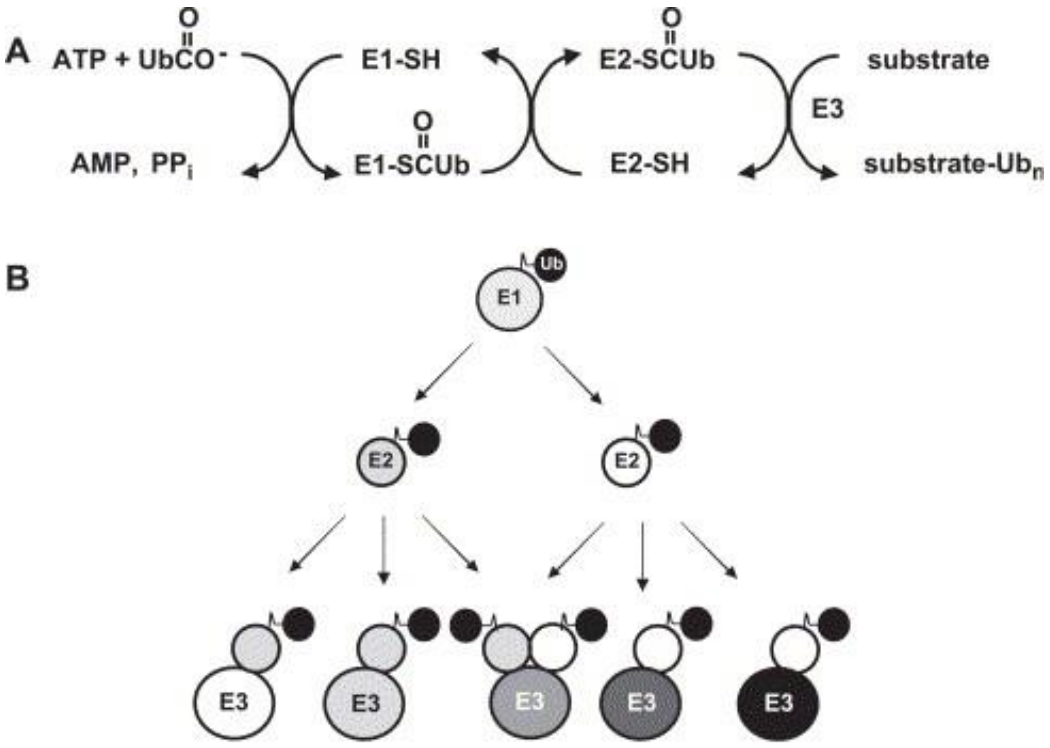


**Figure I-6. Ubiquitin pathway.** (A) Ubiquitin transfer mechanism. (B) Hierarchical diagram of ubiquitin pathway. Reproduced with permission from Pickart and Eddins, *Biochimica et Biophysica Acta* 1695 (2004) 55–72.

Several proteins have been reported to function as E3s for ASK1 and facilitate degradation. It remains unclear whether there are only certain contexts in which each of these proteins functions or if there is some other diversity of function that would explain the apparent redundancy of having multiple distinct E3 ligases. Nonetheless, each of the proteins below has been demonstrated to function as an E3 and promote the degradation of ASK1.

The first E3 reported for ASK1 was the protein C-terminus of heat shock protein 70-interacting protein (STUB1, commonly known and referred to hereafter as CHIP). Overexpression of CHIP and reconstituted *in vitro* systems both demonstrated that CHIP has the ability to ubiquitinate ASK1 (100, 101). Furthermore, this ubiquitination was increased in response to $H_2O_2$ treatment and decreased following CHIP knockdown (101). As part of the CHIP-mediated degradation of ASK1, heat shock protein 70 (HSPA1A and HSPA4, collectively referred to here as HSP-70) has been reported to bind to ASK1 and, together with CHIP, target ASK1 for proteasomal degradation (100). This function of HSP-70 as a co-E3 with CHIP expands upon an earlier report that identified HSP-70 as a negative regulator of ASK1 which interfered with the n-terminal dimerization of ASK1 (102).

Cellular inhibitor of apoptosis protein 1 (BIRC2) was the next E3 identified for ASK1. Evidence similar to that seen for CHIP was presented here, but in this case, TNF$\alpha$ was the stressor used (103). This could suggest that each type of stress activation has at least some unique protein-protein interactions.

Roquin-2 (RC3H2) was recently identified by the Ichijo group as a third E3 for ASK1 (104). RC3H2 was identified using an imaging-based screen to look for increased levels of a fluorescently-tagged ASK1 following siRNA knockdown of a large candidate list of ubiquitin-related proteins. After RC3H2 emerged as the best candidate from the screen, extensive western-based assays were performed to demonstrate that RC3H2 is capable of ubiquitinating ASK1 and thereby promoting its subsequent degradation (104).

Another study found that the protein TNFAIP3 is also capable of interacting with ASK1 as an E3 and promoting its degradation (105). One last pair of E3 ligases reported to ubiquitinate ASK1 are NEDD4 and NEDD4L. ASK1 was found to be a substrate for each of these proteins and a binding partner of NEDD4L in a high-throughput protein microarray study (106).

In addition to the E3s discussed above, other protein-protein interactions with ASK1 have been described that promote ASK1 degradation by means other than directly coupling ubiquitin to ASK1. Suppressor of cytokine signaling 1 (SOCS1) is one such protein that binds to ASK1 only when ASK1 is phosphorylated at Tyr-718 and promotes the degradation of ASK1 (83). SOCS3 was also identified as an ASK1 binding protein in the same study, with an observation that overexpression of SOCS3 resulted in decreased ASK1 expression (83). This suggested that SOCS3 behaves similarly to SOCS1, but no follow-up studies were performed (83). In another study, SOCS1-mediated degradation of ASK1 was shown to be important for IL-6-induced protection against oxidant-induced lung injury in mice (107). Beta-arrestins 1 and 2 (ARRB1 and ARRB2) have both been reported to interact with ASK1 and promote its

degradation by acting as scaffold proteins to bring ASK1 into contact with CHIP (108). These studies highlight the importance of ubiquitin-mediation degradation of ASK1 as a regulatory mechanism to control MAPK signaling.

While degradation of ASK1 can act as an important regulator of ASK1 signaling, there needs to be a way to control the targeting of ASK1 to the proteasome, otherwise efficient signal propagation could not occur. An important means of blocking ubiquitin-mediated proteolysis is through a deubiquitinase called ubiquitin-specific peptidase 9, X-linked (USP9X). This protein can bind to ubiquitinated ASK1 and remove the ubiquitin molecule, thus stabilizing ASK1 and preventing degradation (29). Interestingly, Nagai *et. al*. showed that USP9X only binds ASK1 with kinase activity (it will not bind a kinase null mutant of ASK1) in response to oxidant stress. This study also identified a ubiquitin-like sequence present in the c-terminus of ASK1 (Fig. I-2) that is required for binding (29). Together, this suggests that there is some sort of conformational or protein-protein interaction change that occurs during activation of ASK1 and that exposes the c-terminal USP9X recognition sequence, thereby allowing USP9X to interact with ASK1.

Another protein that seems to decrease degradation of ASK1 is GNA13. The activated form of this protein is able to decrease the interaction between ASK1 and CHIP and thereby promote stabilization of ASK1 (109). GNA13 and GNA12 have also been shown to promote an increase in ASK1 activity, which gives GNA13 the ability to stimulate ASK1 signaling and also assist in maintaining that signaling by blocking CHIP-mediated degradation (109, 110). Interestingly, Um *et. al*. reported that ASK1 could interact with components of the 19S regulatory subunit of the 26S proteasome and that

this interaction had a negative impact on proteasome function. This affect was attributable to phosphorylation of a component of the 19S regulatory subunit by ASK1 (111) and partially relied on the ubiquitin-like sequence present in ASK1 (112). This report adds another layer to the degradation regulatory mechanism of ASK1, whereby upon activation ASK1 becomes ubiquitinated and thus targeted for proteasomal destruction. But at the same time, ASK1 decreases the activity of the proteasome while USP9X works to remove the ubiquitin. Thus, the ultimate fate of ASK1 depends on the interplay of these mechanisms, which likely can be tuned by the cell depending on the source or severity of the stress signal.

*ASK1 scaffold proteins*

Several of the previously studied ASK1-interacting proteins serve as scaffold proteins that help to bring ASK1 into contact with its downstream MAP2Ks and MAPKs and thus enhance signaling through this pathway. One such set of proteins is ARRB1 and ARRB2, which were discussed above for their role as scaffold proteins to promote the degradation of ASK1. In addition to this role, there have been other reports that suggest the beta-arrestins can also act as scaffolds for MAPK signaling downstream of ASK1. Specifically, ARRB1 has been reported to serve as a scaffold for ASK1, MKK4, and JNK3 (113). In this way, ARRB1 brings all three levels of the MAPK cascade together to enhance signaling in response to stress. Another report added support to this scaffolding function of the beta-arrestins by using a peptide array to identify docking sites in ARRB1 and ARRB2 for JNK3, MKK4, and ASK1 (114). It is possible that the

arrestins may perform different regulatory functions for ASK1 depending on the cellular and stress context.

Another well-studied scaffold protein is ASK1-interacting protein 1 (DAB2IP), which was shown to enhance TNF$\alpha$-induced ASK1 signaling by recruiting components of the TNF receptor complex (including TRAF2) to ASK1 (115, 116). Additionally, DAB2IP was shown to recruit PP2A to ASK1 to dephosphorylate Ser966 and promote 14-3-3 dissociation from ASK1 (89, 117). Similarly, the protein RB1CC1 seems to act as an important bridging protein that enhances the ASK1 and TRAF2 interaction and its depletion reduces this binding event (118).

While DAB2IP and RB1CC1 bring some of the upstream TNF$\alpha$ protein machinery into contact with ASK1 to potentiate signaling, other scaffold proteins help link ASK1 with its downstream target kinases. Dual-specificity phosphatase 19 (DUSP19) is one such protein which interacts with ASK1 and MAP2K7 and enhances ASK1 signaling through the JNK pathway (119). Another protein called GEMIN5 was shown to behave similarly to the beta arrestins by acting as a scaffold to bring ASK1, MKK4, and JNK together to enhance ASK1-mediated signaling (120). In a similar fashion, the scaffold protein MAPK8IP3 is known to be phosphorylated by ASK1, and this phosphorylation enhances the ability of MAPK8IP3 to link ASK1 to MAP2K4, MAP2K7, and JNK (121).

A final family of scaffolding proteins that interact with ASK1 and regulate its function are the 14-3-3 proteins (122). These proteins are present in many different multiprotein complexes and are known to bind to phosphoserine and phosphothreonine

motifs in their partner proteins (122). The 14-3-3 proteins were shown to suppress ASK1 signaling by binding to ASK1 at the phospho-Ser-966 residue (123). Reciprocally, another study found that ASK1 activation was dependent on dephosphorylation of Ser-966 and subsequent dissociation of 14-3-3 proteins from ASK1 (88). This negative regulatory role of 14-3-3 proteins on ASK1 was further confirmed in a mouse model of diabetic cardiomyopathy where a dominant negative mutant of a 14-3-3 isoform resulted in an increase in apoptosis (124). Interestingly, the 14-3-3 proteins have been found to act as docking sites for both ASK1 and ASK2 and may play a role in linking the functions of these two kinases (96). In the same study, both knockdown of ASK2 and mutation of the 14-3-3 binding site on ASK2 also resulted in a decrease in 14-3-3 binding to ASK1 and increased ASK1 signaling (96).

*ASK1 positive regulatory interactions*

Several of the protein-protein interactions described above result in an amplification of signaling through the ASK1 pathway by bringing ASK1 into close contact with its downstream target kinases. However, the scaffold proteins are not the only protein-protein interactions that positively regulate the function of ASK1. One of the first positive regulators of ASK1 to be described was the death-domain associated protein DAXX (125). DAXX was shown to promote FAS-mediated apoptosis through the ASK1 pathway by interacting with ASK1 (125, 126). However, this enhancement of ASK1 signaling can be abrogated if DAXX binds to PARK7 or HSP27, which allows for

a highly nuanced control mechanism through just this one protein-protein interaction (127, 128).

Dual-specificity tyrosine-phosphorylation-regulated protein kinase 1A (DYRK1A) has also been reported to increase the activity of ASK1 and possibly even phosphorylate ASK1 (129). Likewise, eukaryotic translation initiation factor 2-alpha kinase 2 (EIF2AK2) also interacts with ASK1 and promotes ASK1 signaling (130). Interestingly, EIF2AK2 also may phosphorylate ASK1 or another protein interacting with ASK1 because a kinase-null mutant of EIF2AK2 abrogated ASK1 signaling (130). Another important positive regulator of ASK1 is the TNF$\alpha$ receptor-associated factor (TRAF) family of proteins. Specifically, TRAF proteins 1, 2, 3, 5, and 6 were initially reported to interact with ASK1 and promote signaling through the MAPK pathway (54). Later studies focused largely on the roles of TRAFs 2 and 6 in ASK1-mediated signaling in response to $H_2O_2$ and TNF$\alpha$ in particular. In all of these studies, the TRAF proteins were shown to be important interacting proteins that bound to ASK1 as TRX dissociated (31, 107, 118, 131, 132).

*ASK1 negative regulatory interactions*

While ASK1 does have several important protein-protein interactions that enhance signaling through its MAPK pathway, there are even more proteins that negatively regulate ASK1 in order to tightly control apoptosis. For instance, apoptosis-linked gene-2 (PDCD6) has been reported to bind to ASK1 and sequester it in the nucleus, thereby abrogating downstream JNK activation (133). Another protein,

microspherule protein 1 (MCRS1), also exhibits a localization change upon binding to ASK1 (134). In this case MCRS1 is largely nuclear, but when it is overexpressed with ASK1 a portion of MCRS1 becomes cytosolic and colocalizes with ASK1 (134). MCRS1 has been shown to negatively regulate ASK1 signaling and to dissociate from ASK1 upon ROS stress (134). PARK7 has also been shown to bind to and negatively regulate ASK1 signaling in a redox-sensitive manner that depends on two key cysteine residues in PARK7 (135, 136). RAF1 has also been shown to interact with ASK1 and negatively regulate ASK1 in a RAF1 kinase-independent manner (137).

Some of the negative mechanisms of ASK1 have only been reported in specific contexts, like cyclin-dependent kinase inhibitor 1A (CDKN1A), which binds to ASK1 and blocks its signaling in response to rapamycin-induced stress (138). Glutaredoxin (GLRX) was reported to interact with and inhibit ASK1 signaling in a redox-dependent manner (139). GLRX association with ASK1 depended on the active site cysteines in GLRX, and overexpressed GLRX blocked ASK1 signaling in response to glucose deprivation (139). Conversely, in a cellular environment with high glutamine levels, ASK1 was found to interact with glutaminyl-tRNA synthetase (QARS), which inhibited ASK1 signaling and dissociated from ASK1 in response to FAS signaling (140). In the context of heat shock stress, GSTM1 was found to interact with and negatively regulate ASK1 (141). Interestingly, in the context of this stressor and cell model system, GSTM1 took the place of TRX for regulating ASK1 (141).

*ASK1 kinase target proteins and pathway crosstalk*

The majority of the ASK1-interacting proteins that have been identified act as regulators of ASK1 in a variety of cellular contexts, but some of them are actually regulated by ASK1. The main target proteins of ASK1 are the four downstream MAP2K kinases in the P38 and JNK pathways. MAP2K4/7 and MAP2K3/6 were elucidated as downstream targets of ASK1 in the same publication that first described ASK1 (27). Since then, many other studies have provided additional evidence for the role of ASK1 in phosphorylating and activating these MAP2Ks (91, 113, 119-121, 126, 136, 138, 142-144). In addition to the MAP2K proteins, ASK1 also phosphorylates some of its adapter proteins like MAPK8IP3 (see previous section for discussion) to enhance ability of the scaffold proteins to bind to ASK1 and downstream targets of ASK1 (121).

ASK1 was recently found to influence the GAPDH-SIAH1 stress response pathway by phosphorylating SIAH1 in response to oxidative stress (145). Thus, ASK1 not only activates its own intrinsic pathway in response to stress, it also can modulate other stress response pathways, which underscores the importance of this stress transducer. Another example of pathway crosstalk involves the death-associated protein DAXX. As discussed above, DAXX is a positive regulator of ASK1 and enhances ASK1 signaling in response to FAS. In addition to that, DAXX is also a downstream target of ASK1 (146). ASK1 phosphorylates DAXX to control its subcellular localization (nuclear vs cytosolic) and to promote polyubiquitination of DAXX (146, 147). This polyubiquitination induces a positive feedback mechanism, whereby ASK1 activation is enhanced by binding to the ubiquitinated DAXX (147). As a final example of pathway crosstalk, ASK1 was shown to interact with MAP3K7 and to

decrease the ability of MAP3K7 to signal through the NF-κB pathway in response to IL-1 (148). More recently, another study showed that this pathway crosstalk be bidirectional when they demonstrated that MAP3K7 and one of its partner proteins (TAB2) could inhibit ASK1 signaling (149).

*Outstanding questions in ASK activation and signal transduction*

As can be seen from all of the protein-protein interactions discussed in the sections above, ASK1 interacts with a wide variety of proteins that each can exert a different regulatory effect on the function of ASK1. From the ubiquitin system controlling ASK1 stability to the scaffold proteins that control ASK1 protein-protein interactions, as well as the myriad interactions that negatively or positively regulate ASK1 and the crosstalk between several stress-signaling cascades, the picture of ASK1 regulation is quite complex. Additional complexity comes from the fact that ASK1 can be activated by several chemically diverse species and that several of the protein-protein interactions may be specific for one type of stressor.

There are two major questions about the function of ASK1 that remain unanswered. Because the many different chemical species to which ASK1 responds are capable of interacting with and modifying proteins in different fashions, it remains unknown how ASK1 senses all of these stress signals and transduces them into a single response. There has been some investigation into this area, but no comparative study between an oxidant and an electrophile has been carried out.

The second major question is whether or not the hypothesized ASK1 signalosome exists and, if it does, what the exact membership of this multiprotein complex might be. The evidence for the presence of an ASK1 signalosome comes from the synthesis of the size exclusion experiment by Noguchi *et. al.* (93) and the large number of identified binary interacting proteins of ASK1 discussed above. Thus, a large multiprotein complex composed of some or all of these interacting proteins is certainly a plausible explanation for the data. However, this hypothesis has not been rigorously tested and a more thorough investigation of the protein-protein interactions that regulate ASK1 needs to be undertaken.

Until now, the vast majority of work in the ASK1 field has used relatively low throughput techniques, including Western blot, yeast-two-hybrid, and *in vitro* kinase assays, to examine how one or a few proteins influence ASK1. What is missing from the literature is a picture of how all of these interactions behave at one time in response to a stimulus. Additionally, most of this work has been performed with techniques that rely on antibodies with poorly characterized specificity and with assays that are largely qualitative or semi-quantitative at best. Using the techniques mentioned above, a complex-wide investigation of the ASK1 signalosome would be nearly impossible; however, by leveraging the speed, specificity, and superior quantitative capabilities of mass spectrometry (MS) techniques, such an examination becomes tenable.

## Analytical techniques to study protein interactions and modifications

*MS-based proteomics overview*

Since the introduction of the electrospray ionization technique by Fenn and Yamashita the field of MS-based proteomics has grown exponentially (150, 151). With the coupling of this ionization technique to tandem MS (MS/MS) instrumentation, the analysis of proteins at a true "omics" level has become routine (152, 153). While early MS-based proteomics studies could identify dozens of proteins in one hour, modern mass spectrometers can identify over five thousand proteins in the same amount of time (154-157). There are many different types of MS assays that are employed to investigate the proteome, but the most common type is the bottom-up or "shotgun" method.

Liquid-chromatography tandem MS (LC-MS/MS or shotgun MS) assays are analyses of a peptide mixture by MS from which the proteins initially present in the mixture are inferred. To start, a protein mixture is digested with a protease (typically trypsin) to generate peptides. These peptides are then separated by reverse phase liquid chromatography in line with the MS instrument. Once eluted from the chromatography column into the MS instrument, a peptide is selected and then fragmented along the peptide bond backbone. These fragments are analyzed and recorded in an MS2 spectrum which contains all of the sequence information for that peptide (Fig, I-7). This procedure is repeated thousands of times in a single experiment, and this collection of MS2 data is analyzed via sophisticated computer

algorithms (152, 158-162). These algorithms predict what the fragmentation pattern for every possible peptide in the proteome is and then match these theoretical spectra to the experimental MS2 spectra to assign an identity to the peptide along with a score for how well the experimental spectrum matches the theoretical one.

Once each MS2 spectrum in a datafile has been assigned to a peptide, a minimum threshold score is applied to the dataset and all peptides that pass this threshold are used to infer the identity of the proteins that were originally present in the sample prior to proteolytic digestion. In addition to the identification of the proteins in the sample, this technique has inherent quantitative data about the abundance of the proteins present in the form of the number of MS2 spectra identified for each protein (termed spectral counting), which can be used to examine expression-level differences in a protein across different conditions (163, 164). There are many other MS-based techniques employed in the field of proteomics, but the basic shotgun analysis with spectral counting outlined above is the foundation for several of the more sophisticated applications discussed below.

*MS-based analysis of phosphorylation and other post-translational modifications*

The majority of the ASK1 phosphorylation sites described above were discovered using mutational analysis to identify the site and the functional importance of having a phosphorylation present on a particular residue. While this is a highly accurate way of describing a phosphosite, it is a slow and laborious process as it is difficult to know what residue to mutate *a priori*. Thus at best, one is able to narrow down to a region by use

of deletion mutants and then begin mutating potential residues one at a time. As discussed above, ASK1 has over 200 serine, threonine, and tyrosine residues so attempting to mutate each one in series to determine if that site is biologically important is not practical. The current state-of-the-art approach to this problem is to utilize MS proteomic assays to identify phosphorylated peptides (and other post-translational modifications [PTMs]), thus removing the guesswork and pin-pointing the exact residue that needs to be mutated for additional analyses (165-172). In fact, MS analyses can even be utilized to determine the biological importance of a particular phosphorylation to a certain extent by tracking the amount of the phosphorylated peptide present under different conditions (173). This is analogous to performing a Western blot with an antibody directed against the phosphorylated form of the protein, but the MS analysis has the advantage of a faster development time and better specificity than an antibody-based approach.

Phosphorylations and other PTMs are typically present at a low amount in the cellular environment with the modified version of the protein only making up a few percent of the total amount of that protein present. Because of this, an enrichment step is often used to aid in identification of the phosphorylated peptide. Depending on the scale of the analysis, this enrichment step could be an epitope tag on a single protein or an antibody against phosphotyrosine residues, or an immobilized metal affinity column to enrich all phosphorylated peptides. In the latter two cases, digestion of the protein is carried out prior to the enrichment step, while in the case of a single protein analysis the enrichment step is carrier out first (166, 174, 175). Following digestion, the most common approach for this kind of experiment is a shotgun MS analysis (Fig. I-7).

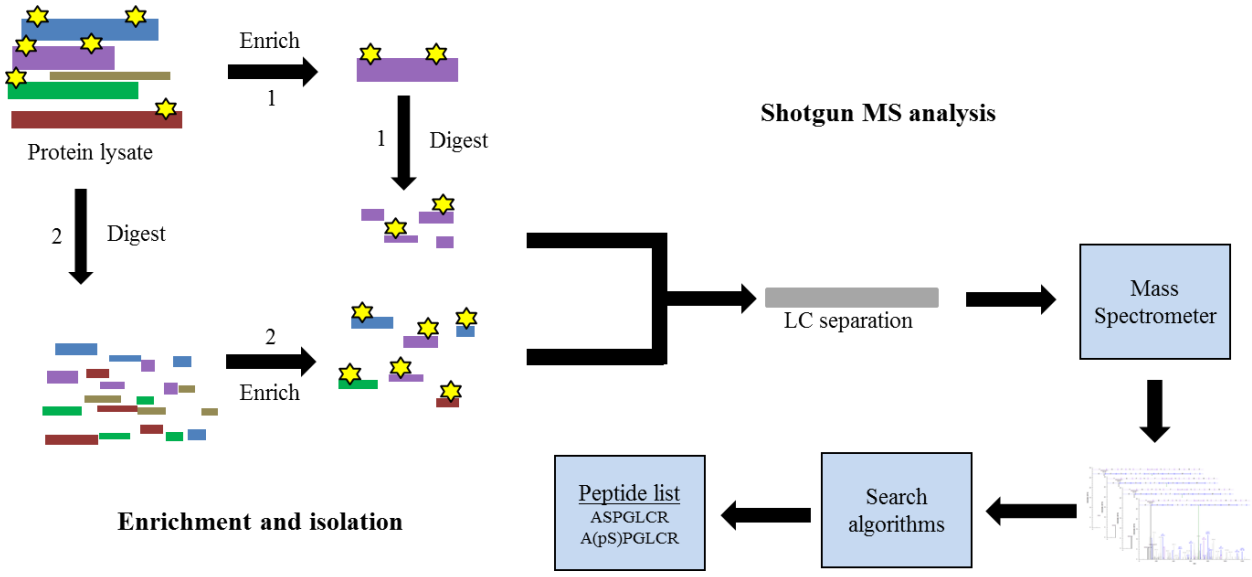


**Figure I-7. Shotgun phosphoproteomics.** Pathway 1 illustrates the concept of purifying a single protein and analyzing it for PTMs (yellow stars) while pathway 2 illustrates a global approach. Following enrichment, the peptides are analyzed via shotgun MS methods.

With the current generation of MS instruments, experiments identifying hundreds or thousands of individual phosphorylated peptides in a single run have become routine (167, 169, 176). The confident identification of phosphopeptides by MS was greatly aided by the introduction of the Thermo Scientific Q Exactive mass spectrometer and the subsequent iterations of it (177-180). The Q Exactive combines two distinct advantages over previous generations of instruments – higher energy collision induced dissociation (HCD) fragmentation and utilizing the Orbitrap as the mass analyzer for both MS1 and MS2 scans. Most previous instrumentation only used a high resolution scan for the MS1 spectrum, which meant that a researcher had high confidence in the mass-to-charge ratio of the peptide precursor with typical mass errors at 10 parts-per-million (ppm) or less, but the MS2 scan was done with a low resolution mass analyzer which could have mass errors of half a dalton or more.

By using a Q Exactive, a researcher could have both MS1 and MS2 scans with less than 10 ppm mass error which greatly increases confidence in identification and especially helps with localizing a phosphorylation to a particular amino acid in a peptide if more than one potential phosphorylation site was present. Phosphorylated peptides are characterized by a mass shift of 79.966 daltons which is observable at both the MS1 and MS2 level – the Q Exactive allows one to very precisely observe this shift and rule out potential false positives. Additionally, by utilizing HCD fragmentation, all fragment ion information is retained as opposed to earlier instrumentation which utilized CID fragmentation in an ion trap that resulted in the loss of any fragment mass less than 1/3 of the precursor mass (181). All of this adds up to better quality spectra that will be

analyzed by the search algorithms mentioned above, which results in improved identifications.

While these matching algorithms are very robust, they are not perfect and do falsely identify some spectra as being a phosphorylated peptide when it is not. In order to combat this, the best practice is to manually validate any automated assignment of a PTM identification. There are well established protocols to ensure that the assignment from the automated algorithm is correct and are covered in detail elsewhere (182-184). In brief, the purity of the collected precursor is confirmed, mass accuracy of MS1 and MS2 fragments are checked and should be within tolerable limits (10 ppm on a Q Exactive), and fragment peaks are assigned to b and y ions and any neutral loss peaks.

The procedure described above can be applied to any post-translational modification of a known mass. For example, HNE Michael adducts could be identified by searching for peptides with a mass shift of 156.115 daltons (158.130 if reduced) on a cysteine, histidine, or lysine residue (185). Here again, the use of a Q Exactive instrument improves the identifications of adducted peptides for the same reasons detailed above – higher accuracy on MS1 and MS2 data coupled with HCD fragmentation provides much more confident identifications. As an example, our lab performed two proteome-wide studies aimed at identifying proteins adducted by HNE through the use of an alkynyl analogue of HNE that was post-coupled to biotin via a copper catalyzed cycloaddition reaction. In the first study, a lower resolution LTQ instrument was used and over 1000 adduct proteins were identified (24). However, no specific adduct sites were mapped due to limitations in the instrumentation and methodology. Thus confirmation of the adducted proteins relied on examining the

concentration-response relationship of the identified proteins. In contrast to this, a later study by our lab used a similar technique, but analyzed on a Q Exactive and identified almost 400 HNE adduct sites on over 300 proteins (25). In this study, the identification of the HNE adduct proteins was much more certain than the earlier study because of the site-specific MS2 annotations, which provided direct evidence of peptide and protein adduction.

*Affinity Purification Mass Spectrometry (AP-MS) methodology*

Classically, protein-protein interaction studies have been done via techniques such as yeast two-hybrid or co-IP westerns, and these types of studies comprise the majority of the ASK1 literature (186, 187). Increasingly, though, mass spectrometry is becoming the method of choice for studying protein interactions (187-192). Typically referred to as affinity purification mass spectrometry (AP-MS), this technique combines an affinity enrichment step to purify the protein of interest (the bait protein) followed by mass spectrometry to identify the interacting proteins (the prey proteins) (193). The bait protein is most often ectopically expressed in a cell model system and is also tagged with an epitope (FLAG, HA, etc.) to allow for immunoaffinity enrichment of it and its prey proteins (Fig. I-8) (193, 194). Many studies have employed variations on this technique, with the majority of the diversity being in the way in which the samples are obtained and the proteins purified. The final mass spectrometry step is almost always a standard shotgun analysis to identify the bait and prey proteins. This type of method has been successfully used to investigate many different proteins and their interactors in several

biological contexts. A recent study established a highly standardized way of preparing samples and validating the data and applied it to a set of over 5,000 bait proteins with more than 50,000 interactions identified so far (195). Another study established the reliability of this type of study by demonstrating that inter-lab reproducibility for AP-MS studies is quite high (196).

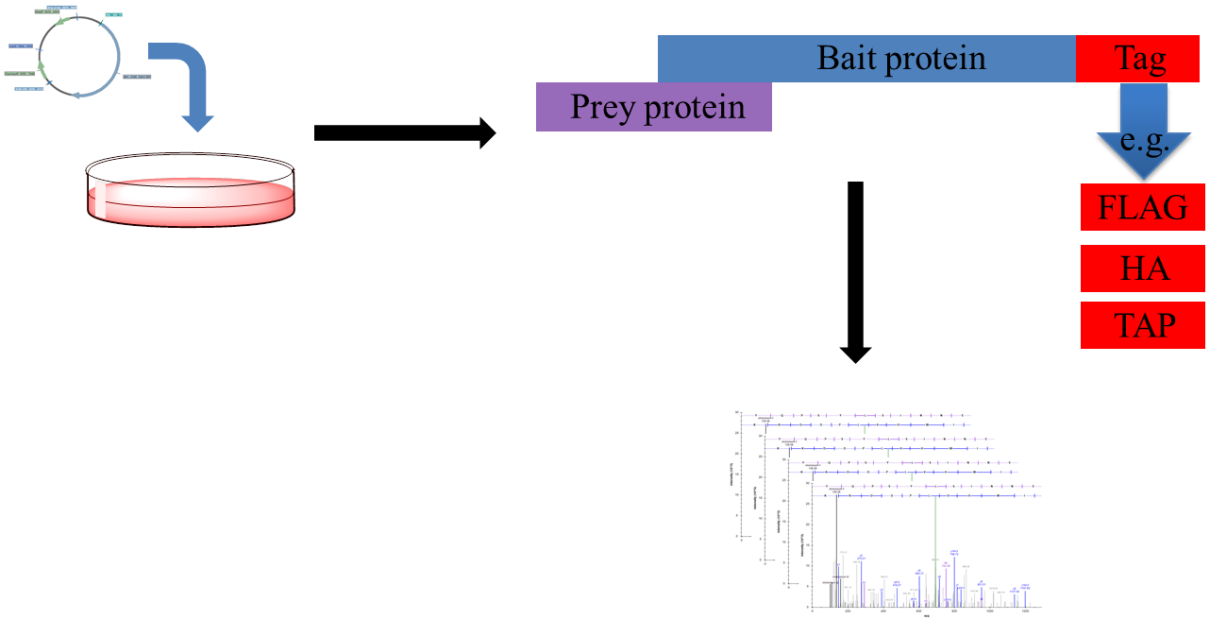


**Figure I-8. General Scheme for an AP-MS experiment.** A tagged bait protein is expressed in cells and then interacting prey proteins are co-purified with the bait protein using the tag. Finally, the purified protein complexes are analyzed via mass spectrometry.

*AP-MS Data analysis and informatics*

One major drawback to an AP-MS experiment is that there are many false positive interactions represented in the inventories obtained in AP-MS analyses. These false positives come from a variety of sources (Fig. I-9) (197). Confidently excluding these while still maintaining high accuracy for the true positive prey proteins is challenging. Initially, false positives could only be managed by carefully designing the affinity purification steps to minimize contaminant proteins and by using negative control experiments to generate a list of proteins to exclude from the final analysis (197). While certainly necessary, these methods are not sufficient on their own to eliminate all of the false positives and often are too stringent – resulting in the removal of true protein-protein interactions that are present in the control at a much lower level.

Recently, there have been several algorithms published that were designed to assign confidence values to AP-MS results by taking advantage of the inherent quantitative data present in MS experiments (186, 198-203). The most widely used of these algorithms is called Significance Analysis of INTeractome (SAINT) and was designed by the Nesvizhskii group (201). SAINT works by comparing spectral count or MS1 intensity distributions from negative control purifications (samples lacking the tagged bait protein that are passed through the full sample workup procedure) to the distributions from the bait purifications and then calculates the probability that each prey is a true interactor with each bait (201, 202). This then allows the user to filter their AP-MS data by a confidence value, which eliminates most of the false positives. A web-based version of this technology was also created along with a pre-populated database

of hundreds of negative control experiments for a variety of conditions to allow anyone to perform a SAINT analysis, even if they did not have their own control data (204).

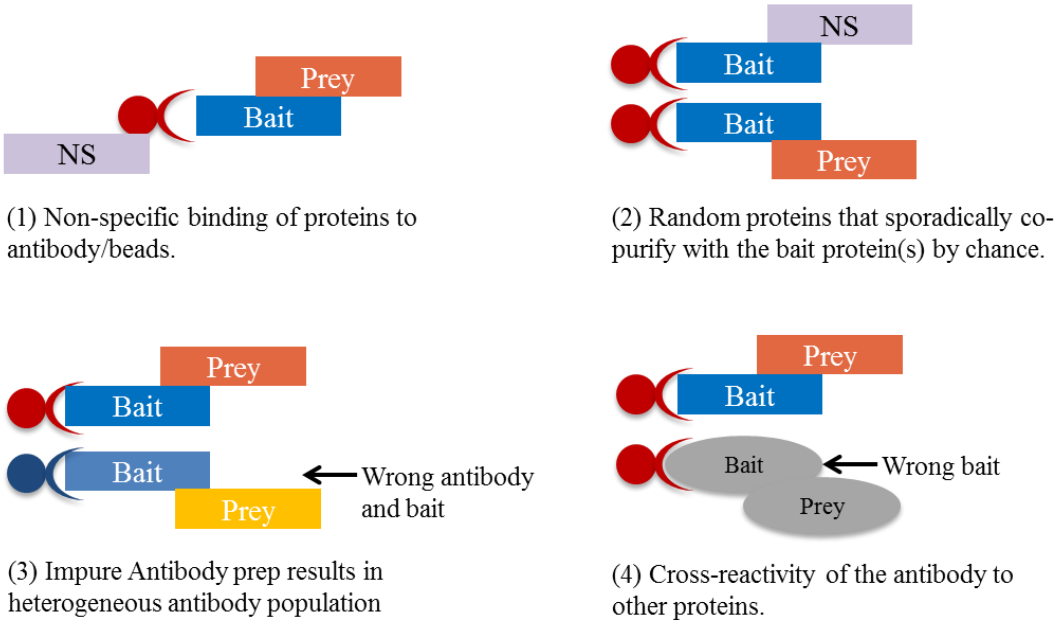


**Figure I-9. Sources of false positive identifications in AP-MS studies.** NS = Non-specific interaction.

*MS-based protein-protein interactions for ASK1*

Only a few mass spectrometry-based studies have reported ASK1 protein-protein interactions and none of them were focused on ASK1. In one study, ASK1 was found to interact with anaplastic lymphoma receptor tyrosine kinase (ALK) via a one-dimensional SDS page LC-MS/MS method (205). Another paper reported a system-wide autophagy study and found ASK1 associated with PRKAA2 and PRKAB2 (206). Finally, a more recent study performed an overexpression-based protein-protein interaction study for over 100 kinases and identified ATPase family, AAA domain containing 3A (ATAD3A) and nucleus accumbens associated 1, BEN and BTB (POZ) domain containing (NACC1) as ASK1 interactors (207).

## Targeted Protein Quantitation

*Parallel Reaction Monitoring (PRM)*

As discussed above, a shotgun MS analysis is the most common MS technique applied in an AP-MS experiment, but it is not the only method that can be used. Another approach is to follow affinity enrichment with a targeted MS analysis using multiple reaction monitoring (MRM) or parallel reaction monitoring (PRM) (208-213). This is not as commonly performed because AP-MS experiments are typically done as discovery experiments when interactions for a protein are not known. If, however, one does know what the interacting proteins for a particular bait protein of interest are, then a targeted assay can be performed to test hypotheses about how these interactions may change in response to various conditions. This MS analysis provides better

quantitation and fewer missing data points, since a particular set of peptides (representing the proteins of interest) are targeted with known elution times and MS/MS spectra.

In a PRM assay, a peptide mixture is eluted off a column into a Q Exactive, where the precursor ion of interest is isolated in the first quadrupole and collected in the C-trap (179, 209). After a sufficient number of ions have been collected, they are fragmented in the HCD cell and then analyzed in the Orbitrap, where a complete MS/MS spectrum is collected (Fig. I-10) (209, 210, 214). After the data are collected, the fragment ions are extracted from the chromatogram and a peptide peak area is calculated. Comparison of this peptide peak area across conditions allows one to see whether the abundance of the targeted protein changes between samples (Fig. I-11). From this information, changes in protein-protein interaction with changing conditions can be inferred. If peptide standards that include lysine or arginine residues uniformly labelled with heavy isotopes (stable isotope dilution – SID) are included in the experiment, then absolute quantitation of the peptides and stoichiometric calculations of the protein-protein interactions can be performed (208, 215-218).

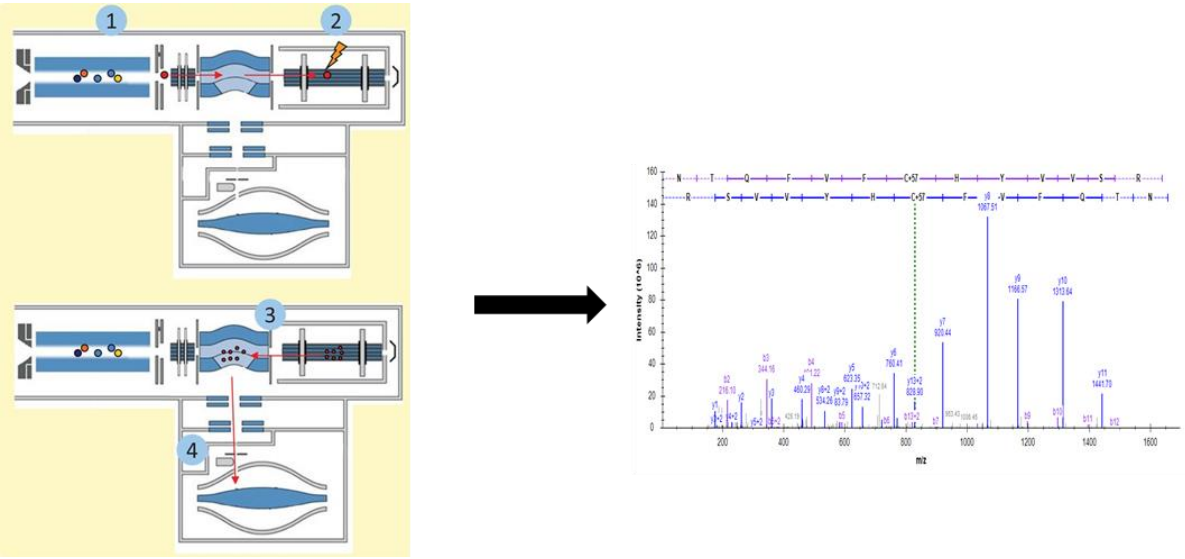


**Figure I-10. PRM method in a Q Exactive.** (1) Targeted peptides are isolated by Q1. (2) Isolated peptides are fragmented in the HCD collision cell. (3) Fragment ions are transferred back into the C-trap. (4) Fragment ions are analyzed in tandem by the Orbitrap and an MS2 spectrum is recorded. Figure adapted from Gallien *et al*. *Mol Cell Proteomics* 2012;11:1709-1723.

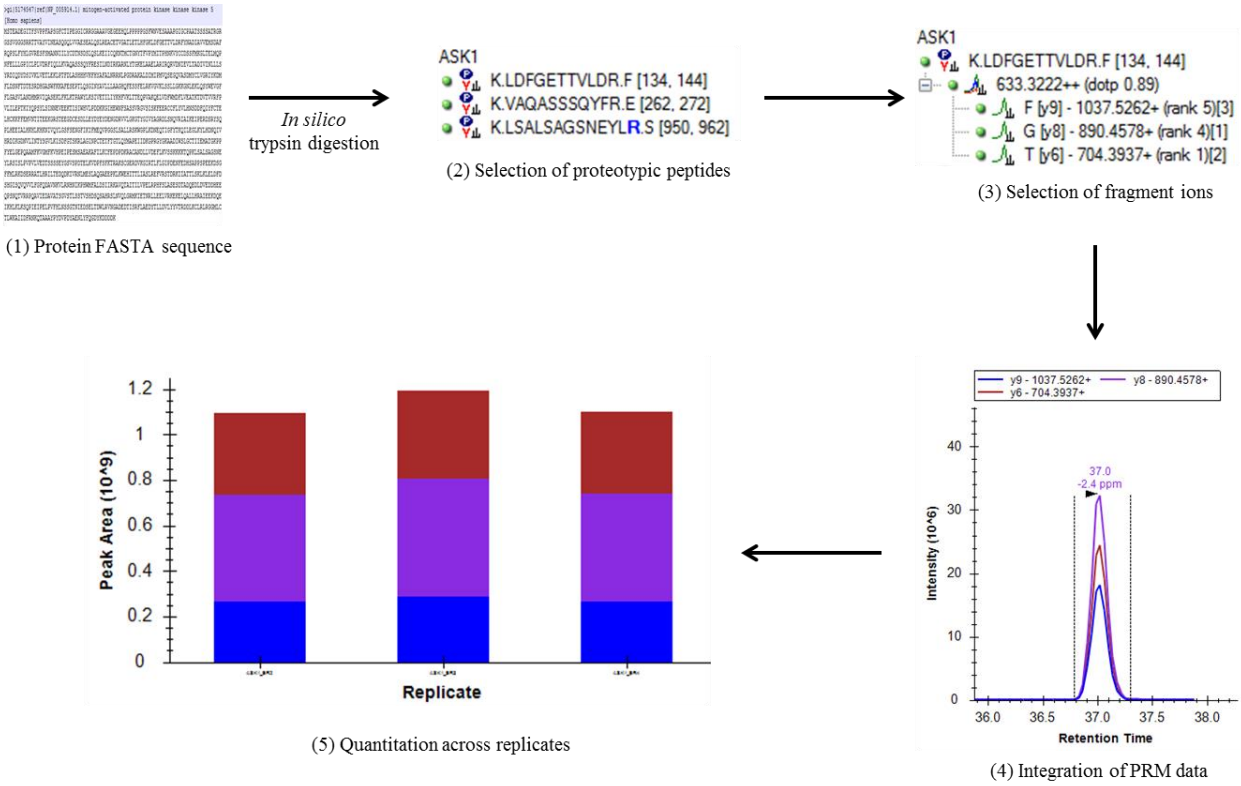


**Figure I-11. Development and analysis of PRM assay.** (1) Target protein FASTA sequence is acquired and digested with trypsin *in silico* (2) Proteotypic peptides of target protein are selected for PRM analysis (3) Peptide fragment ions are selected post-acquisition based on performance (4) The top three fragment ions are integrated across the dataset (5) Integrated peak areas are compared across runs

## Research Objectives and Approach

*Questions and objectives*

As discussed above, there are two major questions in the ASK1 field regarding its activation in response to diverse stress stimuli. The first deals with understanding how ASK1 is able to transduce several chemically distinct stressors into a single biological pathway response. The second question deals with the existence of the hypothesized signalosome as a unifying construct for all of the protein-protein interactions discussed above. The activation of ASK1 has primarily been studied using $H_2O_2$, but for the work presented in this dissertation, I chose to examine ASK1 activation in response to HNE, as it is a relevant, endogenously produced product of lipid oxidation that acts via a completely different mechanism than $H_2O_2$ and thus may present new mechanistic insight into the function and regulation of ASK1. Therefore, the specific questions that this dissertation addresses are: (1) what is the composition of the hypothesized ASK1 signalosome and how does this composition change in response to HNE stress and (2) how does ASK1 respond to alkylation stress by HNE?

I hypothesized that ASK1 or its complex members are modified by electrophiles (represented by HNE), resulting in pathway activation and formation of a consensus post-activation signalosome, along with a change in the phosphorylation pattern on ASK1. Chapter II discusses the application of mass spectrometry methodology to track the dynamic changes in the composition of the putative signalosome complex in response to HNE stress. Chapter III discusses the use of mass spectrometry to identify HNE adduction sites on ASK1 and how that adduction correlates with activation of the

ASK1 pathway and changes in the phosphorylation state of ASK1. The major aims of my dissertation research were:

1. Determine the consensus composition of the pre- and post-activation ASK signalosome in an over-expression and endogenous-expression cell model system.
2. Track the dynamics of the signalosome composition in response to an increasing concentration of HNE treatment.
3. Identify the sites of covalent HNE adduction on ASK1.
4. Map phosphorylation sites on ASK1 and correlate changes in site occupancy with HNE treatment and adduction.

A secondary goal of this research was to demonstrate the utility of AP-PRM for determining the stoichiometry of a protein complex and examining compositional changes in multiprotein complexes in response to stimuli. A discussion of using AP-PRM for these purposes compared to more traditional means is presented in chapter IV.

*Approach*

To test the hypothesis that ASK1 is modified by HNE, resulting in pathway activation and signalosome rearrangement, a suitable model system expressing ASK1 was developed and AP-PRM assays were performed to track changes in signalosome

composition in response to treatment. These studies are discussed in chapter II, in which three different components of the ASK1 signalosome were expressed in cells and the resulting AP-PRM data from these cell lines were combined to generate a comprehensive view of the changes in complex formation that occur as a result of HNE insult. These results were compared to a similar experiment performed in the context of endogenous expression of the ASK1 protein to verify the results. Additionally, in chapter III, immunopurified ASK1 treated with HNE was examined to identify and localize sites of HNE adduction at different HNE concentration levels. These adduction sites were compared with changes in phosphorylation at the same HNE concentrations in order to correlate the consequences of adduction with functional changes in ASK1. The phosphorylation changes in response to HNE were also compared to the changes in phosphorylation that occur on ASK1 in response to $H_2O_2$ and the HNE adduct sites were compared to sites of cysteine oxidation as a function of $H_2O_2$ treatment. This comparison allowed for a detailed look at how ASK1 differentially senses oxidative and electrophilic stress. All of these results together generated a view of how ASK1 responds to electrophile stress (modelled here with HNE) at both the PTM and protein-protein interaction level, which had been completely lacking in our understanding of this important system until now.

**Table I-1. ASK1 Protein-Protein Interaction Table**

| Protein | Regulation (POS/NEG) | Mechanism | Experimental Method(s) | Reference(s) |
|---|---|---|---|---|
| AKT1 | NEG | Phosphorylates ASK1 at Ser-83 | Co-IP Western, OE, Endog. | (85) |
| ALK | - | - | AP-MS | (205) |
| ARRB1 & ARRB2 | POS/NEG | Act as a scaffold to bring ASK1 into contact with CHIP for degradation and into contact with MAP2K4 and JNK for signaling in different contexts | Co-IP Western, OE, RNAi, Peptide array, Kinase assay | (108, 113, 114) |
| ASK1 | POS | Dimerizes and autophosphorylates itself | Co-IP Western | (31) |
| ASK2 | - | Forms heteromeric complex with ASK1. Conflicting reports on regulatory role. | Co-IP Western, OE, AP-MS, Y2H | (36, 71, 94-96, 207) |
| ASK3 | - | - | AP-MS | This study |
| ATAD3A | - | - | AP-MS | (207) |
| BIRC2 | NEG | Ubiquitinates ASK1 | Western, functional KD | (103) |
| CDC25A | NEG | Dephosphorylates ASK1 Thr-838 | Co-IP Western, OE, Endog., Functional. | (92) |
| CDKN1A | NEG | Binds to ASK1 and blocks rapamycin-induced stress | Co-IP Western, OE | (138) |
| CREBBP | - | - | Y2H | (219) |
| DAB2IP | POS | Scaffold protein that links ASK1 to TNF$\alpha$ receptor complex to enhance signaling | Co-IP Western, OE, functional KD | (89, 115-117) |
| DAXX | POS | Promotes ASK1 signaling, target of ASK1 | Co-IP Western, OE, IVK, ICC | (125-128, 146, 147) |
| DMD | - | - | Y2H | (219) |
| DUSP19 | POS | Scaffold protein that links ASK1 to MAP2K7 | Co-IP Western, OE, IVK | (119) |
| DYRK1A | POS | Promotes ASK1 signaling, may phosphorylate ASK1 | Co-IP Western, OE, IVK | (129) |
| EIF2AK2 | POS | Promotes ASK1 signaling | Co-IP Western, OE, IVK, ICC | (130) |
| EP300 | - | - | Y2H | (219) |
| GADD45B | - | Interacts with ASK1 | Co-IP Western, OE | (220) |
| GAPDH | - | Enhances ASK1 binding to SIAH1 | Co-IP Western, OE, Endog. | (145) |
| GEMIN5 | POS | Scaffold protein that links ASK1 to MAP2K4 and JNK | Co-IP Western, OE, IVK | (120) |

| Protein | Regulation (POS/NEG) | Mechanism | Experimental Method(s) | Reference(s) |
|---|---|---|---|---|
| GLRX | NEG | Inhibits ASK1 signaling | CO-IP Western, OE, IVK | (139) |
| GNA12 | POS | Promotes ASK1 activity | Co-IP Western, OE | (109, 110) |
| GNA13 | POS | Blocks ASK1-CHIP interaction, promotes ASK1 activity | Co-IP Western, OE | (109, 110) |
| GSTM1 | NEG | Inhibits ASK1, dissociates after heat shock | Co-IP Western, OE, IVK | (141) |
| HSPA1A/ HSPA4 | NEG | Disrupts ASK1 n-terminal homophilic interaction and works with CHIP as a co-E3 | Co-IP Western, OE, Endog, kinase assay | (100, 102) |
| HSP90AA1 | - | - | Identified in a HTS as an interactor | (221) |
| JAK2 | NEG | Phosphorylates ASK1 Y718 | Co-IP Western, OE, kinase assay | (84) |
| MAP2K3/6 | - | Target of ASK1 | Co-IP Western, OE, Endog., IVK | (27, 91, 136, 138, 142, 143) |
| MAP2K4/7 | - | Target of ASK1 | Co-IP Western, OE, Endog., IVK | (27, 113, 119-121, 126, 144) |
| MAP3K7 | NEG | Target of ASK1, inhibits ASK1 signaling | Co-IP Western, OE | (148, 149) |
| MAPK8IP3 | POS | Scaffold protein that links ASK1 to MAP2K4/7 and JNK | Co-IP Western, OE, Endog. | (121) |
| MCRS1 | NEG | Inhibits ASK1 activity | Co-IP Western, OE, Endog., ICC | (134) |
| NACC1 | - | - | AP-MS | (207) |
| NEDD4 | - | Ubiquitinates ASK1 | HTS, protein microarray | (106) |
| NEDD4L | - | Ubiquitinates ASK1 | HTS, protein microarray | (106) |
| PARK7 | NEG | Inhibits ASK1 activity | Co-IP Western, OE, IVK | (135, 136) |
| PDCD6 | NEG | Binds to ASK1 and translocates it to the nucleus | Co-IP Western, OE, ICC | (133) |
| PIM1 | NEG | Phosphorylates ASK1 Ser-83 | Co-IP Western. OE. Endog. | (86) |
| PPP5C | NEG | Dephosphorylates ASK1 Thr-838 | Co-IP Western Y2H, OE, ICC, Endog | (91) |
| PRDX1 | POS | May form a mixed-disulfide with ASK1 to transduce $H_2O_2$ signaling | Co-IP Western, OE | (222) |

| Protein | Regulation (POS/NEG) | Mechanism | Experimental Method(s) | Reference(s) |
|---|---|---|---|---|
| PRKAA2 | - | - | AP-MS | (206) |
| PRKAB2 | - | - | AP-MS | (206) |
| Proteasome | NEG | Degrades ASK1, but ASK1 can phosphorylate it and decrease activity | Co-IP Western, OE, functional. | (111) |
| PTPN11 | POS | Dephosphorylates ASK1 Y718 | Co-IP Western, OE | (84) |
| QARS | NEG | Binds to ASK1 in context of high glutamine environment and inhibits signaling | Co-IP Western, OE, IVK | (140) |
| RAF1 | NEG | Inhibits ASK1 | Co-IP Western, OE | (137) |
| RB1CC1 | POS | Scaffold protein that links ASK1 to TRAF2 | Co-IP Western, OE | (118) |
| RC3H2 | NEG | Ubiquitinates ASK1 | OE, Endog, Co-IP Western, HTS | (104) |
| SIAH1 | - | Target of ASK1 | Co-IP Western, OE, Endog. | (145) |
| SMN1 | - | ASK1 blocks ubiquitination of SMN1 | Co-IP Western, OE | (223) |
| SOCS1 | NEG | Promotes ASK1 degradation | OE, Co-IP western | (83, 107) |
| SOCS3 | NEG? | Promotes ASK1 degradation | OE, Co-IP western | (83) |
| STUB1 | NEG | Ubiquitinates ASK1 | Western, OE, *in vitro* system, functional KD | (100, 101) |
| TNFAIP3 | NEG | Promotes ASK1 degradation | OE, Co-IP western | (105) |
| TRAFs | POS | Promotes ASK1 activity | Co-IP Western, OE, Endog | (31, 54, 107, 118, 131, 132) |
| TRX | NEG | Binds to ASK1 N-terminus and inhibits activity. Promotes ubiquitination. | Y2H, Co-IP Western, OE | (31, 38, 97) |
| USP9X | POS | Deubiquitinates ASK1 and promotes protein stability | Co-IP Western, OE, Endog., Mutagenesis | (29) |
| 14-3-3 | NEG | Binds to ASK1 at pSer966 and blocks signaling. Acts as a bridge between ASK1 and ASK2 | Co-IP Western, OE, Endog. | (88, 96, 117, 122-124, 224) |

Table 1. Reported ASK signalosome member proteins and their regulation of ASK1. OE=Over Expression, Endog.= Endogenous expression, Co-IP – coimmunoprecipitation, Y2H = yeast two-hybrid, HTS=High Throughput Screen, AP-MS = Affinity Purification Mass Spectrometry, IVK = *in vitro* kinase assay, ICC = immunocytochemistry

## References


1. Nishikawa, T., Edelstein, D., Du, X. L., Yamagishi, S., Matsumura, T., Kaneda, Y., Yorek, M. A., Beebe, D., Oates, P. J., Hammes, H. P., Giardino, I., and Brownlee, M. (2000) Normalizing mitochondrial superoxide production blocks three pathways of hyperglycaemic damage. *Nature* 404, 787-790

2. Christen, Y. (2000) Oxidative stress and Alzheimer disease. *Am J Clin Nutr* 71, 621s-629s

3. Benzi, G., and Moretti, A. (1995) Are reactive oxygen species involved in Alzheimer's disease? *Neurobiol Aging* 16, 661-674

4. Cross, C. E., Halliwell, B., Borish, E. T., Pryor, W. A., Ames, B. N., Saul, R. L., McCord, J. M., and Harman, D. (1987) Oxygen radicals and human disease. *Ann Intern Med* 107, 526-545

5. Evans, J. L., Goldfine, I. D., Maddux, B. A., and Grodsky, G. M. (2003) Are oxidative stress-activated signaling pathways mediators of insulin resistance and beta-cell dysfunction? *Diabetes* 52, 1-8

6. Brownlee, M. (2001) Biochemistry and molecular cell biology of diabetic complications. *Nature* 414, 813-820

7. Lin, M. T., and Beal, M. F. (2006) Mitochondrial dysfunction and oxidative stress in neurodegenerative diseases. *Nature* 443, 787-795

8. Rodrigo, R., González, J., and Paoletto, F. (2011) The role of oxidative stress in the pathophysiology of hypertension. *Hypertension Research* 34, 431-440

9. Förstermann, U. (2008) Oxidative stress in vascular disease: causes, defense mechanisms and potential therapies. *Nature Clinical Practice Cardiovascular Medicine* 5, 338-349

10. Sanyal, A. J. (2005) Mechanisms of Disease: pathogenesis of nonalcoholic fatty liver disease. *Nature Clinical Practice Gastroenterology & Hepatology* 2, 46-53

11. Zhao, Y., and Zhao, B. (2013) Oxidative Stress and the Pathogenesis of Alzheimer's Disease. *Oxid Med Cell Longev* 2013

12. Blesa, J., Trigo-Damas, I., Quiroga-Varela, A., and Jackson-Lewis, V. R. (2015) Oxidative stress and Parkinson's disease. *Front Neuroanat* 9, 91

13. Chiarugi, P., Taddei, M. L., and Giannoni, E. (2016) Principles of Redox Signaling. *Studies on Hepatic Disorders*, pp. 3-40, Springer International Publishing

14. Reczek, C. R., and Chandel, N. S. (2015) ROS-dependent signal transduction. *Curr Opin Cell Biol* 33, 8-13

15. West, J. D., and Marnett, L. J. (2006) Endogenous reactive intermediates as modulators of cell signaling and cell death. *Chem Res Toxicol* 19, 173-194

16. Schopfer, F. J., Cipollina, C., and Freeman, B. A. (2011) Formation and signaling actions of electrophilic lipids. *Chem Rev* 111, 5997-6021

17. Benedetti, A., Comporti, M., and Esterbauer, H. (1980) Identification of 4-hydroxynonenal as a cytotoxic product originating from the peroxidation of liver microsomal lipids. *Biochim Biophys Acta* 620, 281-296

18. Esterbauer, H., Schaur, R. J., and Zollner, H. (1991) Chemistry and biochemistry of 4-hydroxynonenal, malonaldehyde and related aldehydes. *Free Radic Biol Med* 11, 81-128

19. Sayre, L. M., Lin, D., Yuan, Q., Zhu, X., and Tang, X. (2006) Protein adducts generated from products of lipid oxidation: focus on HNE and one. *Drug Metab Rev* 38, 651-675

20. Carini, M., Aldini, G., and Facino, R. M. (2004) Mass spectrometry for detection of 4-hydroxy-trans-2-nonenal (HNE) adducts with peptides and proteins. *Mass Spectrom Rev* 23, 281-305

21. Xu, G., Liu, Y., Kansal, M. M., and Sayre, L. M. (1999) Rapid cross-linking of proteins by 4-ketoaldehydes and 4-hydroxy-2-alkenals does not arise from the lysine-derived monoalkylpyrroles. *Chem Res Toxicol* 12, 855-861

22. Liu, Z., Minkler, P. E., and Sayre, L. M. (2003) Mass spectroscopic characterization of protein modification by 4-hydroxy-2-(E)-nonenal and 4-oxo-2-(E)-nonenal. *Chem Res Toxicol* 16, 901-911

23. Tang, X., Sayre, L. M., and Tochtrop, G. P. (2011) A mass spectrometric analysis of 4-hydroxy-2-(E)-nonenal modification of cytochrome c. *J Mass Spectrom* 46, 290-297

24. Codreanu, S. G., Ullery, J. C., Zhu, J., Tallman, K. A., Beavers, W. N., Porter, N. A., Marnett, L. J., Zhang, B., and Liebler, D. C. (2014) Alkylation damage by lipid electrophiles targets functional protein systems. *Mol Cell Proteomics* 13, 849-859

25. Yang, J., Tallman, K. A., Porter, N. A., and Liebler, D. C. (2015) Quantitative chemoproteomics for site-specific analysis of protein alkylation by 4-hydroxy-2-nonenal in cells. *Anal Chem* 87, 2535-2541

26. Yang, J., Carroll, K. S., and Liebler, D. C. (2016) The Expanding Landscape of the Thiol Redox Proteome. *Mol Cell Proteomics* 15, 1-11

27. Ichijo, H., Nishida, E., Irie, K., ten Dijke, P., Saitoh, M., Moriguchi, T., Takagi, M., Matsumoto, K., Miyazono, K., and Gotoh, Y. (1997) Induction of apoptosis by ASK1, a mammalian MAPKKK that activates SAPK/JNK and p38 signaling pathways. *Science* 275, 90-94

28. Bunkoczi, G., Salah, E., Filippakopoulos, P., Fedorov, O., Muller, S., Sobott, F., Parker, S. A., Zhang, H., Min, W., Turk, B. E., and Knapp, S. (2007) Structural and functional characterization of the human protein kinase ASK1. *Structure* 15, 1215-1226

29. Nagai, H., Noguchi, T., Homma, K., Katagiri, K., Takeda, K., Matsuzawa, A., and Ichijo, H. (2009) Ubiquitin-like sequence in ASK1 plays critical roles in the recognition and stabilization by USP9X and oxidative stress-induced cell death. *Mol Cell* 36, 805-818

30. Tobiume, K., Saitoh, M., and Ichijo, H. (2002) Activation of apoptosis signal-regulating kinase 1 by the stress-induced activating phosphorylation of pre-formed oligomer. *J Cell Physiol* 191, 95-104

31. Fujino, G., Noguchi, T., Matsuzawa, A., Yamauchi, S., Saitoh, M., Takeda, K., and Ichijo, H. (2007) Thioredoxin and TRAF family proteins regulate reactive oxygen species-dependent activation of ASK1 through reciprocal modulation of the N-terminal homophilic interaction of ASK1. *Mol Cell Biol* 27, 8152-8163

32. Takeda, K., Noguchi, T., Naguro, I., and Ichijo, H. (2008) Apoptosis signal-regulating kinase 1 in stress and immune response. *Annu Rev Pharmacol Toxicol* 48, 199-225

33. Widmann, C., Gibson, S., Jarpe, M. B., and Johnson, G. L. (1999) Mitogen-activated protein kinase: conservation of a three-kinase module from yeast to human. *Physiol Rev* 79, 143-180

34. Kaji, T., Yoshida, S., Kawai, K., Fuchigami, Y., Watanabe, W., Kubodera, H., and Kishimoto, T. (2010) ASK3, a novel member of the apoptosis signal-regulating kinase family, is essential for stress-induced cell death in HeLa cells. *Biochem Biophys Res Commun* 395, 213-218

35. Naguro, I., Umeda, T., Kobayashi, Y., Maruyama, J., Hattori, K., Shimizu, Y., Kataoka, K., Kim-Mitsuyama, S., Uchida, S., Vandewalle, A., Noguchi, T., Nishitoh, H., Matsuzawa, A., Takeda, K., and Ichijo, H. (2012) ASK3 responds to osmotic stress and regulates blood pressure by suppressing WNK1-SPAK/OSR1 signaling in the kidney. *Nat Commun* 3, 1285

36. Takeda, K., Shimozono, R., Noguchi, T., Umeda, T., Morimoto, Y., Naguro, I., Tobiume, K., Saitoh, M., Matsuzawa, A., and Ichijo, H. (2007) Apoptosis signal-regulating kinase (ASK) 2 functions as a mitogen-activated protein kinase kinase kinase in a heteromeric complex with ASK1. *J Biol Chem* 282, 7522-7531

37. Hatai, T., Matsuzawa, A., Inoshita, S., Mochida, Y., Kuroda, T., Sakamaki, K., Kuida, K., Yonehara, S., Ichijo, H., and Takeda, K. (2000) Execution of apoptosis signal-regulating kinase 1 (ASK1)-induced apoptosis by the mitochondria-dependent caspase activation. *J Biol Chem* 275, 26576-26581

38. Saitoh, M., Nishitoh, H., Fujii, M., Takeda, K., Tobiume, K., Sawada, Y., Kawabata, M., Miyazono, K., and Ichijo, H. (1998) Mammalian thioredoxin is a direct inhibitor of apoptosis signal-regulating kinase (ASK) 1. *The EMBO journal* 17, 2596-2606

39. Matsuzawa, A., Saegusa, K., Noguchi, T., Sadamitsu, C., Nishitoh, H., Nagai, S., Koyasu, S., Matsumoto, K., Takeda, K., and Ichijo, H. (2005) ROS-dependent activation of the TRAF6-ASK1-p38 pathway is selectively required for TLR4-mediated innate immunity. *Nature immunology* 6, 587-592

40. Takeda, K., Matsuzawa, A., Nishitoh, H., Tobiume, K., Kishida, S., Ninomiya-Tsuji, J., Matsumoto, K., and Ichijo, H. (2004) Involvement of ASK1 in Ca2+-induced p38 MAP kinase activation. *EMBO reports* 5, 161-166

41. Nishitoh, H., Matsuzawa, A., Tobiume, K., Saegusa, K., Takeda, K., Inoue, K., Hori, S., Kakizuka, A., and Ichijo, H. (2002) ASK1 is essential for endoplasmic reticulum stress-induced neuronal cell death triggered by expanded polyglutamine repeats. *Genes & development* 16, 1345-1355

42. Lim, P. L., Liu, J., Go, M. L., and Boelsterli, U. A. (2008) The mitochondrial superoxide/thioredoxin-2/Ask1 signaling pathway is critically involved in troglitazone-induced cell injury to human hepatocytes. *Toxicol Sci* 101, 341-349

43. Usuki, F., Fujita, E., and Sasagawa, N. (2008) Methylmercury activates ASK1/JNK signaling pathways, leading to apoptosis due to both mitochondria- and endoplasmic reticulum (ER)-generated processes in myogenic cell lines. *Neurotoxicology* 29, 22-30

44. Nakagawa, H., Maeda, S., Hikiba, Y., Ohmae, T., Shibata, W., Yanai, A., Sakamoto, K., Ogura, K., Noguchi, T., Karin, M., Ichijo, H., and Omata, M. (2008) Deletion of apoptosis signal-regulating kinase 1 attenuates acetaminophen-induced liver injury by inhibiting c-Jun N-terminal kinase activation. *Gastroenterology* 135, 1311-1321

45. Shinkai, Y., Iwamoto, N., Miura, T., Ishii, T., Cho, A. K., and Kumagai, Y. (2012) Redox cycling of 1,2-naphthoquinone by thioredoxin1 through Cys32 and Cys35 causes inhibition of its catalytic activity and activation of ASK1/p38 signaling. *Chem Res Toxicol* 25, 1222-1230

46. Kuo, C. T., Chen, B. C., Yu, C. C., Weng, C. M., Hsu, M. J., Chen, C. C., Chen, M. C., Teng, C. M., Pan, S. L., Bien, M. Y., Shih, C. H., and Lin, C. H. (2009) Apoptosis signal-regulating kinase 1 mediates denbinobin-induced apoptosis in human lung adenocarcinoma cells. *J Biomed Sci* 16, 43

47. Kwon, M. J., Jeong, K. S., Choi, E. J., and Lee, B. H. (2003) 2,3,7,8-Tetrachlorodibenzo-p-dioxin (TCDD)-induced activation of mitogen-activated protein kinase signaling pathway in Jurkat T cells. *Pharmacol Toxicol* 93, 186-190

48. Myers, C. R., Myers, J. M., Kufahl, T. D., Forbes, R., and Szadkowski, A. (2011) The effects of acrolein on the thioredoxin system: implications for redox-sensitive signaling. *Mol Nutr Food Res* 55, 1361-1374

49. Pramanik, K. C., and Srivastava, S. K. (2012) Apoptosis signal-regulating kinase 1-thioredoxin complex dissociation by capsaicin causes pancreatic tumor growth suppression by inducing apoptosis. *Antioxid Redox Signal* 17, 1417-1432

50. Lee, K. W., Zhao, X., Im, J. Y., Grosso, H., Jang, W. H., Chan, T. W., Sonsalla, P. K., German, D. C., Ichijo, H., Junn, E., and Mouradian, M. M. (2012) Apoptosis signal-regulating kinase 1 mediates MPTP toxicity and regulates glial activation. *PLoS One* 7, e29935

51. Ouyang, M., and Shen, X. (2006) Critical role of ASK1 in the 6-hydroxydopamine-induced apoptosis in human neuroblastoma SH-SY5Y cells. *J Neurochem* 97, 234-244

52. Yang, W., Tiffany-Castiglioni, E., Koh, H. C., and Son, I. H. (2009) Paraquat activates the IRE1/ASK1/JNK cascade associated with apoptosis in human neuroblastoma SH-SY5Y cells. *Toxicol Lett* 191, 203-210

53. Tobiume, K., Matsuzawa, A., Takahashi, T., Nishitoh, H., Morita, K., Takeda, K., Minowa, O., Miyazono, K., Noda, T., and Ichijo, H. (2001) ASK1 is required for sustained activations of JNK/p38 MAP kinases and apoptosis. *EMBO reports* 2, 222-228

54. Nishitoh, H., Saitoh, M., Mochida, Y., Takeda, K., Nakano, H., Rothe, M., Miyazono, K., and Ichijo, H. (1998) ASK1 is essential for JNK/SAPK activation by TRAF2. *Mol Cell* 2, 389-395

55. Liu, H., Nishitoh, H., Ichijo, H., and Kyriakis, J. M. (2000) Activation of apoptosis signal-regulating kinase 1 (ASK1) by tumor necrosis factor receptor-associated factor 2 requires prior dissociation of the ASK1 inhibitor thioredoxin. *Molecular and cellular biology* 20, 2198-2208

56. Gotoh, Y., and Cooper, J. A. (1998) Reactive oxygen species- and dimerization-induced activation of apoptosis signal-regulating kinase 1 in tumor necrosis factor-alpha signal transduction. *J Biol Chem* 273, 17477-17482

57. Soh, Y., Jeong, K. S., Lee, I. J., Bae, M. A., Kim, Y. C., and Song, B. J. (2000) Selective activation of the c-Jun N-terminal protein kinase pathway during 4-hydroxynonenal-induced apoptosis of PC12 cells. *Molecular pharmacology* 58, 535-541

58. Rudolph, T. K., and Freeman, B. A. (2009) Transduction of redox signaling by electrophile-protein reactions. *Sci Signal* 2, re7

59. Ji, C., Kozak, K. R., and Marnett, L. J. (2001) IkappaB kinase, a molecular target for inhibition by 4-hydroxy-2-nonenal. *J Biol Chem* 276, 18223-18228

60. Levonen, A. L., Landar, A., Ramachandran, A., Ceaser, E. K., Dickinson, D. A., Zanoni, G., Morrow, J. D., and Darley-Usmar, V. M. (2004) Cellular mechanisms of redox cell signalling: role of cysteine modification in controlling antioxidant defences in response to electrophilic lipid oxidation products. *Biochem J* 378, 373-382

61. Ishii, T., Itoh, K., Ruiz, E., Leake, D. S., Unoki, H., Yamamoto, M., and Mann, G. E. (2004) Role of Nrf2 in the regulation of CD36 and stress protein expression in murine macrophages: activation by oxidatively modified LDL and 4-hydroxynonenal. *Circ Res* 94, 609-616

62. Pettazzoni, P., Ciamporcero, E., Medana, C., Pizzimenti, S., Dal Bello, F., Minero, V. G., Toaldo, C., Minelli, R., Uchida, K., Dianzani, M. U., Pili, R., and Barrera, G. (2011) Nuclear factor erythroid 2-related factor-2 activity controls 4-hydroxynonenal metabolism and activity in prostate cancer cells. *Free Radic Biol Med* 51, 1610-1618

63. Jung, K. A., and Kwak, M. K. (2013) Enhanced 4-hydroxynonenal resistance in KEAP1 silenced human colon cancer cells. *Oxid Med Cell Longev* 2013, 423965

64. Manning, A. M., and Davis, R. J. (2003) Targeting JNK for therapeutic benefit: from junk to gold? *Nat Rev Drug Discov* 2, 554-565

65. Lawrence, M. C., Jivan, A., Shao, C., Duan, L., Goad, D., Zaganjor, E., Osborne, J., McGlynn, K., Stippec, S., Earnest, S., Chen, W., and Cobb, M. H. (2008) The roles of MAPKs in disease. *Cell Res* 18, 436-442

66. Tabas, I., and Ron, D. (2011) Integrating the mechanisms of apoptosis induced by endoplasmic reticulum stress. *Nat Cell Biol* 13, 184-190

67. Berdichevsky, A., Guarente, L., and Bose, A. (2010) Acute oxidative stress can reverse insulin resistance by inactivation of cytoplasmic JNK. *J Biol Chem* 285, 21581-21589

68. Sekine, Y., Takeda, K., and Ichijo, H. (2006) The ASK1-MAP kinase signaling in ER stress and neurodegenerative diseases. *Curr Mol Med* 6, 87-97

69. Fujisawa, T., Takeda, K., and Ichijo, H. (2007) ASK family proteins in stress response and disease. *Mol Biotechnol* 37, 13-18

70. Kawarazaki, Y., Ichijo, H., and Naguro, I. (2014) Apoptosis signal-regulating kinase 1 as a therapeutic target. *Expert Opin Ther Targets* 18, 651-664

71. Iriyama, T., Takeda, K., Nakamura, H., Morimoto, Y., Kuroiwa, T., Mizukami, J., Umeda, T., Noguchi, T., Naguro, I., Nishitoh, H., Saegusa, K., Tobiume, K., Homma, T., Shimada, Y., Tsuda, H., Aiko, S., Imoto, I., Inazawa, J., Chida, K., Kamei, Y., Kozuma, S., Taketani, Y., Matsuzawa, A., and Ichijo, H. (2009) ASK1 and ASK2 differentially regulate the counteracting roles of apoptosis and inflammation in tumorigenesis. *Embo j* 28, 843-853

72. Hayakawa, Y., Hirata, Y., Nakagawa, H., Sakamoto, K., Hikiba, Y., Kinoshita, H., Nakata, W., Takahashi, R., Tateishi, K., Tada, M., Akanuma, M., Yoshida, H., Takeda, K., Ichijo, H., Omata, M., Maeda, S., and Koike, K. (2011) Apoptosis signal-regulating kinase 1 and cyclin D1 compose a positive feedback loop contributing to tumor growth in gastric cancer. *Proc Natl Acad Sci U S A* 108, 780-785

73. Hayakawa, Y., Hirata, Y., Sakitani, K., Nakagawa, H., Nakata, W., Kinoshita, H., Takahashi, R., Takeda, K., Ichijo, H., Maeda, S., and Koike, K. (2012) Apoptosis signal-regulating kinase-1 inhibitor as a potent therapeutic drug for the treatment of gastric cancer. *Cancer Sci* 103, 2181-2185

74. Song, J., Park, K. A., Lee, W. T., and Lee, J. E. (2014) Apoptosis signal regulating kinase 1 (ASK1): potential as a therapeutic target for Alzheimer's disease. *Int J Mol Sci* 15, 2119-2129

75. Kadowaki, H., Nishitoh, H., Urano, F., Sadamitsu, C., Matsuzawa, A., Takeda, K., Masutani, H., Yodoi, J., Urano, Y., Nagano, T., and Ichijo, H. (2005) Amyloid beta induces neuronal cell death through ROS-mediated ASK1 activation. *Cell Death Differ* 12, 19-24

76. Nishitoh, H., Kadowaki, H., Nagai, A., Maruyama, T., Yokota, T., Fukutomi, H., Noguchi, T., Matsuzawa, A., Takeda, K., and Ichijo, H. (2008) ALS-linked mutant SOD1 induces ER stress- and ASK1-dependent motor neuron death by targeting Derlin-1. *Genes Dev* 22, 1451-1464

77. Guo, X., Harada, C., Namekata, K., Matsuzawa, A., Camps, M., Ji, H., Swinnen, D., Jorand-Lebrun, C., Muzerelle, M., Vitte, P. A., Ruckle, T., Kimura, A., Kohyama, K., Matsumoto, Y., Ichijo, H., and Harada, T. (2010) Regulation of the severity of neuroinflammation and demyelination by TLR-ASK1-p38 pathway. *EMBO Mol Med* 2, 504-515

78. Okazaki, T., Higuchi, M., Takeda, K., Iwatsuki-Horimoto, K., Kiso, M., Miyagishi, M., Yanai, H., Kato, A., Yoneyama, M., Fujita, T., Taniguchi, T., Kawaoka, Y., Ichijo, H., and Gotoh, Y. (2015) The ASK family kinases differentially mediate induction of type I interferon and apoptosis during the antiviral response. *Sci Signal* 8, ra78

79. Bhattacharyya, A., Pathak, S., Basak, C., Law, S., Kundu, M., and Basu, J. (2003) Execution of macrophage apoptosis by Mycobacterium avium through apoptosis signal-regulating kinase 1/p38 mitogen-activated protein kinase signaling and caspase 8 activation. *J Biol Chem* 278, 26517-26525

80. Maruoka, S., Hashimoto, S., Gon, Y., Nishitoh, H., Takeshita, I., Asai, Y., Mizumura, K., Shimizu, K., Ichijo, H., and Horie, T. (2003) ASK1 regulates influenza virus infection-induced apoptotic cell death. *Biochem Biophys Res Commun* 307, 870-876

81. Geleziunas, R., Xu, W., Takeda, K., Ichijo, H., and Greene, W. C. (2001) HIV-1 Nef inhibits ASK1-dependent death signalling providing a potential mechanism for protecting the infected host cell. *Nature* 410, 834-838

82. Miyakawa, K., Matsunaga, S., Kanou, K., Matsuzawa, A., Morishita, R., Kudoh, A., Shindo, K., Yokoyama, M., Sato, H., Kimura, H., Tamura, T., Yamamoto, N., Ichijo, H., Takaori-Kondo, A., and Ryo, A. (2015) ASK1 restores the antiviral activity of APOBEC3G by disrupting HIV-1 Vif-mediated counteraction. *Nat Commun* 6, 6945

83. He, Y., Zhang, W., Zhang, R., Zhang, H., and Min, W. (2006) SOCS1 inhibits tumor necrosis factor-induced activation of ASK1-JNK inflammatory signaling by mediating ASK1 degradation. *J Biol Chem* 281, 5559-5566

84. Yu, L., Min, W., He, Y., Qin, L., Zhang, H., Bennett, A. M., and Chen, H. (2009) JAK2 and SHP2 reciprocally regulate tyrosine phosphorylation and stability of proapoptotic protein ASK1. *J Biol Chem* 284, 13481-13488

85. Kim, A. H., Khursigara, G., Sun, X., Franke, T. F., and Chao, M. V. (2001) Akt phosphorylates and negatively regulates apoptosis signal-regulating kinase 1. *Molecular and cellular biology* 21, 893-901

86. Gu, J. J., Wang, Z., Reeves, R., and Magnuson, N. S. (2009) PIM1 phosphorylates and negatively regulates ASK1-mediated apoptosis. *Oncogene* 28, 4261-4271

87. Seong, H. A., Jung, H., Ichijo, H., and Ha, H. (2010) Reciprocal negative regulation of PDK1 and ASK1 signaling by direct interaction and phosphorylation. *J Biol Chem* 285, 2397-2414

88. Goldman, E. H., Chen, L., and Fu, H. (2004) Activation of apoptosis signal-regulating kinase 1 by reactive oxygen species through dephosphorylation at serine 967 and 14-3-3 dissociation. *J Biol Chem* 279, 10442-10449

89. Min, W., Lin, Y., Tang, S., Yu, L., Zhang, H., Wan, T., Luhn, T., Fu, H., and Chen, H. (2008) AIP1 recruits phosphatase PP2A to ASK1 in tumor necrosis factor-induced ASK1-JNK activation. *Circ Res* 102, 840-848

90. Fujii, K., Goldman, E. H., Park, H. R., Zhang, L., Chen, J., and Fu, H. (2004) Negative control of apoptosis signal-regulating kinase 1 through phosphorylation of Ser-1034. *Oncogene* 23, 5099-5104

91. Morita, K., Saitoh, M., Tobiume, K., Matsuura, H., Enomoto, S., Nishitoh, H., and Ichijo, H. (2001) Negative feedback regulation of ASK1 by protein phosphatase 5 (PP5) in response to oxidative stress. *The EMBO journal* 20, 6028-6036

92. Cho, Y. C., Park, J. E., Park, B. C., Kim, J. H., Jeong, D. G., Park, S. G., and Cho, S. (2015) Cell cycle-dependent Cdc25C phosphatase determines cell survival by regulating apoptosis signal-regulating kinase 1. *Cell Death Differ*

93. Noguchi, T., Takeda, K., Matsuzawa, A., Saegusa, K., Nakano, H., Gohda, J., Inoue, J., and Ichijo, H. (2005) Recruitment of tumor necrosis factor receptor-associated factor family proteins to apoptosis signal-regulating kinase 1 signalosome is essential for oxidative stress-induced cell death. *J Biol Chem* 280, 37033-37040

94. Wang, X. S., Diener, K., Tan, T. H., and Yao, Z. (1998) MAPKKK6, a novel mitogen-activated protein kinase kinase kinase, that associates with MAPKKK5. *Biochem Biophys Res Commun* 253, 33-37

95. Ortner, E., and Moelling, K. (2007) Heteromeric complex formation of ASK2 and ASK1 regulates stress-induced signaling. *Biochem Biophys Res Commun* 362, 454-459

96. Cockrell, L. M., Puckett, M. C., Goldman, E. H., Khuri, F. R., and Fu, H. (2010) Dual engagement of 14-3-3 proteins controls signal relay from ASK2 to the ASK1 signalosome. *Oncogene* 29, 822-830

97. Liu, Y., and Min, W. (2002) Thioredoxin promotes ASK1 ubiquitination and degradation to inhibit ASK1-mediated apoptosis in a redox activity-independent manner. *Circulation research* 90, 1259-1266

98. Pickart, C. M., and Eddins, M. J. (2004) Ubiquitin: structures, functions, mechanisms. 1695, 55–72

99. Clague, M. J., Heride, C., and Urbe, S. (2015) The demographics of the ubiquitin system. *Trends Cell Biol* 25, 417-426

100. Gao, Y., Han, C., Huang, H., Xin, Y., Xu, Y., Luo, L., and Yin, Z. (2010) Heat shock protein 70 together with its co-chaperone CHIP inhibits TNF-alpha induced apoptosis by promoting proteasomal degradation of apoptosis signal-regulating kinase1. *Apoptosis* 15, 822-833

101. Hwang, J. R., Zhang, C., and Patterson, C. (2005) C-terminus of heat shock protein 70-interacting protein facilitates degradation of apoptosis signal-regulating kinase 1 and inhibits apoptosis signal-regulating kinase 1-dependent apoptosis. *Cell Stress Chaperones* 10, 147-156

102. Park, H. S., Cho, S. G., Kim, C. K., Hwang, H. S., Noh, K. T., Kim, M. S., Huh, S. H., Kim, M. J., Ryoo, K., Kim, E. K., Kang, W. J., Lee, J. S., Seo, J. S., Ko, Y. G., Kim, S., and Choi, E. J. (2002) Heat shock protein hsp72 is a negative regulator of apoptosis signal-regulating kinase 1. *Mol Cell Biol* 22, 7721-7730

103. Zhao, Y., Conze, D. B., Hanover, J. A., and Ashwell, J. D. (2007) Tumor necrosis factor receptor 2 signaling induces selective c-IAP1-dependent ASK1 ubiquitination and terminates mitogen-activated protein kinase signaling. *J Biol Chem* 282, 7777-7782

104. Maruyama, T., Araki, T., Kawarazaki, Y., Naguro, I., Heynen, S., Aza-Blanc, P., Ronai, Z., Matsuzawa, A., and Ichijo, H. (2014) Roquin-2 promotes ubiquitin-mediated degradation of ASK1 to regulate stress responses. *Sci Signal* 7, ra8

105. Won, M., Park, K. A., Byun, H. S., Sohn, K. C., Kim, Y. R., Jeon, J., Hong, J. H., Park, J., Seok, J. H., Kim, J. M., Yoon, W. H., Jang, I. S., Shen, H. M., Liu, Z. G., and Hur, G. M. (2010) Novel anti-apoptotic mechanism of A20 through targeting ASK1 to suppress TNF-induced JNK activation. *Cell Death Differ* 17, 1830-1841

106. Persaud, A., Alberts, P., Amsen, E. M., Xiong, X., Wasmuth, J., Saadon, Z., Fladd, C., Parkinson, J., and Rotin, D. (2009) Comparison of substrate specificity of the ubiquitin ligases Nedd4 and Nedd4-2 using proteome arrays. *Mol Syst Biol* 5, 333

107. Kolliputi, N., and Waxman, A. B. (2009) IL-6 cytoprotection in hyperoxic acute lung injury occurs via suppressor of cytokine signaling-1-induced apoptosis signal-regulating kinase-1 degradation. *Am J Respir Cell Mol Biol* 40, 314-324

108. Zhang, Z., Hao, J., Zhao, Z., Ben, P., Fang, F., Shi, L., Gao, Y., Liu, J., Wen, C., Luo, L., and Yin, Z. (2009) beta-Arrestins facilitate ubiquitin-dependent degradation of apoptosis signal-regulating kinase 1 (ASK1) and attenuate H2O2-induced apoptosis. *Cell Signal* 21, 1195-1206

109. Kutuzov, M. A., Andreeva, A. V., and Voyno-Yasenetskaya, T. A. (2007) Regulation of apoptosis signal-regulating kinase 1 degradation by G alpha13. *Faseb j* 21, 3727-3736

110. Berestetskaya, Y. V., Faure, M. P., Ichijo, H., and Voyno-Yasenetskaya, T. A. (1998) Regulation of apoptosis by alpha-subunits of G12 and G13 proteins via apoptosis signal-regulating kinase-1. *J Biol Chem* 273, 27816-27823

111. Um, J. W., Im, E., Park, J., Oh, Y., Min, B., Lee, H. J., Yoon, J. B., and Chung, K. C. (2010) ASK1 negatively regulates the 26 S proteasome. *J Biol Chem* 285, 36434-36446

112. Schneider, J. R., Lodolce, J. P., and Boone, D. L. (2013) An Ubiquitin-like Motif in ASK1 Mediates its Association with and Inhibition of the Proteasome. *J Biochem Pharmacol Res* 1, 161-167

113. McDonald, P. H., Chow, C. W., Miller, W. E., Laporte, S. A., Field, M. E., Lin, F. T., Davis, R. J., and Lefkowitz, R. J. (2000) Beta-arrestin 2: a receptor-regulated MAPK scaffold for the activation of JNK3. *Science* 290, 1574-1577

114. Li, X., MacLeod, R., Dunlop, A. J., Edwards, H. V., Advant, N., Gibson, L. C., Devine, N. M., Brown, K. M., Adams, D. R., Houslay, M. D., and Baillie, G. S. (2009) A scanning peptide array approach uncovers association sites within the JNK/beta arrestin signalling complex. *FEBS Lett* 583, 3310-3316

115. Zhang, H., Zhang, R., Luo, Y., D'Alessio, A., Pober, J. S., and Min, W. (2004) AIP1/DAB2IP, a novel member of the Ras-GAP family, transduces TRAF2-induced ASK1-JNK activation. *J Biol Chem* 279, 44955-44965

116. Xie, D., Gore, C., Zhou, J., Pong, R. C., Zhang, H., Yu, L., Vessella, R. L., Min, W., and Hsieh, J. T. (2009) DAB2IP coordinates both PI3K-Akt and ASK1 pathways for cell survival and apoptosis. *Proc Natl Acad Sci U S A* 106, 19878-19883

117. Zhang, R., He, X., Liu, W., Lu, M., Hsieh, J. T., and Min, W. (2003) AIP1 mediates TNF-alpha-induced ASK1 activation by facilitating dissociation of ASK1 from its inhibitor 14-3-3. *J Clin Invest* 111, 1933-1943

118. Gan, B., Peng, X., Nagy, T., Alcaraz, A., Gu, H., and Guan, J. L. (2006) Role of FIP200 in cardiac and liver development and its regulation of TNFalpha and TSC-mTOR signaling pathways. *J Cell Biol* 175, 121-133

119. Zama, T., Aoki, R., Kamimoto, T., Inoue, K., Ikeda, Y., and Hagiwara, M. (2002) Scaffold role of a mitogen-activated protein kinase phosphatase, SKRP1, for the JNK signaling pathway. *J Biol Chem* 277, 23919-23926

120. Kim, E. K., Noh, K. T., Yoon, J. H., Cho, J. H., Yoon, K. W., Dreyfuss, G., and Choi, E. J. (2007) Positive regulation of ASK1-mediated c-Jun NH(2)-terminal kinase signaling pathway by the WD-repeat protein Gemin5. *Cell Death Differ* 14, 1518-1528

121. Matsuura, H., Nishitoh, H., Takeda, K., Matsuzawa, A., Amagasa, T., Ito, M., Yoshioka, K., and Ichijo, H. (2002) Phosphorylation-dependent scaffolding role of JSAP1/JIP3 in the ASK1-JNK signaling pathway. A new mode of regulation of the MAP kinase cascade. *J Biol Chem* 277, 40703-40709

122. Subramanian, R. R., Zhang, H., Wang, H., Ichijo, H., Miyashita, T., and Fu, H. (2004) Interaction of apoptosis signal-regulating kinase 1 with isoforms of 14-3-3 proteins. *Exp Cell Res* 294, 581-591

123. Zhang, L., Chen, J., and Fu, H. (1999) Suppression of apoptosis signal-regulating kinase 1-induced cell death by 14-3-3 proteins. *Proc Natl Acad Sci U S A* 96, 8511-8515

124. Thandavarayan, R. A., Watanabe, K., Ma, M., Veeraveedu, P. T., Gurusamy, N., Palaniyandi, S. S., Zhang, S., Muslin, A. J., Kodama, M., and Aizawa, Y. (2008) 14-3-3 protein regulates Ask1 signaling and protects against diabetic cardiomyopathy. *Biochem Pharmacol* 75, 1797-1806

125. Chang, H. Y., Nishitoh, H., Yang, X., Ichijo, H., and Baltimore, D. (1998) Activation of apoptosis signal-regulating kinase 1 (ASK1) by the adapter protein Daxx. *Science* 281, 1860-1863

126. Song, J. J., and Lee, Y. J. (2004) Daxx deletion mutant (amino acids 501-625)-induced apoptosis occurs through the JNK/p38-Bax-dependent mitochondrial pathway. *J Cell Biochem* 92, 1257-1270

127. Junn, E., Taniguchi, H., Jeong, B. S., Zhao, X., Ichijo, H., and Mouradian, M. M. (2005) Interaction of DJ-1 with Daxx inhibits apoptosis signal-regulating kinase 1 activity and cell death. *Proc Natl Acad Sci U S A* 102, 9691-9696

128. Charette, S. J., Lavoie, J. N., Lambert, H., and Landry, J. (2000) Inhibition of Daxx-mediated apoptosis by heat shock protein 27. *Mol Cell Biol* 20, 7602-7612

129. Choi, H. K., and Chung, K. C. (2011) Dyrk1A Positively Stimulates ASK1-JNK Signaling Pathway during Apoptotic Cell Death. *Exp Neurobiol* 20, 35-44

130. Takizawa, T., Tatematsu, C., and Nakanishi, Y. (2002) Double-stranded RNA-activated protein kinase interacts with apoptosis signal-regulating kinase 1. Implications for apoptosis signaling pathways. *Eur J Biochem* 269, 6126-6132

131. Hoeflich, K. P., Yeh, W. C., Yao, Z., Mak, T. W., and Woodgett, J. R. (1999) Mediation of TNF receptor-associated factor effector functions by apoptosis signal-regulating kinase-1 (ASK1). *Oncogene* 18, 5814-5820

132. Wu, Y., Fan, Y., Xue, B., Luo, L., Shen, J., Zhang, S., Jiang, Y., and Yin, Z. (2006) Human glutathione S-transferase P1-1 interacts with TRAF2 and regulates TRAF2-ASK1 signals. *Oncogene* 25, 5787-5800

133. Hwang, I. S., Jung, Y. S., and Kim, E. (2002) Interaction of ALG-2 with ASK1 influences ASK1 localization and subsequent JNK activation. *FEBS Lett* 529, 183-187

134. Xu, M., Zhang, F., Da, L., Li, T., and Zhao, M. (2012) Microspherule protein 2 associates with ASK1 and acts as a negative regulator of stress-induced ASK1 activation. *FEBS Lett* 586, 1678-1686

135. Waak, J., Weber, S. S., Gorner, K., Schall, C., Ichijo, H., Stehle, T., and Kahle, P. J. (2009) Oxidizable residues mediating protein stability and cytoprotective interaction of DJ-1 with apoptosis signal-regulating kinase 1. *J Biol Chem* 284, 14245-14257

136. Mo, J. S., Jung, J., Yoon, J. H., Hong, J. A., Kim, M. Y., Ann, E. J., Seo, M. S., Choi, Y. H., and Park, H. S. (2010) DJ-1 modulates the p38 mitogen-activated protein kinase pathway through physical interaction with apoptosis signal-regulating kinase 1. *J Cell Biochem* 110, 229-237

137. Chen, J., Fujii, K., Zhang, L., Roberts, T., and Fu, H. (2001) Raf-1 promotes cell survival by antagonizing apoptosis signal-regulating kinase 1 through a MEK-ERK independent mechanism. *Proc Natl Acad Sci U S A* 98, 7783-7788

138. Huang, S., Shu, L., Dilling, M. B., Easton, J., Harwood, F. C., Ichijo, H., and Houghton, P. J. (2003) Sustained activation of the JNK cascade and rapamycin-induced apoptosis are suppressed by p53/p21(Cip1). *Mol Cell* 11, 1491-1501

139. Song, J. J., Rhee, J. G., Suntharalingam, M., Walsh, S. A., Spitz, D. R., and Lee, Y. J. (2002) Role of glutaredoxin in metabolic oxidative stress. Glutaredoxin as a sensor of oxidative stress mediated by H2O2. *J Biol Chem* 277, 46566-46575

140. Ko, Y. G., Kim, E. Y., Kim, T., Park, H., Park, H. S., Choi, E. J., and Kim, S. (2001) Glutamine-dependent antiapoptotic interaction of human glutaminyl-tRNA synthetase with apoptosis signal-regulating kinase 1. *J Biol Chem* 276, 6030-6036

141. Dorion, S., Lambert, H., and Landry, J. (2002) Activation of the p38 signaling pathway by heat shock involves the dissociation of glutathione S-transferase Mu from Ask1. *J Biol Chem* 277, 30792-30797

142. McLaughlin, N. J., Banerjee, A., Kelher, M. R., Gamboni-Robertson, F., Hamiel, C., Sheppard, F. R., Moore, E. E., and Silliman, C. C. (2006) Platelet-activating factor-induced clathrin-mediated endocytosis requires beta-arrestin-1 recruitment and activation of the p38 MAPK signalosome at the plasma membrane for actin bundle formation. *J Immunol* 176, 7039-7050

143. Takekawa, M., Tatebayashi, K., and Saito, H. (2005) Conserved docking site is essential for activation of mammalian MAP kinase kinases by specific MAP kinase kinase kinases. *Mol Cell* 18, 295-306

144. Ryoo, K., Huh, S. H., Lee, Y. H., Yoon, K. W., Cho, S. G., and Choi, E. J. (2004) Negative regulation of MEKK1-induced signaling by glutathione S-transferase Mu. *J Biol Chem* 279, 43589-43594

145. Tristan, C. A., Ramos, A., Shahani, N., Emiliani, F. E., Nakajima, H., Noeh, C. C., Kato, Y., Takeuchi, T., Noguchi, T., Kadowaki, H., Sedlak, T. W., Ishizuka, K., Ichijo, H., and Sawa, A. (2015) Role of apoptosis signal-regulating kinase 1 (ASK1) as an activator of the GAPDH-Siah1 stress-signaling cascade. *J Biol Chem* 290, 56-64

146. Ko, Y. G., Kang, Y. S., Park, H., Seol, W., Kim, J., Kim, T., Park, H. S., Choi, E. J., and Kim, S. (2001) Apoptosis signal-regulating kinase 1 controls the proapoptotic function of death-associated protein (Daxx) in the cytoplasm. *J Biol Chem* 276, 39103-39106

147. Fukuyo, Y., Kitamura, T., Inoue, M., Horikoshi, N. T., Higashikubo, R., Hunt, C. R., Usheva, A., and Horikoshi, N. (2009) Phosphorylation-dependent Lys63-linked polyubiquitination of Daxx is essential for sustained TNF-{alpha}-induced ASK1 activation. *Cancer Res* 69, 7512-7517

148. Mochida, Y., Takeda, K., Saitoh, M., Nishitoh, H., Amagasa, T., Ninomiya-Tsuji, J., Matsumoto, K., and Ichijo, H. (2000) ASK1 inhibits interleukin-1-induced NF-kappa B activity through disruption of TRAF6-TAK1 interaction. *J Biol Chem* 275, 32747-32752

149. Kim, S. Y., Shim, J. H., Chun, E., and Lee, K. Y. (2012) Reciprocal inhibition between the transforming growth factor-beta-activated kinase 1 (TAK1) and apoptosis signal-regulating kinase 1 (ASK1) mitogen-activated protein kinase kinase kinases and

its suppression by TAK1-binding protein 2 (TAB2), an adapter protein for TAK1. *J Biol Chem* 287, 3381-3391

150. Yamashita, M., and Fenn, J. B. (1984) Electrospray ion source. Another variation on the free-jet theme. *J. Phys. Chem* 88, 4451-4459

151. Fenn, J. B., Mann, M., Meng, C. K., Wong, S. F., and Whitehouse, C. M. (1989) Electrospray ionization for mass spectrometry of large biomolecules. *Science* 246, 64-71

152. Eng, J. K., McCormack, A. L., and Yates, J. R. (1994) An approach to correlate tandem mass spectral data of peptides with amino acid sequences in a protein database. *J Am Soc Mass Spectrom* 5, 976-989

153. Aebersold, R., and Mann, M. (2003) Mass spectrometry-based proteomics. *Nature* 422, 198-207

154. Zhang, B., Wang, J., Wang, X., Zhu, J., Liu, Q., Shi, Z., Chambers, M. C., Zimmerman, L. J., Shaddox, K. F., Kim, S., Davies, S. R., Wang, S., Wang, P., Kinsinger, C. R., Rivers, R. C., Rodriguez, H., Townsend, R. R., Ellis, M. J., Carr, S. A., Tabb, D. L., Coffey, R. J., Slebos, R. J., and Liebler, D. C. (2014) Proteogenomic characterization of human colon and rectal cancer. *Nature* 513, 382-387

155. Williamson, J. C., Edwards, A. V., Verano-Braga, T., Schwammle, V., Kjeldsen, F., Jensen, O. N., and Larsen, M. R. (2016) High-performance hybrid Orbitrap mass spectrometers for quantitative proteome analysis: observations and implications. *Proteomics*

156. Kelstrup, C. D., Jersie-Christensen, R. R., Batth, T. S., Arrey, T. N., Kuehn, A., Kellmann, M., and Olsen, J. V. (2014) Rapid and deep proteomes by faster sequencing on a benchtop quadrupole ultra-high-field Orbitrap mass spectrometer. *J Proteome Res* 13, 6187-6195

157. Richards, A. L., Hebert, A. S., Ulbrich, A., Bailey, D. J., Coughlin, E. E., Westphall, M. S., and Coon, J. J. (2015) One-hour proteome analysis in yeast. *Nat Protoc* 10, 701-714

158. Tabb, D. L., Fernando, C. G., and Chambers, M. C. (2007) MyriMatch: highly accurate tandem mass spectral peptide identification by multivariate hypergeometric analysis. *J Proteome Res* 6, 654-661

159. Kim, S., and Pevzner, P. A. (2014) MS-GF+ makes progress towards a universal database search tool for proteomics. *Nat Commun* 5, 5277

160. Dasari, S., Chambers, M. C., Slebos, R. J., Zimmerman, L. J., Ham, A. J., and Tabb, D. L. (2010) TagRecon: high-throughput mutation identification through sequence tagging. *J Proteome Res* 9, 1716-1726

161. Dasari, S., Chambers, M. C., Codreanu, S. G., Liebler, D. C., Collins, B. C., Pennington, S. R., Gallagher, W. M., and Tabb, D. L. (2011) Sequence tagging reveals unexpected modifications in toxicoproteomics. *Chem Res Toxicol* 24, 204-216

162. Tabb, D. L. (2015) The SEQUEST Family Tree. *J Am Soc Mass Spectrom*

163. Liu, H., Sadygov, R. G., and Yates, J. R., 3rd (2004) A model for random sampling and estimation of relative protein abundance in shotgun proteomics. *Anal Chem* 76, 4193-4201

164. Old, W. M., Meyer-Arendt, K., Aveline-Wolf, L., Pierce, K. G., Mendoza, A., Sevinsky, J. R., Resing, K. A., and Ahn, N. G. (2005) Comparison of label-free methods for quantifying human proteins by shotgun proteomics. *Mol Cell Proteomics* 4, 1487-1502

165. Schmelzle, K., and White, F. M. (2006) Phosphoproteomic approaches to elucidate cellular signaling networks. *Curr Opin Biotechnol* 17, 406-414

166. Junger, M. A., and Aebersold, R. (2014) Mass spectrometry-driven phosphoproteomics: patterning the systems biology mosaic. *Wiley Interdiscip Rev Dev Biol* 3, 83-112

167. Parker, R., Clifton-Bligh, R., and Molloy, M. P. (2014) Phosphoproteomics of MAPK inhibition in BRAF-mutated cells and a role for the lethal synergism of dual BRAF and CK2 inhibition. *Mol Cancer Ther* 13, 1894-1906

168. von Stechow, L., Francavilla, C., and Olsen, J. V. (2015) Recent findings and technological advances in phosphoproteomics for cells and tissues. *Expert Rev Proteomics* 12, 469-487

169. Li, J., Li, Q., Tang, J., Xia, F., Wu, J., and Zeng, R. (2015) Quantitative Phosphoproteomics Revealed Glucose-stimulated Responses of Islet Associated with Insulin Secretion. *J Proteome Res*

170. Humphrey, S. J., Azimifar, S. B., and Mann, M. (2015) High-throughput phosphoproteomics reveals in vivo insulin signaling dynamics. *Nat Biotechnol* 33, 990-995

171. Larance, M., and Lamond, A. I. (2015) Multidimensional proteomics for cell biology. *Nat Rev Mol Cell Biol* 16, 269-280

172. Doll, S., and Burlingame, A. L. (2015) Mass spectrometry-based detection and assignment of protein posttranslational modifications. *ACS Chem Biol* 10, 63-71

173. Kennedy, J. J., Yan, P., Zhao, L., Ivey, R. G., Voytovich, U. J., Moore, H. D., Lin, C., Pogosova-Agadjanyan, E. L., Stirewalt, D. L., Reding, K. W., Whiteaker, J. R., and Paulovich, A. G. (2016) Immobilized Metal Affinity Chromatography Coupled to Multiple

Reaction Monitoring Enables Reproducible Quantification of Phospho-signaling. *Mol Cell Proteomics* 15, 726-739

174. Huang, J., Wang, F., Ye, M., and Zou, H. (2014) Enrichment and separation techniques for large-scale proteomics analysis of the protein post-translational modifications. *J Chromatogr A* 1372C, 1-17

175. van der Mijn, J. C., Labots, M., Piersma, S. R., Pham, T. V., Knol, J. C., Broxterman, H. J., Verheul, H. M., and Jimenez, C. R. (2015) Evaluation of different phospho-tyrosine antibodies for label-free phosphoproteomics. *J Proteomics*

176. Wandinger, S. K., Lahortiga, I., Jacobs, K., Klammer, M., Jordan, N., Elschenbroich, S., Parade, M., Jacoby, E., Linders, J. T., Brehmer, D., Cools, J., and Daub, H. (2016) Quantitative Phosphoproteomics Analysis of ERBB3/ERBB4 Signaling. *PLoS One* 11, e0146100

177. Michalski, A., Damoc, E., Hauschild, J. P., Lange, O., Wieghaus, A., Makarov, A., Nagaraj, N., Cox, J., Mann, M., and Horning, S. (2011) Mass spectrometry-based proteomics using Q Exactive, a high-performance benchtop quadrupole Orbitrap mass spectrometer. *Mol Cell Proteomics* 10, M111.011015

178. Lee, Y. Y., Kim, H. P., Kang, M. J., Cho, B. K., Han, S. W., Kim, T. Y., and Yi, E. C. (2013) Phosphoproteomic analysis identifies activated MET-axis PI3K/AKT and MAPK/ERK in lapatinib-resistant cancer cell line. *Exp Mol Med* 45, e64

179. Scheltema, R. A., Hauschild, J. P., Lange, O., Hornburg, D., Denisov, E., Damoc, E., Kuehn, A., Makarov, A., and Mann, M. (2014) The Q Exactive HF, a Benchtop mass spectrometer with a pre-filter, high-performance quadrupole and an ultra-high-field Orbitrap analyzer. *Mol Cell Proteomics* 13, 3698-3708

180. Oppermann, F. S., Klammer, M., Bobe, C., Cox, J., Schaab, C., Tebbe, A., and Daub, H. (2013) Comparison of SILAC and mTRAQ quantification for phosphoproteomics on a quadrupole orbitrap mass spectrometer. *J Proteome Res* 12, 4089-4100

181. Olsen, J. V., Macek, B., Lange, O., Makarov, A., Horning, S., and Mann, M. (2007) Higher-energy C-trap dissociation for peptide modification analysis. *Nat Methods* 4, 709-712

182. Nichols, A. M., and White, F. M. (2009) Manual validation of peptide sequence and sites of tyrosine phosphorylation from MS/MS spectra. *Methods Mol Biol* 492, 143-160

183. Holman, J. D., Dasari, S., and Tabb, D. L. (2013) Informatics of protein and posttranslational modification detection via shotgun proteomics. *Methods Mol Biol* 1002, 167-179

184. Tabb, D. L., Friedman, D. B., and Ham, A. J. (2006) Verification of automated peptide identifications from proteomic tandem mass spectra. *Nat Protoc* 1, 2213-2222

185. Fritz, K. S., Kellersberger, K. A., Gomez, J. D., and Petersen, D. R. (2012) 4-HNE adduct stability characterized by collision-induced dissociation and electron transfer dissociation mass spectrometry. *Chem Res Toxicol* 25, 965-970

186. Armean, I. M., Lilley, K. S., and Trotter, M. W. (2013) Popular computational methods to assess multiprotein complexes derived from label-free affinity purification and mass spectrometry (AP-MS) experiments. *Mol Cell Proteomics* 12, 1-13

187. Ngounou Wetie, A. G., Sokolowska, I., Woods, A. G., Roy, U., Deinhardt, K., and Darie, C. C. (2014) Protein-protein interactions: switch from classical methods to proteomics and bioinformatics-based approaches. *Cell Mol Life Sci* 71, 205-228

188. Morris, J. H., Knudsen, G. M., Verschueren, E., Johnson, J. R., Cimermancic, P., Greninger, A. L., and Pico, A. R. (2014) Affinity purification-mass spectrometry and network analysis to understand protein-protein interactions. *Nat Protoc* 9, 2539-2554

189. Kohli, P., Bartram, M. P., Habbig, S., Pahmeyer, C., Lamkemeyer, T., Benzing, T., Schermer, B., and Rinschen, M. M. (2014) Label-free quantitative proteomic analysis of the YAP/TAZ interactome. *Am J Physiol Cell Physiol* 306, C805-818

190. Diner, B. A., Li, T., Greco, T. M., Crow, M. S., Fuesler, J. A., Wang, J., and Cristea, I. M. (2015) The functional interactome of PYHIN immune regulators reveals IFIX is a sensor of viral DNA. *Mol Syst Biol* 11, 787

191. Dong, Y., Yang, J., Ye, W., Wang, Y., Ye, C., Weng, D., Gao, H., Zhang, F., Xu, Z., and Lei, Y. (2015) Isolation of Endogenously Assembled RNA-Protein Complexes Using Affinity Purification Based on Streptavidin Aptamer S1. *Int J Mol Sci* 16, 22456-22472

192. Bernaudo, F., Monteleone, F., Mesuraca, M., Krishnan, S., Chiarella, E., Scicchitano, S., Cuda, G., Morrone, G., Bond, H. M., and Gaspari, M. (2015) Validation of a novel shotgun proteomic workflow for the discovery of protein-protein interactions: focus on ZNF521. *J Proteome Res* 14, 1888-1899

193. Dunham, W. H., Mullin, M., and Gingras, A. C. (2012) Affinity-purification coupled to mass spectrometry: basic principles and strategies. *Proteomics* 12, 1576-1590

194. Gingras, A. C., Gstaiger, M., Raught, B., and Aebersold, R. (2007) Analysis of protein complexes using mass spectrometry. *Nat Rev Mol Cell Biol* 8, 645-654

195. Huttlin, E. L., Ting, L., Bruckner, R. J., Gebreab, F., Gygi, M. P., Szpyt, J., Tam, S., Zarraga, G., Colby, G., Baltier, K., Dong, R., Guarani, V., Vaites, L. P., Ordureau, A., Rad, R., Erickson, B. K., Wuhr, M., Chick, J., Zhai, B., Kolippakkam, D., Mintseris, J., Obar, R. A., Harris, T., Artavanis-Tsakonas, S., Sowa, M. E., De Camilli, P., Paulo, J.

A., Harper, J. W., and Gygi, S. P. (2015) The BioPlex Network: A Systematic Exploration of the Human Interactome. *Cell* 162, 425-440

196. Varjosalo, M., Sacco, R., Stukalov, A., van Drogen, A., Planyavsky, M., Hauri, S., Aebersold, R., Bennett, K. L., Colinge, J., Gstaiger, M., and Superti-Furga, G. (2013) Interlaboratory reproducibility of large-scale human protein-complex analysis by standardized AP-MS. *Nat Methods* 10, 307-314

197. Li, K. W., Chen, N., Klemmer, P., Koopmans, F., Karupothula, R., and Smit, A. B. (2012) Identifying true protein complex constituents in interaction proteomics: the example of the DMXL2 protein complex. *Proteomics* 12, 2428-2432

198. Sowa, M. E., Bennett, E. J., Gygi, S. P., and Harper, J. W. (2009) Defining the human deubiquitinating enzyme interaction landscape. *Cell* 138, 389-403

199. Lavallee-Adam, M., Cloutier, P., Coulombe, B., and Blanchette, M. (2011) Modeling contaminants in AP-MS/MS experiments. *J Proteome Res* 10, 886-895

200. Goldfarb, D., Hast, B. E., Wang, W., and Major, M. B. (2014) Spotlite: web application and augmented algorithms for predicting co-complexed proteins from affinity purification--mass spectrometry data. *J Proteome Res* 13, 5944-5955

201. Choi, H., Larsen, B., Lin, Z. Y., Breitkreutz, A., Mellacheruvu, D., Fermin, D., Qin, Z. S., Tyers, M., Gingras, A. C., and Nesvizhskii, A. I. (2011) SAINT: probabilistic scoring of affinity purification-mass spectrometry data. *Nat Methods* 8, 70-73

202. Teo, G., Liu, G., Zhang, J., Nesvizhskii, A. I., Gingras, A. C., and Choi, H. (2014) SAINTexpress: improvements and additional features in Significance Analysis of INTeractome software. *J Proteomics* 100, 37-43

203. Jager, S., Cimermancic, P., Gulbahce, N., Johnson, J. R., McGovern, K. E., Clarke, S. C., Shales, M., Mercenne, G., Pache, L., Li, K., Hernandez, H., Jang, G. M., Roth, S. L., Akiva, E., Marlett, J., Stephens, M., D'Orso, I., Fernandes, J., Fahey, M., Mahon, C., O'Donoghue, A. J., Todorovic, A., Morris, J. H., Maltby, D. A., Alber, T., Cagney, G., Bushman, F. D., Young, J. A., Chanda, S. K., Sundquist, W. I., Kortemme, T., Hernandez, R. D., Craik, C. S., Burlingame, A., Sali, A., Frankel, A. D., and Krogan, N. J. (2012) Global landscape of HIV-human protein complexes. *Nature* 481, 365-370

204. Mellacheruvu, D., Wright, Z., Couzens, A. L., Lambert, J. P., St-Denis, N. A., Li, T., Miteva, Y. V., Hauri, S., Sardiu, M. E., Low, T. Y., Halim, V. A., Bagshaw, R. D., Hubner, N. C., Al-Hakim, A., Bouchard, A., Faubert, D., Fermin, D., Dunham, W. H., Goudreault, M., Lin, Z. Y., Badillo, B. G., Pawson, T., Durocher, D., Coulombe, B., Aebersold, R., Superti-Furga, G., Colinge, J., Heck, A. J., Choi, H., Gstaiger, M., Mohammed, S., Cristea, I. M., Bennett, K. L., Washburn, M. P., Raught, B., Ewing, R. M., Gingras, A. C., and Nesvizhskii, A. I. (2013) The CRAPome: a contaminant repository for affinity purification-mass spectrometry data. *Nat Methods* 10, 730-736

205. Crockett, D. K., Lin, Z., Elenitoba-Johnson, K. S., and Lim, M. S. (2004) Identification of NPM-ALK interacting proteins by tandem mass spectrometry. *Oncogene* 23, 2617-2629

206. Behrends, C., Sowa, M. E., Gygi, S. P., and Harper, J. W. (2010) Network organization of the human autophagy system. *Nature* 466, 68-76

207. So, J., Pasculescu, A., Dai, A. Y., Williton, K., James, A., Nguyen, V., Creixell, P., Schoof, E. M., Sinclair, J., Barrios-Rodiles, M., Gu, J., Krizus, A., Williams, R., Olhovsky, M., Dennis, J. W., Wrana, J. L., Linding, R., Jorgensen, C., Pawson, T., and Colwill, K. (2015) Integrative analysis of kinase networks in TRAIL-induced apoptosis provides a source of potential targets for combination therapy. *Sci Signal* 8, rs3

208. Schmidt, C., Lenz, C., Grote, M., Luhrmann, R., and Urlaub, H. (2010) Determination of protein stoichiometry within protein complexes using absolute quantification and multiple reaction monitoring. *Anal Chem* 82, 2784-2796

209. Gallien, S., Duriez, E., Crone, C., Kellmann, M., Moehring, T., and Domon, B. (2012) Targeted proteomic quantification on quadrupole-orbitrap mass spectrometer. *Mol Cell Proteomics* 11, 1709-1723

210. Peterson, A. C., Russell, J. D., Bailey, D. J., Westphall, M. S., and Coon, J. J. (2012) Parallel reaction monitoring for high resolution and high mass accuracy quantitative, targeted proteomics. *Mol Cell Proteomics* 11, 1475-1488

211. Kuhn, E., Wu, J., Karl, J., Liao, H., Zolg, W., and Guild, B. (2004) Quantification of C-reactive protein in the serum of patients with rheumatoid arthritis using multiple reaction monitoring mass spectrometry and 13C-labeled peptide standards. *Proteomics* 4, 1175-1186

212. Picotti, P., Bodenmiller, B., Mueller, L. N., Domon, B., and Aebersold, R. (2009) Full dynamic range proteome analysis of S. cerevisiae by targeted proteomics. *Cell* 138, 795-806

213. Anderson, L., and Hunter, C. L. (2006) Quantitative mass spectrometric multiple reaction monitoring assays for major plasma proteins. *Mol Cell Proteomics* 5, 573-588

214. Gallien, S., Bourmaud, A., Kim, S. Y., and Domon, B. (2014) Technical considerations for large-scale parallel reaction monitoring analysis. *J Proteomics* 100, 147-159

215. Kirkpatrick, D. S., Gerber, S. A., and Gygi, S. P. (2005) The absolute quantification strategy: a general procedure for the quantification of proteins and post-translational modifications. *Methods* 35, 265-273

216. Kuzyk, M. A., Smith, D., Yang, J., Cross, T. J., Jackson, A. M., Hardie, D. B., Anderson, N. L., and Borchers, C. H. (2009) Multiple reaction monitoring-based,

multiplexed, absolute quantitation of 45 proteins in human plasma. *Mol Cell Proteomics* 8, 1860-1877

217. Keshishian, H., Addona, T., Burgess, M., Mani, D. R., Shi, X., Kuhn, E., Sabatine, M. S., Gerszten, R. E., and Carr, S. A. (2009) Quantification of cardiovascular biomarkers in patient plasma by targeted mass spectrometry and stable isotope dilution. *Mol Cell Proteomics* 8, 2339-2349

218. Gerber, S. A., Rush, J., Stemman, O., Kirschner, M. W., and Gygi, S. P. (2003) Absolute quantification of proteins and phosphoproteins from cell lysates by tandem MS. *Proc Natl Acad Sci U S A* 100, 6940-6945

219. Bandyopadhyay, S., Chiang, C. Y., Srivastava, J., Gersten, M., White, S., Bell, R., Kurschner, C., Martin, C., Smoot, M., Sahasrabudhe, S., Barber, D. L., Chanda, S. K., and Ideker, T. (2010) A human MAP kinase interactome. *Nat Methods* 7, 801-805

220. Papa, S., Zazzeroni, F., Bubici, C., Jayawardena, S., Alvarez, K., Matsuda, S., Nguyen, D. U., Pham, C. G., Nelsbach, A. H., Melis, T., De Smaele, E., Tang, W. J., D'Adamio, L., and Franzoso, G. (2004) Gadd45 beta mediates the NF-kappa B suppression of JNK signalling by targeting MKK7/JNKK2. *Nat Cell Biol* 6, 146-153

221. Taipale, M., Krykbaeva, I., Koeva, M., Kayatekin, C., Westover, K. D., Karras, G. I., and Lindquist, S. (2012) Quantitative analysis of HSP90-client interactions reveals principles of substrate recognition. *Cell* 150, 987-1001

222. Jarvis, R. M., Hughes, S. M., and Ledgerwood, E. C. (2012) Peroxiredoxin 1 functions as a signal peroxidase to receive, transduce, and transmit peroxide signals in mammalian cells. *Free Radic Biol Med* 53, 1522-1530

223. Kwon, J. E., Kim, E. K., and Choi, E. J. (2011) Stabilization of the survival motor neuron protein by ASK1. *FEBS Lett* 585, 1287-1292

224. Zhang, H., Lin, Y., Li, J., Pober, J. S., and Min, W. (2007) RIP1-mediated AIP1 phosphorylation at a 14-3-3-binding site is critical for tumor necrosis factor-induced ASK1-JNK/p38 activation. *J Biol Chem* 282, 14788-14796

# CHAPTER II

# ASSEMBLY DYNAMICS AND STOICHIOMETRY OF THE APOPTOSIS SIGNAL-REGULATING KINASE (ASK) SIGNALOSOME IN RESPONSE TO ELECTROPHILE STRESS

## Introduction

As discussed in chapter 1, ASK1 is hypothesized to be regulated by a large multiprotein complex termed the ASK signalosome (1) where proteins dynamically assemble around ASK1 as either an inactive or active signaling complex [recently reviewed in (2)]. The exact composition of this complex has not yet been determined, but over 90 proteins have been identified as ASK1-interacting proteins (see Table I-1). These interacting proteins have most commonly been identified using co-immunoprecipitation (co-IP) and Western blot methods in ASK1-overexpressing cells. Thus, although the ASK1 system is currently best understood as a series of binary interactions, there is evidence that ASK1 exists in a high molecular mass "pre-activation" complex of ~1500 kDa that undergoes protein compositional or stoichiometric remodeling to form an even higher mass "post-activation" complex upon treatment with $H_2O_2$ (3).

The majority of the reported ASK1 protein-protein interactions have been investigated in the context of $H_2O_2$-mediated activation of the system but many other chemicals are known to activate ASK1 (1, 4-20). I chose to investigate the ASK1

system in the context of exposure to the lipid electrophile 4-hydroxy-2-nonenal (HNE), which is a physiologically relevant stressor generated endogenously under conditions of oxidative stress (21, 22) that I and others (5) have shown to be capable of activating the ASK1 pathway. Unlike the reversible oxidation caused by $H_2O_2$, electrophile stress is characterized by covalent (non-reversible) adduction of cellular nucleophiles, particularly protein Cys residues (21-24). Due to this mechanistic difference between $H_2O_2$-induced oxidative stress and HNE-induced electrophile stress, I reasoned that the mechanisms of ASK1 regulation may vary between these two stressors. Thus, studies of HNE-induced electrophile stress may reveal new insights into how the ASK system is able to respond to diverse stress signals.

To better define the molecular composition of the ASK system and its regulation in response to HNE, I used quantitative mass spectrometry to gain an “all components” view of ASK1-interacting proteins. I hypothesized that a subset of the previously reported ASK1-interacting proteins would constitute the ASK signalosome in unstressed cells and that the composition and stoichiometry of the complex would change in response to HNE stress. Here I report a systematic investigation of ASK signalosome components and the response of this signalosome to HNE treatment. I employed an affinity purification-mass spectrometry (AP-MS) approach with data-dependent shotgun liquid chromatography-tandem mass spectrometry (LC-MS/MS) and parallel reaction monitoring (PRM) methods to study four related cell models with both over-expression and endogenous expression of ASK1, ASK2, and ASK3 proteins.

## Experimental Procedures

*DNA constructs*

Tandem-tagged constructs for ASK1, ASK2, and ASK3 were generated in pcDNA3.1 plasmids (V790-20, Life Technologies, Grand Island, NY) from Genscript (Piscataway, NJ). The ASK1 sequence previously described (25) was modified by substituting the HA tag with a tandem HA-FLAG tag. Partial clones of ASK2 containing the catalytic portion of each protein (plasmid # 23853) and ASK3 (plasmid # 23499) were obtained from Addgene (Cambridge, MA) and were originally created by William Hahn & David Root (26). The missing gene fragments were synthesized by Genscript and a tandem tag sequence was added to each gene (HA-V5 for ASK2 and HA-Myc for ASK3). All three plasmids are available from Addgene (ASK1 - #69726, ASK2 - #69727, ASK3 - #69728).

*Antibodies*

Co-IPs of epitope-tagged proteins were performed with either EZview red anti-HA beads (Sigma-Aldrich, St. Louis, MO, E6779), EZview red anti-FLAG beads (Sigma-Aldrich, F2426), EZview red anti-Myc beads (Sigma-Aldrich, E6654), or Anti-V5 agarose affinity gel (Sigma-Aldrich, A7345). The endogenous ASK1 IPs were performed using sc-5294 AC (Santa Cruz Biotechnology, Dallas, TX).

ICC staining was performed with the following primary antibodies at 1:500 dilutions: Beta Tubulin (ab7792), V5 (ab9116), and Myc (ab9132) purchased from Abcam (Cambridge, MA); ASK1 (sc-5294) purchased from Santa Cruz Biotechnology;

HA (71-5500) purchased from Life Technologies (Carlsbad, CA); and FLAG (8146S) purchased from Cell Signaling Technology (Danvers, MA). Secondary staining for ICC was done with the following antibodies from Life Technologies at 1:500 dilutions: anti-rabbit 633 (A21071), anti-goat 546 (A11056), and anti-mouse 488 (A21202).

Western blots were performed with the following primary antibodies: FLAG (8146S), ASK1 phospo-T845 (3765S), JNK (9252S), phospho-JNK (4668S), p38 (9212S), and phospho-p38 (9211S) purchased from Cell Signaling Technology; ASK1 (sc-5294) purchased from Santa Cruz Biotechnology; ASK2 (ab99426) and ASK3 (ab76806) purchased from Abcam; and ATAD3A (H00055210-D01P) and ATAD3B (H00083858-B01P) purchased from Novus Biologicals (Littleton, CO). Secondary antibodies were from Life Technologies: anti-mouse 680 (A21058), anti-rabbit 680 (A21109), and anti-goat 680 (A21084).

*Cell lines and cell culture*

HEK-293 cells (CRL-1573, ATCC) were grown in DMEM (Life Technology, 12430) supplemented with 10% fetal bovine serum (Atlas Biologicals, Fort Collins, CO) at 37°C in a humidified atmosphere with 5% $CO_2$. ASK1, 2, and 3 expressing cell lines were generated from HEK-293 cells by transfecting the corresponding expression plasmids into cells using Lipofectamine 2000 (Life Technologies, 11668019) following the manufacturer's instructions. Twenty-four hours following transfection, cells were split 1:10 and after an additional 24 hr were switched into selection medium consisting of the HEK-293 medium described above supplemented with 1.5 mg/mL Geneticin (Life Technologies, 10131-027) and maintained in this medium for 2 weeks to select for cells

expressing the plasmid of interest. Stock cell cultures were maintained thereafter in HEK-293 media supplemented with 1mg/mL Geneticin. Prior to harvesting, cells were plated in 15 cm dishes in HEK-293 media supplemented with 0.5 mg/mL Geneticin.

All cell lines were treated prior to harvesting with ethanol (vehicle control, 0.08% v/v), 10 μM HNE, or 50 μM HNE. The three treatments were prepared in serum-free media and placed on the cells for 1 hr at 37°C. Cells were harvested with a cell scraper in the treatment medium and immediately centrifuged at 100 x g for 5 min at 4°C. Following this, the cell pellets were washed twice with ice cold phosphate buffered saline (PBS) and stored at -80°C until use.

For the ASK protein colocalization imaging studies, ASK1, ASK2, and ASK3 constructs were transiently co-transfected into HEK-293 cells using an Amaxa Nucleofector 2b (Lonza, Allendale, NJ) and the cell line Nucleofector Kit V (Lonza, VCA-1003) using the manufacturer's recommended HEK-293 electroporation protocol.

*RNA interference*

HEK-293 cells were plated in 10 cm dishes and transfected at 30% confluence using Lipofectamine RNAiMAX (Life Technologies, 13778-150) following the manufacturer's suggested protocol. Forty-eight hours after transfection, cells were split into two new 10 cm dishes. Twenty-four hours later, cells were harvested, washed twice in PBS, and frozen at -80°C until use. Anti-ASK1 Stealth siRNA duplexes with the following sequences: 5'-AAACAUUUCAGUAUGAAUGCCUUGG -3' and 5'-CCAAGGCAUUCAUACAAAAUGUUU-3' (Life Technologies) specific for ASK1 (with no overlapping targeting on ASK2 or ASK3) were used at a concentration of 10 nM.

Negative control siRNA (Life Technologies, 12935-300) designed for use with medium GC content Stealth siRNA was used at the same concentration.

*Immunocytochemistry*

Cells were plated in a 6-well plate at a density of 100,000 cells per well with five 12 mm glass coverslips in each well (Carolina Biological Supply, Burlington, NC, 633029). Three days later, the coverslips were washed once in PBS, fixed for 10 min at room temperature (RT) in 4% paraformaldehyde, blocked for 20 min at RT in 8% bovine serum albumin (BSA), washed twice with PBS and either stored at 4°C in PBS or used immediately for immunostaining.

Fixed cells were imaged with either a Zeiss (Thornwood, NY) LSM510 META inverted confocal microscope (for the triple transfection) or a Zeiss Axioplan microscope equipped with an Apotome optical sectioning slider (for sub-cellular localization) and acquired images were analyzed using ZEN software (Zeiss). For slides imaged with the Zeiss LSM510 META microscope, cells were permeabilized in 0.1% Triton X100 for 5 min at RT, washed once with PBS, incubated with primary antibody in 1% BSA for 1 hr at 37°C in a humidified chamber, washed once with PBS, incubated with secondary antibody in 1% BSA for 30 min at 37°C in a humidified chamber, washed twice with PBS, and then mounted onto a slide with Prolong Gold (Life Technologies, P-36931). For slides imaged with the Zeiss Axioplan microscope, cells were permeabilized in 0.1% Triton X100 for 5 min at RT, washed three times with PBS, incubated with primary antibody in 1% BSA overnight at 4°C, washed six times with PBS, incubated with

secondary antibody in 1% BSA for 1 hr at RT, washed five times with PBS, and then mounted using Prolong Gold onto glass slides (VWR, 48312-003).

*Cell viability assays*

Cells were plated in a 96-well plate at a density of 10,000 cells/well and allowed to grow for 24 hr. Medium was then removed and replaced with 100 μL/well of serum-free DMEM containing the appropriate concentration of HNE and the cells were incubated at 37°C for 24 hr. To measure cell viability, 10 μL/well of WST reagent (Sigma, 11644807001) was added and the cells were incubated for 1 hr. Absorbance readings then were taken at 450 nm and 650 nm with a Spectramax M4 spectrophotometer (Molecular Devices, Sunnyvale, CA) according to the manufacturer's protocol.

*Co-immunoprecipitation and western blotting*

Frozen cell pellets were lysed on ice in 500 μL of NETN buffer (50 mM HEPES pH 7.5, 150 mM NaCl, and 1% Igepal supplemented with 10 μL/mL of HALT [Life technologies, 78444] protease and phosphatase inhibitor), per 15 cm plate for 30 min with occasional inversion. Lysates then were clarified by centrifugation at 10,000 × g for 10 min at 4°C. Protein in the clarified lysates was measured with the BCA assay (Life Technology, 23225). Protein concentrations were adjusted to 2 mg/mL and 5 mg of total protein was added in a final volume of 2.5 mL to antibody beads pre-washed with NETN. For each IP, a 50 μL slurry of antibody-bead conjugate was washed twice with 1 mL of NETN prior to incubation with protein lysates. After addition of the protein lysate,

the beads were rotated at 4°C for 1 hr to allow for capture of the target protein. Following incubation, the beads were pelleted by centrifugation at 100 × g and the supernatant was discarded. The beads were then washed twice with 1 mL of NETN buffer and the bound protein complexes were resuspended in 80 μL of lithium dodecyl sulfate (LDS) sample buffer diluted 1:1 with NETN and supplemented with 50 mM dithiothreitol (DTT). The samples were then frozen at -80°C until use.

For western blot analysis, cell lysis and IP were carried out as described above. Gels were loaded with either 50 μg of input protein or 5 μL of IP and run for 50 min at a constant 180 V. Proteins were then electrophoretically transferred to PVDF membranes (Life Technology, LC2002) using the BioRad (Hercules, California) wet transfer system (1703930) operated at a constant 300 mA current for 90 min at 4°C. Membranes were blocked in a 1:1 mixture of Tris-buffered saline plus 0.05% Tween-20 (TBST) and blocking buffer (Rockland, Limerick, PA, MB-070) for 1 hr at RT while rocking. Primary antibodies were diluted (1:2000 for tag antibodies, 1:1000 for protein antibodies, and 1:750 for phospho antibodies) in the same buffer used for blocking, added to the membrane, and incubated at 4°C overnight with rocking. After incubation, the membranes were washed three times with TBST, incubated with the appropriate secondary antibody diluted 1:10,000 in the same buffer used for the primary antibody, and allowed to rock for 30 min at RT. The membranes were then washed three times with TBST, visualized using a LiCor Odyssey (Lincoln, Nebraska), and analyzed using Odyssey v3.0 software.

*Size exclusion chromatography of ASK complexes*

Size exclusion chromatography (SEC) was performed as described previously (3) with minor modifications (see supplemental Fig. A10A). For the IP-PRM assays, 6 column runs were pooled and each target fraction (1-9) was immunopurified following the procedure described above with the exception of the buffer which consisted of the SEC buffer supplemented with 10 μL/mL of HALT.

*Preparation of peptides for MS analyses*

Bead-bound protein complexes were eluted in LDS buffer and heated at 95°C for 10 min prior to being loaded on a 10% Bis-Tris gel (Life Technologies, NP0301). The gels were loaded with 35 μL of each sample elution in alternate lanes (with a blank lane between sample lanes) and then were run at a constant 180 V for 3 min, after which the run was paused. Each sample lane was then re-loaded with the remaining 35 μL of each sample and the gel runs were resumed for an additional 7 min to complete loading of proteins into the gel. Gels were then stained with Simply Blue safe stain (Life Technologies, LC6060) for 1 min in a microwave oven at maximum power and then allowed to destain in distilled water for 2-3 hr. Each sample lane was cut as a single band and diced into ~1 mm cubes. The gel pieces were placed into individual Eppendorf tubes and washed twice with 200 μL of 100 mM ammonium bicarbonate (AmBic). Samples were then reduced with 5 mM DTT in AmBic for 30 min at 60°C while shaking at 1000 rpm and then alkylated with 10 mM iodoacetamide in AmBic for 20 min in the dark at RT. Excess blue dye was then removed with three 200 μL washes in 50 mM AmBic:acetonitrile (1:1, v/v) and the gel pieces were dehydrated in 100%

acetonitrile. The gel pieces were rehydrated in 200 μL of 25 mM AmBic with 300 ng of trypsin gold (Promega, Madison, WI) per sample and placed in a 37°C incubator for 16 hr. Peptides were extracted from the SDS gel with three 20 min incubations in 200 μL of 60% acetonitrile / 40% water containing 1% formic acid and evaporated to dryness *in vacuo*. The peptides were resuspended in 30% acetonitrile / 70% water containing 0.1% formic acid and stored at -80°C until use. Labelled peptide standards for quantitative analyses (see below) were spiked in at this reconstitution step.

*Mass spectrometry*

Shotgun analyses of the single gel fraction samples were carried out on a Q Exactive Plus mass spectrometer (ThermoFisher Scientific, San Jose, CA) equipped with a Proxeon nLC1000 LC (ThermoFisher Scientific) and a Nanoflex source (ThermoFisher Scientific). Peptide mixtures were evaporated *in vacuo* and resuspended in 2% acetonitrile / 98% water containing 0.1% formic acid and loaded onto an 11 cm long column with a 75 μm internal diameter (New Objective, Woburn, MA, PF360-75-10-N-5) packed with 3 μm particle size and 120 Å pore size ReproSil-Pur C18-AQ resin (Dr. Maisch GmbH, Ammerbuch-Entringen, Germany) and separated over a 100 min gradient with a mobile phase containing aqueous acetonitrile and 0.1% formic acid programmed from 2-5% acetonitrile over 5 min, then 5 to 35% acetonitrile over 80 min, then 35-90% acetonitrile over 5 min, followed by 10 min at 90% acetonitrile, all at a flow rate of 300 nL/min. A single MS1 scan from *m/z* 300-1800 at 70,000 resolution with an automatic gain control (AGC) value of 3e6 and max injection time of 64 msec was recorded as profile data. A top 12 method was used, whereby the

12 most intense precursors were automatically chosen for MS2 analysis and a dynamic exclusion window of 20 sec was employed. For each MS2 scan, a resolution of 17,500, an AGC value of 2e5, a max injection time of 100 msec, a 2.0 *m/z* isolation window, and a normalized collision energy of 27 was used and centroid data were recorded.

PRM assays were also performed on the ThermoFisher Scientific Q Exactive Plus instrument and LC system described above. For PRM analyses, peptides were separated over a 70 min gradient: from 2-5% acetonitrile over 5 min, then 5 to 35% acetonitrile over 50 min, then 35-90% acetonitrile over 5 min, followed by 10 min at 90% acetonitrile, all at a flow rate of 300 nL/min. The PRM method consisted of an MS1 scan at 17,500 resolution with an AGC value of 3e6, max injection time of 64 msec, and scan range from *m/z* 380-1500 recorded as profile data. This was followed by 14 targeted MS2 scans at a resolution of 17,500 and with an AGC value of 5e5, a max injection time of 80 msec, a 0.5 *m/z* isolation window, a fixed first mass of 150 *m/z*, normalized collision energy of 27, and recorded as profile data. The targeted-MS2 methods were controlled with a timed inclusion list containing the target precursor *m/z* value, charge, and a 3 min retention time window that was determined from prior analyses of synthetic peptide standards as described (27). Lists of all peptides targeted for PRM analysis are given in Tables S1-S3.

*Targeted protein quantitation*

Two targeted protein analysis methods were employed in this study, the labelled reference peptide (LRP) and stable isotope dilution (SID) methods. The first relied on normalization of each unlabelled target peptide to a heavy isotope labelled peptide

standard called the labelled reference peptide (LRP) for relative quantitation (27). Three LRP standards (GYSFTTTAER^, AAQGDITAPGGAR^, and APLDNDIGVSEATR^) were purchased from New England Peptide (Gardner, MA) at >98% purity and quantified by amino acid analysis. For all LRP assays, the heavy peptide was spiked in at 2.5 fmol/μL to enable normalization.

The second method was stable isotope dilution (SID), whereby a heavy isotope labelled analog of each target peptide was spiked into each sample to allow for absolute quantitation and stoichiometry determination. Light and heavy peptide pairs for 26 peptides representing 26 proteins (Table S14) were purchased from New England Peptide. Each heavy peptide was synthesized with a terminal lysine or arginine that was uniformly labelled with $C^{13}$ and $N^{15}$ resulting in a mass shift of +8 Da for lysine and +10 Da for arginine. Heavy labelled peptides were of >99% isotopic purity and >98% peptide purity as determined by HPLC-UV and LC-MS analysis. Absolute concentration of the heavy labelled peptides was determined by amino acid analysis. Eight-point reverse calibration curves (Fig. A5) were generated for each peptide pair by spiking in a constant level of 2.5 fmol/μL of light peptide and varying the amount of heavy peptide from a high value of 100 fmol/μL to a low value of 0.0064 fmol/μL. Assay linearity across all concentration points was assessed and an equation for determining the analyte concentration using the peak area ratio of light/heavy isotopologues was defined using QuaSAR (28), which was implemented through the Skyline interface as described (29). The lower limit of quantitation (LLOQ) for each peptide was defined as the lowest point on the calibration curve with a coefficient of variation <25% across three technical replicates. The lower limit of detection (LLOD) was defined as one-third

of the LLOQ. For all SID assays, the heavy peptide was spiked in at 2.5 fmol/μL to enable normalization and absolute quantitation. Data below the LLOQ was excluded from all analyses.

*Data analysis*

Thermo .raw datafiles from shotgun LC-MS/MS runs were converted to mzml format using Proteowizard version 3.0.5211 (30). The mzml files were searched using MyriMatch version 2.1.132 (31), Pepitome version 1.0.42 (32), Comet version 2014.01.1 (33), and MS-GF+ version 9517 (34) against the human Refseq version 54 database (Sep 25, 2012; 34,590 entries). A semi-tryptic search was employed with a maximum of four missed cleavages allowed. A fixed carbimidomethyl modification on Cys, a variable oxidation on Met, and a pyro-glu on Gln were allowed with a maximum of 3 dynamic modifications per peptide with a precursor ion tolerance of 10 ppm and a fragment ion tolerance of 20 ppm. A target-decoy search was employed using a reverse sequence database to allow calculation of FDR for peptide-spectrum matches (35). Protein-level FDR was calculated by dividing the number of reverse sequence proteins identified by the total number of proteins identified, multiplying by two and converting to a percent. All search result files were parsimoniously assembled in IDPicker 3 version 3.1.643.0 (36). SAINTexpress version 3.1.0 (37, 38) was used with the Spotlight (39) interface to identify non-specific ASK protein interactions detected by the IP analyses.

PRM runs were designed and analyzed using Skyline (40) and three transitions per peptide were used for quantitative analyses. For LRP quantitation, the summed peak areas of all three transitions of the target peptides were normalized against those

of a heavy labelled peptide that was spiked into all runs at a constant concentration to correct for run-to-run variation caused by the instrument. Of the three LRP peptide standards spiked into all samples, the one used for normalization within each experimental system (e.g., ASK1-TAG cells, ASK2-TAG cells, etc.) had the lowest coefficient of variation for that system. LRP-normalized peak areas were further corrected for variances in protein concentration due to IP efficiency differences across experiments using an internal reference peptide (IRP) (41) from the ASK bait protein. Thus, all peptide results reported from the PRM assays are ratios of the amount of peak area for the analyte peptide divided by the peak area for the LRP peptide; this ratio was then divided by the peak area for the light SID peptide from the ASK bait protein. This final correction step minimizes measurement variation due to differing efficiencies of protein capture in each IP.

Peptides targeted for SID measurements were first normalized to the appropriate heavy labelled standard and then further normalized to an IRP as described above. Specifically, the peak area for the light target peptide was divided by the peak area of the corresponding heavy peptide; this ratio was then further divided by the light SID peptide signal for the ASK bait protein. This final correction step minimizes measurement variation due to differing efficiencies of protein capture in each IP. For stoichiometric analysis, absolute molar amounts of each peptide present in the IP were calculated using the standard curve and these were expressed as a percent of total ASK bait protein present in order to estimate the stoichiometry of the complex.

*Experimental Design and Statistical Rationale*

For initial data-dependent LC-MS/MS studies to compare IP methods, three biological replicate samples were analyzed for each of the IP methods, together with 3 negative control replicates. Similarly, for data-dependent LC-MS/MS analyses of the composition of ASK signalosome complexes, three biological replicate samples were analyzed for each of the IP methods, together with 3 negative control replicates. These sample sizes and datasets enable confident estimates of measurement variation and protein complex composition based on spectral count data (42) and application of the SAINT algorithm and software (37, 38).

To evaluate the dynamics of ASK signalosome changes in response to HNE electrophile stress, four biological replicate samples were performed for each cell line (five for ASK1-TAG). For these ASK signalosome dynamics experiments, 24 control replicates were prepared and each was run as two technical replicates interspersed between the IP samples to control for both non-specific binding and any potential carryover. The 48 control PRM analyses were divided among the 4 cell lines based on run order and all technical replicates were treated as independent for statistical testing. For PRM studies of the effects of ASK1 knockdown, four biological replicates and six controls were prepared and run as described above. For studies of the composition of ASK signalosome fractions prepared by size exclusion chromatography, two biological replicates were performed for each sample along with one negative control replicate that was run as two technical PRM injections as described above. These sample sizes were chosen to be sufficiently large enough to document measurement variation and assess significance of differences with the tests enumerated below.

Concentration-dependent differences in protein-protein interactions with the bait protein were assessed using both the two-tailed Jonckheere-Terpstra test (43, 44) to identify trends in the concentration-response relationships and the Kruskal Wallis test (45) with Dunn's post-hoc testing (46) to identify significant differences in the means of each concentration point via the DescTools package in R. The Wilcoxon rank sum test (47) was used to determine if the peptides targeted were significantly enriched over the negative control IPs. These non-parametric test methods were chosen as the IP data in this study was found to be non-normally distributed. All statistical tests were carried out in the R environment. Raw data files can be downloaded at: ftp://MSV000079399@massive.ucsd.edu and processed Skyline files can be downloaded at https://panoramaweb.org/labkey/Liebler_ASK.url.

## Results

*ASK-expressing HEK-293 cell lines*

I first generated cell lines that express epitope-tagged versions of ASK1 and the related MAP3Ks, ASK2 and ASK3. ASK2 was chosen as it is a known interacting protein of ASK1 (48-53). ASK3 (54, 55) is a highly similar MAP3K that I identified as a potential ASK1-interacting protein in a pilot shotgun study of ASK1 (data not shown). HEK-293 cells were chosen as they have been used for much of the published ASK1 research to date and are easily transfected. Because of the low endogenous expression of ASK1 and the lack of suitable antibodies for immunoprecipitating endogenous ASK2 and ASK3, I chose to clone a unique tandem affinity purification tag

(TAG) in-frame with each of the ASK genes (Fig. II-1A). These tags allowed us to conduct very clean immunofluorescent assays and highly efficient and specific immunopurifications. I transfected each of the ASK-TAG constructs into separate HEK-293 cells, thus creating three different cell lines, each stably expressing one of the tagged ASK proteins. I confirmed the transfections by Western blotting (Fig. II-1B).

I further confirmed that the tagging and overexpression of these three proteins did not cause aberrant sub-cellular localization via immunocytochemistry staining. Overexpressed and endogenous ASK1 both showed cytosolic and perinuclear localization (Fig. II-1D & E), consistent with published literature (56-58). In addition, no aberrant aggregation of the overexpressed proteins in the three cell lines was detected (Fig. A1). To verify the function of ASK1-TAG in transfected cells, I treated the cells with HNE (Fig. A2). HNE activated the ASK1 MAPK pathway in a time- and dose-dependent fashion, as shown by Western blot, which detected increased activating phosphorylation of ASK1 (pT838), as well as increased phospho-JNK and phospho-p38 staining, all of which are consistent with previous reports (5, 25).

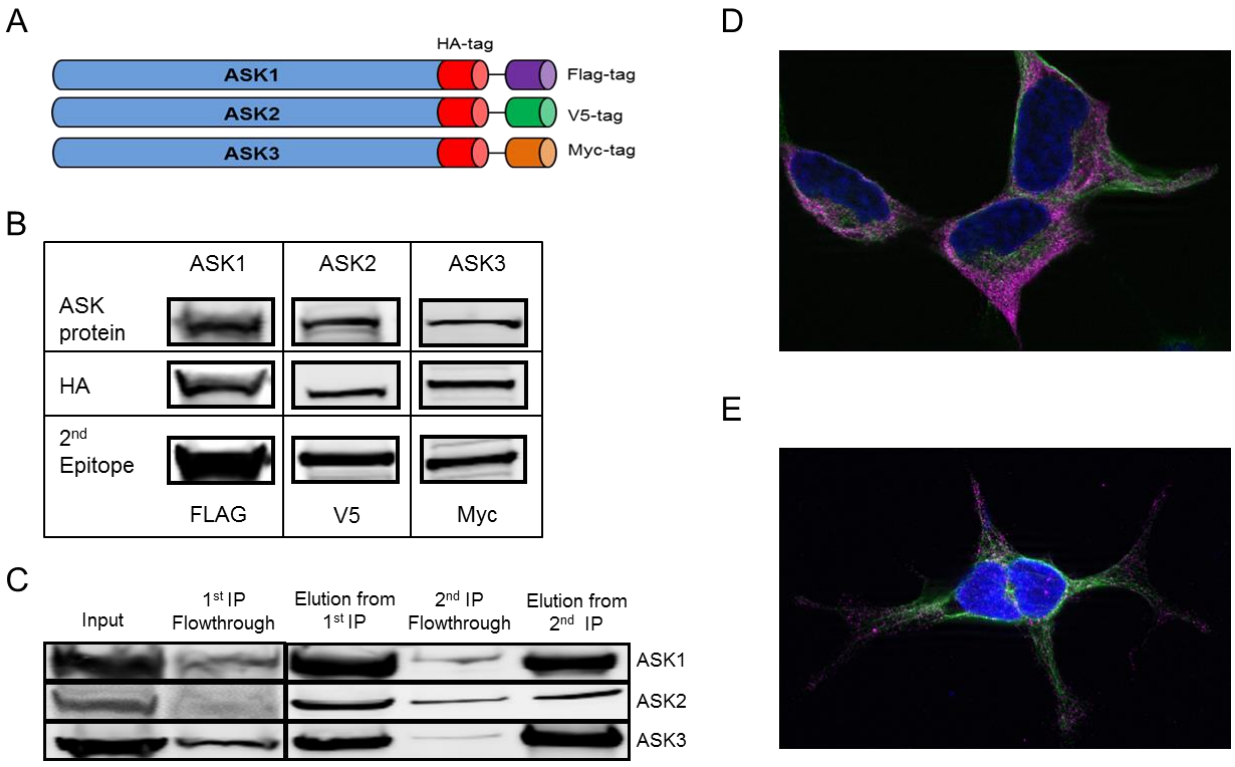


**Figure II-1. ASK-TAG cell lines.** (A) Design of tandem-tagged ASK proteins. (B) Western blots showing expression of ASK proteins and their epitope tags in HEK-293 cells. (C) Western blots demonstrating the tandem-IP procedure for each of the ASK-TAG proteins. (D & E) Immunocytochemistry of HEK-293 parental (D) and ASK1-TAG (E) cells showing similar localization of ASK1 (magenta) in both cell systems. Blue = DAPI, Green = Tubulin.

*Shotgun LC-MS/MS analysis of ASK1-interacting proteins*

I optimized a tandem-IP method to minimize potential non-specific interactions through the sequential IP steps (Fig. II-1C). While a tandem IP can reduce non-specific interactions, it can also fail to detect true interactions that do not survive both capture steps. I performed an IP method comparison using the ASK1-TAG cells, as ASK1 has the largest number of reported interactors among the three ASK proteins. I tested three different purifications using the FLAG and/or HA tags: a) anti-FLAG IP, followed by FLAG peptide release and recapture with anti-HA, b) anti-FLAG IP, and c) anti-HA IP. Each IP was performed in triplicate along with three negative control IPs consisting of untransfected HEK-293 cells. After shotgun LC-MS/MS analyses of the IPs, the data were searched and assembled together at a protein FDR of 0.88%.

The complete list of protein identifications from this experiment are provided in Table S4. Across all three IP methods, I identified 28 out of 94 (30%) previously reported ASK1-interacting proteins.

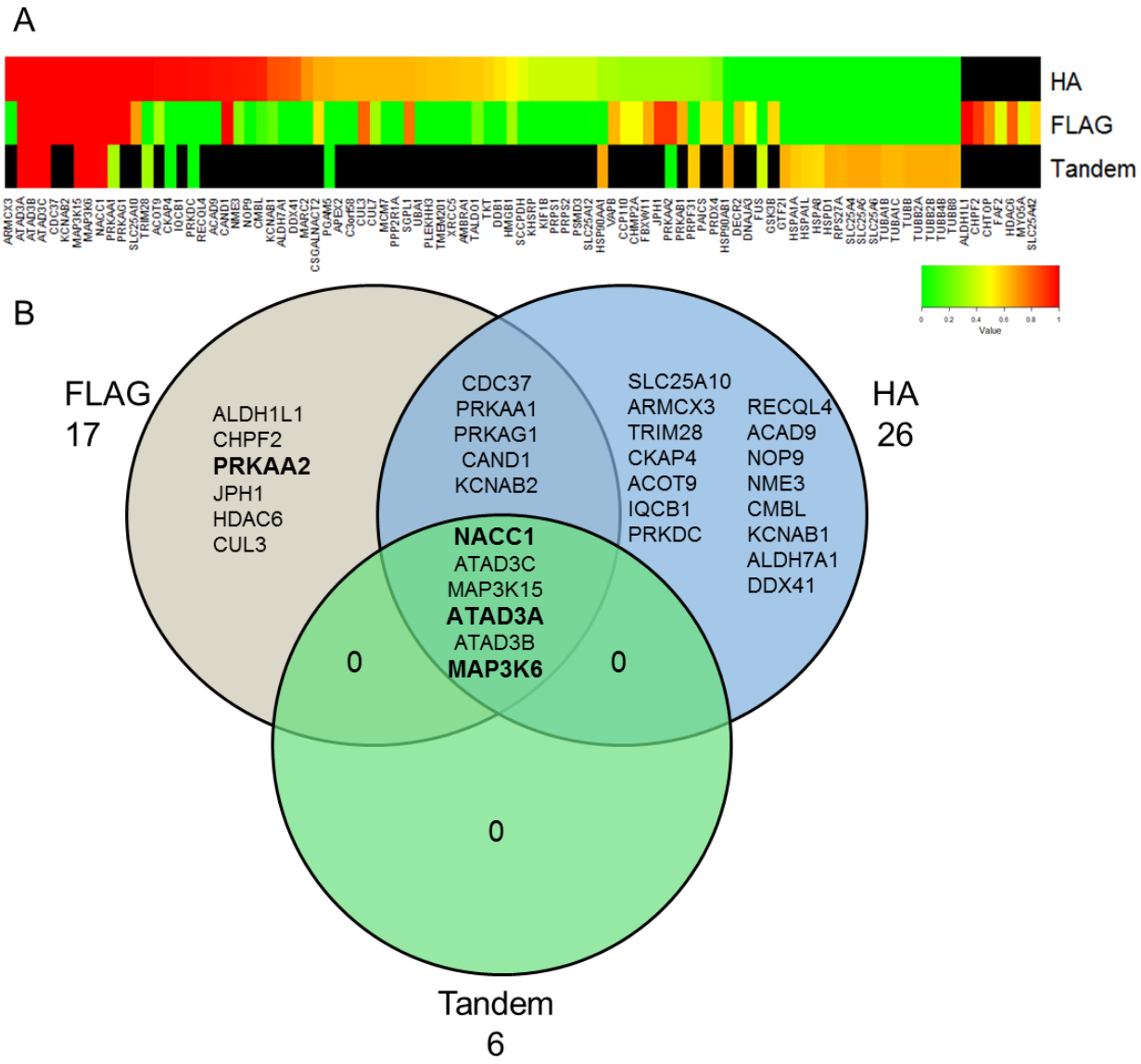


**Figure II-2. Comparison of ASK1 IP methods.** Three IP methods for ASK1 were analyzed by data-dependent shotgun MS and the proteins identified in each IP were scored by SAINT. The heat map shows SaintScores for all proteins that were at least 0.4 in one IP method. The proteins listed in the Venn diagram are those with a high-confidence SaintScore of at least 0.8. Proteins listed in bold are previously reported ASK1-interacting proteins.

I then applied the SAINT algorithm to determine which of the identified proteins in each IP experiment were best supported by the spectral count data as specific binding partners of the ASK proteins. SAINT uses the negative control data to generate a probability score for each protein present in a purification, which allows for a comparison of the robustness of each IP method employed for ASK1. The SAINT scores for all proteins identified in each IP are provided in Tables S5-S7. The HA IP generated the most interactions with a high SaintScore, whereas the FLAG IP generated the most identified interactions overall, and the tandem IP generated the fewest interactions (Fig. 2). However, application of a SAINTScore threshold of ≥0.8 yielded only 32 proteins that passed the filter (Venn diagram in Fig. II-2), of which only four were previously reported as ASK1-interactors (bold proteins in Venn diagram). Three of the reported interacting proteins were identified in all three IP methods; of these, ASK2 is a well-documented ASK1 interactor, whereas ATAD3A and NACC1 were only recently reported in another AP-MS study (53).

I decided to further examine the putative ATAD3A interaction, because it (along with ATAD3B) represented the highest number of spectral counts for ASK1 interacting proteins other than ASK2. I confirmed the interaction between ASK1 and both ATAD3A and ATAD3B in the ASK1-TAG cells (Fig. A3A) by co-IP Western blot analysis, but I was not able to confirm this interaction in the HEK-293 cells (Fig. A3B). I also could not detect the interaction between ASK1 and ATAD3A by co-IP and Western blotting in another cell line (RT4 cells) with a higher endogenous level of ASK1 expression (Fig. A3B). I therefore concluded that the apparent ASK1-ATAD3A/ATAD3B interaction was an artifact of the ASK1-TAG model.

*Interaction between ASK1, ASK2, and ASK3*

Another protein of interest identified in all three IP methods was ASK3 (MAP3K15). I had previously identified this protein as a potential ASK1-interactor in a preliminary shotgun screen of ASK1-expressing cells and the presence of ASK3 in all three IP methods seemed to support this conclusion. To further investigate the association of the three ASK proteins (ASK1, ASK2, and ASK3), I transiently electroporated all three proteins into HEK-293 cells in order to perform co-localization studies. As can be seen in Fig. II-3A, all three of the ASK proteins show similar subcellular distributions and co-localization (white color in the Merge panel of Fig. II-3A).

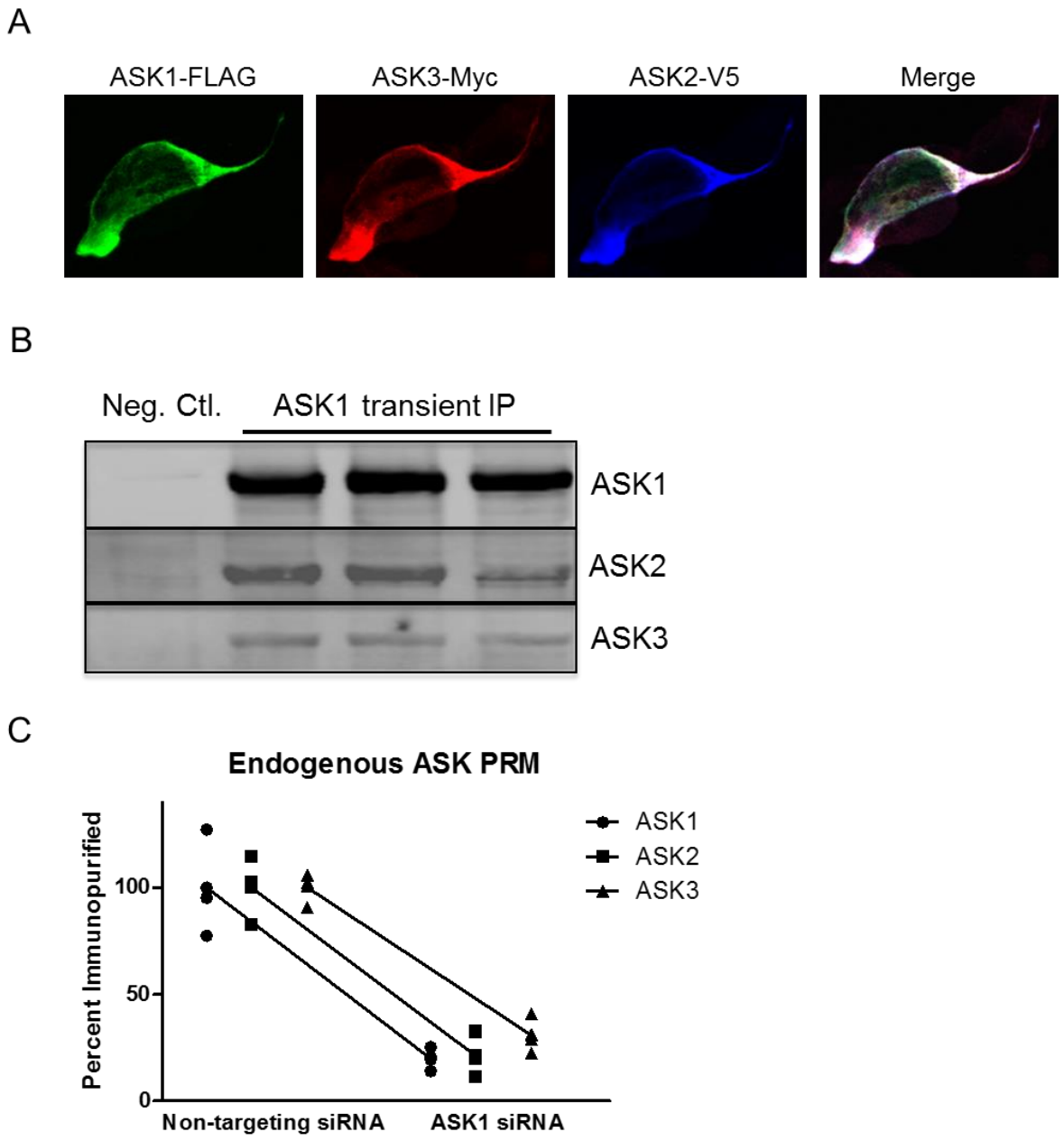


**Figure II-3. Validation of ASK protein interactions.** (A) ICC imaging of all three ASK proteins co-transfected into HEK-293 cells shows co-localization (white color in right-most panel). (B) Co-IP western of ASK2 and ASK3 interacting with transiently expressed ASK1. (C) PRM analysis of immunopurified endogenous ASK1 complexes from cells treated with non-targeting (left) and ASK1-targeting (right) siRNA shows a decreased amount of ASK1 purified and a concomitant decrease in ASK2 and ASK3.

I also performed a transient transfection of only ASK1 and used co-IP and Western blotting to detect ASK2 and ASK3 association with overexpressed ASK1 (Fig II-3B). The available antibodies for ASK2 and ASK3 did not enable sufficiently sensitive detection for co-IP Western analysis at their endogenous expression levels in HEK-293 cells. Instead, I used a parallel reaction monitoring (PRM) targeted MS assay to demonstrate the association of all three ASK proteins in an endogenous ASK1 IP (Fig II-3C). Furthermore, I performed siRNA knockdown of endogenous ASK1 in HEK-293 cells (Fig. A4A) and showed with PRM analysis that decreasing the amount of expressed ASK1 also decreased the amount of associated ASK2 and ASK3 in co-IP analyses (Fig. II-3C). In addition, I monitored many of the previously reported ASK1-interacting proteins, but saw no other proteins that followed the same trend seen with ASK2 and ASK3 (see Fig. A4B&C and Tables S8-S9). This series of experiments confirmed the previously reported association of ASK2 with ASK1 and identified ASK3 as a new ASK1-interacting protein. Furthermore, the siRNA knockdown experiment suggested a proportional interaction among the three ASK proteins.

*Targeted MS analysis of ASK1-interacting proteins*

My inability to detect previously reported ASK1-interacting proteins in data-dependent LC-MS/MS analyses of co-IPs suggested that they were present at relatively low levels compared to the overexpressed ASK1 and that more sensitive targeted methods would be required to detect these proteins. Thus, I re-analyzed the same co-IP samples described above with a PRM assay, which targeted 66 previously reported ASK1-interacting proteins listed in Table S1. For these experiments I used the LRP

method, which employs a single heavy isotope labelled peptide as a normalization standard for all target peptides in the analysis and provides a cost-effective means to quantitatively compare abundance of larger numbers of proteins between samples (27). This LRP-PRM assay was thus used to detect significant enrichment of the target proteins in ASK1-TAG co-IPs.

These analyses detected 61 of the 66 targeted ASK1-interacting proteins (92%) (Tables S10-S13). Significant enrichment was defined as either a) detection in at least 2 of 3 biological replicates for proteins not detected in the control samples or b) by a significant ($p \leq 0.05$; Wilcoxon rank test) and at least 3-fold enrichment over control samples (Fig. II-4). Of the sixty-two enriched proteins, I detected 60 in the HA IP while only observing 29 in the FLAG IP and 6 in the tandem IP. These results thus confirmed the association of most previously reported ASK1 interacting proteins; albeit at levels that appeared to be much lower than ASK1.

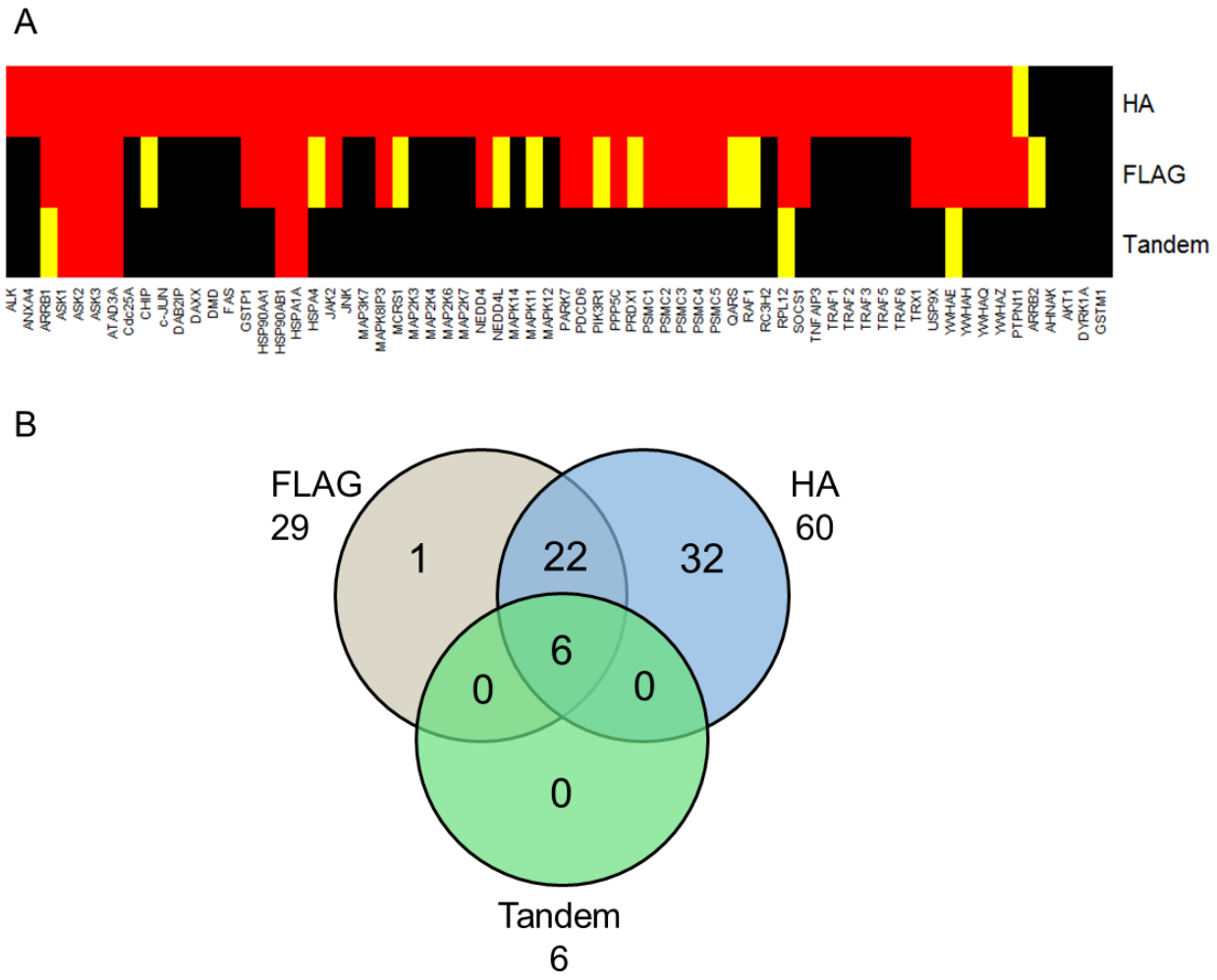


**Figure II-4. Comparison of ASK1 IP methods by targeted proteomics.** PRM analyses of the same samples as Fig. 2 identified 61 out of 66 reported ASK1-interacting proteins targeted. Sixty of those proteins were detected in the HA IP at an enriched level over control. Black signifies that the protein was not detected, yellow that the protein was detected but was not enriched, and red that the protein was detected and enriched over background.

*Targeted assay strategy for ASK1 complex dynamics and stoichiometry studies*

Because PRM analyses enabled detection of many previously reported ASK1-interacting proteins in the co-IP analyses, I pursued a targeted analysis strategy for studies of the dynamics of ASK signalosome components in response to HNE electrophile stress and to further characterize the stoichiometry of ASK1 interaction with other putative signalosome protein components. A targeted analysis strategy employing a combination of LRP-PRM and SID-PRM assays for these studies is represented in Fig. II-5. I employed the LRP-PRM approach to target 94 proteins, including the 68 targeted in the co-IP analyses described above, as well as additional proteins hypothesized to have ASK1 interactions. These proteins and the targeted peptides and precursor *m/z* values are listed in Table S2. Because normalization to the LRP standard provides ratios for each peptide (peak area for peptide/peak area for LRP standard), these values can be used for relative quantitation between HNE exposures for the dynamics experiments.

For measurements of stoichiometry of ASK1-interacting proteins, I required absolute quantitation and therefore performed SID-PRM analyses for 26 peptide targets (Table S3) corresponding to a subset of 26 ASK1-interacting proteins identified as significant interactors in the co-IP experiments above. Calibration curves for all 26 peptides are shown in Fig. A5 and the specific features of each assay (target peptides, transitions, LLOD, LLOQ, linearity) are presented in Table S14.

These two quantitative strategies were applied simultaneously in the same study of the dynamics of ASK signalosome proteins in response to HNE treatment. The combined LRP-PRM and SID-PRM analysis targeted 254 peptide precursors from the

94 proteins, three LRP standard peptide precursors, and 26 stable isotope labelled SID standard peptide precursors. For LRP-based quantitation, multiple peptides were targeted for most of the proteins. For SID-based quantitation, a single peptide per protein and its heavy isotopologue standard were measured. Quantitative comparisons of each protein between conditions were based on the data for a single peptide per protein generated either by LRP (normalized ratio) or by SID (molar quantity) measurements. For the 26 proteins for which SID measurements were possible, these were used in preference to LRP measurements. For proteins for which multiple peptides were targeted for LRP measurements, the one with the highest average peak area across all IPs was used for quantitative comparisons.

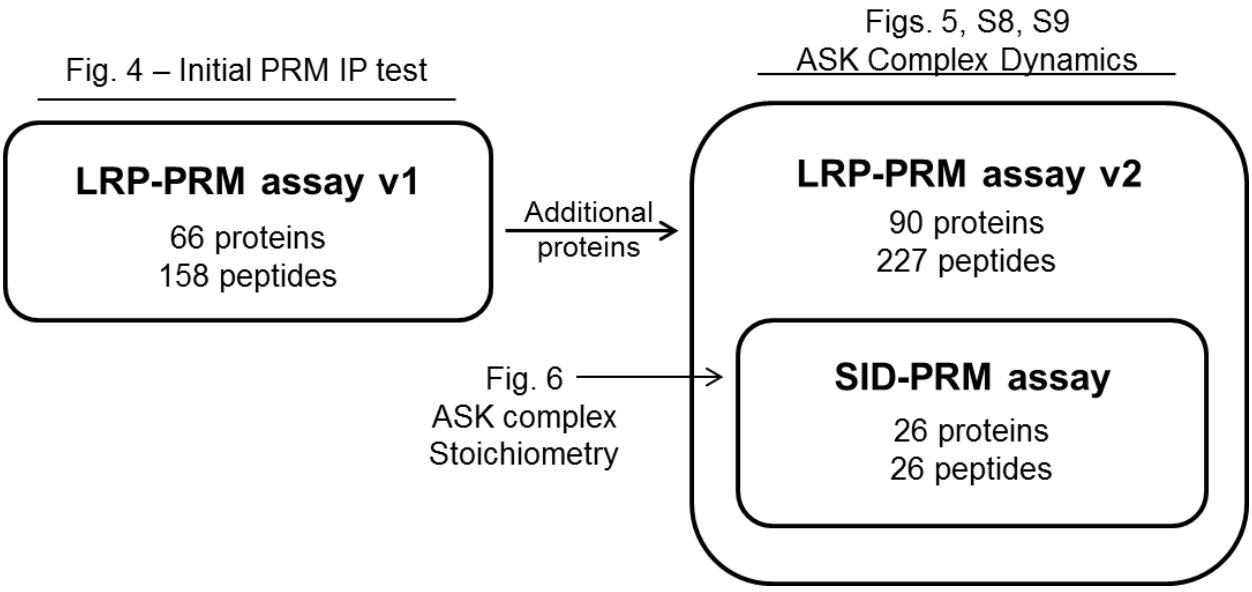


**Figure II-5. ASK PRM assay development.** An LRP-PRM assay was used to target reported ASK1 complex members in the samples previously analyzed by shotgun MS. For the subsequent assays examining ASK complex dynamics, I added additional protein targets and developed an expanded LRP-PRM (see text for discussion). Of the 94 proteins in the expanded assay, 26 were selected for concurrent SID analyses with the addition of stable isotope-labelled standards for use in the complex stoichiometry study.

*Dynamic changes in ASK signalosome composition in response to HNE*

I performed WST cell death assays to determine the HNE concentrations to use for studies of ASK1 protein interaction dynamics. All three ASK-overexpressing cell lines and the non-transfected HEK-293 cell line yielded a similar $EC_{50}$ value (approximately 10 μM) for HNE (Figure A6A). The effectiveness of this HNE concentration in triggering electrophile stress was confirmed by Western blot analysis of the activating Thr838 phosphorylation of ASK1 in the ASK1-TAG cell line, which showed a much higher level of activation at 20 μM than 5 μM (2-fold above and below the $EC_{50}$ value, respectively) (Fig. A6B). These assays, along with evidence of maximal ASK1 MAPK pathway activation after 1 hr of treatment (Fig. A2), led us to select a treatment time of 1 hr with three concentrations: 0 μM HNE (ethanol vehicle control - below $EC_{50}$), 10 μM HNE ($EC_{50}$), and 50 μM HNE (above $EC_{50}$).

I treated the four cell lines with HNE in quadruplicate (quintuplicate for ASK1-TAG) at each concentration and confirmed the success and uniformity of the IPs by Western blotting (Fig. A7A) prior to running the PRM analyses of the corresponding samples. I first determined the amount of the ASK1, ASK2, and ASK3 proteins present in IPs from ASK1-TAG, ASK2-TAG, and ASK3-TAG cells, as well as from non-transfected control HEK-293 cells (Fig. A7B). ASK1 and ASK2 were both purified at higher amounts from their respective cell lines, whereas amounts of immunoprecipitated ASK3 from ASK3-TAG cells and ASK1 from non-transfected cells were over an order of magnitude lower.

To detect HNE-induced changes in the ASK protein complex composition for each cell line, I employed two different strategies. First, I compared the means of the

LRP- and SID-normalized peak areas for each detected peptide at each concentration using the Kruskal-Wallis test with a Dunn's post-test. Differences between the means are indicated by blue connecting bars in the graphs in Figure II-6A and B. I also performed a Jonckheere-Terpstra (JT) test to detect trends in response consistent with a concentration-dependent relationship. Figure II-6A and B depict measurements of NACC1, YWHAG, PSMC2, and HSP90AB1, all of which have significant ($p \leq 0.05$) JT test values, indicating that these four peptides exhibit increased abundance with increasing HNE concentration.

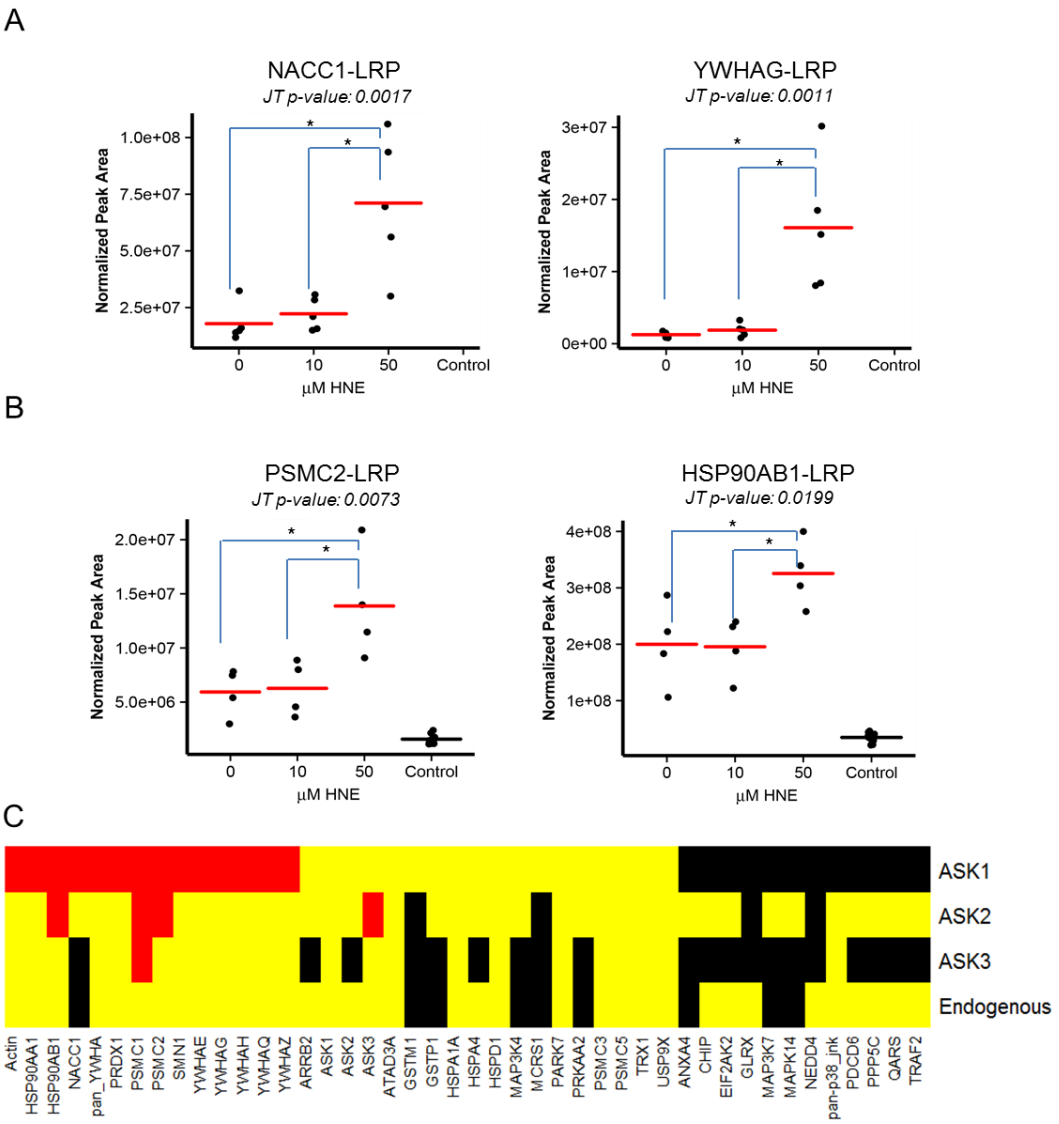


**Figure II-6. ASK complex dynamics in response to HNE treatment.** (A & B) Four proteins that exhibited a positive concentration-response relationship to HNE in the ASK1-TAG cells (A) and the ASK2-TAG cells (B). (C) Summary of all the peptides detected in the ASK complex dynamics study. Black signifies that the peptide was not detected in the IP; yellow indicates that the peptide was detected, but did not change significantly in response to HNE; and red indicates that the peptide was detected, was enriched above the negative control, and exhibited a significant HNE-dependent change for at least one treatment concentration.

As a further test of specificity, I performed Wilcoxon rank sum tests between each treatment condition and the negative control to access whether or not the peptide was part of a true protein-protein interaction with the bait protein or if it was merely non-specifically purified. A red mean bar was used to denote peptides that were enriched over the negative control at that concentration point with either a Wilcoxon p-value ≤ 0.05 or detection in at least half of the replicates at a given concentration point and no detection in any of the negative control replicates.

Figure II-6C summarizes the findings of the concentration-response relationships in the ASK complex in all four cell lines. I detected 79 peptides corresponding to 44 proteins in at least one of the cell lines. The ASK1-TAG cells had the largest number of significant changes in protein complex composition (red bars), whereas the ASK2 and ASK3 cell lines only had a few each. In total, 15 proteins exhibited concentration-dependent shifts in association with the three ASK proteins and 14 of these were observed with ASK1 alone. Furthermore, because of the low expression level of ASK3 in the ASK3-TAG cell line, the majority of the detected peptides were not significantly enriched over the negative control samples. Measurements in non-transfected HEK-293 cells expressing endogenous ASK1 had no significantly changing ASK-interacting proteins in response to HNE, probably because the low abundance of ASK1 made it difficult to quantify interactors. Data for the individual protein measurements summarized in Figure II-6C are presented in Figures A8 and A9; the normalized protein measurements with statistical test results can be found in Tables S15-S19.

A well-known caveat with AP-MS studies is that artifactual protein-protein associations may be observed in studies with overexpressed, epitope-tagged proteins.

To address this possibility for the 14 proteins found to exhibit a dynamic association change with ASK1-TAG in response to HNE treatment, I measured levels of these proteins in the ASK1 IPs from the HEK-293 cells. Most (11 of 14) were detected in the endogenous ASK1 IPs at a higher level than in the negative control IPs (Figure A10). Those 112 proteins thus are significantly associated with ASK1 at endogenous levels and the association is independent of an epitope tag. Moreover, if these associations had been driven simply by overexpression of ASK1-TAG protein, association differences upon HNE treatment would not be expected. The failure to observe this HNE-dependent dynamic in untransfected cells may reflect the difficulty of measuring changes in association at the low abundance levels of endogenous ASK1.

*Analysis of ASK signalosome populations prepared by size exclusion chromatography*

Although several proteins displayed concentration-dependent changes in response to HNE treatment, there were fewer changes than might be anticipated from the ASK1-signalosome remodeling hypothesis (2, 3). I hypothesized that some of the dynamic shifts in the ASK complex composition could have been masked by a potentially heterogeneous mixture of pre- and post-activation ASK signalosome complexes. ASK1 has been reported to undergo a shift in complex size upon activation by oxidants and thereby change from a ~1500 kDa pre-activation complex to a much higher molecular weight post-activation complex (3).

To assess this possibility, I repeated the size exclusion chromatography (SEC) fractionation of the ASK complex as described by Ichijo and colleagues (3) with minor modifications (Fig. A11A). My measurements suggested a minimum complex size of

approximately 669 kDa, which is consistent with the analysis by Ichijo and colleagues (21). However, I did not observe a shift in the distribution of ASK1 or phospho-ASK1 across SEC fractions (Fig. A11B&C). PRM analysis of ASK1, ASK2, and ASK3 in IPs from SEC-fractionated ASK1 complexes revealed a similar distribution of the ASK proteins as was seen for ASK1 in the Western blot analyses (Fig. A11D).

*ASK protein complex stoichiometry*

SID-PRM measurements in the ASK signalosome dynamics study provided absolute quantitative estimates of ASK1-interacting proteins in the IPs. I used these measurements to estimate protein stoichiometry relative to bait protein as has been done for other systems (59-62). The apparent stoichiometry varied somewhat depending on the cellular context. In the ASK1-TAG cell co-IPs (Fig. II-7A), ASK2, ASK3, 14-3-3 proteins (YWHAQ, YWHAB, YWHAH, and YWHAE measured collectively by a common peptide), PARK7, PRDX1, and USP9X were present at a few percent of the level of ASK1. Analyses of the ASK2-TAG cell co-IPs (Fig. II-7C) yielded data similar to the ASK1-TAG IPs, with ASK1, ASK3, 14-3-3 proteins, PARK7, PRDX1, and USP9X present at a few percent of the level of ASK2. Interestingly, measured levels of some of the interacting proteins appeared to increase with increasing HNE treatment concentration.

In co-IPs of endogenous ASK1 from untransfected cells (Fig. II-7B), the stoichiometry of ASK2 relative to ASK1 was approximately 1:1 and that of 14-3-3 proteins to ASK1 was approximately 0.5:1. The other proteins measured at low levels in co-IPs of ASK1-TAG and ASK2-TAG were also present at less than 10% of

endogenous ASK1 and PRDX1 was not detected as a partner of endogenously expressed ASK1.

ASK3-TAG co-IPs expressed a level of ASK3 lower than that of endogenous ASK1 in co-IPs from untransfected cells (Fig. II-S7B) and 14-3-3 proteins and PRDX1 were present in stoichiometries of approximately 0.5:1 and 0.7:1 relative to ASK3, respectively (Fig. II-7D). Other detected interactors were present at levels less than 10% of ASK3.

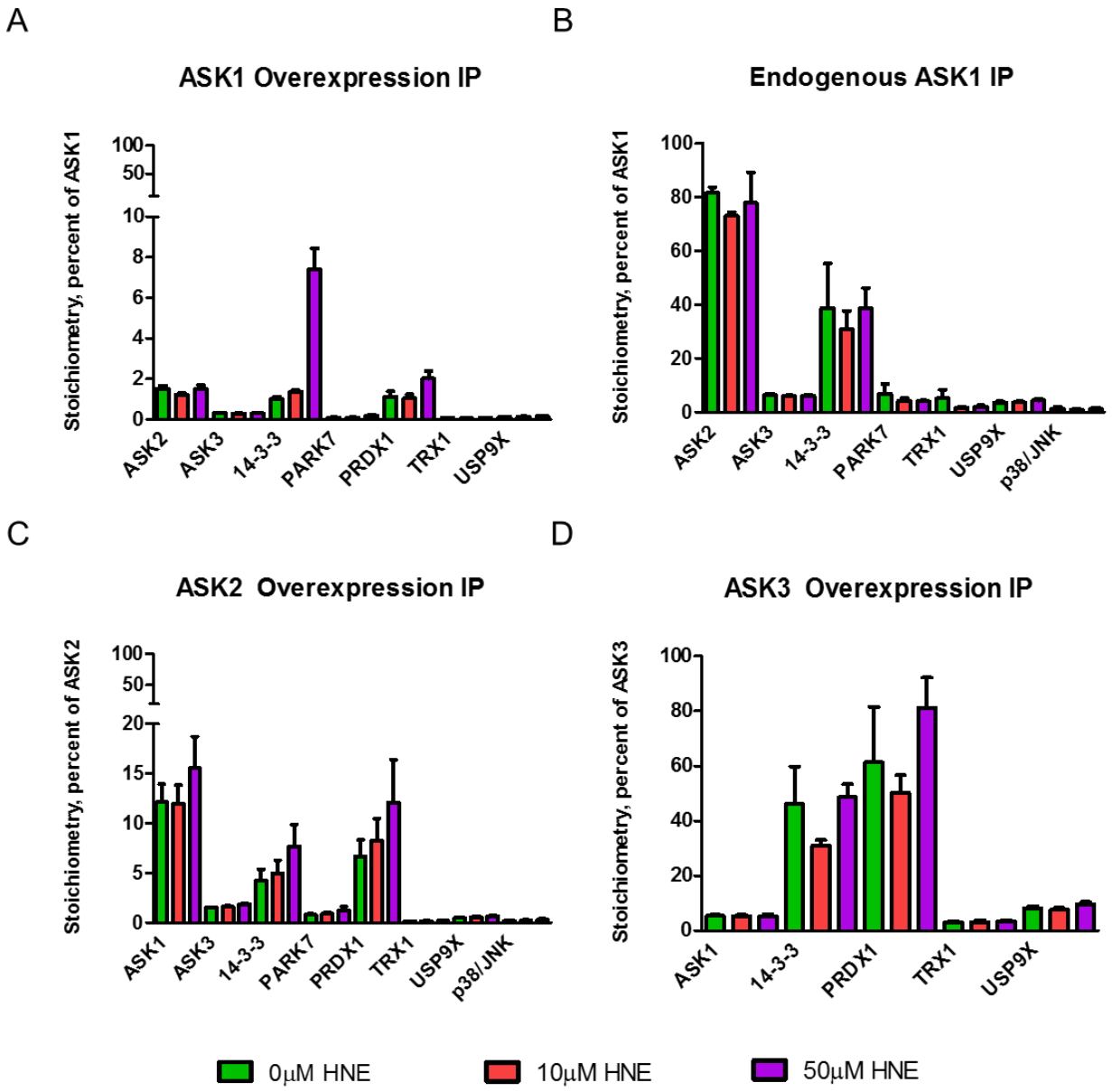


**Figure II-7. ASK1 complex stoichiometry.** Apparent stoichiometry of the ASK complexes present in each cell relative to the ASK bait protein component as assessed by SID-PRM measurements. For ASK1-TAG (A), ASK2-TAG (C), and ASK3-TAG (D), all detected proteins were calculated relative to the overexpressed protein in each cell line. For the endogenous ASK IP from non-transfected cells (B), all detected proteins were calculated relative to endogenous ASK1.

## Discussion

ASK1 is thought to be regulated by a large multiprotein complex that changes composition dynamically in response to oxidative stress. The candidate membership list—ASK1 and its 90 reported interacting proteins—together would be too large to comprise a signalosome complex of the reported 1,500 kDa size (3). I therefore asked which members of this candidate list are constitutively bound to ASK1 and how does this repertoire of interacting molecules change upon activation of the ASK1 pathway by HNE electrophile stress. I first confirmed ASK1 interactions with most of the reported interactors with shotgun and targeted MS analyses. Using targeted PRM assays, I also identified 14 proteins that demonstrated dynamic shifts in their association with ASK1 under stress. Using precise SID-based measurements, I next provided the first ever quantitative examination of the ASK complex. I detected ASK2 as a 1:1 stoichiometric binding partner of ASK1 and several 14-3-3 proteins as ASK1 interactors with a collective stoichiometry of approximately 0.5:1. ASK3 and several other proteins exhibited stoichiometries of 0.1:1 or lower. These stoichiometries were consistent between ASK1-TAG and ASK2-TAG complexes and immunoprecipitates of endogenous ASK1. Moreover, the complex size calculated from the stoichiometry measurements is consistent with SEC analyses of ASK1 complexes. The data suggest a core ASK signalosome consisting of ASK1, ASK2 and 14-3-3 proteins, which interacts with a variety of other proteins to mediate MAPK activation and possibly other diverse signaling events.

Most previous studies of the ASK1 multiprotein complex have been done using IP/Western blot methods to identify binary interactions, but these methods provide little insight into the composition and dynamics of multiprotein complexes. Shotgun proteomics analyses have been extensively used to inventory members of multiprotein complexes and enable unbiased discovery of novel components. Targeted proteomics assays can provide quantitative information that enables insights into complex function. Here I used LRP- and SID-PRM assays to examine the compositional changes of the ASK signalosome in response to HNE stress.

These two targeted quantitation approaches are complementary in the way they were applied here. The LRP method requires only a single labeled reference standard and thus offers the most cost-effective approach to a targeted survey of 90 candidate binding partners. However, the method is potentially subject to ionization suppression and interferences due to the lack of labeled standards for all analytes (29). Thus, my use of SID-PRM analyses of a single peptide for each of 26 candidate ASK1-interacting proteins enabled highly precise quantitation, which was sufficient for estimates of complex stoichiometries. Although measurement of a single peptide per protein could be subject to interference by unanticipated protein modification or cleavage, all of the SID measurement trends were consistent with multiple estimates from the LRP method with the same samples.

I identified 14 proteins that showed an increased association with ASK1 in response to HNE, including two HSP genes (HSP90AA1 and HSP90AB1), two proteasome components (PSMC1 and PSMC2), several 14-3-3 family proteins (YWHAE, YWHAG, YWHAH, YWHAQ, and YWHAZ), and the antioxidant protein

PRDX1. Most of these proteins were also found to be enriched (though not dynamic) in ASK1 IPs over the negative controls in the endogenous HEK-293 cell line, which lends further support to the validity of these proteins as components of a dynamic ASK multiprotein complex. This precise, multiplexed quantitative assessment of component dynamics would be impossible with IP/Western methods.

An important element of my approach is the use of complementary epitope-tagged overexpression cell models for ASK proteins, which provided reinforcing data on the ASK signalosome. The proteins detected in all of the ASK-TAG cell line IPs were similar (Figs. II-6 & II-7), especially those analyzed by SID-PRM in the ASK1-TAG and ASK2-TAG cell lines with regard to both the proteins identified and the trends in association observed. The composition of ASK IPs from both cell lines was also remarkably similar to that of native ASK IPs from untransfected cells (compare Figs. II-7A & II-7C with Fig. II-7B). SID-PRM data from the endogenous ASK1 IP revealed an approximately 1:1:0.5 stoichiometry of ASK1:ASK2:14-3-3 proteins. Even though ASK1 and ASK2 levels were much higher in the overexpressing cell models, the SID-PRM analyses of the ASK2/14-3-3 binding partners in the ASK1-TAG complex and ASK1/14-3-3 binding partners in the ASK2-TAG complex revealed stoichiometries similar to those in native ASK1 complexes from untransfected cells. Additionally, by overexpressing ASK1 and ASK2, I were able to detect dynamic protein-protein associations that could not be observed at endogenous ASK1 expression levels, likely due to the approximately 40-fold lower expression level of the ASK proteins in untransfected cells (Fig. A7). Thus, examining a multiprotein complex at multiple expression levels can provide insights that would otherwise be missed.

One of the disadvantages of overexpression systems is that they can generate false-positive associations. In the shotgun analysis of ASK1-TAG IPs, I identified the previously reported ASK1-interacting protein ATAD3A (53) as a putative ASK1 interactor by all three IP methods. I then attempted to validate this interaction by Western blotting and was able to do so in the overexpressing cell line, but not in two different non-transfected systems (Fig. A3). This suggested that the interaction between ATAD3A and ASK1 may be mediated by the presence of the affinity tags. The previous study by So *et. al*. reporting an ASK1-ATAD3A interaction used a triple FLAG tag on ASK1 (53). I used a single FLAG epitope as part of my tandem tag on ASK1, so it is possible that the interaction between ASK1 and ATAD3A is mediated by the FLAG sequence. By utilizing the endogenously expressing cell line, I was able to identify this interaction as a likely artifact.

Through quantitative MS analyses of ASK-TAG protein overexpression and native ASK protein expression in non-transfected cells, I was able to confirm the essential elements of the ASK signalosome hypothesis (2) and further extend our understanding of this system. Through my SEC experiments, I confirmed previous observations of the distribution of the ASK1 protein across multiple high molecular weight complexes (3). In contrast to a report that $H_2O_2$ led to the formation of a higher molecular weight ASK signalosome complex (3), I did not observe the same shift with a similar degree of MAPK activation by HNE. I also detected most previously reported ASK1-interacting proteins at a significant enrichment over negative control IPs, thus confirming their associations with ASK1. Several of these proteins exhibited dynamic associations with the overexpressed ASK1 upon HNE treatment, which is consistent

with previous observations of dynamic protein-protein associations with ASK1 in response to stress activation.

While I did observe several dynamic protein-protein interactions with ASK1, most of these proteins associated with ASK1 in a low stoichiometric ratio. The SID-PRM assay targeted 26 of the previously reported ASK1-interacting proteins and quantified 7 of them in ASK1 IPs from non-transfected cells. Of these 7 proteins, ASK2 was present at a nearly 1:1 ratio with ASK1 and several 14-3-3 family proteins were collectively present at an approximately 0.5:1 ratio with ASK1. The remaining proteins were observed at a 0.1:1 or lower ratio with ASK1. Thus, my data points toward a core ASK1 complex that consists of ASK1, ASK2, and 14-3-3 family members that associates with other proteins to execute MAPK pathway signaling.

Interestingly, the expected size of a stoichiometric core ASK1 complex as I have described it here would be approximately 625 kDa (2 ASK1, 2 ASK2, and 1 14-3-3 family protein), which corresponds well with the smallest commonly observed ASK1 complex mass (approximately 669 kDa) in both my SEC experiments (Fig. A11B & C) and similar SEC analyses reported by Noguchi *et. al*. (21). This suggests a core ASK1 complex that may transiently associate with other proteins in a context-dependent fashion. Indeed, the MW range for ASK1 complexes in the SEC analyses extends from approximately 669 kDa to as much as 3000 kDa (21), which could indicate the simultaneous co-existence of many different ASK1 signalosome complexes.

The presence of multiple 14-3-3 family members in the ASK1 core complex suggests that they may serve a key role as adapter proteins for bringing the ASK complex into contact with many other identified ASK interacting proteins. Indeed,

finding equal stoichiometry between ASK1 and ASK2 in the signalosome complex raises the possibility that previously reported ASK1-interacting proteins may interact with both ASK proteins. Regardless of ASK protein binding specificity, the diversity of ASK-interacting protein partners likely enables the ASK signaling pathway to respond to a wide variety of environmental stressors. ASK1 has been reported to interact with several other proteins to influence different signaling pathways (63-66) and recent studies explored the role of ASK1 in antiviral response and innate immunity (67-69). The core ASK complex thus may play a broader cellular role beyond activation of the MAPK pathway. The large number of identified interacting proteins certainly points toward multifunctional roles of the core ASK complex in the cell. Future investigations of the ASK1 core complex associations through targeted MS in different physiological contexts will be essential to test these hypotheses.

## References


1. Fujino, G., Noguchi, T., Matsuzawa, A., Yamauchi, S., Saitoh, M., Takeda, K., and Ichijo, H. (2007) Thioredoxin and TRAF family proteins regulate reactive oxygen species-dependent activation of ASK1 through reciprocal modulation of the N-terminal homophilic interaction of ASK1. *Mol Cell Biol* 27, 8152-8163

2. Shiizaki, S., Naguro, I., and Ichijo, H. (2013) Activation mechanisms of ASK1 in response to various stresses and its significance in intracellular signaling. *Adv Biol Regul* 53, 135-144

3. Noguchi, T., Takeda, K., Matsuzawa, A., Saegusa, K., Nakano, H., Gohda, J., Inoue, J., and Ichijo, H. (2005) Recruitment of tumor necrosis factor receptor-associated factor family proteins to apoptosis signal-regulating kinase 1 signalosome is essential for oxidative stress-induced cell death. *J Biol Chem* 280, 37033-37040

4. Saitoh, M., Nishitoh, H., Fujii, M., Takeda, K., Tobiume, K., Sawada, Y., Kawabata, M., Miyazono, K., and Ichijo, H. (1998) Mammalian thioredoxin is a direct inhibitor of apoptosis signal-regulating kinase (ASK) 1. *EMBO J* 17, 2596-2606

5. Soh, Y., Jeong, K. S., Lee, I. J., Bae, M. A., Kim, Y. C., and Song, B. J. (2000) Selective activation of the c-Jun N-terminal protein kinase pathway during 4-hydroxynonenal-induced apoptosis of PC12 cells. *Mol Pharmacol* 58, 535-541

6. Nishitoh, H., Matsuzawa, A., Tobiume, K., Saegusa, K., Takeda, K., Inoue, K., Hori, S., Kakizuka, A., and Ichijo, H. (2002) ASK1 is essential for endoplasmic reticulum stress-induced neuronal cell death triggered by expanded polyglutamine repeats. *Genes Dev* 16, 1345-1355

7. Takeda, K., Matsuzawa, A., Nishitoh, H., Tobiume, K., Kishida, S., Ninomiya-Tsuji, J., Matsumoto, K., and Ichijo, H. (2004) Involvement of ASK1 in Ca2+-induced p38 MAP kinase activation. *EMBO Rep* 5, 161-166

8. Takeda, K., Noguchi, T., Naguro, I., and Ichijo, H. (2008) Apoptosis signal-regulating kinase 1 in stress and immune response. *Annu Rev Pharmacol Toxicol* 48, 199-225

9. Matsuzawa, A., Saegusa, K., Noguchi, T., Sadamitsu, C., Nishitoh, H., Nagai, S., Koyasu, S., Matsumoto, K., Takeda, K., and Ichijo, H. (2005) ROS-dependent activation of the TRAF6-ASK1-p38 pathway is selectively required for TLR4-mediated innate immunity. *Nat Immunol* 6, 587-592

10. Lee, K. W., Zhao, X., Im, J. Y., Grosso, H., Jang, W. H., Chan, T. W., Sonsalla, P. K., German, D. C., Ichijo, H., Junn, E., and Mouradian, M. M. (2012) Apoptosis signal-regulating kinase 1 mediates MPTP toxicity and regulates glial activation. *PLoS One* 7, e29935

11. Lim, P. L., Liu, J., Go, M. L., and Boelsterli, U. A. (2008) The mitochondrial superoxide/thioredoxin-2/Ask1 signaling pathway is critically involved in troglitazone-induced cell injury to human hepatocytes. *Toxicol Sci* 101, 341-349

12. Usuki, F., Fujita, E., and Sasagawa, N. (2008) Methylmercury activates ASK1/JNK signaling pathways, leading to apoptosis due to both mitochondria- and endoplasmic reticulum (ER)-generated processes in myogenic cell lines. *Neurotoxicology* 29, 22-30

13. Nakagawa, H., Maeda, S., Hikiba, Y., Ohmae, T., Shibata, W., Yanai, A., Sakamoto, K., Ogura, K., Noguchi, T., Karin, M., Ichijo, H., and Omata, M. (2008) Deletion of apoptosis signal-regulating kinase 1 attenuates acetaminophen-induced liver injury by inhibiting c-Jun N-terminal kinase activation. *Gastroenterology* 135, 1311-1321

14. Shinkai, Y., Iwamoto, N., Miura, T., Ishii, T., Cho, A. K., and Kumagai, Y. (2012) Redox cycling of 1,2-naphthoquinone by thioredoxin1 through Cys32 and Cys35 causes inhibition of its catalytic activity and activation of ASK1/p38 signaling. *Chem Res Toxicol* 25, 1222-1230

15. Kuo, C. T., Chen, B. C., Yu, C. C., Weng, C. M., Hsu, M. J., Chen, C. C., Chen, M. C., Teng, C. M., Pan, S. L., Bien, M. Y., Shih, C. H., and Lin, C. H. (2009) Apoptosis signal-regulating kinase 1 mediates denbinobin-induced apoptosis in human lung adenocarcinoma cells. *J Biomed Sci* 16, 43

16. Kwon, M. J., Jeong, K. S., Choi, E. J., and Lee, B. H. (2003) 2,3,7,8-Tetrachlorodibenzo-p-dioxin (TCDD)-induced activation of mitogen-activated protein kinase signaling pathway in Jurkat T cells. *Pharmacol Toxicol* 93, 186-190

17. Myers, C. R., Myers, J. M., Kufahl, T. D., Forbes, R., and Szadkowski, A. (2011) The effects of acrolein on the thioredoxin system: implications for redox-sensitive signaling. *Mol Nutr Food Res* 55, 1361-1374

18. Pramanik, K. C., and Srivastava, S. K. (2012) Apoptosis signal-regulating kinase 1-thioredoxin complex dissociation by capsaicin causes pancreatic tumor growth suppression by inducing apoptosis. *Antioxid Redox Signal* 17, 1417-1432

19. Ouyang, M., and Shen, X. (2006) Critical role of ASK1 in the 6-hydroxydopamine-induced apoptosis in human neuroblastoma SH-SY5Y cells. *J Neurochem* 97, 234-244

20. Yang, W., Tiffany-Castiglioni, E., Koh, H. C., and Son, I. H. (2009) Paraquat activates the IRE1/ASK1/JNK cascade associated with apoptosis in human neuroblastoma SH-SY5Y cells. *Toxicol Lett* 191, 203-210

21. Benedetti, A., Comporti, M., and Esterbauer, H. (1980) Identification of 4-hydroxynonenal as a cytotoxic product originating from the peroxidation of liver microsomal lipids. *Biochim Biophys Acta* 620, 281-296

22. Schopfer, F. J., Cipollina, C., and Freeman, B. A. (2011) Formation and signaling actions of electrophilic lipids. *Chem Rev* 111, 5997-6021

23. Fritz, K. S., Kellersberger, K. A., Gomez, J. D., and Petersen, D. R. (2012) 4-HNE adduct stability characterized by collision-induced dissociation and electron transfer dissociation mass spectrometry. *Chem Res Toxicol* 25, 965-970

24. West, J. D., and Marnett, L. J. (2006) Endogenous reactive intermediates as modulators of cell signaling and cell death. *Chem Res Toxicol* 19, 173-194

25. Ichijo, H., Nishida, E., Irie, K., ten Dijke, P., Saitoh, M., Moriguchi, T., Takagi, M., Matsumoto, K., Miyazono, K., and Gotoh, Y. (1997) Induction of apoptosis by ASK1, a mammalian MAPKKK that activates SAPK/JNK and p38 signaling pathways. *Science* 275, 90-94

26. Johannessen, C. M., Boehm, J. S., Kim, S. Y., Thomas, S. R., Wardwell, L., Johnson, L. A., Emery, C. M., Stransky, N., Cogdill, A. P., Barretina, J., Caponigro, G., Hieronymus, H., Murray, R. R., Salehi-Ashtiani, K., Hill, D. E., Vidal, M., Zhao, J. J., Yang, X., Alkan, O., Kim, S., Harris, J. L., Wilson, C. J., Myer, V. E., Finan, P. M., Root, D. E., Roberts, T. M., Golub, T., Flaherty, K. T., Dummer, R., Weber, B. L., Sellers, W. R., Schlegel, R., Wargo, J. A., Hahn, W. C., and Garraway, L. A. (2010) COT drives resistance to RAF inhibition through MAP kinase pathway reactivation. *Nature* 468, 968-972

27. Zhang, H., Liu, Q., Zimmerman, L. J., Ham, A. J., Slebos, R. J., Rahman, J., Kikuchi, T., Massion, P. P., Carbone, D. P., Billheimer, D., and Liebler, D. C. (2011) Methods for peptide and protein quantitation by liquid chromatography-multiple reaction monitoring mass spectrometry. *Mol Cell Proteomics* 10, M110.006593

28. Mani, D. R., Abbatiello, S. E., and Carr, S. A. (2012) Statistical characterization of multiple-reaction monitoring mass spectrometry (MRM-MS) assays for quantitative proteomics. *BMC Bioinformatics* 13 Suppl 16, S9

29. Addona, T. A., Abbatiello, S. E., Schilling, B., Skates, S. J., Mani, D. R., Bunk, D. M., Spiegelman, C. H., Zimmerman, L. J., Ham, A. J., Keshishian, H., Hall, S. C., Allen, S., Blackman, R. K., Borchers, C. H., Buck, C., Cardasis, H. L., Cusack, M. P., Dodder, N. G., Gibson, B. W., Held, J. M., Hiltke, T., Jackson, A., Johansen, E. B., Kinsinger, C. R., Li, J., Mesri, M., Neubert, T. A., Niles, R. K., Pulsipher, T. C., Ransohoff, D., Rodriguez, H., Rudnick, P. A., Smith, D., Tabb, D. L., Tegeler, T. J., Variyath, A. M., Vega-Montoto, L. J., Wahlander, A., Waldemarson, S., Wang, M., Whiteaker, J. R., Zhao, L., Anderson, N. L., Fisher, S. J., Liebler, D. C., Paulovich, A. G., Regnier, F. E., Tempst, P., and Carr, S. A. (2009) Multi-site assessment of the precision and reproducibility of multiple reaction monitoring-based measurements of proteins in plasma. *Nat Biotechnol* 27, 633-641

30. Kessner, D., Chambers, M., Burke, R., Agus, D., and Mallick, P. (2008) ProteoWizard: open source software for rapid proteomics tools development. *Bioinformatics* 24, 2534-2536

31. Tabb, D. L., Fernando, C. G., and Chambers, M. C. (2007) MyriMatch: highly accurate tandem mass spectral peptide identification by multivariate hypergeometric analysis. *J Proteome Res* 6, 654-661

32. Dasari, S., Chambers, M. C., Martinez, M. A., Carpenter, K. L., Ham, A. J., Vega-Montoto, L. J., and Tabb, D. L. (2012) Pepitome: evaluating improved spectral library search for identification complementarity and quality assessment. *J Proteome Res* 11, 1686-1695

33. Eng, J. K., Jahan, T. A., and Hoopmann, M. R. (2013) Comet: an open-source MS/MS sequence database search tool. *Proteomics* 13, 22-24

34. Kim, S., and Pevzner, P. A. (2014) MS-GF+ makes progress towards a universal database search tool for proteomics. *Nat Commun* 5, 5277

35. Elias, J. E., and Gygi, S. P. (2007) Target-decoy search strategy for increased confidence in large-scale protein identifications by mass spectrometry. *Nat Methods* 4, 207-214

36. Ma, Z. Q., Dasari, S., Chambers, M. C., Litton, M. D., Sobecki, S. M., Zimmerman, L. J., Halvey, P. J., Schilling, B., Drake, P. M., Gibson, B. W., and Tabb, D. L. (2009) IDPicker 2.0: Improved protein assembly with high discrimination peptide identification filtering. *J Proteome Res* 8, 3872-3881

37. Choi, H., Larsen, B., Lin, Z. Y., Breitkreutz, A., Mellacheruvu, D., Fermin, D., Qin, Z. S., Tyers, M., Gingras, A. C., and Nesvizhskii, A. I. (2011) SAINT: probabilistic scoring of affinity purification-mass spectrometry data. *Nat Methods* 8, 70-73

38. Teo, G., Liu, G., Zhang, J., Nesvizhskii, A. I., Gingras, A. C., and Choi, H. (2014) SAINTexpress: improvements and additional features in Significance Analysis of INTeractome software. *J Proteomics* 100, 37-43

39. Goldfarb, D., Hast, B. E., Wang, W., and Major, M. B. (2014) Spotlite: web application and augmented algorithms for predicting co-complexed proteins from affinity purification--mass spectrometry data. *J Proteome Res* 13, 5944-5955

40. MacLean, B., Tomazela, D. M., Shulman, N., Chambers, M., Finney, G. L., Frewen, B., Kern, R., Tabb, D. L., Liebler, D. C., and MacCoss, M. J. (2010) Skyline: an open source document editor for creating and analyzing targeted proteomics experiments. *Bioinformatics* 26, 966-968

41. Sherrod, S. D., Myers, M. V., Li, M., Myers, J. S., Carpenter, K. L., Maclean, B., Maccoss, M. J., Liebler, D. C., and Ham, A. J. (2012) Label-free quantitation of protein modifications by pseudo selected reaction monitoring with internal reference peptides. *J Proteome Res* 11, 3467-3479

42. Liu, H., Sadygov, R. G., and Yates, J. R., 3rd (2004) A model for random sampling and estimation of relative protein abundance in shotgun proteomics. *Anal Chem* 76, 4193-4201

43. Jonckheere, A. R. (1954) A distribution-free k-sample test against ordered alternatives. *Biometrika* 41, 133-145

44. Terpstra, T. (1952) The asymptotic normality and consistency of Kendall's test against trend, when ties are present in one ranking. *Indagationes Mathematicae* 14, 327-333

45. Kruskal, W. H., and Wallis, W. A. (2012) Use of Ranks in One-Criterion Variance Analysis.

46. Dunn, O. J. (1964) Multiple comparisons using rank sums. *Technometrics* 6, 241-252

47. Mann, H. B., and Whitney, D. R. (1947) On a test of whether one of two random variables is stochastically larger than the other. *The annals of mathematical statistics*, 50-60

48. Takeda, K., Shimozono, R., Noguchi, T., Umeda, T., Morimoto, Y., Naguro, I., Tobiume, K., Saitoh, M., Matsuzawa, A., and Ichijo, H. (2007) Apoptosis signal-regulating kinase (ASK) 2 functions as a mitogen-activated protein kinase kinase kinase in a heteromeric complex with ASK1. *J Biol Chem* 282, 7522-7531

49. Iriyama, T., Takeda, K., Nakamura, H., Morimoto, Y., Kuroiwa, T., Mizukami, J., Umeda, T., Noguchi, T., Naguro, I., Nishitoh, H., Saegusa, K., Tobiume, K., Homma, T., Shimada, Y., Tsuda, H., Aiko, S., Imoto, I., Inazawa, J., Chida, K., Kamei, Y., Kozuma, S., Taketani, Y., Matsuzawa, A., and Ichijo, H. (2009) ASK1 and ASK2 differentially regulate the counteracting roles of apoptosis and inflammation in tumorigenesis. *Embo j* 28, 843-853

50. Wang, X. S., Diener, K., Tan, T. H., and Yao, Z. (1998) MAPKKK6, a novel mitogen-activated protein kinase kinase kinase, that associates with MAPKKK5. *Biochem Biophys Res Commun* 253, 33-37

51. Ortner, E., and Moelling, K. (2007) Heteromeric complex formation of ASK2 and ASK1 regulates stress-induced signaling. *Biochem Biophys Res Commun* 362, 454-459

52. Cockrell, L. M., Puckett, M. C., Goldman, E. H., Khuri, F. R., and Fu, H. (2010) Dual engagement of 14-3-3 proteins controls signal relay from ASK2 to the ASK1 signalosome. *Oncogene* 29, 822-830

53. So, J., Pasculescu, A., Dai, A. Y., Williton, K., James, A., Nguyen, V., Creixell, P., Schoof, E. M., Sinclair, J., Barrios-Rodiles, M., Gu, J., Krizus, A., Williams, R., Olhovsky, M., Dennis, J. W., Wrana, J. L., Linding, R., Jorgensen, C., Pawson, T., and

Colwill, K. (2015) Integrative analysis of kinase networks in TRAIL-induced apoptosis provides a source of potential targets for combination therapy. *Sci Signal* 8, rs3

54. Naguro, I., Umeda, T., Kobayashi, Y., Maruyama, J., Hattori, K., Shimizu, Y., Kataoka, K., Kim-Mitsuyama, S., Uchida, S., Vandewalle, A., Noguchi, T., Nishitoh, H., Matsuzawa, A., Takeda, K., and Ichijo, H. (2012) ASK3 responds to osmotic stress and regulates blood pressure by suppressing WNK1-SPAK/OSR1 signaling in the kidney. *Nat Commun* 3, 1285

55. Kaji, T., Yoshida, S., Kawai, K., Fuchigami, Y., Watanabe, W., Kubodera, H., and Kishimoto, T. (2010) ASK3, a novel member of the apoptosis signal-regulating kinase family, is essential for stress-induced cell death in HeLa cells. *Biochem Biophys Res Commun* 395, 213-218

56. Subramanian, R. R., Zhang, H., Wang, H., Ichijo, H., Miyashita, T., and Fu, H. (2004) Interaction of apoptosis signal-regulating kinase 1 with isoforms of 14-3-3 proteins. *Exp Cell Res* 294, 581-591

57. Sturchler, E., Feurstein, D., Chen, W., McDonald, P., and Duckett, D. (2013) Stress-induced nuclear import of apoptosis signal-regulating kinase 1 is mediated by karyopherin alpha2/beta1 heterodimer. *Biochim Biophys Acta* 1833, 583-592

58. Hwang, I. S., Jung, Y. S., and Kim, E. (2002) Interaction of ALG-2 with ASK1 influences ASK1 localization and subsequent JNK activation. *FEBS Lett* 529, 183-187

59. Schmidt, C., Lenz, C., Grote, M., Luhrmann, R., and Urlaub, H. (2010) Determination of protein stoichiometry within protein complexes using absolute quantification and multiple reaction monitoring. *Anal Chem* 82, 2784-2796

60. Hochleitner, E. O., Kastner, B., Frohlich, T., Schmidt, A., Luhrmann, R., Arnold, G., and Lottspeich, F. (2005) Protein stoichiometry of a multiprotein complex, the human spliceosomal U1 small nuclear ribonucleoprotein: absolute quantification using isotope-coded tags and mass spectrometry. *J Biol Chem* 280, 2536-2542

61. Cheng, D., Hoogenraad, C. C., Rush, J., Ramm, E., Schlager, M. A., Duong, D. M., Xu, P., Wijayawardana, S. R., Hanfelt, J., Nakagawa, T., Sheng, M., and Peng, J. (2006) Relative and absolute quantification of postsynaptic density proteome isolated from rat forebrain and cerebellum. *Mol Cell Proteomics* 5, 1158-1170

62. van Nuland, R., Smits, A. H., Pallaki, P., Jansen, P. W., Vermeulen, M., and Timmers, H. T. (2013) Quantitative dissection and stoichiometry determination of the human SET1/MLL histone methyltransferase complexes. *Mol Cell Biol* 33, 2067-2077

63. Ko, Y. G., Kang, Y. S., Park, H., Seol, W., Kim, J., Kim, T., Park, H. S., Choi, E. J., and Kim, S. (2001) Apoptosis signal-regulating kinase 1 controls the proapoptotic function of death-associated protein (Daxx) in the cytoplasm. *J Biol Chem* 276, 39103-39106

64. Tristan, C. A., Ramos, A., Shahani, N., Emiliani, F. E., Nakajima, H., Noeh, C. C., Kato, Y., Takeuchi, T., Noguchi, T., Kadowaki, H., Sedlak, T. W., Ishizuka, K., Ichijo, H., and Sawa, A. (2015) Role of apoptosis signal-regulating kinase 1 (ASK1) as an activator of the GAPDH-Siah1 stress-signaling cascade. *J Biol Chem* 290, 56-64

65. Mochida, Y., Takeda, K., Saitoh, M., Nishitoh, H., Amagasa, T., Ninomiya-Tsuji, J., Matsumoto, K., and Ichijo, H. (2000) ASK1 inhibits interleukin-1-induced NF-kappa B activity through disruption of TRAF6-TAK1 interaction. *J Biol Chem* 275, 32747-32752

66. Kwon, J. E., Kim, E. K., and Choi, E. J. (2011) Stabilization of the survival motor neuron protein by ASK1. *FEBS Lett* 585, 1287-1292

67. Miyakawa, K., Matsunaga, S., Kanou, K., Matsuzawa, A., Morishita, R., Kudoh, A., Shindo, K., Yokoyama, M., Sato, H., Kimura, H., Tamura, T., Yamamoto, N., Ichijo, H., Takaori-Kondo, A., and Ryo, A. (2015) ASK1 restores the antiviral activity of APOBEC3G by disrupting HIV-1 Vif-mediated counteraction. *Nat Commun* 6, 6945

68. Okazaki, T., Higuchi, M., Takeda, K., Iwatsuki-Horimoto, K., Kiso, M., Miyagishi, M., Yanai, H., Kato, A., Yoneyama, M., Fujita, T., Taniguchi, T., Kawaoka, Y., Ichijo, H., and Gotoh, Y. (2015) The ASK family kinases differentially mediate induction of type I interferon and apoptosis during the antiviral response. *Sci Signal* 8, ra78

69. Kawarazaki, Y., Ichijo, H., and Naguro, I. (2014) Apoptosis signal-regulating kinase 1 as a therapeutic target. *Expert Opin Ther Targets* 18, 651-664

# CHAPTER III

# DYNAMIC PHOSPHORYLATION OF APOPTOSIS SIGNAL REGULATING KINASE 1 (ASK1) IN RESPONSE TO OXIDATIVE AND ELECTROPHILIC STRESS

## Introduction

Apoptosis signal-regulating kinase 1 (ASK1) is a mitogen-activated protein kinase kinase kinase that acts as a critical sensor for cell stress. Activation of ASK1 results in downstream activation of p38 and JNK and subsequent stress response and apoptosis (1, 2). ASK1 is known to be activated by a number of stress signals (3-18) and has been most notably studied for its role in transducing cellular responses to oxidative stress (3-5, 19). Because ASK1 can be activated by such a broad range of signals, its activity must be carefully regulated by the cell. One such means of regulation is the dynamic assembly of a multiprotein complex around ASK1 to control its function (see chapters 1 and 2).

A second important method of ASK1 regulation is through differential phosphorylation. Five phosphorylated residues have been reported as important for ASK1 regulation (Ser-83, Tyr-718, Thr-838, Ser-966, and Ser-1033), and another 24 phosphorylations are listed on PhosphoSitePlus out of a total of 231 potential phosphorylation sites in the full-length protein (19-29). The additional 24 sites were identified by global MS profiling studies and have not been examined for dynamic changes in response to activation of ASK1. The five known dynamic sites (four

inactivating and one activating – Thr-838) have all been studied in the context of oxidative stress through treatment of cells with either TNF$\alpha$ or $H_2O_2$. What is not known is whether these five sites (and potentially others) serve as master phospho-regulators of ASK1 function for all stress signals or if dynamic phosphorylation at these sites is specific for oxidative stress only. Indeed, the broader question of whether chemically distinct activators of ASK1 signaling produce distinct sets of dynamic phosphorylations has never been addressed.

In order to test the generalizability of the phosphoregulation of ASK1, I chose to map phosphorylation sites in response to treatment of cells with either $H_2O_2$ or 4-hydroxy-2-nonenal (HNE). HNE is a prototypical electrophile that is generated endogenously under conditions of oxidative stress, but which acts through covalent adduction of protein cysteine thiol residues, as opposed to the reversible oxidation of protein thiols by $H_2O_2$ (30-33). HNE has been previously shown to activate ASK1 and the downstream pathway to a similar degree as $H_2O_2$ (8) but whether or not ASK1 senses these two chemicals by the same method is unknown.

Because of the mechanistic difference between the reversible modification of ASK1 by $H_2O_2$ and the irreversible modification of ASK1 by HNE, I hypothesized that unique dynamic phosphorylation sites of ASK1 would be observed for each stressor, ultimately culminating in activation of the same stress pathway. To test this hypothesis, I used both data-dependent shotgun liquid chromatography-tandem mass spectrometry (LC-MS/MS) and parallel reaction monitoring (PRM) methods to map sites of phosphorylation and HNE adduction on ASK1 in response to treatment of an ASK1-expressing cell line with $H_2O_2$ and HNE. I report here the interplay between oxidative

and electrophilic activation of ASK1 and the phosphorylative response of the protein to these stressors. This work was performed in collaboration with Carlos Morales Betanzos, Ph.D., a postdoctoral fellow in the Liebler laboratory.

## Experimental Procedures

*DNA construct*

The tandem-tagged construct for ASK1 (ASK1-TAG) was generated in a pcDNA3.1 plasmid (Life Technology, Grand Island, NY) by Genscript (Piscataway, NJ). The ASK1 sequence previously described (1) was modified to exchange the HA tag to a tandem HA-FLAG tag and is available from Addgene (#69726).

*Antibodies*

All ASK1 protein IPs were performed with EZview red anti-FLAG beads (Sigma-Aldrich, St. Louis, MO). Western blots were performed with the following primary antibodies: FLAG (8146S), phosphoP38 (9211S), P38 (9212S), phosphoJNK (4668S), JNK (9252S), ASK1 phosphoSer-83 (3761S), ASK1 phosphoSer-966 (3764S), and ASK1 phosphoThr-838 (3765S) from Cell Signaling Technology (Danvers, MA), and ASK1 (SC-5294; Santa Cruz Biotechnology, Dallas, TX). Secondary antibodies were from Life Technology: anti-mouse 680 (A21058) and anti-rabbit 680 (A21109).

*Cell lines and cell culture*

HEK-293 cells (CRL-1573; ATCC) were grown in DMEM (12430; Life Technology) supplemented with 10% fetal bovine serum (Atlas Biologicals, Fort Collins, CO) at 37°C in a humidified atmosphere with 5% $CO_2$. The ASK1-expressing cell line was generated from HEK-293 cells by transfecting the ASK1-TAG plasmid into cells using Lipofectamine 2000 (Life Technology) following the manufacturer's instructions. Twenty-four hr following transfection, cells were split 1:10 and, after an additional 24 hr, were switched into selection medium consisting of the HEK-293 medium described above supplemented with 1.5 mg/mL Geneticin (Life Technology) and maintained in this medium for two weeks to select for cells expressing the plasmid of interest. Stock cell cultures were maintained thereafter in HEK-293 media supplemented with 1 mg/mL Geneticin. Prior to harvesting, cells were plated in 15 cm dishes in HEK-293 media supplemented with 0.5 mg/mL Geneticin.

For the phosphorylation site studies, all cells were treated with 20 μM MG-132 (M8699; Sigma-Aldrich) in serum-free media for 2 hr at 37 °C prior to treatment with stressors. Following proteasomal inhibition, cells were treated with ethanol (vehicle control-HNE, 0.08% v/v), 10 μM HNE, 50 μM HNE, PBS (vehicle control $H_2O_2$), 500 μM $H_2O_2$, or 5,000 μM $H_2O_2$. The treatments were prepared in serum-free media and placed on the cells for 1 hr at 37°C. Cells were then harvested with a cell scraper in the treatment medium and immediately centrifuged at 100 x g for 5 min at 4 °C. The cell pellets then were washed twice with ice cold PBS and stored at -80 °C until use.

For the HNE adduct site-mapping studies, HEK-293 cells transiently expressing ASK1-TAG were generated by transfection with Lipofectamine according to the

manufacturer's instructions. These cells were then treated with 20 μM MG-132 for 2 hr at 37 °C prior to treatment with 50 μM HNE for 1 hr at 37 °C. These cells were then harvested and pelleted as described above.

*Cell viability assays*

Cells were plated in a 96-well plate at a density of 10,000 cells/well and allowed to grow for 24 hr. Medium was then removed and replaced with 100 μL/well of serum-free DMEM containing the appropriate concentration of HNE or $H_2O_2$ and the cells were incubated at 37°C for 24 hr. To measure cell viability, 10 μL/well of WST reagent (Sigma, 11644807001) was added and the cells were incubated for 1 hr. Absorbance readings then were taken at 450 nm and 650 nm with a Spectramax M4 spectrophotometer (Molecular Devices, Sunnyvale, CA) according to the manufacturer's protocol.

*Immunoprecipitation and western blotting*

Frozen cell pellets were lysed on ice in 500 μL of NETN buffer (50 mM HEPES pH 7.5, 150 mM NaCl, and 1% Igepal supplemented with 10 μL/mL of HALT [78444; Life Technology] protease and phosphatase inhibitor), per 15 cm plate for 30 min with occasional inversion. Lysates then were clarified by centrifugation at 10,000 × g for 10 min at 4 °C. Protein in the clarified lysates was measured with the BCA assay (Life Technology). Protein concentrations then were adjusted to 2 mg/mL. HNE-treated samples that were used for adduction site-mapping studies were further reduced with 2 mM sodium borohydride (Sigma Aldrich) for 2 hr at room temperature with occasional

inversion; all other samples were not reduced. Next, 5 mg of total protein was added in a final volume of 2.5 mL to antibody beads pre-washed with NETN. For each IP, a 50 μL slurry of antibody-bead conjugate was washed twice with 1 mL of NETN prior to incubation with protein lysates. After addition of the protein lysate, the beads were rotated at 4 °C for 1 hr to allow for capture of the target protein. Following incubation, the beads were pelleted by centrifugation at 100 × g and the supernatant was discarded. The beads were then washed twice with 1 mL of NETN buffer and the bound protein was resuspended in 80 μL of lithium dodecyl sulfate (LDS) sample buffer diluted 1:1 with NETN and supplemented with 50 mM dithiothreitol (DTT). The samples were then frozen at -80 °C until use.

For western blot analysis, cell lysis and IP were carried out as described above. Gels were loaded with either 20 μg of input protein or 2 μL of IP and run for 50 min at a constant 180 V. Proteins then were electrophoretically transferred to PVDF membranes (Life Technology) using the BioRad (Hercules, California) wet transfer system operated at a constant 300 mA current for 90 min at 4 °C. Membranes were blocked in a 1:1 mixture of Tris-buffered saline plus 0.05% Tween-20 (TBST) and blocking buffer (MB-070; Rockland, Limerick, PA) for 1 hr at room temperature while rocking. Primary antibodies were diluted (1:2000 for tag antibodies, 1:1000 for protein antibodies, and 1:750 for phospho antibodies) in the same buffer used for blocking, added to the membrane, and incubated at 4 °C overnight with rocking. After incubation, the membranes were washed three times with TBST, incubated with the appropriate secondary antibody diluted 1:10,000 in the same buffer used for the primary antibody, and allowed to rock for 30 min at room temperature. The membranes were then

washed three times with TBST, visualized using a LiCor Odyssey (Lincoln, Nebraska), and analyzed using the Image Studio Lite software (LiCor).

*Preparation of peptides for MS analyses*

Bead-bound ASK1 protein was eluted in LDS buffer and heated at 95 °C for 10 min prior to being loaded on a 10% Bis-Tris gel (NP0301; Life Technology). The gels were loaded with 35 μL of each sample elution and then were run at a constant 180 V for 3 min, after which the run was paused. Each sample lane was then re-loaded with the remaining 35 μL of each sample and the gel runs were resumed for an additional 47 min. Gels were then stained with Simply Blue safe stain (Life Technology) for 1 min in a microwave oven at maximum power and then allowed to destain in distilled water for 2-3 hr. For each sample, a single band from 100-200 kDa was cut and diced into ~1 mm cubes. The gel pieces were placed into individual Eppendorf tubes and washed twice with 200 μL of 100 mM ammonium bicarbonate (AmBic). Samples were then reduced with 5 mM DTT in AmBic for 30 min at 60 °C while shaking at 1000 rpm and then alkylated with 10 mM iodoacetamide in AmBic for 20 min in the dark at room temperature. Excess blue dye was then removed with three 200 μL washes in 50 mM AmBic:acetonitrile (1:1, v/v) and the gel pieces were dehydrated in 100% acetonitrile. The gel pieces were rehydrated in 200 μL of 25 mM AmBic with 200 ng of trypsin gold (Promega, Madison, WI) per sample and placed in a 37 °C incubator for 16 hr. Peptides were extracted from the SDS gel with three 20 min incubations in 200 μL of 60% acetonitrile / 40% water containing 1% formic acid and evaporated to dryness *in*

*vacuo*. The peptides were resuspended in 30% acetonitrile / 70% water containing 0.1% formic acid and stored at -80 °C until use.

*Mass spectrometry*

Shotgun analyses of the single gel fraction samples were carried out on a Q Exactive Plus mass spectrometer (ThermoFisher Scientific, San Jose, CA) equipped with a Proxeon nLC1000 LC (ThermoFisher Scientific) and a Nanoflex source (ThermoFisher Scientific). Peptide mixtures were evaporated *in vacuo* and resuspended in 2% acetonitrile / 98% water containing 0.1% formic acid and loaded onto an 20 cm long column with a 75 μm internal diameter (PF360-75-10-N-5; New Objective, Woburn, MA) packed with 3 μm particle size and 120 Å pore size ReproSil-Pur C18-AQ resin (Dr. Maisch GmbH, Ammerbuch-Entringen, Germany) and separated over a 180 min gradient with a mobile phase containing aqueous acetonitrile and 0.1% formic acid programmed from 2-5% acetonitrile over 5 min, then 5 to 25% acetonitrile over 150 min, then 25-90% acetonitrile over 5 min, followed by 20 min at 90% acetonitrile, all at a flow rate of 300 nL/min. A single MS1 scan from *m/z* 300-1800 at 70,000 resolution with an automatic gain control (AGC) value of 3e6 and max injection time of 64 msec was recorded as profile data. A top 10 method was used, whereby the 10 most intense precursors were automatically chosen for MS2 analysis and a dynamic exclusion window of 20 sec was employed. For each MS2 scan, a resolution of 17,500, an AGC value of 1e5, a max injection time of 175 msec, a 1.4 *m/z* isolation window, and a normalized collision energy of 27 were used and centroid data were recorded.

PRM assays were performed on the same Q Exactive Plus instrument and LC system using the same gradient described above. The PRM method consisted of an MS1 scan at 17,500 resolution with an AGC value of 3e6, max injection time of 30 msec, and scan range from *m/z* 380-1500 recorded as profile data. This was followed by 10 targeted MS2 scans at a resolution of 17,500 and with an AGC value of 1e5, a max injection time of 175 msec, a 0.5 *m/z* isolation window, a fixed first mass of 150 *m/z*, normalized collision energy of 27, and recorded as profile data. The targeted-MS2 methods were controlled with a timed inclusion list containing the target precursor *m/z* value, charge, and a 10 min retention time window that was determined from shotgun analyses.

*Data analysis*

Shotgun runs were converted to mzml format using Proteowizard version 3.0.5211 (34). The mzml files were searched using MS-GF+ version 9517 (35). A semi-tryptic search was employed with a maximum of four missed cleavages allowed. A fixed carbimidomethyl modification on cysteine, a variable oxidation on methionine, and a pyro-glu on glutamine were allowed with a maximum of 3 dynamic modifications per peptide with a precursor ion tolerance of 10 ppm and a fragment ion tolerance of 20 ppm. For phosphorylation studies, an additional variable modification of 79.966331 Da on serine, threonine, or tyrosine was employed. For the HNE adduction studies, the carbimidomethylation modification on cysteine was changed to a variable search parameter and a variable mass of 158.130680 Da for reduced HNE adducts on cysteine was used. A target-decoy search was employed using a reverse sequence database to

allow calculation of FDR for peptide-spectrum matches (36). Protein-level FDR was calculated by dividing the number of reverse sequence proteins identified by the total number of proteins identified, multiplying by 2 and converting to a percent. All search result files were parsimoniously assembled in IDPicker 3 version 3.1.8754.0 (37).

PRM runs were designed and analyzed using Skyline (38) and 3 transitions per peptide were used for quantitation. To normalize the data between independent runs, the integrated peak area for each peptide was divided by the total quantifiable signal observed in each run. This normalization corrected for both instrumental variance and slight sample to sample discrepancies that occurred during immunoprecipitation.

All phosphorylation site assignments were confirmed by manual spectrum annotation as previously described (39). In summary, for each peptide, precursor purity was confirmed by MS1, major peaks were unambiguously assigned, and direct evidence of site modifications was required. The precursor purity was confirmed by examining the MS1 scan immediately prior to peptide isolation to determine if any mass aside from the targeted peptide fell within the isolation window employed for the run (1.4 m/z for shotgun or 0.5 m/z for PRM). If any other mass was present at more than 10% of the intensity of the targeted precursor, this spectrum was not considered for further evaluation. Additionally, the selected peptide peak was required to have no more than 10 ppm mass error in the MS1 scan. Spectra that passed this filter were then manually annotated using mMass version 5.5.0 (40, 41), which allowed for automated spectral annotations of b- and y-ions, internal fragment ions, neutral loss ions for $H_2O$, $NH_3$, CO, and $H_3PO_4$, as well as annotations of phospho-specific mass-shifted ions. Assigned peaks were required to explain at least half of the total ion current for each spectrum to

be considered acceptable. Furthermore, for peptides with phosphorylated threonine or serine residues, the presence of a phosphoric acid neutral loss peak (from either the precursor or a fragment ion) was required for the spectrum to be accepted. Peptides that passed all of these filters were then divided into two categories: peptides with or without ambiguous site localizations. Peptides with ambiguous PTM site localizations were those where more than one modifiable residue was present in the sequence such that the PTM could not be definitively assigned to one residue (e.g. a peptide with two side-by-side serines). Unambiguous PTM assignments were those spectra where no other site-assignment of the PTM could reasonably explain the MS/MS data.

*Experimental Design and Statistical Rationale*

Treatment of ASK1-TAG cells by HNE and $H_2O_2$ were each performed in biological quadruplicate (i.e., in four separate cultures of cells). PRM analyses of phosphorylated peptides in HNE-treated cells were performed in triplicate; all other MS assays for phosphopeptide detection and quantitation were performed in quadruplicate. The HNE adduct site-mapping experiments were performed in biological triplicate. Statistical comparisons of the relative amount of each phosphorylated peptide were performed using the Student's t-test as pair-wise comparisons of each treatment concentration to the zero level treatment. Replicate numbers were chosen to be sufficient to evaluate reproducibility and provide enough data points for the t-test.

## Results

*Establishment of experimental system*

In order to investigate the differential stress-sensing ability of ASK1, I first stably expressed a tandem-tagged version of the ASK1 protein (ASK1-TAG) in HEK-293 cells. I then characterized the response of these cells to HNE and $H_2O_2$ treatment using WST cell survivability assays and Western blot-based MAPK pathway activation assays. In the 24 hr WST assay, the treated cells were found to have an $EC_{50}$ concentration of approximately 10 μM for HNE and 36 μM for $H_2O_2$ (Fig III-1 A & B). Despite the low $EC_{50}$ value obtained for the $H_2O_2$ cells, use of this concentration in a one hr exposure produced minimal stress activation of the ASK1 MAPK pathway (data not shown). Thus, I conducted a dose-escalation experiment at higher concentrations of $H_2O_2$ to find a treatment level at which the downstream pathway was activated similarly to treatment with HNE at 10 μM and 50 μM (Fig. III-1C). Based on the results of the pathway activation Western analyses, I chose to use 0, 10, and 50 μM HNE and 0, 500, and 5,000 μM $H_2O_2$ for all further studies.

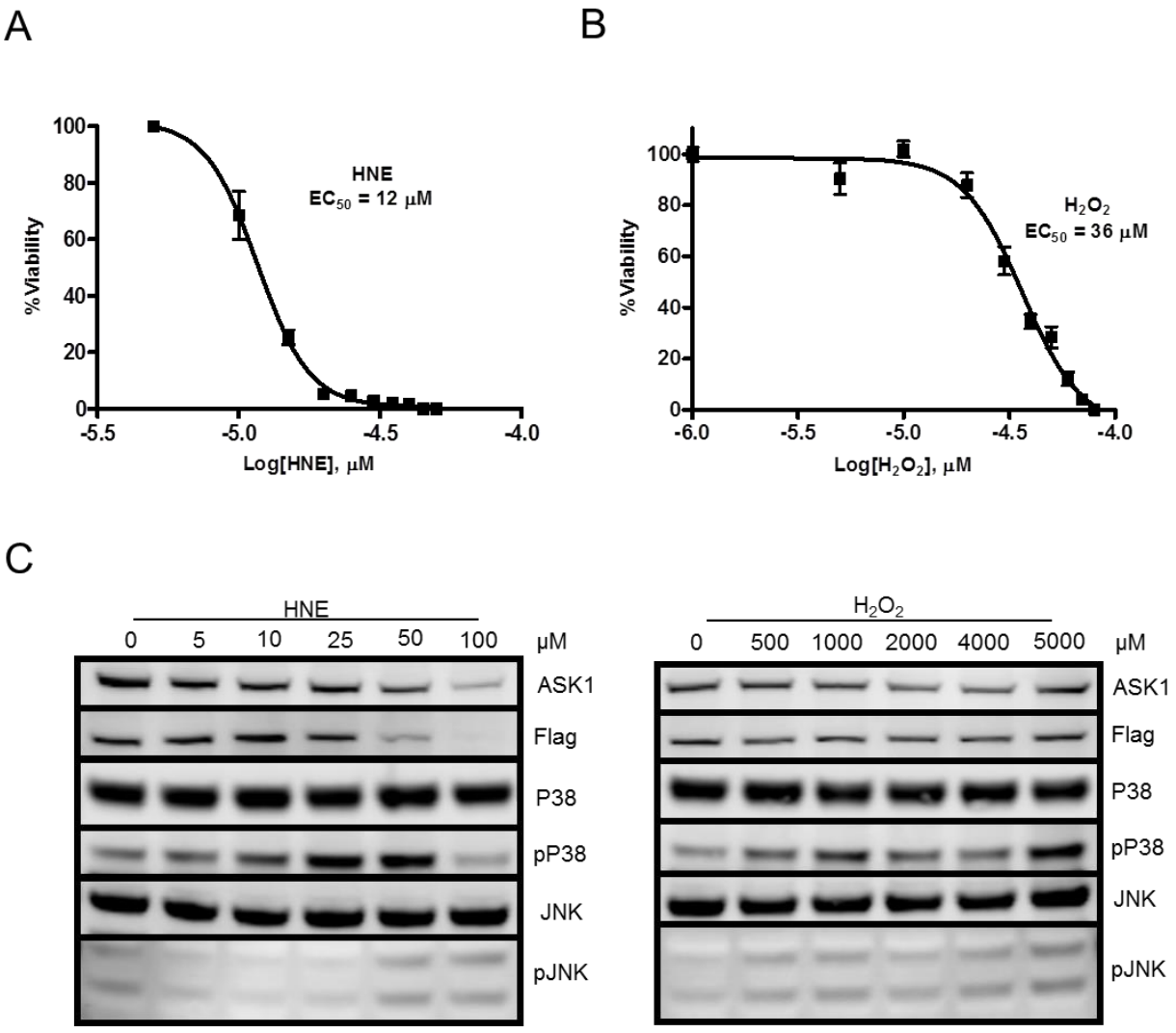


**Figure III-1. ASK1-TAG cell characterization.** Twenty-four hr WST-based cell death assays were performed with (A) HNE and (B) $H_2O_2$ to determine the $EC_{50}$ concentration for each compound in the cell line. (C) Western blot showing activation of the ASK1 MAPK pathway after 1 hr with each compound at varying concentrations.

*Purification of phosphorylated ASK1 peptides*

In order to identify phosphorylated ASK1 peptides, the ASK1 cells were first blocked with MG-132 to inhibit proteasomal degradation and then treated with either HNE or $H_2O_2$ at the concentrations described above. Following treatment, cells were harvested and lysed, and the tagged ASK1 protein was immunopurified with anti-FLAG beads. The purified ASK1 was separated by one-dimensional gel electrophoresis and analyzed by MS as shown in figure III-2.

I chose to employ a biphasic approach to identifying phosphorylated ASK1 peptides by first performing a data-dependent shotgun analysis on the immunopurified samples in order to identify as many potential sites of phosphorylation as possible (phase 1). I next targeted all of these sites by reanalyzing the same samples with a scheduled PRM method to quantify each peptide (phase 2). I then performed manual annotation of the putative phosphopeptide spectra obtained in the PRM analysis to confirm which sites were truly phosphorylated. Integrated peak areas for this final list of validated sites were used for concentration-dependent quantitation of each phosphopeptide at each concentration level compared to the control (0 μM) level. Table III-1 lists all of the phosphopeptides in each treatment condition that were found in the shotgun and PRM analyses and passed manual validation criteria.

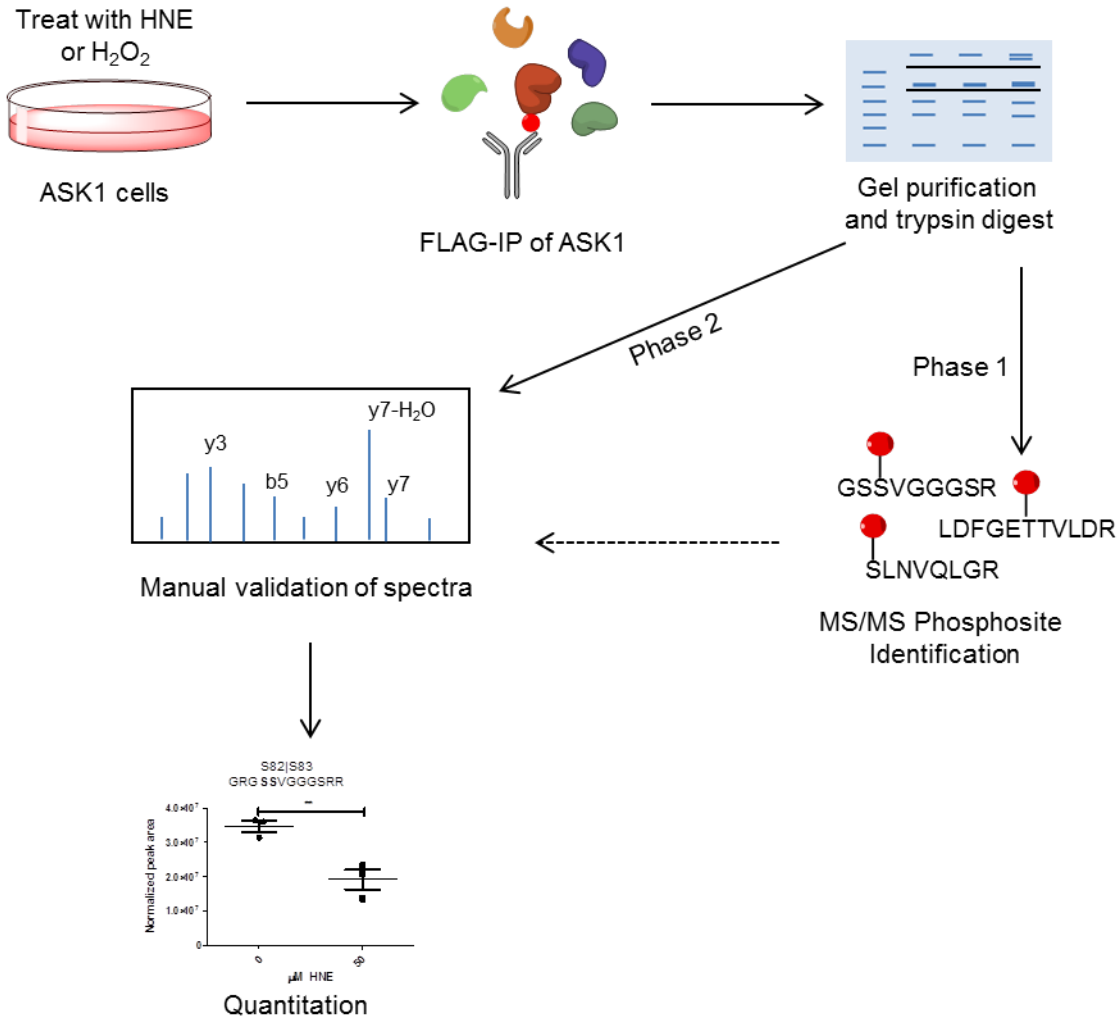


**Figure III-2. Workflow for identification, validation, and quantitation of phosphorylated peptides on ASK1.**

**Table III-1. Manually validated phosphorylation sites identified by MS in ASK1 under two different stress stimuli.**

| Status[1] | A.A. site[2] | Stimulation | Identified sequences |
|---|---|---|---|
| Known | S82/83 | Both | G**SS**VGGGSRR |
| Known | S82/83 | Both | GRG**SS**VGGGSR |
| Known | S82/83 | Both | GRG**SS**VGGGSRR |
| Known | S82/83 | $H_2O_2$ | G**SS**VGGGSR |
| Novel | T140/141 | HNE | LDFGE**TT**VLDR |
| Novel | S268/269 | $H_2O_2$ | VAQAS**SS**QYFR |
| Novel | Y355 | $H_2O_2$ | FH**Y**AFALNR |
| Known | T947/S952 | HNE | KKK**T**QPKL**S**ALSAGSNEYLR |
| Known | T947/S952 | Both | KK**T**QPKL**S**ALSAGSNEYLR |
| Novel | S955 | Both | LSAL**S**AGSNEYLR |
| Known | S958 | Both | LSALSAG**S**NEYLR |
| | S955/S958 | HNE | TQPKLSAL**S**AG**S**NEYLR |
| | S955/S958 | HNE | KTQPKLSAL**S**AG**S**NEYLR |
| Novel | T1000/S1004 | HNE | **T**RAK**S**CGERDVKGIR |
| Novel | T1000/S1004 | HNE | TRAK**S**CGERDVK |
| Novel | S1004 | Both | AK**S**CGERDVK |
| Known | T1059 | $H_2O_2$ | IL**T**EDQDKIVR |
| Novel | S1240 | HNE | **S**LNVQLGR |

[1]Known=previously reported site, Novel=unreported phosphorylation site
[2]In some cases, site assignment may remain ambiguous even after manual validation. Here, site assignment is presented for the residues with the most supporting evidence.

For the HNE-treated samples, an initial list of 25 putative phosphosites from the shotgun data was reduced to 13 manually validated sites. In the $H_2O_2$-treated samples, an initial 23 putative phosphorylation sites were reduced to 12 manually validated sites. For many of these peptides, the exact site of phosphorylation could not be localized by the MS/MS evidence. However, in all cases, I was able to narrow the potential list of sites down to a maximum of two residues, which were often adjacent, but was unable to distinguish between them due to a lack of definitive evidence for one site over the other. In total, there were 10 unique sites identified between both treatments and four of these were present in both HNE and $H_2O_2$ treated samples. Of these 10 sites, six have not previously been reported. Annotated MS/MS spectra for each of these sites are provided in Fig. B-1.

Of the five known dynamic phosphorylation sites, only one (Ser-83) was detected in my MS experiments. For the other four sites, Tyr-718 and Ser-1033 were originally identified in different stress and cellular contexts than were employed here and have not been observed in response to $H_2O_2$ stress. Ser-966 was been observed to be dynamic in response to oxidative stress before but was not observed here, possibly due to the fact that the tryptic peptide would have been fairly long (28 amino acids) and may not have ionized well. Even if it had been detected, it would have contained 8 serine residues, which would have made site localization impossible. Thr-838 is the sole known activating site on ASK1 and is expected to be observed as dynamic in response to both stressors used here. However the peptide containing this site was not detected in the PRM runs, is also somewhat long (24 amino acids), and contains four threonine residues. In an effort to obtain information on this site, I purchased a synthetic standard

for the phosphorylated peptide but was unable to reliably detect it except at very high concentrations (data not shown) which indicates that this peptide may be poorly ionized.

*Validation of MS methodology and comparison to antibody-based methods*

In order to validate the MS methodology, I compared Western blot-based results for a well-characterized phosphorylation in ASK1 (Ser-83) to the PRM results (Fig. III-3). In response to treatment with HNE, both the Western blot and the PRM results show a decrease in the amount of phosphorylation at Ser-83. Because the peptide that contains Ser-83 also contains a serine at position 82, I was not able to differentiate between the two potential phosphorylation sites with the MS/MS data. However, in this case the assignment to Ser-83 is supported also by previous literature evidence, which includes mutational analyses (22, 42).

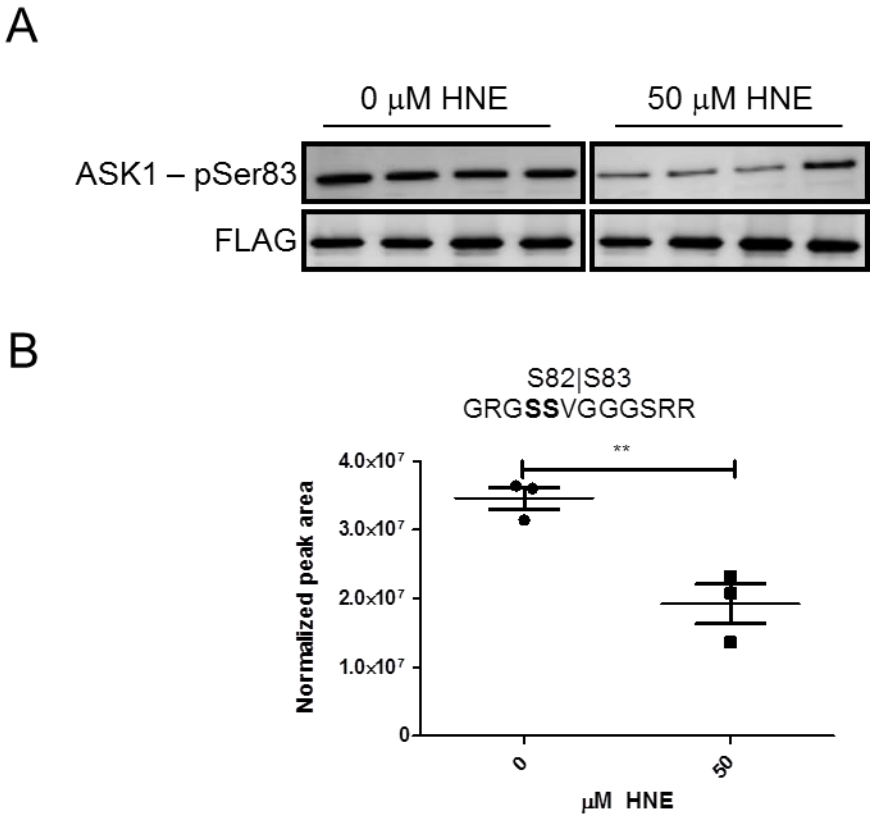


**Figure III-3. Comparison of Western blot and PRM for pS83 detection.** (A) Western blot of ASK1-pS83 and the FLAG tag in ASK1-TAG cells with or without HNE treatment. (B) Quantitation of the pS83 containing peptide in PRM assays at both concentration points.

*Dynamics of phosphorylation sites in HNE- and $H_2O_2$- treated samples*

In ASK1-TAG cells treated with three concentrations of HNE, 13 phosphopeptides covering six different phosphorylation sites were quantified (Fig. B-2). Of the six phosphosites, five exhibited a significant dynamic response to HNE treatment in at least one of the two treatment levels compared to the zero treatment samples (Fig. III-4A).

After treatment of the cells with $H_2O_2$, 12 phosphopeptides covering nine different phosphorylation sites were quantified (Fig. B-3). Of these nine phosphosites, seven displayed significant concentration-based dynamic responses to at least one of the treatment levels compared to the zero treatment level (Fig. III-4B).

In some cases, peptides exhibited consistent trends across both concentration levels for one of the stressors, but failed to show a significant difference in one of the comparisons due to a high variance in the measurements for that treatment level. For example, in Fig. III-4A, the peptide for S82|S83 shows significance for only the 50 μM v 0 μM comparison, even though the average fold change is very similar for the 10 μM v 0 μM comparison. As can be seen from Fig. B-2A (2), there is one high measured value in the 10 μM treatment that eliminates the ability to statistically characterize this peptide at this concentration.

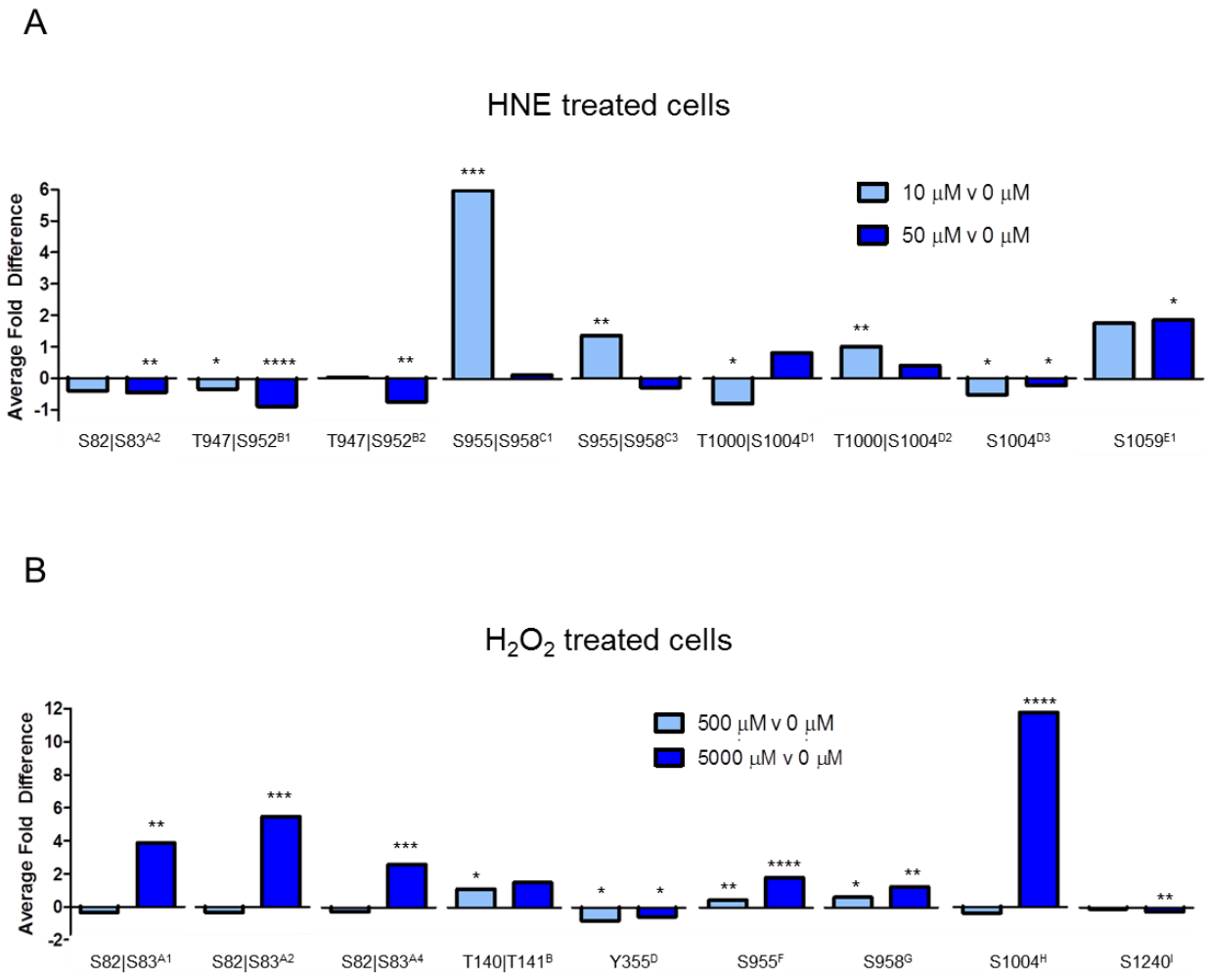


**Figure III-4. Phosphopeptides significantly different at each concentration point.** ASK1-TAG cells were treated with (A) HNE and (B) $H_2O_2$ at two different concentrations for each molecule. Average peak areas for each peptide were normalized to the 0 μM treatment level and a fold change was calculated. Peptides with significant differences from the zero point were denoted with asterisks. Each site is denoted by a superscript, which maps to supporting supplemental data figures. See figures B-2 for (A) and B-3 for (B).

*Antibody-based investigation of phosphorylation dynamics*

Of the previously reported dynamic phosphorylation sites, I only was able to observe Ser-83 with the MS method. Many of the other phosphorylation sites were on peptides that were not amenable to tryptic digestion. In order to track the activation status of ASK1, I performed Western blots with the Thr-838 ASK1 phospho-antibody (Fig. III-5). Phosphorylation of Thr-838 increased with increasing treatment of $H_2O_2$, but only exhibited a modest increase with HNE-treatment. This is in contrast to data from the previous chapter (see Figs. A-2 & A-6B) where concentration- and time-dependent increasing phosphorylation of Thr-838 was observed in response to HNE treatment. The HNE-treated lysates used here had been stored at -80 $^{o}$C for several months and it is possible that this phosphosite is labile in lysate over time.

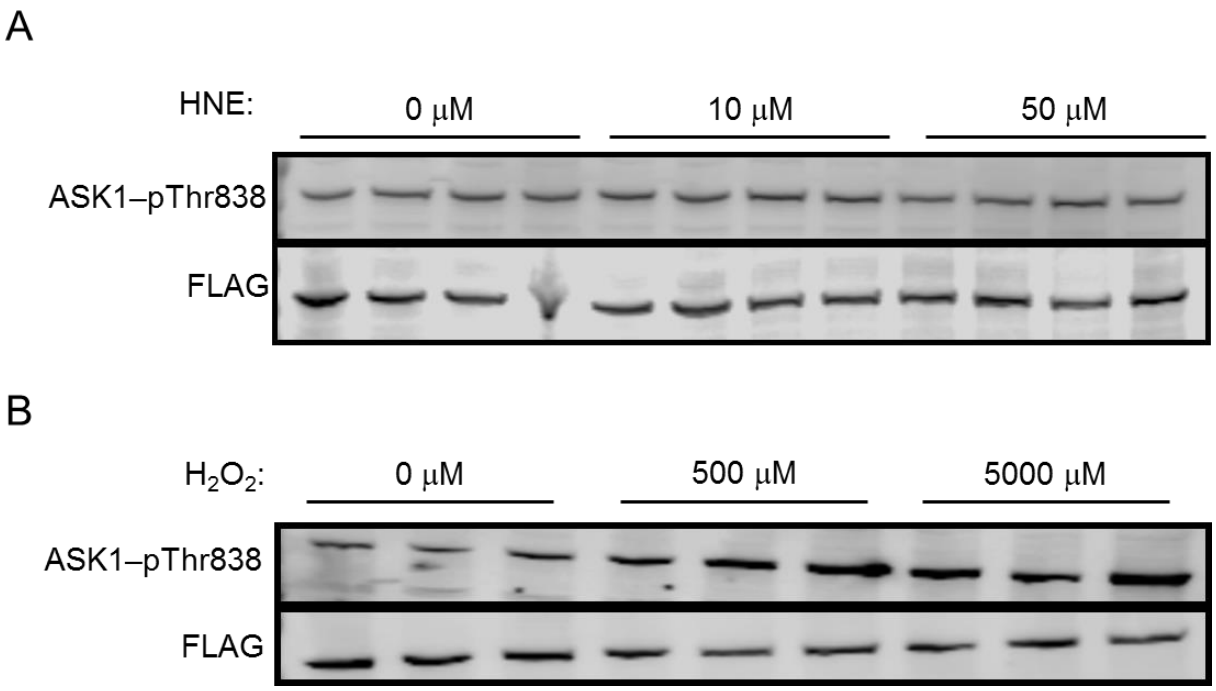


**Figure III-5. Western blot data for ASK1 activation.** Phosphorylation of Thr-838 on ASK1 was increased with increasing concentration of (A) HNE and (B) $H_2O_2$ after a 1 hr treatment.

*Identification of HNE adduction sites in HNE-treated samples*

HEK-293 cells transiently expressing ASK1-TAG were treated with MG-132 followed by 50 μM HNE treatment. Cys-928 and Cys-1005 were identified as two unique adduct sites in this experiment (Fig. B-4). Interestingly, both sites were near the C-terminus of ASK1 and the Cys-1005 site is located immediately adjacent to Ser-1004, while the Cys-928 site is located in the kinase domain.

*Comparison of phosphosites across treatments*

Between both the HNE- and the $H_2O_2$-treated cells with MS and Western blot methodologies, I identified a total of 11 phosphosites, with five of those shared between the two treatments. Figure III-6 diagrams the nine dynamic phosphosites identified by MS and summarizes how each site changes in response to each treatment as well as lists the sites of HNE adduction. Of these nine dynamic sites, five were not previously reported.

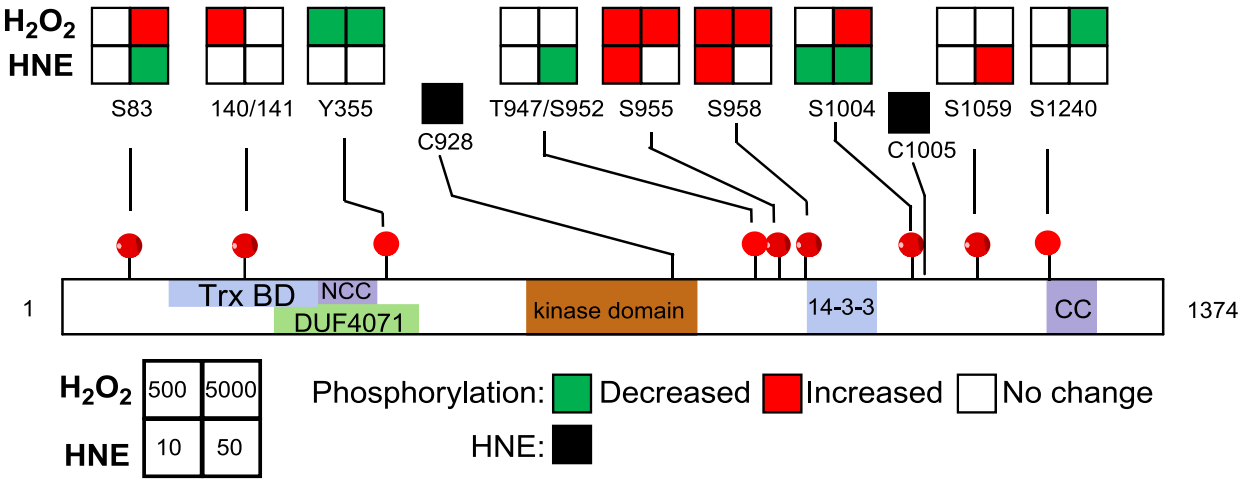


**Figure III-6. Summary of significantly dynamic phosphosites on ASK1.** Each large square represents a single phosphosite detected on ASK1. The top two interior squares are the two doses of $H_2O_2$ used (low to high -> left to right) and the bottom two interior squares are for HNE. A red square indicates that the phosphosite significantly increased in phosphorylation at the corresponding treatment level over the zero level and a green square indicates that the site significantly decreased. White squares indicate either no change or non-detection. Black squares indicate HNE adduction sites.

## Discussion

ASK1 contains 231 serine, threonine, and tyrosine residues that could be phosphorylated and has been shown to be regulated by phosphorylations on at least five of these. Four sites (Ser-83, Tyr-718, Ser-966, and Ser-1033) have been reported to negatively regulate the function of ASK1, whereas one site (Thr-838) has been reported to enhance it. All five previously reported dynamic sites were only studied via perturbation with $H_2O_2$ and TNF$\alpha$. However, ASK1 is responsive to more stress signals than just these, including the lipid electrophile HNE. It is unknown whether ASK1 senses all activating stressors by the same mechanism. I therefore asked how phosphorylation of ASK1 changes in response to HNE stress as compared to $H_2O_2$ stress in order to see if there were different sensing mechanisms for these two molecules. I first performed shotgun MS in cells treated with differing concentrations of HNE and $H_2O_2$ to identify potential sites of phosphorylation on ASK1 in response to both stressors and created a target list of putative phosphopeptides. I then utilized targeted PRM assays to track the dynamics of these putative sites in the same samples. I identified and quantified a total of 10 phosphosites on 18 different peptide forms and monitored one additional phosphosite via Western blot across both treatment groups. Of these 11 sites, 10 exhibited a dynamic response to at least one treatment condition and five were dynamic in both HNE- and $H_2O_2$-treated cells.

Most previous studies of ASK1 phosphorylation have utilized mutagenesis and Western blot methods to identify important modification sites. All of the studies describing the five previously known dynamic sites have been done in this way. However, this is a slow and laborious process that requires *a priori* knowledge of which

residues to mutate. With so many potential sites of phosphorylation in ASK1, an unbiased approach to phosphosite identification is needed. Shotgun proteomic assays have been used extensively in recent years to identify phosphorylation sites on thousands of proteins. Although MS assays have greatly expedited the identification of phosphosites, obtaining dynamic information about those sites still typically relies on mutagenesis or phospho-specific antibody generation. The approach in this study was to utilize targeted proteomics to track the dynamics of phosphorylation on all detected phosphosites in ASK1 in response to two different treatments. With this approach, I rapidly pinpointed which sites were more responsive in each treatment condition. This generated a smaller list of interesting sites that could be examined in future studies.

Of the nine phosphosites listed in Figure III-6, four were found to be dynamic in both $H_2O_2$- and HNE-treated cells, along with Thr-838 as shown in the Western blot in Figure III-5. One of these sites (pSer-83) is well known as a dynamically-modified site in ASK1. Previous reports described a decrease in phosphorylation upon treatment with oxidants and subsequent activation of ASK1. My HNE data was in line with this observation and suggests that this site may act as a general activity readout for ASK1. However, in the $H_2O_2$-treated samples, I observed an increase in the amount of pSer-83 upon treatment with 5000 μM $H_2O_2$. This is counter to what has been previously reported; although previous reports typically only examined phosphorylation of this residue after $H_2O_2$ treatments of 500 μM or less (23, 43) and once at 2 mM (24). It is therefore possible that this residue is dephosphorylated at lower oxidant concentrations and then increasingly phosphorylated at higher oxidant levels. While not significant, my data do show a downward trend in the phosphorylation level of Ser-83 at 500 μM $H_2O_2$

treatment prior to the significant increase at the highest treatment level. Importantly, AKT1 is the kinase known to phosphorylate ASK1 at Ser-83 and $H_2O_2$ has been shown to stimulate AKT1 activity in a time- and dose-dependent manner (44-46). Thus, there may be a switch point at which the activity of AKT1 outcompetes the activity of the phosphatase that dephosphorylates Ser-83.

Of the other four sites that were found to be in common between the two stress types, three exhibited consistent dynamics between both HNE and $H_2O_2$. The previously known dynamic site Thr-838 increased in phosphorylation here in response to treatment with $H_2O_2$ and in previous studies in response to treatment with HNE. This observation is consistent with previous reports in the literature and confirms the validity of this site as a marker of ASK1 activity. Additionally, Ser-955 and Ser-958 both exhibited an increase in phosphorylation upon treatment with either stressor, which suggests that these two sites may also be good markers for ASK1 activity.

The final phosphosite that was observed on ASK1 in both treatments was Ser-1004. In the $H_2O_2$-treated cells, Ser-1004 was increasingly phosphorylated at the higher concentration level. However, in the HNE-treated cells, Ser-1004 phosphorylation decreased with increasing HNE treatment. Interestingly, one of the two identified HNE adduct sites was on Cys-1005. It is possible that the decreased phosphorylation observed at this residue in HNE-treated samples was due to interference by the adjacent adducted cysteine residue, although the stoichiometries of HNE adduction and serine phosphorylation remain to be investigated.

HNE and $H_2O_2$ treatments also resulted in several novel changes. The HNE-treated cells had two phosphosites that were uniquely dynamic and the $H_2O_2$-treated

cells had three uniquely dynamic residues, as well as one unique non-dynamic residue. The presence of phosphosites that are specific to one stress type could serve as a cellular readout of what specific type of stress is being sensed by ASK1 and could indicate that ASK1 senses these two stressors in different ways.

Although ASK1 seems to sense HNE and $H_2O_2$ through different mechanisms, the end result of activation by either of these molecules is the same. The presence of a core group of phosphorylated residues in ASK1 that exhibit similar dynamics between two dissimilar stress molecules could start to explain how a single sensor protein is able to transduce so many different chemical signals into a single pathway response. It is possible that many or all of the stressors that activate ASK1 will exert fine control over the phosphorylation of Thr-838, Ser-955, and Ser-958 residues to control the activity of ASK1. Future studies with additional stress activators of ASK1 will be necessary to test this hypothesis.

## References


1. Ichijo, H., Nishida, E., Irie, K., ten Dijke, P., Saitoh, M., Moriguchi, T., Takagi, M., Matsumoto, K., Miyazono, K., and Gotoh, Y. (1997) Induction of apoptosis by ASK1, a mammalian MAPKKK that activates SAPK/JNK and p38 signaling pathways. *Science* 275, 90-94

2. Shiizaki, S., Naguro, I., and Ichijo, H. (2013) Activation mechanisms of ASK1 in response to various stresses and its significance in intracellular signaling. *Adv Biol Regul* 53, 135-144

3. Takeda, K., Noguchi, T., Naguro, I., and Ichijo, H. (2008) Apoptosis signal-regulating kinase 1 in stress and immune response. *Annu Rev Pharmacol Toxicol* 48, 199-225

4. Saitoh, M., Nishitoh, H., Fujii, M., Takeda, K., Tobiume, K., Sawada, Y., Kawabata, M., Miyazono, K., and Ichijo, H. (1998) Mammalian thioredoxin is a direct inhibitor of apoptosis signal-regulating kinase (ASK) 1. *The EMBO journal* 17, 2596-2606

5. Matsuzawa, A., Saegusa, K., Noguchi, T., Sadamitsu, C., Nishitoh, H., Nagai, S., Koyasu, S., Matsumoto, K., Takeda, K., and Ichijo, H. (2005) ROS-dependent activation of the TRAF6-ASK1-p38 pathway is selectively required for TLR4-mediated innate immunity. *Nat Immunol* 6, 587-592

6. Takeda, K., Matsuzawa, A., Nishitoh, H., Tobiume, K., Kishida, S., Ninomiya-Tsuji, J., Matsumoto, K., and Ichijo, H. (2004) Involvement of ASK1 in Ca2+-induced p38 MAP kinase activation. *EMBO reports* 5, 161-166

7. Nishitoh, H., Matsuzawa, A., Tobiume, K., Saegusa, K., Takeda, K., Inoue, K., Hori, S., Kakizuka, A., and Ichijo, H. (2002) ASK1 is essential for endoplasmic reticulum stress-induced neuronal cell death triggered by expanded polyglutamine repeats. *Genes & development* 16, 1345-1355

8. Soh, Y., Jeong, K. S., Lee, I. J., Bae, M. A., Kim, Y. C., and Song, B. J. (2000) Selective activation of the c-Jun N-terminal protein kinase pathway during 4-hydroxynonenal-induced apoptosis of PC12 cells. *Mol Pharmacol* 58, 535-541

9. Lee, K. W., Zhao, X., Im, J. Y., Grosso, H., Jang, W. H., Chan, T. W., Sonsalla, P. K., German, D. C., Ichijo, H., Junn, E., and Mouradian, M. M. (2012) Apoptosis signal-regulating kinase 1 mediates MPTP toxicity and regulates glial activation. *PLoS One* 7, e29935

10. Lim, P. L., Liu, J., Go, M. L., and Boelsterli, U. A. (2008) The mitochondrial superoxide/thioredoxin-2/Ask1 signaling pathway is critically involved in troglitazone-induced cell injury to human hepatocytes. *Toxicol Sci* 101, 341-349

11. Usuki, F., Fujita, E., and Sasagawa, N. (2008) Methylmercury activates ASK1/JNK signaling pathways, leading to apoptosis due to both mitochondria- and endoplasmic reticulum (ER)-generated processes in myogenic cell lines. *Neurotoxicology* 29, 22-30

12. Nakagawa, H., Maeda, S., Hikiba, Y., Ohmae, T., Shibata, W., Yanai, A., Sakamoto, K., Ogura, K., Noguchi, T., Karin, M., Ichijo, H., and Omata, M. (2008) Deletion of apoptosis signal-regulating kinase 1 attenuates acetaminophen-induced liver injury by inhibiting c-Jun N-terminal kinase activation. *Gastroenterology* 135, 1311-1321

13. Shinkai, Y., Iwamoto, N., Miura, T., Ishii, T., Cho, A. K., and Kumagai, Y. (2012) Redox cycling of 1,2-naphthoquinone by thioredoxin1 through Cys32 and Cys35 causes inhibition of its catalytic activity and activation of ASK1/p38 signaling. *Chem Res Toxicol* 25, 1222-1230

14. Kuo, C. T., Chen, B. C., Yu, C. C., Weng, C. M., Hsu, M. J., Chen, C. C., Chen, M. C., Teng, C. M., Pan, S. L., Bien, M. Y., Shih, C. H., and Lin, C. H. (2009) Apoptosis signal-regulating kinase 1 mediates denbinobin-induced apoptosis in human lung adenocarcinoma cells. *J Biomed Sci* 16, 43

15. Kwon, M. J., Jeong, K. S., Choi, E. J., and Lee, B. H. (2003) 2,3,7,8-Tetrachlorodibenzo-p-dioxin (TCDD)-induced activation of mitogen-activated protein kinase signaling pathway in Jurkat T cells. *Pharmacol Toxicol* 93, 186-190

16. Pramanik, K. C., and Srivastava, S. K. (2012) Apoptosis signal-regulating kinase 1-thioredoxin complex dissociation by capsaicin causes pancreatic tumor growth suppression by inducing apoptosis. *Antioxid Redox Signal* 17, 1417-1432

17. Ouyang, M., and Shen, X. (2006) Critical role of ASK1 in the 6-hydroxydopamine-induced apoptosis in human neuroblastoma SH-SY5Y cells. *J Neurochem* 97, 234-244

18. Yang, W., Tiffany-Castiglioni, E., Koh, H. C., and Son, I. H. (2009) Paraquat activates the IRE1/ASK1/JNK cascade associated with apoptosis in human neuroblastoma SH-SY5Y cells. *Toxicol Lett* 191, 203-210

19. Gotoh, Y., and Cooper, J. A. (1998) Reactive oxygen species- and dimerization-induced activation of apoptosis signal-regulating kinase 1 in tumor necrosis factor-alpha signal transduction. *J Biol Chem* 273, 17477-17482

20. He, Y., Zhang, W., Zhang, R., Zhang, H., and Min, W. (2006) SOCS1 inhibits tumor necrosis factor-induced activation of ASK1-JNK inflammatory signaling by mediating ASK1 degradation. *J Biol Chem* 281, 5559-5566

21. Yu, L., Min, W., He, Y., Qin, L., Zhang, H., Bennett, A. M., and Chen, H. (2009) JAK2 and SHP2 reciprocally regulate tyrosine phosphorylation and stability of proapoptotic protein ASK1. *J Biol Chem* 284, 13481-13488

22. Kim, A. H., Khursigara, G., Sun, X., Franke, T. F., and Chao, M. V. (2001) Akt phosphorylates and negatively regulates apoptosis signal-regulating kinase 1. *Mol Cell Biol* 21, 893-901

23. Gu, J. J., Wang, Z., Reeves, R., and Magnuson, N. S. (2009) PIM1 phosphorylates and negatively regulates ASK1-mediated apoptosis. *Oncogene* 28, 4261-4271

24. Seong, H. A., Jung, H., Ichijo, H., and Ha, H. (2010) Reciprocal negative regulation of PDK1 and ASK1 signaling by direct interaction and phosphorylation. *J Biol Chem* 285, 2397-2414

25. Goldman, E. H., Chen, L., and Fu, H. (2004) Activation of apoptosis signal-regulating kinase 1 by reactive oxygen species through dephosphorylation at serine 967 and 14-3-3 dissociation. *J Biol Chem* 279, 10442-10449

26. Min, W., Lin, Y., Tang, S., Yu, L., Zhang, H., Wan, T., Luhn, T., Fu, H., and Chen, H. (2008) AIP1 recruits phosphatase PP2A to ASK1 in tumor necrosis factor-induced ASK1-JNK activation. *Circ Res* 102, 840-848

27. Fujii, K., Goldman, E. H., Park, H. R., Zhang, L., Chen, J., and Fu, H. (2004) Negative control of apoptosis signal-regulating kinase 1 through phosphorylation of Ser-1034. *Oncogene* 23, 5099-5104

28. Morita, K., Saitoh, M., Tobiume, K., Matsuura, H., Enomoto, S., Nishitoh, H., and Ichijo, H. (2001) Negative feedback regulation of ASK1 by protein phosphatase 5 (PP5) in response to oxidative stress. *EMBO J* 20, 6028-6036

29. Cho, Y. C., Park, J. E., Park, B. C., Kim, J. H., Jeong, D. G., Park, S. G., and Cho, S. (2015) Cell cycle-dependent Cdc25C phosphatase determines cell survival by regulating apoptosis signal-regulating kinase 1. *Cell Death Differ*

30. Benedetti, A., Comporti, M., and Esterbauer, H. (1980) Identification of 4-hydroxynonenal as a cytotoxic product originating from the peroxidation of liver microsomal lipids. *Biochim Biophys Acta* 620, 281-296

31. Schopfer, F. J., Cipollina, C., and Freeman, B. A. (2011) Formation and signaling actions of electrophilic lipids. *Chem Rev* 111, 5997-6021

32. Fritz, K. S., Kellersberger, K. A., Gomez, J. D., and Petersen, D. R. (2012) 4-HNE adduct stability characterized by collision-induced dissociation and electron transfer dissociation mass spectrometry. *Chem Res Toxicol* 25, 965-970

33. West, J. D., and Marnett, L. J. (2006) Endogenous reactive intermediates as modulators of cell signaling and cell death. *Chem Res Toxicol* 19, 173-194

34. Kessner, D., Chambers, M., Burke, R., Agus, D., and Mallick, P. (2008) ProteoWizard: open source software for rapid proteomics tools development. *Bioinformatics* 24, 2534-2536

35. Kim, S., and Pevzner, P. A. (2014) MS-GF+ makes progress towards a universal database search tool for proteomics. *Nature communications* 5, 5277

36. Elias, J. E., and Gygi, S. P. (2007) Target-decoy search strategy for increased confidence in large-scale protein identifications by mass spectrometry. *Nat Methods* 4, 207-214

37. Ma, Z. Q., Dasari, S., Chambers, M. C., Litton, M. D., Sobecki, S. M., Zimmerman, L. J., Halvey, P. J., Schilling, B., Drake, P. M., Gibson, B. W., and Tabb, D. L. (2009) IDPicker 2.0: Improved protein assembly with high discrimination peptide identification filtering. *Journal of proteome research* 8, 3872-3881

38. MacLean, B., Tomazela, D. M., Shulman, N., Chambers, M., Finney, G. L., Frewen, B., Kern, R., Tabb, D. L., Liebler, D. C., and MacCoss, M. J. (2010) Skyline: an open source document editor for creating and analyzing targeted proteomics experiments. *Bioinformatics* 26, 966-968

39. Nichols, A. M., and White, F. M. (2009) Manual validation of peptide sequence and sites of tyrosine phosphorylation from MS/MS spectra. *Methods Mol Biol* 492, 143-160

40. Strohalm, M., Kavan, D., Novak, P., Volny, M., and Havlicek, V. (2010) mMass 3: a cross-platform software environment for precise analysis of mass spectrometric data. *Anal Chem* 82, 4648-4651

41. Niedermeyer, T. H., and Strohalm, M. (2012) mMass as a software tool for the annotation of cyclic peptide tandem mass spectra. *PLoS One* 7, e44913

42. Yuan, Z. Q., Feldman, R. I., Sussman, G. E., Coppola, D., Nicosia, S. V., and Cheng, J. Q. (2003) AKT2 inhibition of cisplatin-induced JNK/p38 and Bax activation by phosphorylation of ASK1: implication of AKT2 in chemoresistance. *J Biol Chem* 278, 23432-23440

43. Zhang, R., Luo, D., Miao, R., Bai, L., Ge, Q., Sessa, W. C., and Min, W. (2005) Hsp90-Akt phosphorylates ASK1 and inhibits ASK1-mediated apoptosis. *Oncogene* 24, 3954-3963

44. Blanc, A., Pandey, N. R., and Srivastava, A. K. (2004) Distinct roles of Ca2+, calmodulin, and protein kinase C in H2O2-induced activation of ERK1/2, p38 MAPK, and protein kinase B signaling in vascular smooth muscle cells. *Antioxid Redox Signal* 6, 353-366

45. Cui, X. L., Ding, Y., Alexander, L. D., Bao, C., Al-Khalili, O. K., Simonson, M., Eaton, D. C., and Douglas, J. G. (2006) Oxidative signaling in renal epithelium: Critical role of cytosolic phospholipase A2 and p38(SAPK). *Free Radic Biol Med* 41, 213-221

46. Shaw, M., Cohen, P., and Alessi, D. R. (1998) The activation of protein kinase B by H2O2 or heat shock is mediated by phosphoinositide 3-kinase and not by mitogen-activated protein kinase-activated protein kinase-2. *Biochem J* 336 ( Pt 1), 241-246

# CHAPTER IV

# PERSPECTIVE

## Summary

There were two driving questions for this body of work. The first was how ASK1 is able to act as a sensor protein capable of detecting molecules of diverse chemotypes and integrate them into a single response pathway. The second question was whether the hypothesized ASK1 signalosome exists and, if it does, what the exact membership of this multiprotein complex might be. In answer to these questions, I hypothesized that ASK1 or its complex members are modified by electrophiles (represented by HNE), resulting in pathway activation and formation of a consensus post-activation signalosome, along with a change in the phosphorylation pattern on ASK1. The studies presented in chapter II addressed the existence of the signalosome and proved that there is a multiprotein ASK1 complex present in the cell. However, the large two-state signalosome concept as it has been presented in the literature is inconsistent with my data, which suggests the concurrent presence of many diverse signalosomes in the cell that all share a core set of proteins. The work presented in chapter III begins to suggest how ASK1 is able to integrate such a diverse array of chemical signals. I utilized PRM assays to demonstrate that two distinct chemical species were capable of activating ASK1 to a similar degree with both a core set of common phosphorylations and a unique phosphorylation signature for each stress.

## ASK1 protein complex composition and dynamics

*Current practices and understanding in the ASK1 field*

In the field of multiprotein complex analysis in general, and for ASK1 in particular, the predominate method for both detection of protein-protein interactions and description of dynamic associations has been co-IP Western blot (1). In most cases, this results in a limited view of the biophysical processes taking place as the co-IP Western assays are inherently binary in nature. Thus, a complex like that of ASK1, which is composed of several different proteins, will only be analyzed in a pair-wise fashion (ASK1 and one other protein) for any given stimulus or cellular context. After a series of these studies have been conducted in the literature, a more complete picture of the potential behavior of the entire complex will begin to be assembled.

This is how the ASK1 field has developed and why the current view of the ASK1 signalosome is that of a consensus two-state system with many different protein-protein interactions that all dynamically shift in association with ASK1 upon treatment (2-4). The inherent assumption with this type of analysis is that the individual studies are cumulative and that the unmeasured components of the signalosome behave similarly between analyses. This assumption is not necessarily true. In order to truly understand how a multiprotein complex is responding to any given stimulus or circumstance, all components of the complex must be observed concurrently. For most complexes, an "all-components" view is not possible via Western blot methodologies. Other major shortcomings for immunoassays include relatively poor quantitative characteristics and reliance on poorly characterized antibodies.

The increased speed and high mass accuracy of modern instruments has resulted in an increased use of affinity purification coupled with mass spectrometry to analyze multiple proteins in a complex concurrently (5-9). This advance addresses many of the issues inherent to Western blot-based studies but still has a few weaknesses. Typically, AP-MS studies are performed with shotgun MS techniques that are good for defining complex membership and can give some evidence for dynamic shifts in protein associations with the complex (10, 11). However, the quantitative data from shotgun methods is typically limited by a large degree of missing values from the inherent stochastic nature of peptide selection based on signal intensity, which undersamples some sequences. Additionally, protein associations with low stoichiometry may not be captured by shotgun analyses due to thresholding effects and dynamic range limitations in the method (12).

*Technical and conceptual advances in ASK1 complex understanding*

In the studies presented in chapter II, I developed a targeted PRM method for precisely monitoring ASK1 protein interaction changes in response to treatment. The information presented in that chapter dealt specifically with the dynamics of the ASK1 complex in response to HNE treatment, but the method is generalizable to any multiprotein complex perturbed by any stimulus. By utilizing the superior quantitative aspects of a targeted MS assay, I bypassed the missing value limitations inherent in shotgun MS quantitation and was able to more confidently assay the protein-protein interactions with ASK1 across different treatment conditions. Additionally, because of the high throughput capabilities of the PRM assay on a Q Exactive mass spectrometer, I

was able to target all known components of the ASK1 multiprotein complex concurrently to generate the first “all-components” view of this important stress-transducing system. As a step toward an even more quantitative understanding of the ASK1 complex protein-protein interaction dynamics, I performed stable isotope dilution assays for many of the complex members in order to generate the first ever stoichiometric estimate of the composition of this complex.

The end result of these assays was the identification of several proteins that demonstrated concurrent dynamic shifts in association with ASK1 in response to HNE treatment. This was the first time that protein-protein interactions with ASK1 have been studied in response to activation by electrophile stress. Additionally, the SID assays allowed me to determine the composition of a minimal ASK1 complex consisting of ASK1, ASK2, and 14-3-3 family proteins that were present in a ratio of 2:2:1 respectively. This complex composition is supported by not only the SID assays, but the distribution of ASK1 in size exclusion experiments. This minimal complex composition coupled with the dynamic rearrangements noted under conditions of HNE stress activation generated a new image of how the ASK1 complex operates. Rather than a consensus two-state super-complex composed of many different proteins, as has been presented in the literature (3, 4), my data supports the idea of many different ASK1 complexes present concurrently in the cell – all as variations of a core complex composed of ASK1, ASK2, and a 14-3-3 protein – that transiently associates with other reported ASK1-interacting proteins in order to carry out necessary signaling functions in response to stress.

The use of PRM assays coupled with SID-based measurements of multiprotein complex constituents has broader implications than just a better understanding of how the ASK1 signalosome functions. Most of the previously described multiprotein complex dynamics in the literature were investigated through the use of immunoassays or reconstituted complexes. As discussed above, the dynamic data obtained from IP-Western assays is inherently binary, limited in quantitative capacity, and requires high quality antibodies for each protein component of the complex. The information from reconstitution experiments has helped to define the behavior of several complexes, but this type of assay is difficult to perform. In many cases, a reconstituted complex may not be possible because of the number of proteins involved. By utilizing targeted PRM assays with SID quantitation, all of these limitations are avoided and high quality dynamic data can be obtained for almost any multiprotein complex.

## ASK1 phosphorylation and stress sensing

*Current practices and understanding in the ASK1 field*

ASK1 can translate the chemical properties of different chemotypes (e.g., oxidants, electrophiles) into a single stress response pathway (3, 13-25). Until now, no investigation of how this single sensor protein is able to detect many molecules of different chemotypes has been carried out. It is therefore unknown whether ASK1 senses all of these stressors via the same mechanism or if each stressor is detected through a different means.

ASK1 is reported to be phosphorylated on at least 29 residues, and 5 of these have been previously identified as dynamic, with phosphorylation states that change in response to treatment with oxidants. All 5 of these residues were discovered through mutational analysis and antibodies were generated to track the phosphorylation status in response to stress (26-32). While mutational analysis and phospho-specific antibody generation is an established method for describing dynamic phosphorylation sites, it is relatively inefficient and time- and labor-intensive.

Shotgun proteomics has become the method of choice in recent years for discovering phosphosites on proteins in an unbiased fashion. This methodology has been tangentially applied to ASK1, as multiple phosphorylation sites have been reported through global shotgun analyses in several different contexts that were not focused on the ASK1 system. None of these reported sites have been investigated further to determine if they are dynamic in response to stress signaling. Recently, advances in MS technology have enabled the use of targeted MS techniques to track phosphorylation status in signaling network proteins (33).

*Technical and conceptual advances in ASK1 stress sensing*

In chapter III, I began to address the question of how ASK1 is able to integrate chemicals with different chemotypes into a single pathway response by comparing the effect of HNE and $H_2O_2$ treatment on the phosphorylation status of ASK1. This was the first comparative study of the phosphorylation state of ASK1 in response to activation by two chemically distinct molecules and is the first study to suggest that ASK1 possesses different sensing mechanisms for different chemical species. I utilized shotgun MS for

the unbiased discovery of phosphorylation sites on ASK1 in response to both of these treatments. This was the first time that discovery proteomics was performed specifically on ASK1 for the purpose of phosphosite identification. I identified several phosphosites, both previously known and novel, that exhibited dynamic responses to stress activation. For each stressor used, I detected a unique set of phosphorylated residues, which suggested that ASK1 was able to respond to $H_2O_2$ and HNE via different mechanisms. Interestingly, I also detected a core set of phosphorylations that were shared between the two stressors and which exhibited consistent dynamic changes for both HNE and $H_2O_2$. This suggested that ASK1 sensed each of these two molecules via a different mechanism but was capable of integrating these two signals into a common activation of the pathway.

In this study, I utilized targeted PRM assays to track the dynamics of the identified phosphorylation sites in response to treatment. This technique allowed me to determine which sites were dynamic without the need to perform any mutations or generate any antibodies. Thus, this study can serve as a proof of concept for the use of targeted MS assays for the assessment of phosphosite dynamics in general. It is unlikely that MS assays will ever completely replace mutational studies or antibody generation, but targeted MS assays can serve as an initial step to narrow down the list of potential sites for further assay development via more traditional means.

## Conclusions and future directions

The studies presented here have enhanced understanding of two unanswered questions in the ASK1 field. First, I have shown that the ASK1 signalosome is likely not a two-state system as it has been conceived of in the literature. Instead, my data supports the idea of a core ASK1 complex that transiently associates with additional proteins as needed, with the functional outcome being the concurrent presence of multiple different ASK1 complexes in the cell. However, the studies that support this idea of a core ASK1 complex were all performed with HNE as the stress signal activating ASK1. Because of this, it is possible that the two different models of the ASK1 signalosome are not in fact mutually exclusive. It is possible that the way in which the ASK1 signalosome functions is dependent on stress activation context. Additional experiments examining not only HNE and $H_2O_2$, but also several of the other known ASK1-activating molecules need to be performed to test this hypothesis.

The second question in the ASK1 field that my work began to answer is whether or not ASK1 senses different stressors via the same mechanism. Through the analysis of the phosphorylation state of ASK1 in response to two chemically distinct stressors, I have shown that ASK1 is likely capable of sensing each through different mechanisms, but that both of these sensing mechanisms are capable of activating the ASK1 pathway through a common set of phosphorylations on ASK1. This idea of different stress sensing mechanisms present in ASK1 brings up a new major question of how this sensing works mechanistically. In order to understand how the differential phosphorylations identified in chapter III allow ASK1 to detect different stressors, a

structural biology based investigation needs to be undertaken. By examining the crystal structure of ASK1 as it is activated via different chemical stressors, the role of the individual phosphosites in stress sensing may become clear. In addition to these studies, further examination of ASK1 phosphorylation in response to activation by some of the other known ASK1-activating molecules should be performed in order to better understand how specifically ASK1 is able to sense distinct stressors. In the studies that I performed, ASK1 exhibited two distinct stress sensing mechanisms, but it is unclear if there are others. Given the large number of phosphorylatable residues in ASK1, it is likely that there will be several other distinct stress sensing mechanisms present in ASK1.

Both of the questions in the ASK field discussed above were answered through the use of discovery and targeted MS proteomics. This series of studies has demonstrated the value of targeted proteomics for analysis of dynamic processes, both in the case of multiprotein complex analysis and phosphoproteomic analysis, and I predict that this technique will become the new gold standard for these fields.

## References


1. Ngounou Wetie, A. G., Sokolowska, I., Woods, A. G., Roy, U., Deinhardt, K., and Darie, C. C. (2014) Protein-protein interactions: switch from classical methods to proteomics and bioinformatics-based approaches. *Cell Mol Life Sci* 71, 205-228

2. Kawarazaki, Y., Ichijo, H., and Naguro, I. (2014) Apoptosis signal-regulating kinase 1 as a therapeutic target. *Expert Opin Ther Targets* 18, 651-664

3. Shiizaki, S., Naguro, I., and Ichijo, H. (2013) Activation mechanisms of ASK1 in response to various stresses and its significance in intracellular signaling. *Adv Biol Regul* 53, 135-144

4. Fujino, G., Noguchi, T., Matsuzawa, A., Yamauchi, S., Saitoh, M., Takeda, K., and Ichijo, H. (2007) Thioredoxin and TRAF family proteins regulate reactive oxygen species-dependent activation of ASK1 through reciprocal modulation of the N-terminal homophilic interaction of ASK1. *Mol Cell Biol* 27, 8152-8163

5. Morris, J. H., Knudsen, G. M., Verschueren, E., Johnson, J. R., Cimermancic, P., Greninger, A. L., and Pico, A. R. (2014) Affinity purification-mass spectrometry and network analysis to understand protein-protein interactions. *Nat Protoc* 9, 2539-2554

6. Bernaudo, F., Monteleone, F., Mesuraca, M., Krishnan, S., Chiarella, E., Scicchitano, S., Cuda, G., Morrone, G., Bond, H. M., and Gaspari, M. (2015) Validation of a novel shotgun proteomic workflow for the discovery of protein-protein interactions: focus on ZNF521. *J Proteome Res* 14, 1888-1899

7. Dunham, W. H., Mullin, M., and Gingras, A. C. (2012) Affinity-purification coupled to mass spectrometry: basic principles and strategies. *Proteomics* 12, 1576-1590

8. Huttlin, E. L., Ting, L., Bruckner, R. J., Gebreab, F., Gygi, M. P., Szpyt, J., Tam, S., Zarraga, G., Colby, G., Baltier, K., Dong, R., Guarani, V., Vaites, L. P., Ordureau, A., Rad, R., Erickson, B. K., Wuhr, M., Chick, J., Zhai, B., Kolippakkam, D., Mintseris, J., Obar, R. A., Harris, T., Artavanis-Tsakonas, S., Sowa, M. E., De Camilli, P., Paulo, J. A., Harper, J. W., and Gygi, S. P. (2015) The BioPlex Network: A Systematic Exploration of the Human Interactome. *Cell* 162, 425-440

9. Varjosalo, M., Sacco, R., Stukalov, A., van Drogen, A., Planyavsky, M., Hauri, S., Aebersold, R., Bennett, K. L., Colinge, J., Gstaiger, M., and Superti-Furga, G. (2013) Interlaboratory reproducibility of large-scale human protein-complex analysis by standardized AP-MS. *Nat Methods* 10, 307-314

10. Diner, B. A., Li, T., Greco, T. M., Crow, M. S., Fuesler, J. A., Wang, J., and Cristea, I. M. (2015) The functional interactome of PYHIN immune regulators reveals IFIX is a sensor of viral DNA. *Mol Syst Biol* 11, 787

11. Kohli, P., Bartram, M. P., Habbig, S., Pahmeyer, C., Lamkemeyer, T., Benzing, T., Schermer, B., and Rinschen, M. M. (2014) Label-free quantitative proteomic analysis of the YAP/TAZ interactome. *Am J Physiol Cell Physiol* 306, C805-818

12. Liebler, D. C., and Zimmerman, L. J. (2013) Targeted quantitation of proteins by mass spectrometry. *Biochemistry* 52, 3797-3806

13. Lim, P. L., Liu, J., Go, M. L., and Boelsterli, U. A. (2008) The mitochondrial superoxide/thioredoxin-2/Ask1 signaling pathway is critically involved in troglitazone-induced cell injury to human hepatocytes. *Toxicol Sci* 101, 341-349

14. Usuki, F., Fujita, E., and Sasagawa, N. (2008) Methylmercury activates ASK1/JNK signaling pathways, leading to apoptosis due to both mitochondria- and endoplasmic reticulum (ER)-generated processes in myogenic cell lines. *Neurotoxicology* 29, 22-30

15. Nakagawa, H., Maeda, S., Hikiba, Y., Ohmae, T., Shibata, W., Yanai, A., Sakamoto, K., Ogura, K., Noguchi, T., Karin, M., Ichijo, H., and Omata, M. (2008) Deletion of apoptosis signal-regulating kinase 1 attenuates acetaminophen-induced liver injury by inhibiting c-Jun N-terminal kinase activation. *Gastroenterology* 135, 1311-1321

16. Shinkai, Y., Iwamoto, N., Miura, T., Ishii, T., Cho, A. K., and Kumagai, Y. (2012) Redox cycling of 1,2-naphthoquinone by thioredoxin1 through Cys32 and Cys35 causes inhibition of its catalytic activity and activation of ASK1/p38 signaling. *Chem Res Toxicol* 25, 1222-1230

17. Kuo, C. T., Chen, B. C., Yu, C. C., Weng, C. M., Hsu, M. J., Chen, C. C., Chen, M. C., Teng, C. M., Pan, S. L., Bien, M. Y., Shih, C. H., and Lin, C. H. (2009) Apoptosis signal-regulating kinase 1 mediates denbinobin-induced apoptosis in human lung adenocarcinoma cells. *J Biomed Sci* 16, 43

18. Kwon, M. J., Jeong, K. S., Choi, E. J., and Lee, B. H. (2003) 2,3,7,8-Tetrachlorodibenzo-p-dioxin (TCDD)-induced activation of mitogen-activated protein kinase signaling pathway in Jurkat T cells. *Pharmacol Toxicol* 93, 186-190

19. Myers, C. R., Myers, J. M., Kufahl, T. D., Forbes, R., and Szadkowski, A. (2011) The effects of acrolein on the thioredoxin system: implications for redox-sensitive signaling. *Mol Nutr Food Res* 55, 1361-1374

20. Pramanik, K. C., and Srivastava, S. K. (2012) Apoptosis signal-regulating kinase 1-thioredoxin complex dissociation by capsaicin causes pancreatic tumor growth suppression by inducing apoptosis. *Antioxid Redox Signal* 17, 1417-1432

21. Lee, K. W., Zhao, X., Im, J. Y., Grosso, H., Jang, W. H., Chan, T. W., Sonsalla, P. K., German, D. C., Ichijo, H., Junn, E., and Mouradian, M. M. (2012) Apoptosis signal-regulating kinase 1 mediates MPTP toxicity and regulates glial activation. *PLoS One* 7, e29935

22. Ouyang, M., and Shen, X. (2006) Critical role of ASK1 in the 6-hydroxydopamine-induced apoptosis in human neuroblastoma SH-SY5Y cells. *J Neurochem* 97, 234-244

23. Yang, W., Tiffany-Castiglioni, E., Koh, H. C., and Son, I. H. (2009) Paraquat activates the IRE1/ASK1/JNK cascade associated with apoptosis in human neuroblastoma SH-SY5Y cells. *Toxicol Lett* 191, 203-210

24. Takeda, K., Noguchi, T., Naguro, I., and Ichijo, H. (2008) Apoptosis signal-regulating kinase 1 in stress and immune response. *Annu Rev Pharmacol Toxicol* 48, 199-225

25. Soh, Y., Jeong, K. S., Lee, I. J., Bae, M. A., Kim, Y. C., and Song, B. J. (2000) Selective activation of the c-Jun N-terminal protein kinase pathway during 4-hydroxynonenal-induced apoptosis of PC12 cells. *Mol Pharmacol* 58, 535-541

26. Kim, A. H., Khursigara, G., Sun, X., Franke, T. F., and Chao, M. V. (2001) Akt phosphorylates and negatively regulates apoptosis signal-regulating kinase 1. *Mol Cell Biol* 21, 893-901

27. Yu, L., Min, W., He, Y., Qin, L., Zhang, H., Bennett, A. M., and Chen, H. (2009) JAK2 and SHP2 reciprocally regulate tyrosine phosphorylation and stability of proapoptotic protein ASK1. *J Biol Chem* 284, 13481-13488

28. Seong, H. A., Jung, H., Ichijo, H., and Ha, H. (2010) Reciprocal negative regulation of PDK1 and ASK1 signaling by direct interaction and phosphorylation. *J Biol Chem* 285, 2397-2414

29. Fujii, K., Goldman, E. H., Park, H. R., Zhang, L., Chen, J., and Fu, H. (2004) Negative control of apoptosis signal-regulating kinase 1 through phosphorylation of Ser-1034. *Oncogene* 23, 5099-5104

30. Goldman, E. H., Chen, L., and Fu, H. (2004) Activation of apoptosis signal-regulating kinase 1 by reactive oxygen species through dephosphorylation at serine 967 and 14-3-3 dissociation. *J Biol Chem* 279, 10442-10449

31. Tobiume, K., Saitoh, M., and Ichijo, H. (2002) Activation of apoptosis signal-regulating kinase 1 by the stress-induced activating phosphorylation of pre-formed oligomer. *J Cell Physiol* 191, 95-104

32. Morita, K., Saitoh, M., Tobiume, K., Matsuura, H., Enomoto, S., Nishitoh, H., and Ichijo, H. (2001) Negative feedback regulation of ASK1 by protein phosphatase 5 (PP5) in response to oxidative stress. *EMBO J* 20, 6028-6036

33. Kennedy, J. J., Yan, P., Zhao, L., Ivey, R. G., Voytovich, U. J., Moore, H. D., Lin, C., Pogosova-Agadjanyan, E. L., Stirewalt, D. L., Reding, K. W., Whiteaker, J. R., and Paulovich, A. G. (2016) Immobilized Metal Affinity Chromatography Coupled to Multiple

Reaction Monitoring Enables Reproducible Quantification of Phospho-signaling. *Mol Cell Proteomics* 15, 726-739

Appendix A

Data to Chapter II:

# ASSEMBLY DYNAMICS AND STOICHIOMTERY OF THE APOPTOSIS SIGNAL-REGULATING KINASE (ASK) SIGNALOSOME IN RESPONSE TO ELECTROPHILE STRESS

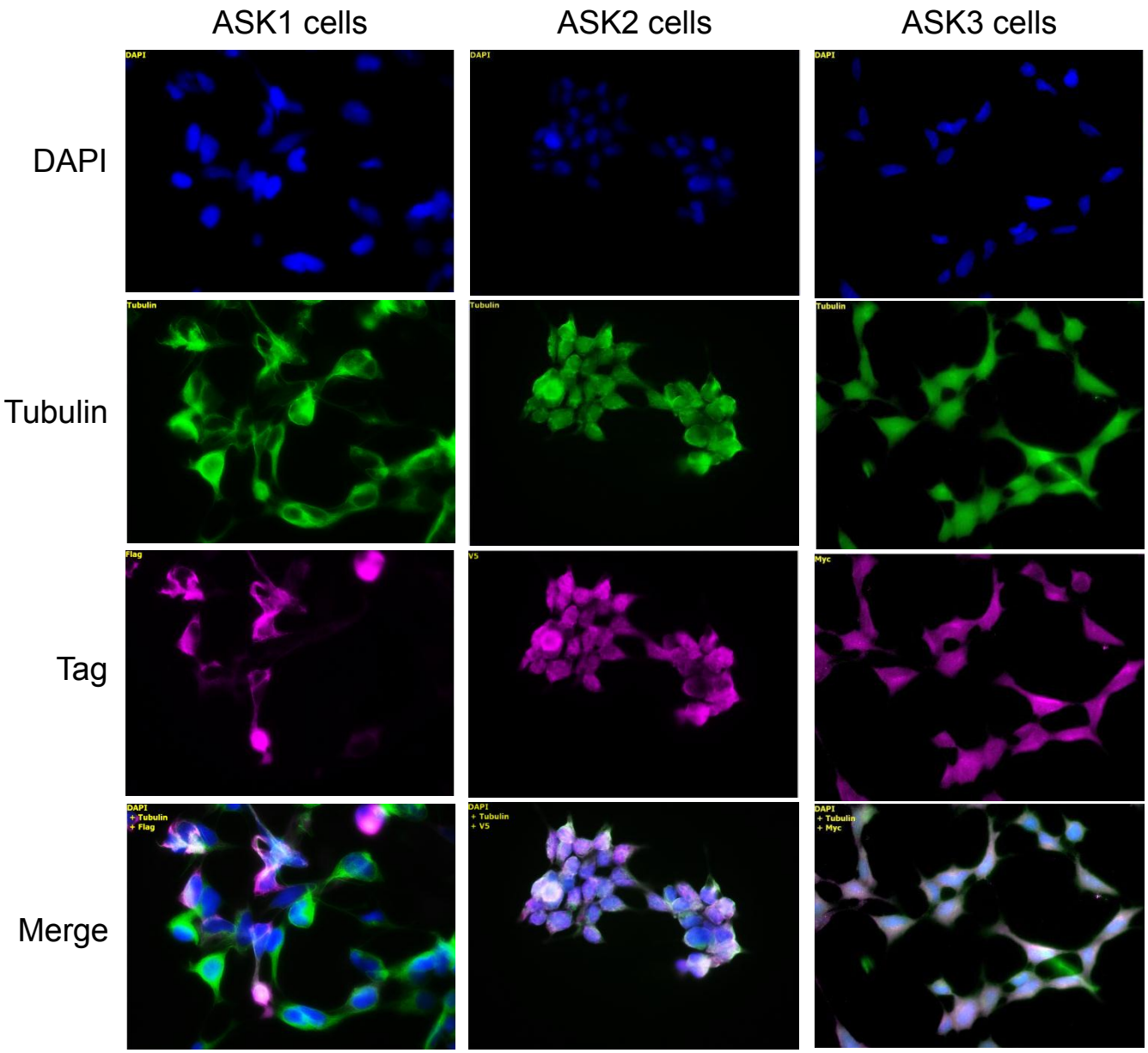


**Figure A-1.** ICC images of the three ASK proteins. ICC results showing proper localization of the three ASK proteins with no evidence of aberrant aggregation.

A

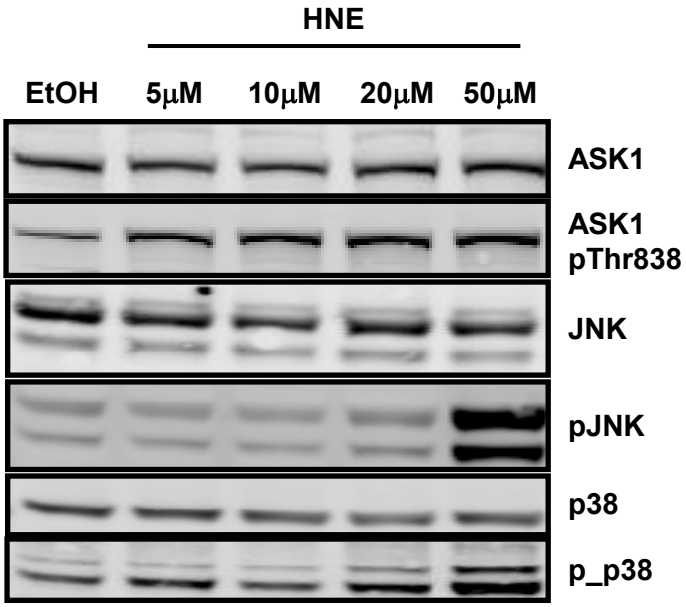


B

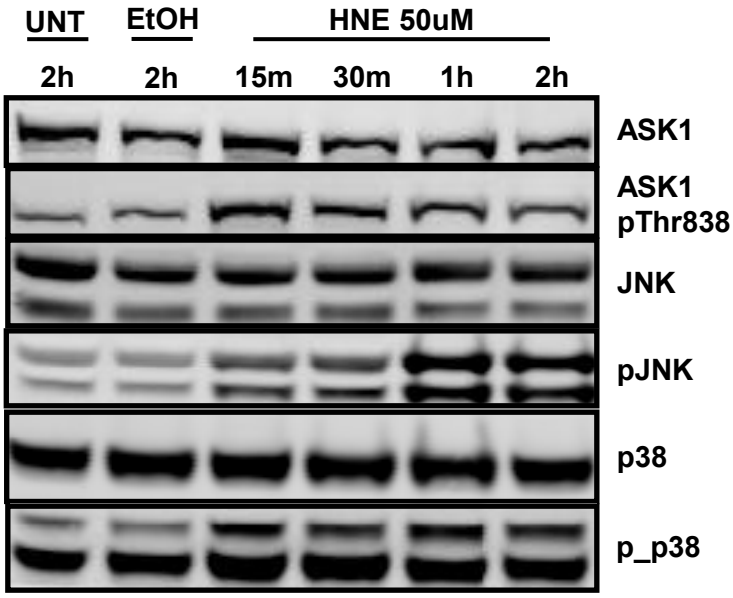


**Figure A-2.** Dose- and time-dependent activation of the ASK1 MAPK pathway. (A) ASK1-TAG cells were treated with increasing concentrations of HNE for 1hr. Activation of ASK1 was observed at all concentrations of HNE used (compare to EtOH) and maximal activation of the downstream kinase JNK and p38 was seen at 50μM. (B) ASK1-TAG cells were treated with 50μM HNE for the times indicated. Activation of ASK1 was detected at all time points but activation of the downstream kinases was strongest at 1-2hrs.

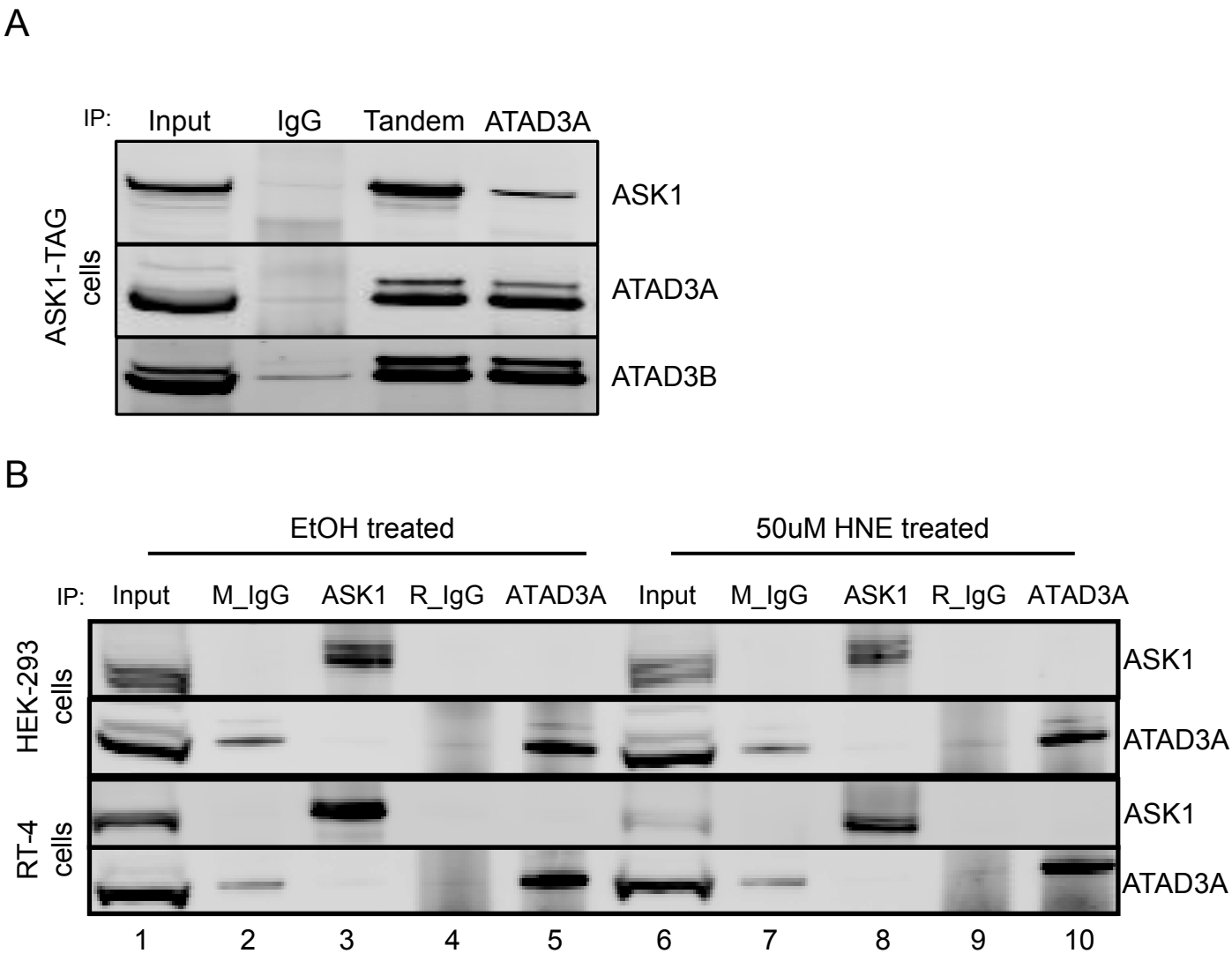


**Figure A-3.** ASK1-ATAD3A interaction test. (A) The interaction of ATAD3A and ATAD3B with ASK1 seen in the over-expressing (ASK1-TAG) cells was confirmed by Co-IP Western. (B) However, in the context of endogenous expression in parental HEK-293 cells (top two panels) and RT-4 cells (which have a higher expression of ASK1), ASK1 and ATAD3A did not co-purify (compare lanes 3 and 5). Additionally, activation status of ASK1 did not seem to produce an association (compare lanes 8 and 10). In fact, there was a higher level of ATAD3A precipitation with the pre-immune IPs than with the ASK1 IPs (compare lanes 2 and 4 with 3 and lanes 7 and 9 with 8).

**A**

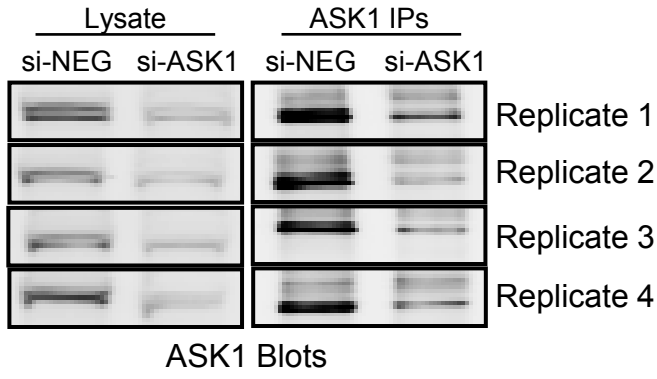


**Figure A-4**. ASK1 knockdown IPs. An si-RNA knockdown of ASK1 was performed in 293 cells. (A) Western blot analysis of cells treated with non-targeting siRNA and ASK1-targeting siRNA shows that ASK1 expression was successfully knocked down. This can be seen at the whole cell lysate level (left panel) and the IP level (right panel). LRP normalized (B) and SID normalized (C) PRM analysis of non-targeting and ASK1-targeting siRNA treated cells show the decrease of ASK1 with siRNA treatment. The majority of the interacting proteins showed no difference with the sole exceptions of ASK2 and ASK3. Black bars denote the mean of each replicate and blue connecting lines show the si-RNA dependent drop in the effected peptides.

**B**

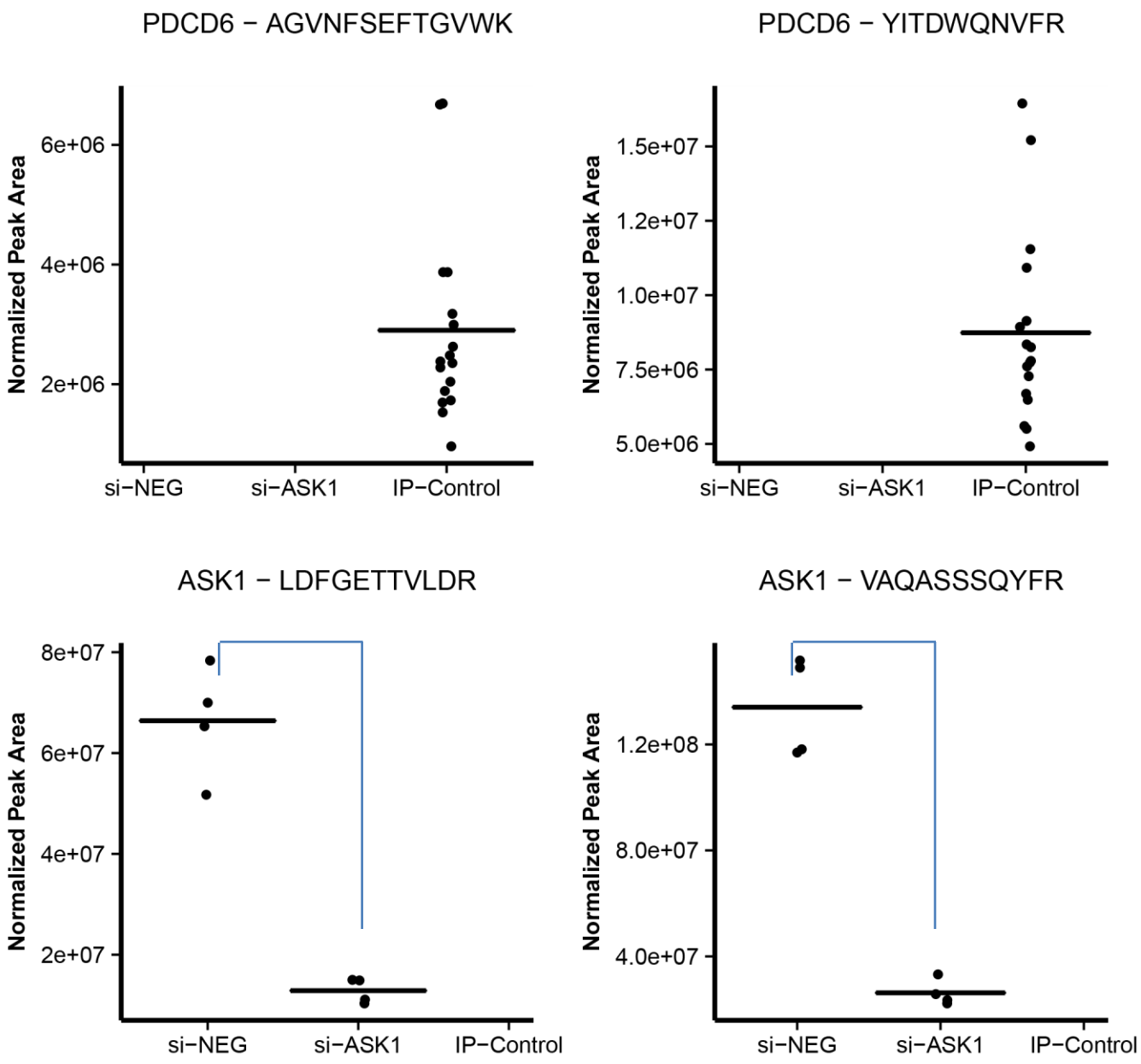


LRP-based results

**Figure A-4**

**B**

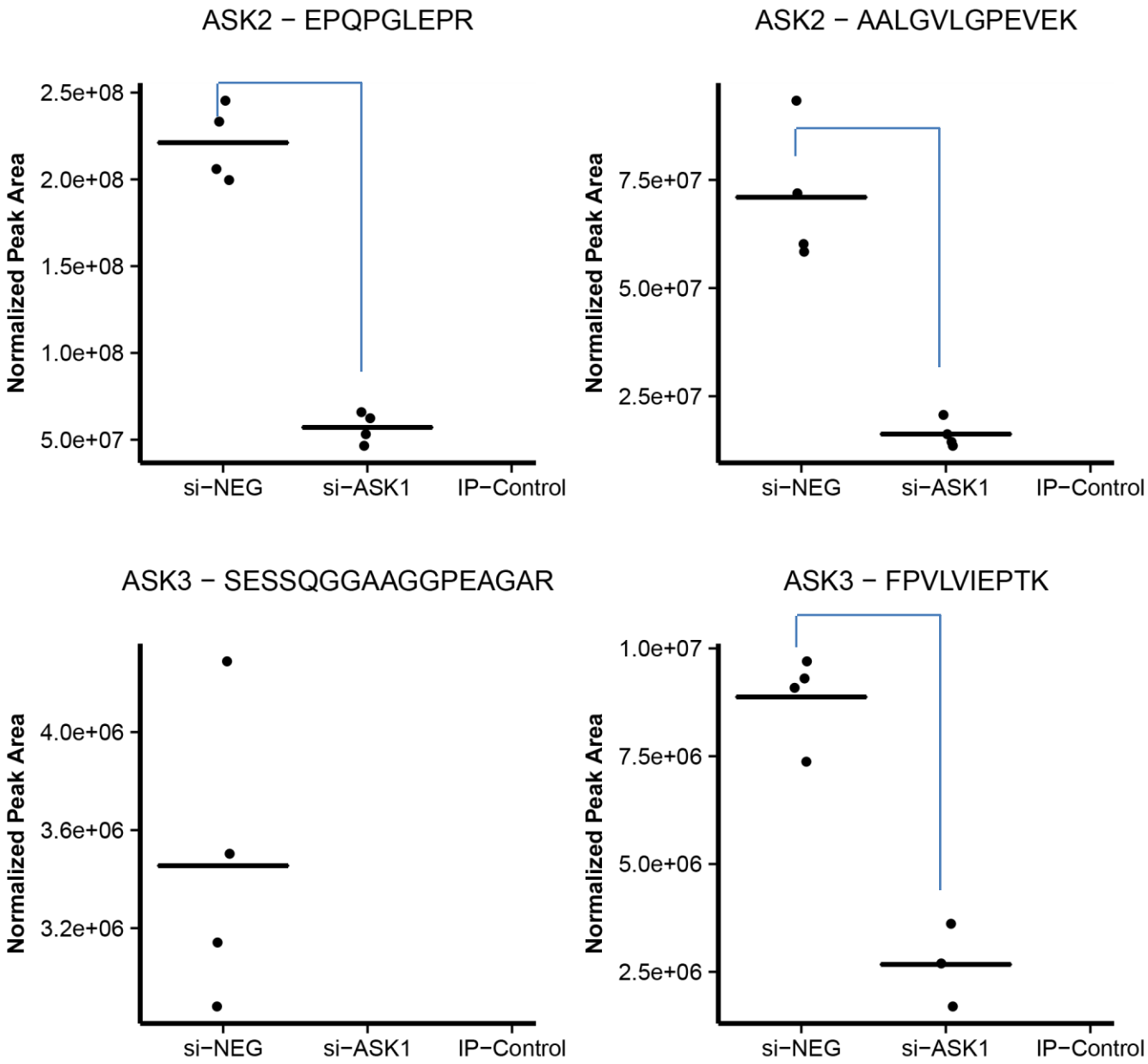


LRP-based results

**Figure A-4**

**B**

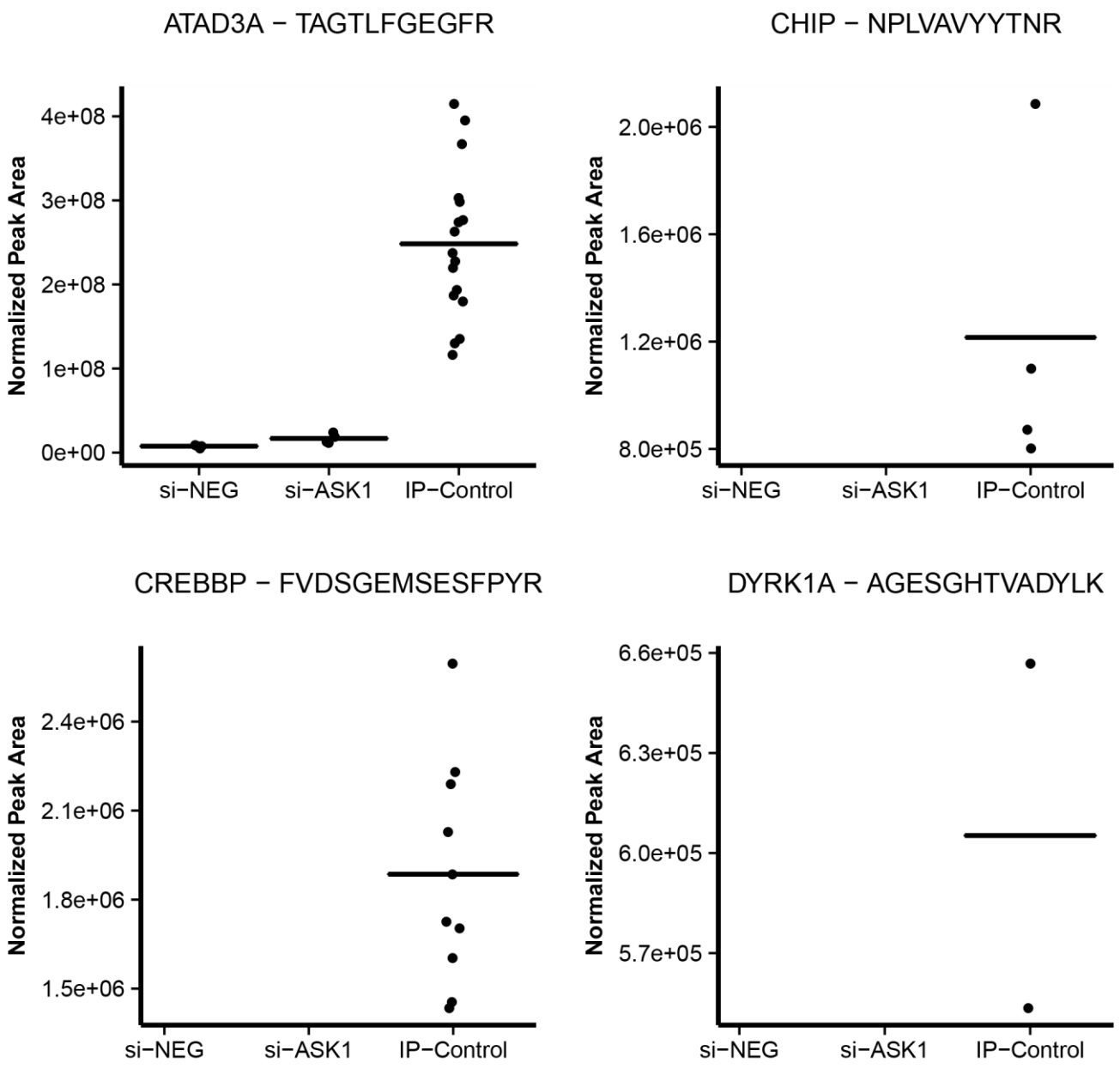


LRP-based results

**Figure A-4**

**B**

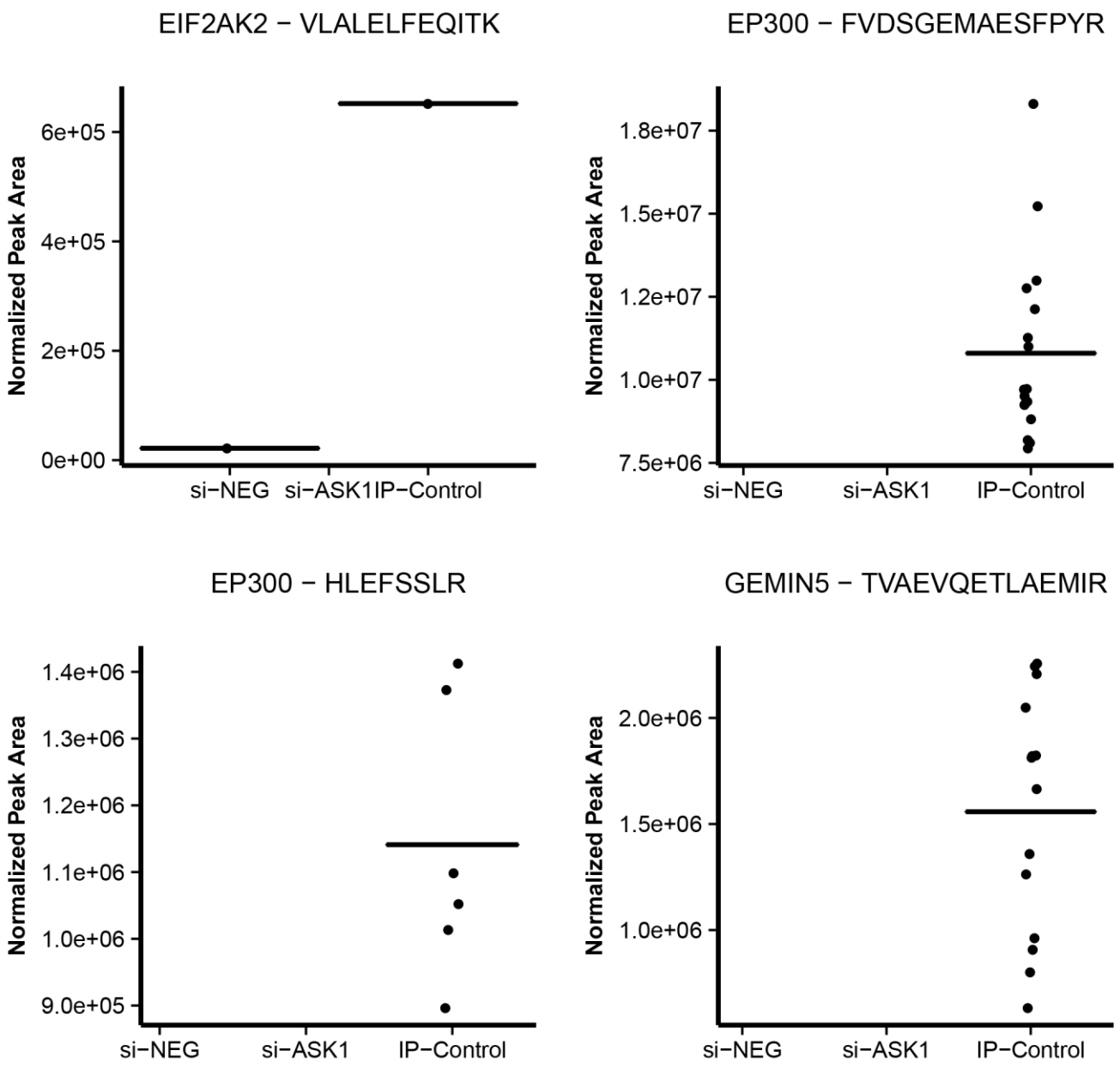


LRP-based results

**Figure A-4**

**B**

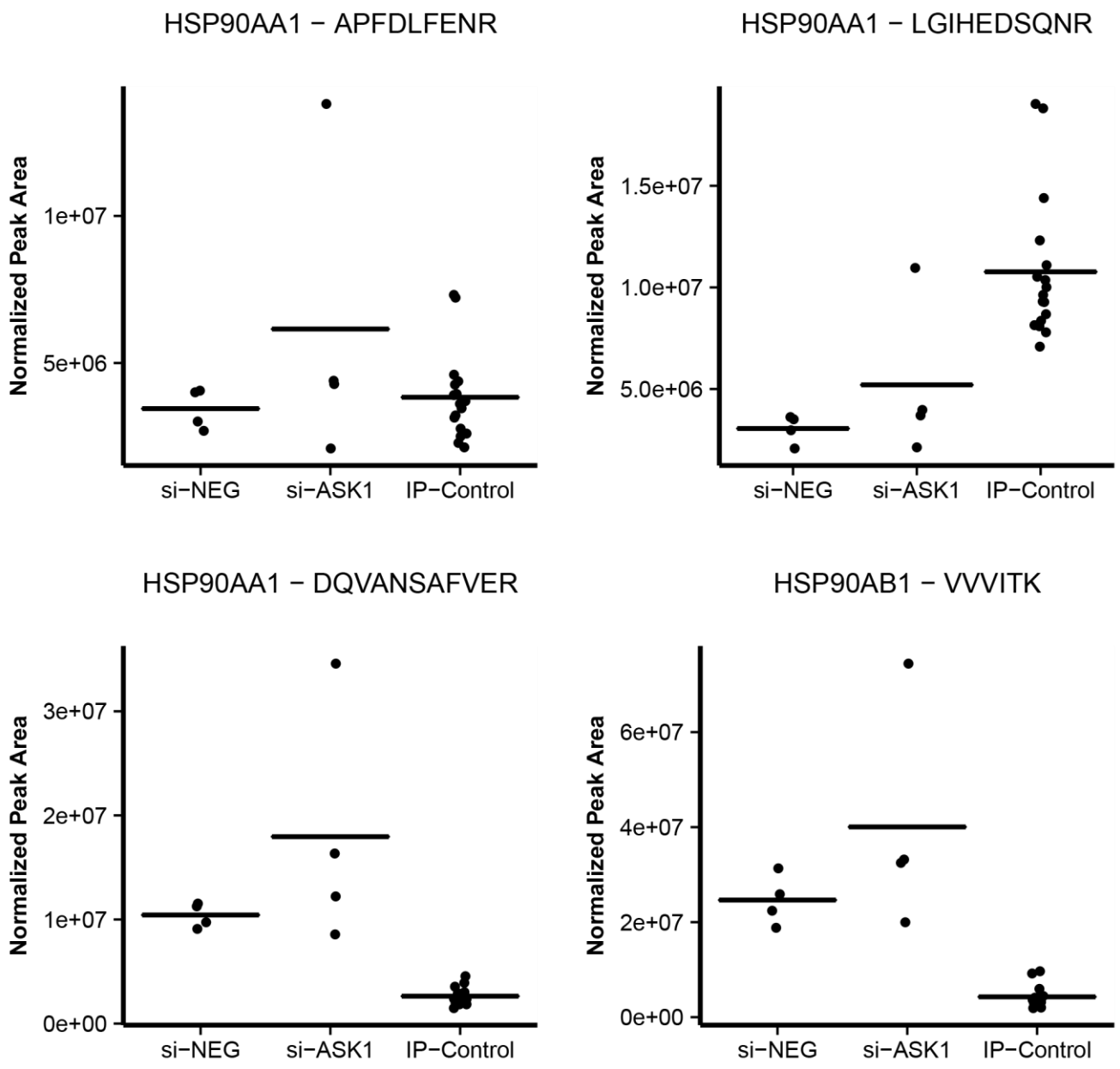


LRP-based results

**Figure A-4**

**B**

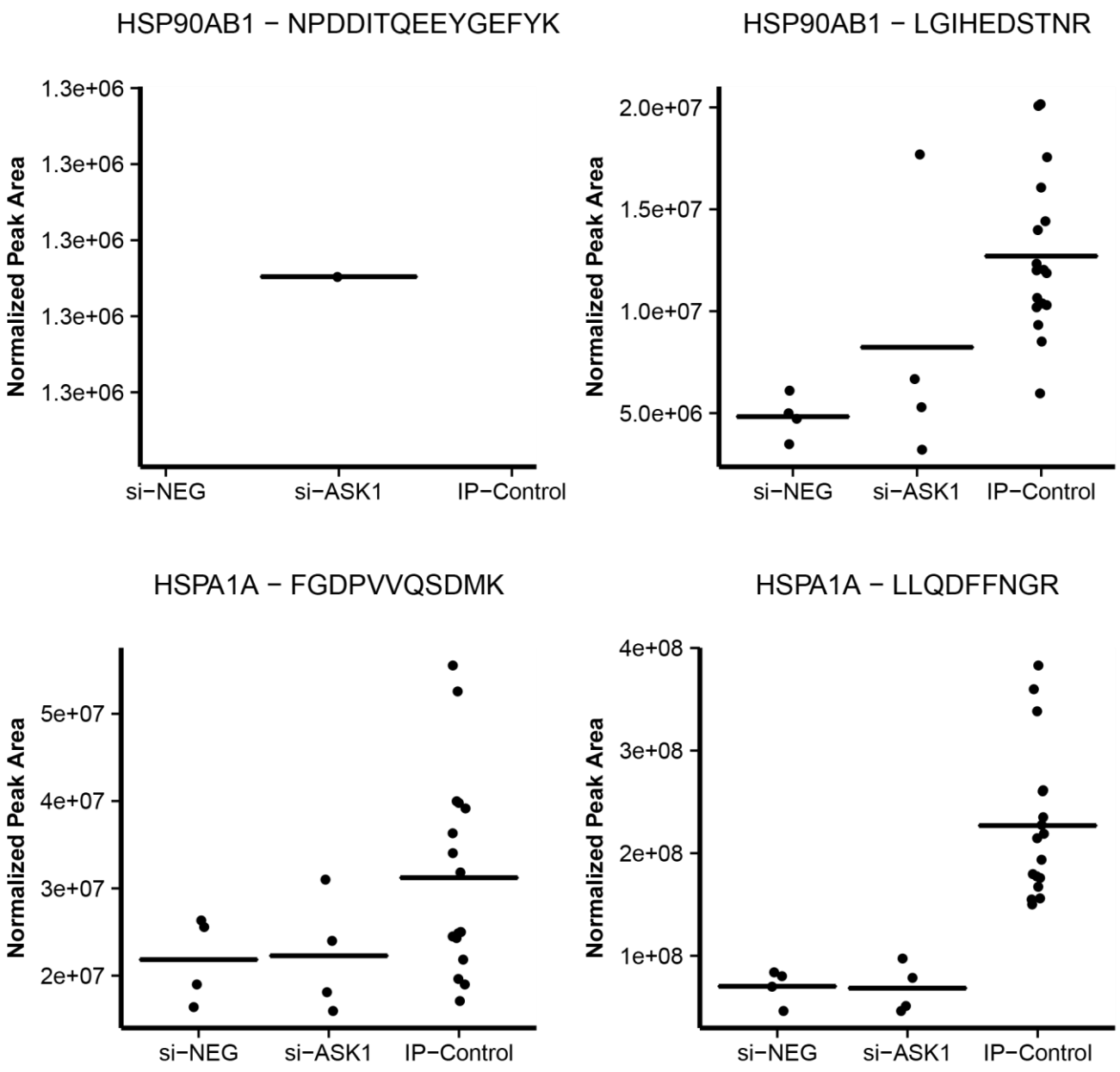


LRP-based results

**Figure A-4**

**B**

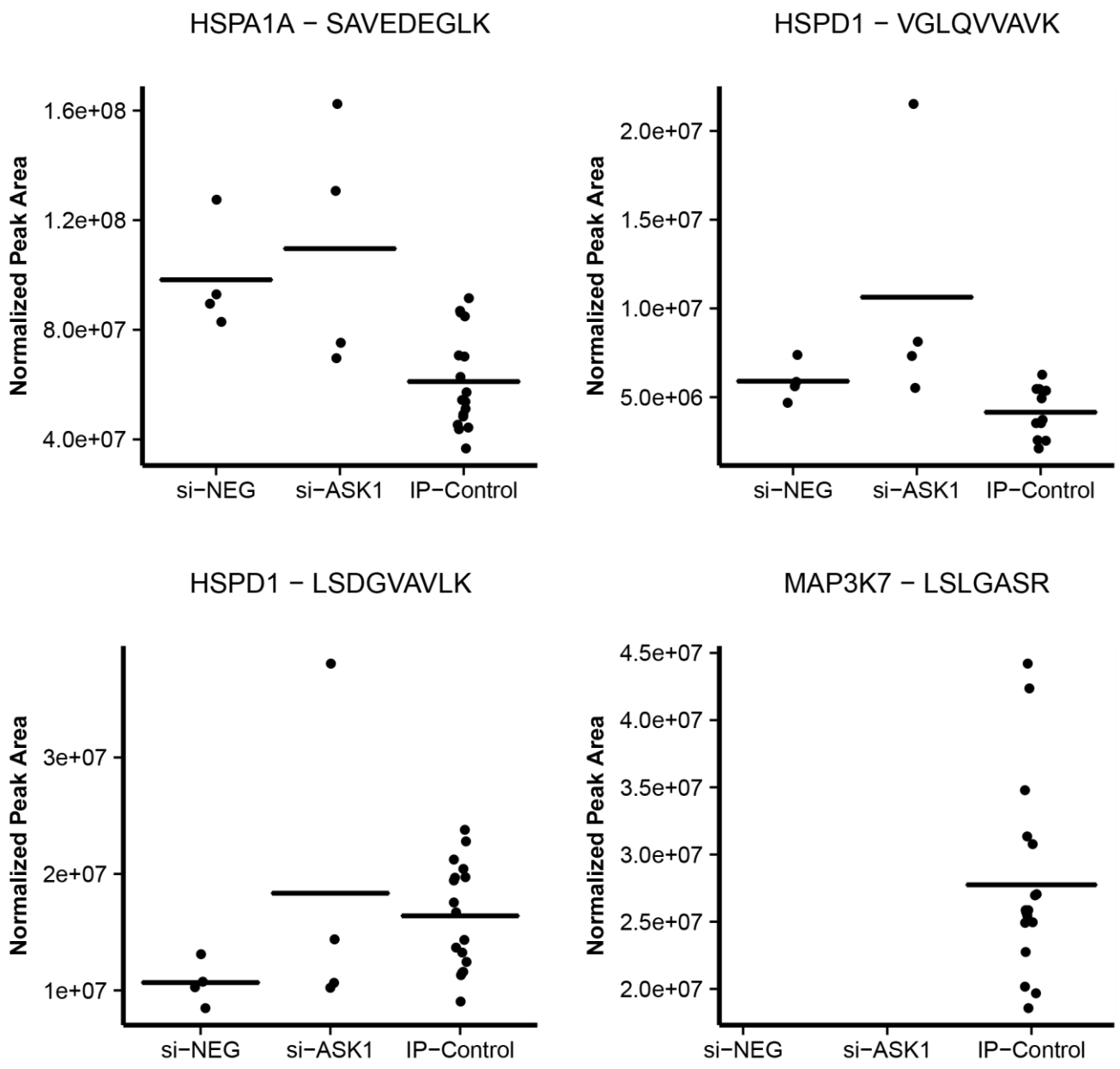


LRP-based results

**Figure A-4**

**B**

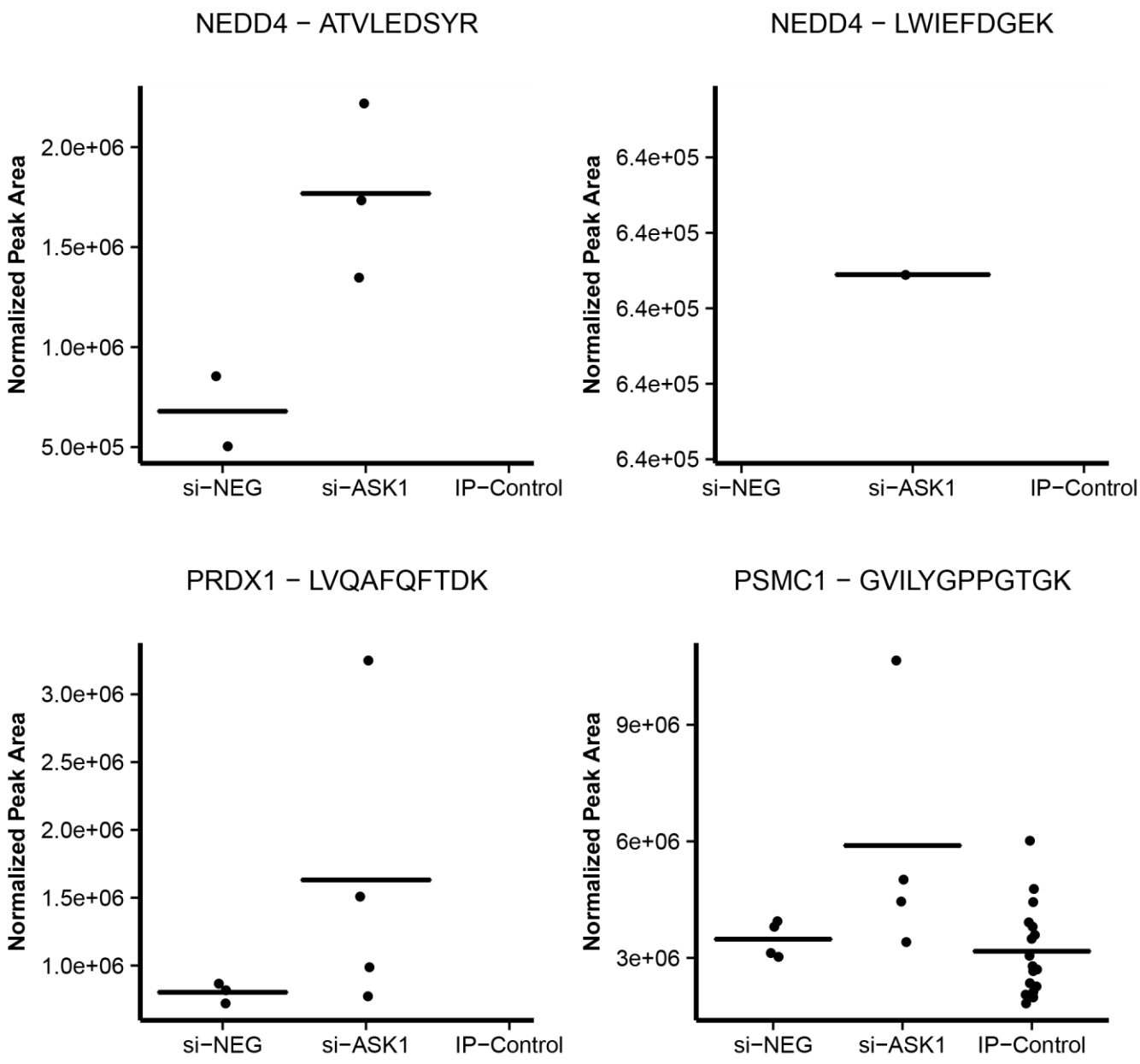


LRP-based results

**Figure A-4**

**B**

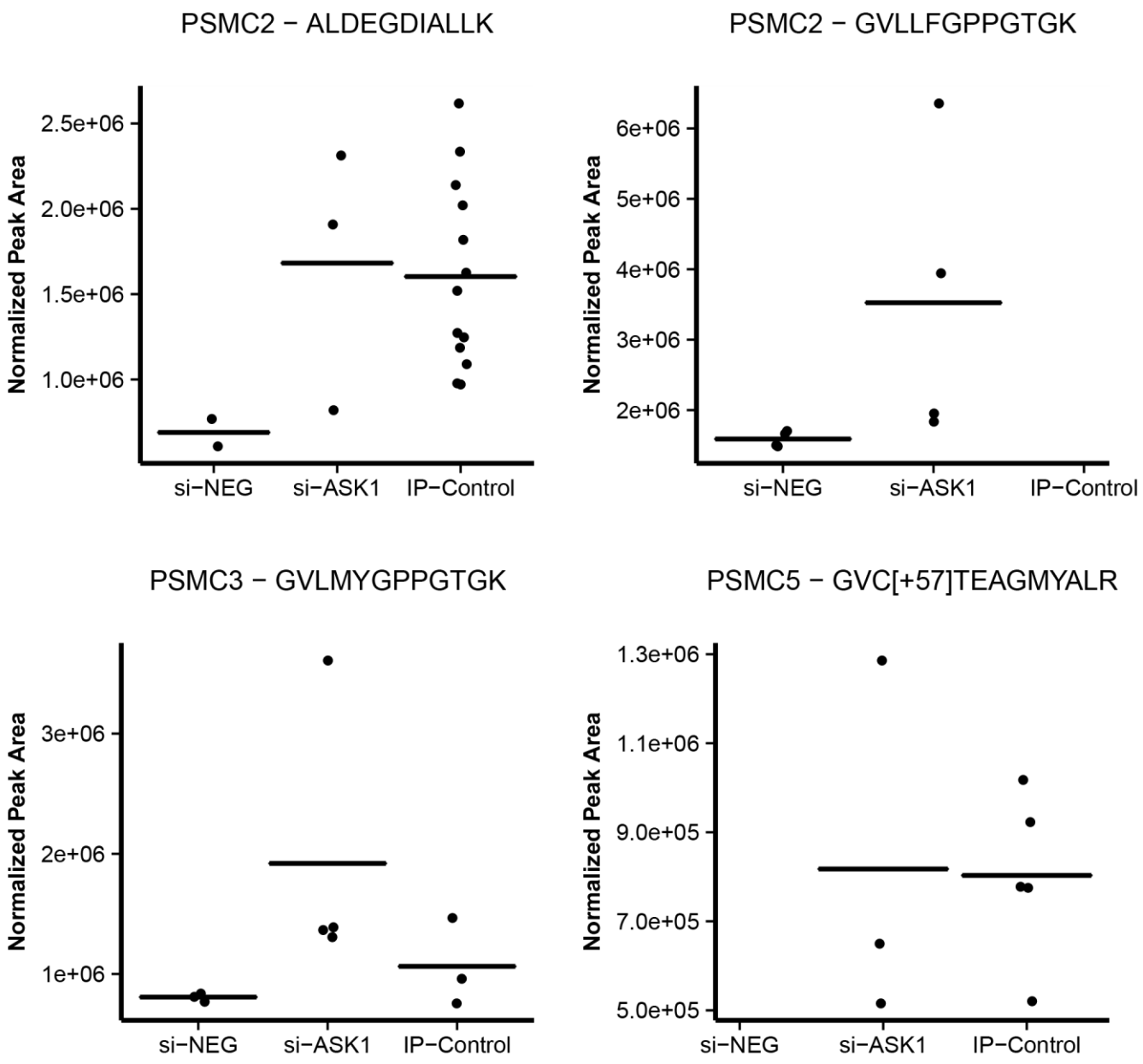


LRP-based results

**Figure A-4**

**B**

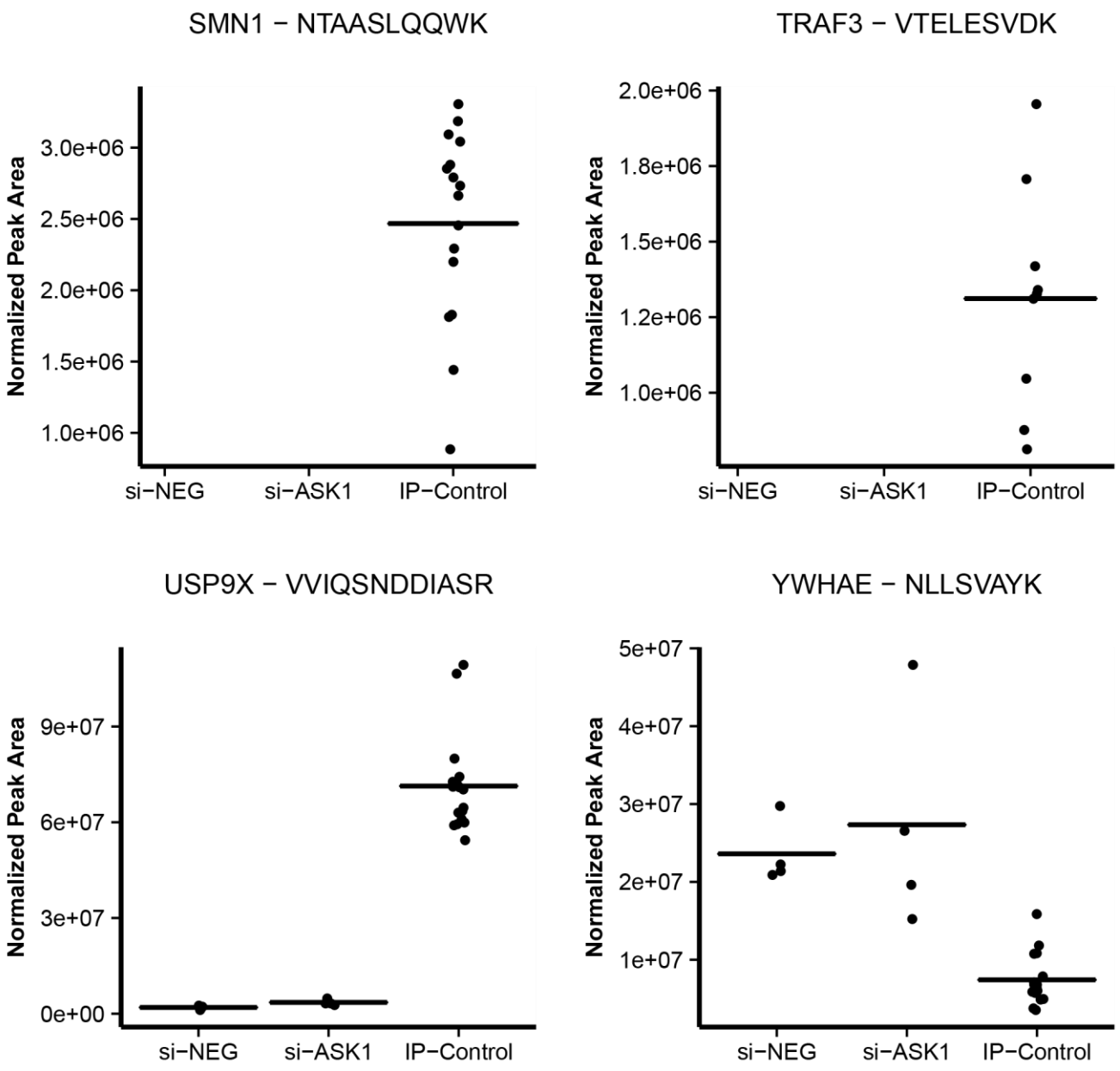


LRP-based results

**Figure A-4**

**B**

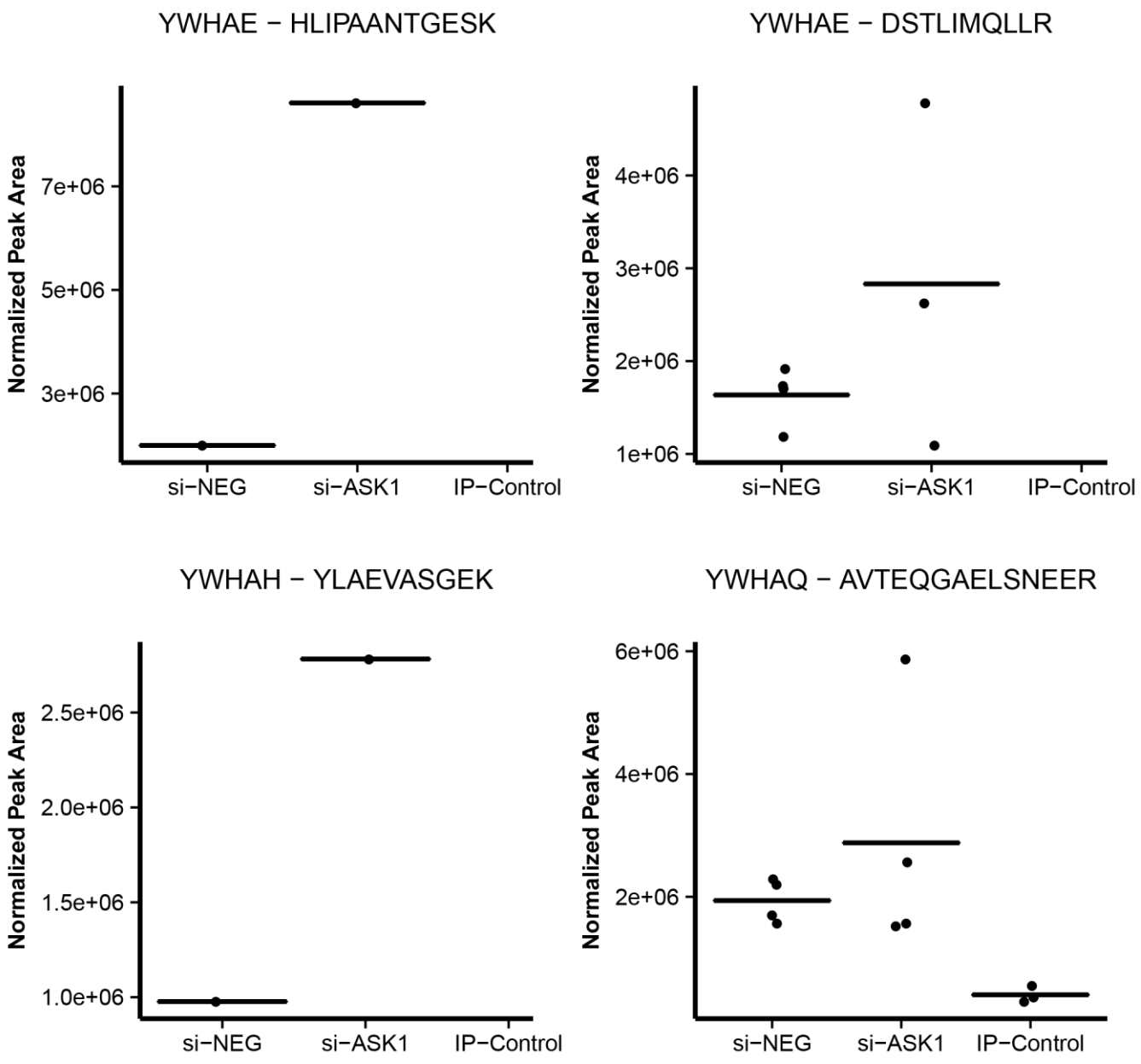
YWHAE − HLIPAANTGESK
YWHAE − DSTLIMQLLR
YWHAH − YLAEVASGEK
YWHAQ − AVTEQGAELSNEER
Normalized Peak Area
7e+06
5e+06
3e+06
4e+06
2e+06
1e+06
2.5e+06
2.0e+06
1.5e+06
1.0e+06
6e+06
si−NEG
si−ASK1
IP−Control
LRP-based results

**Figure A-4**

**B**

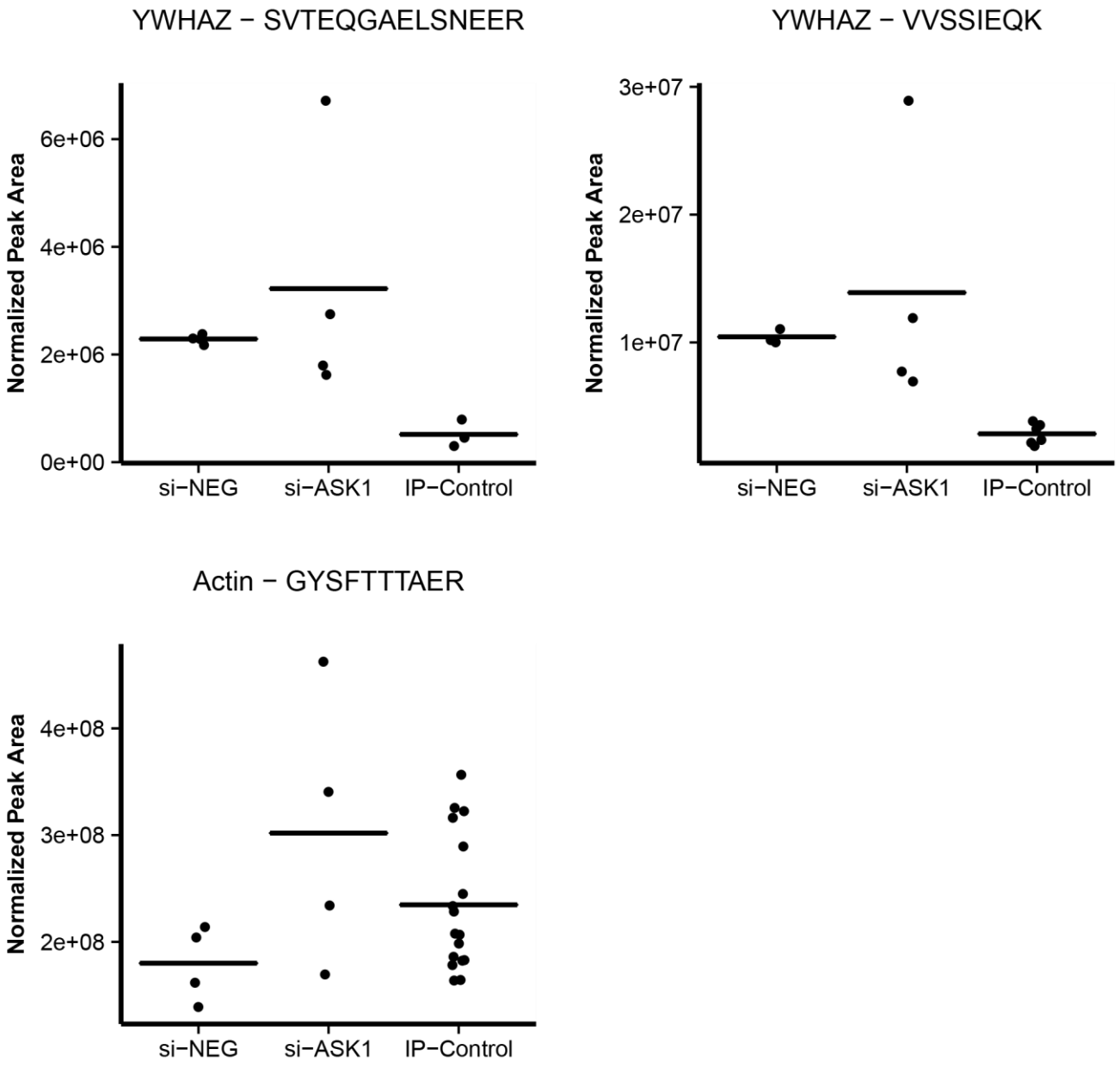


LRP-based results

**Figure A-4**

C

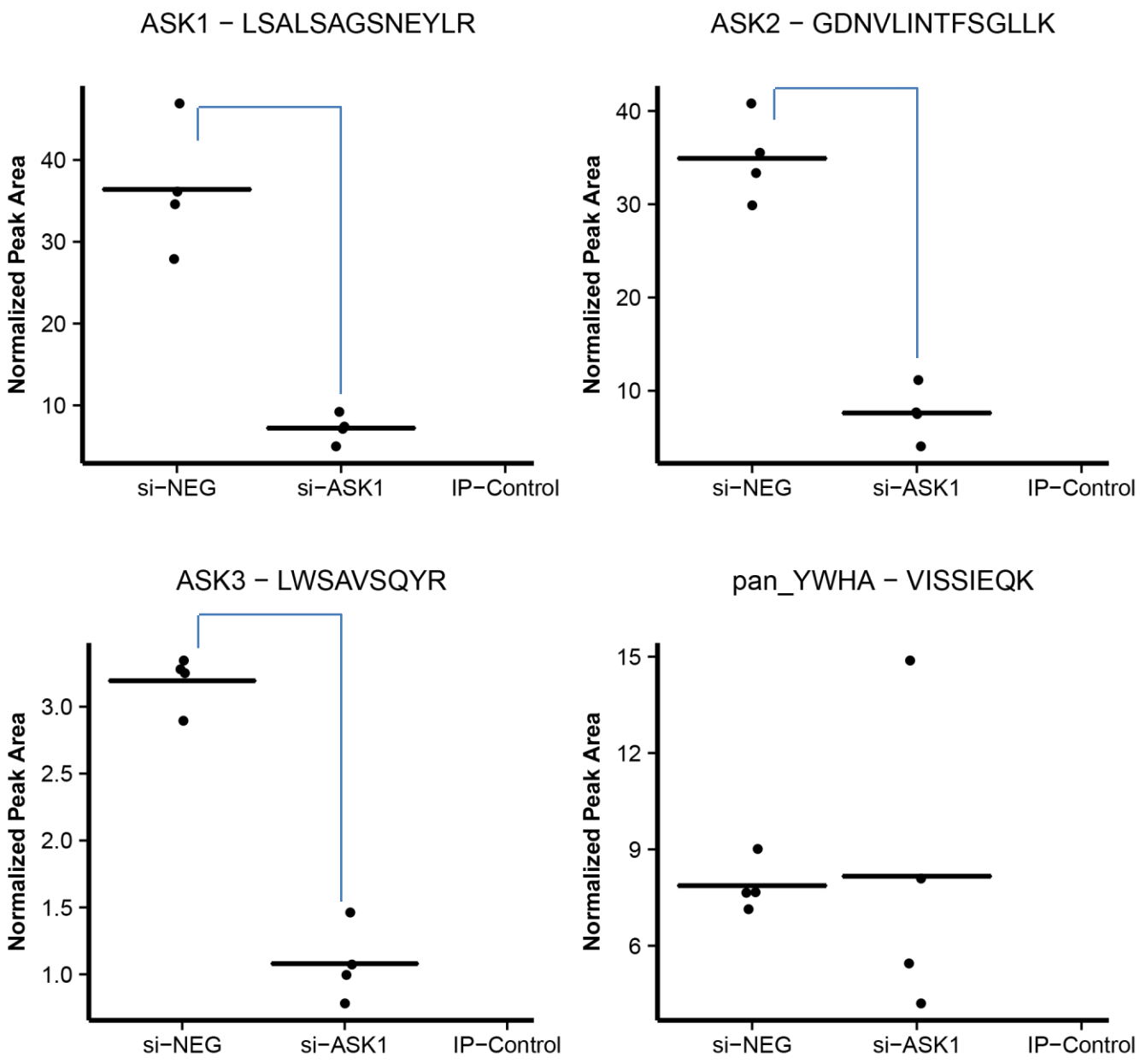


SID-based results

**Figure A-4**

C

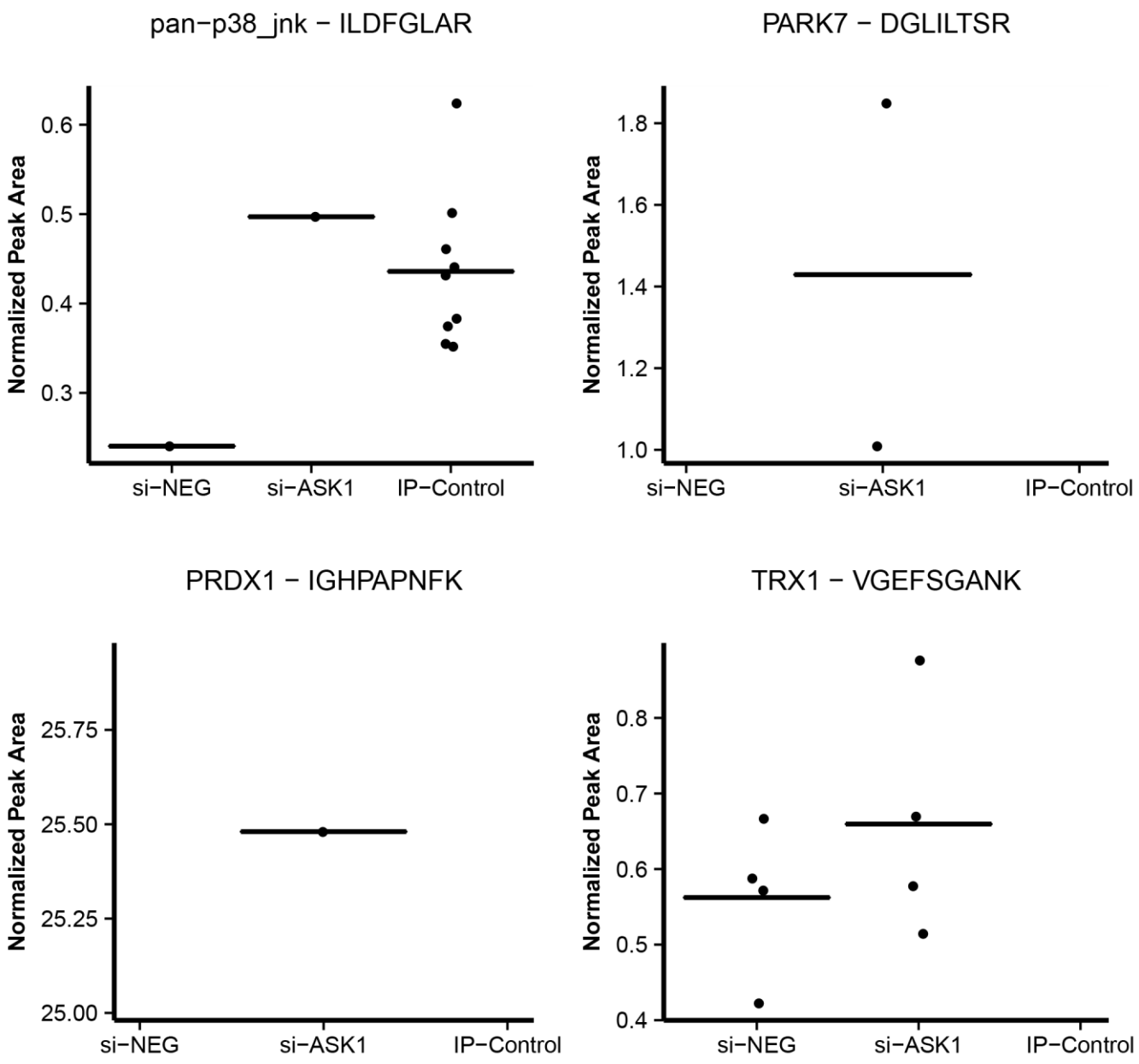


SID-based results

**Figure A-4**

**C**

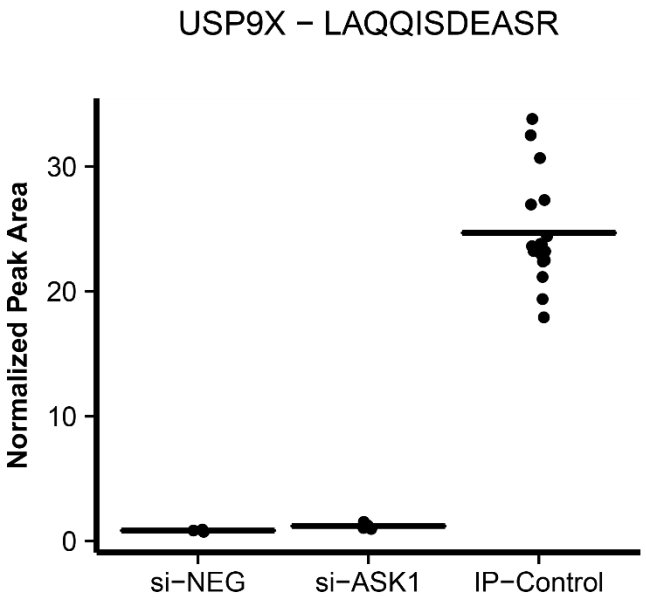


SID-based results

**Figure A-4**

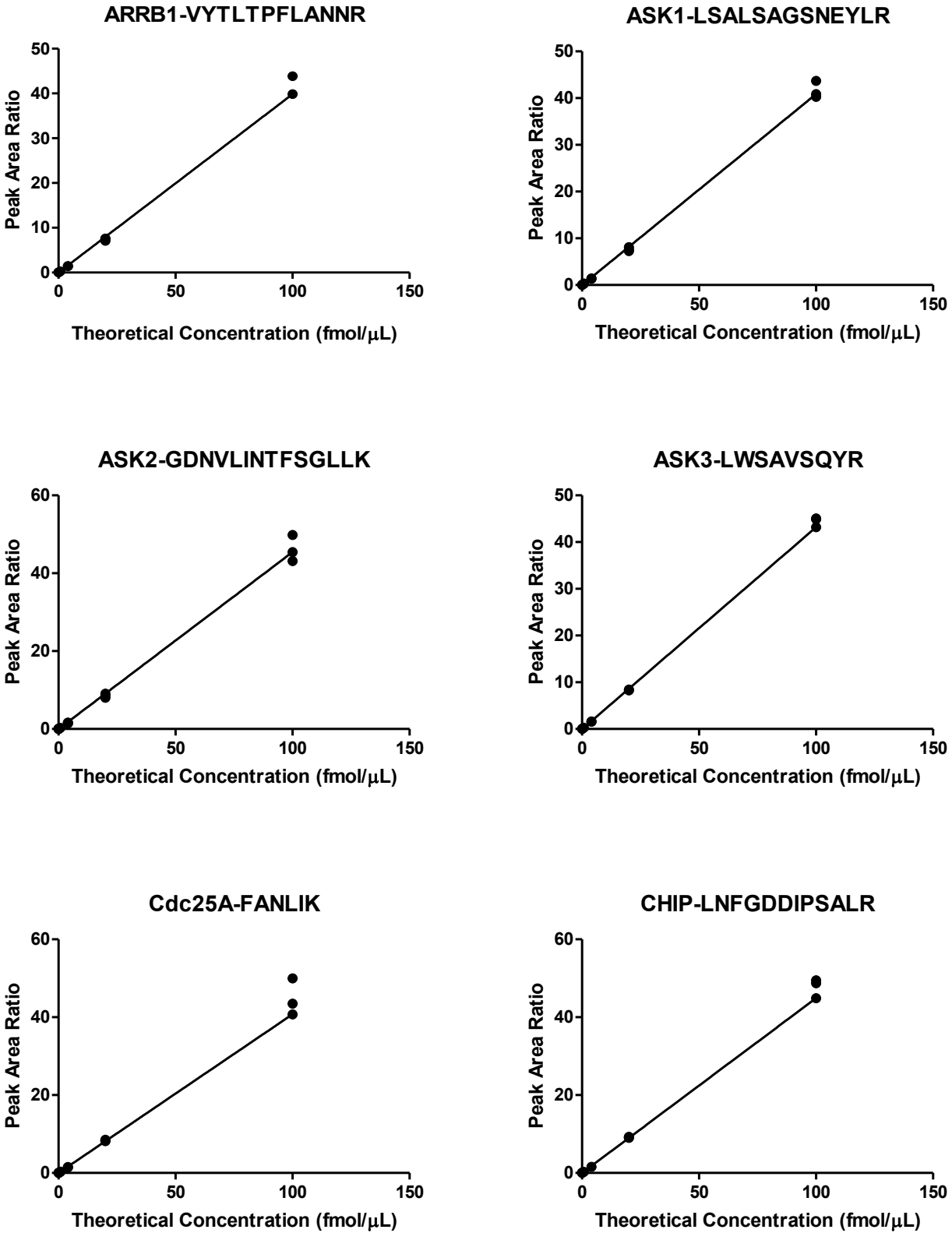


**Figure A-5.** SID calibration curve data. Linear regression curves of all 26 SID peptides with theoretical concentration on the x-axis and peak area ratio on the y-axis.

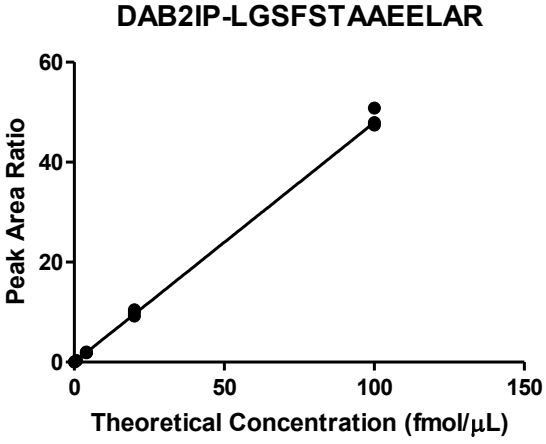
DAB2IP-LGSFSTAAEELAR
Peak Area Ratio
Theoretical Concentration (fmol/μL)
0
20
40
60
0
50
100
150

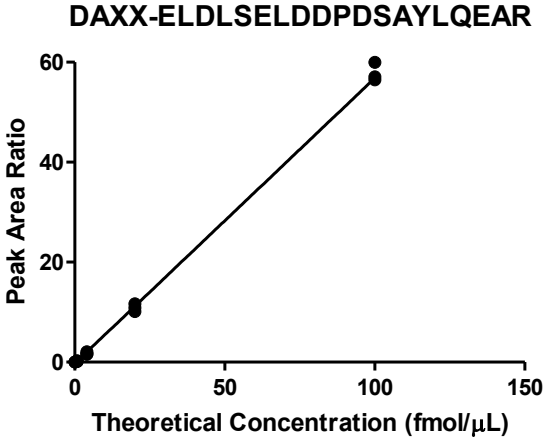
DAXX-ELDLSELDDPDSAYLQEAR
Peak Area Ratio
Theoretical Concentration (fmol/μL)
0
20
40
60
0
50
100
150

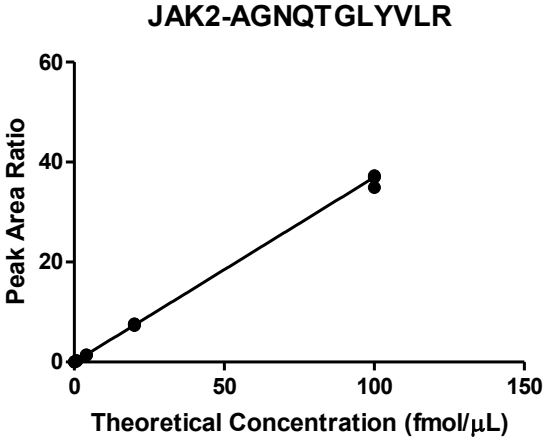
JAK2-AGNQTGLYVLR
Peak Area Ratio
Theoretical Concentration (fmol/μL)
0
20
40
60
0
50
100
150

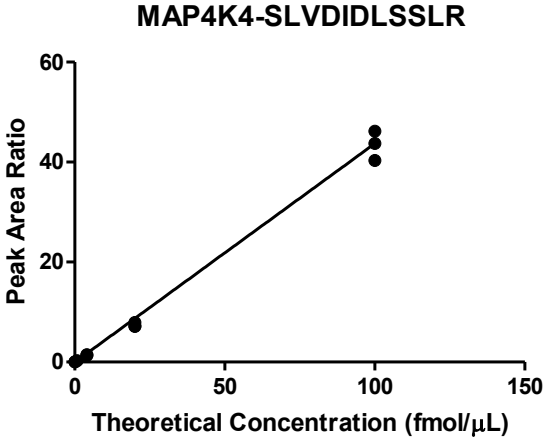
MAP4K4-SLVDIDLSSLR
Peak Area Ratio
Theoretical Concentration (fmol/μL)
0
20
40
60
0
50
100
150

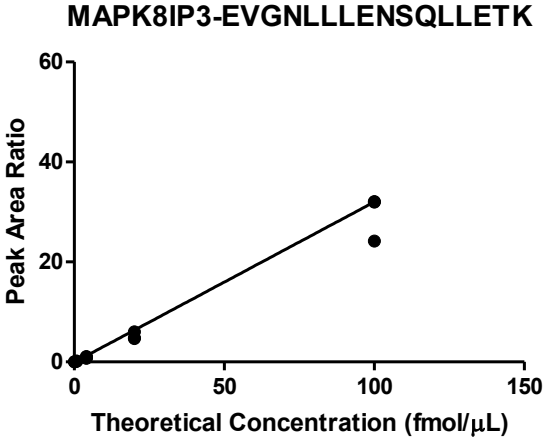
MAPK8IP3-EVGNLLLENSQLLETK
Peak Area Ratio
Theoretical Concentration (fmol/μL)
0
20
40
60
0
50
100
150

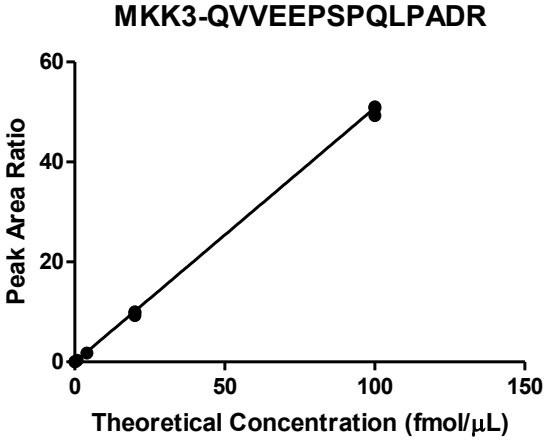
MKK3-QVVEEPSPQLPADR
Peak Area Ratio
Theoretical Concentration (fmol/μL)
0
20
40
60
0
50
100
150

**Figure A-5.**

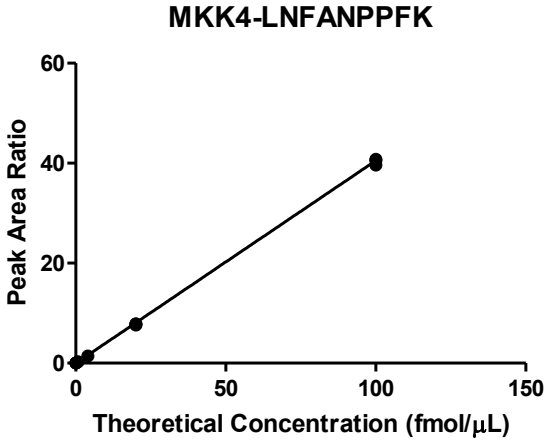
MKK4-LNFANPPFK
Peak Area Ratio
Theoretical Concentration (fmol/μL)
0
20
40
60
0
50
100
150

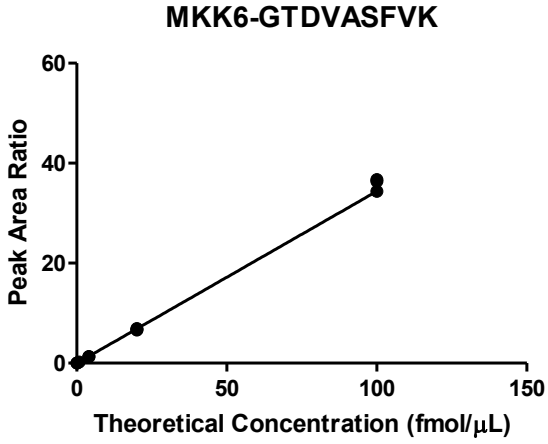
MKK6-GTDVASFVK
Peak Area Ratio
Theoretical Concentration (fmol/μL)
0
20
40
60
0
50
100
150

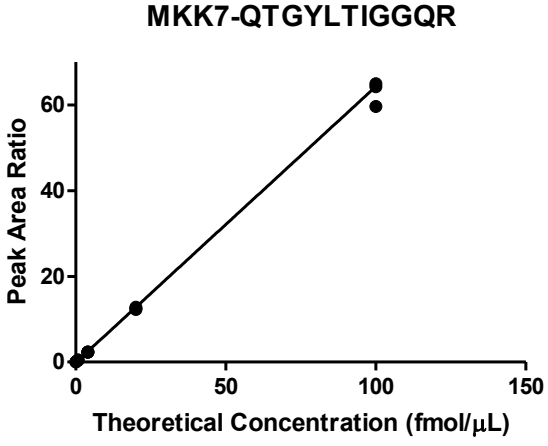
MKK7-QTGYLTIGGQR
Peak Area Ratio
Theoretical Concentration (fmol/μL)
0
20
40
60
0
50
100
150

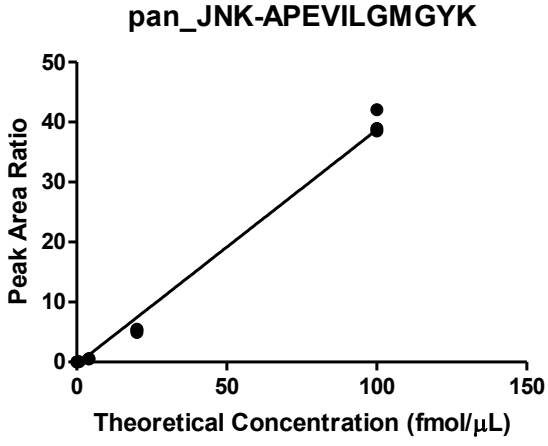
pan_JNK-APEVILGMGYK
Peak Area Ratio
Theoretical Concentration (fmol/μL)
0
10
20
30
40
50
0
50
100
150

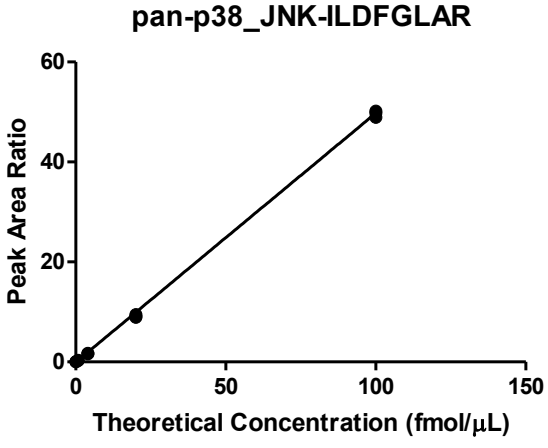
pan-p38_JNK-ILDFGLAR
Peak Area Ratio
Theoretical Concentration (fmol/μL)
0
20
40
60
0
50
100
150

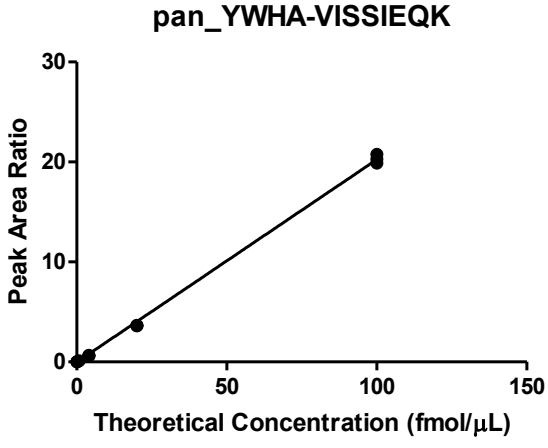
pan_YWHA-VISSIEQK
Peak Area Ratio
Theoretical Concentration (fmol/μL)
0
10
20
30
0
50
100
150

**Figure A-5.**

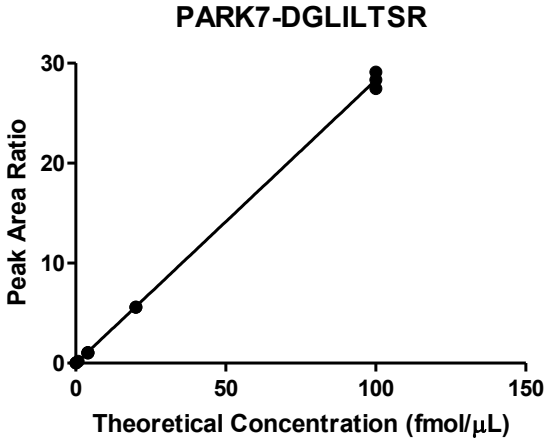
PARK7-DGLILTSR
Peak Area Ratio
0
10
20
30
0
50
100
150
Theoretical Concentration (fmol/μL)

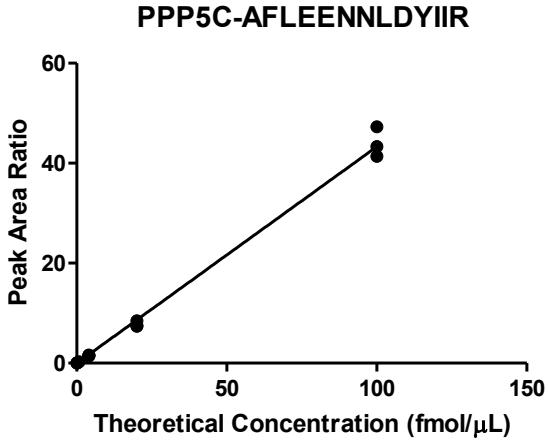
PPP5C-AFLEENNLDYIIR
Peak Area Ratio
0
20
40
60
0
50
100
150
Theoretical Concentration (fmol/μL)

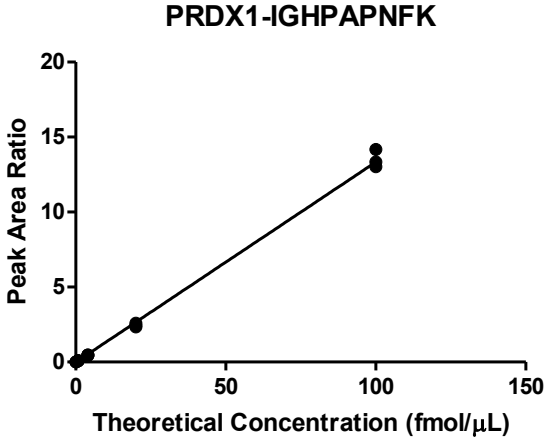
PRDX1-IGHPAPNFK
Peak Area Ratio
0
5
10
15
20
0
50
100
150
Theoretical Concentration (fmol/μL)

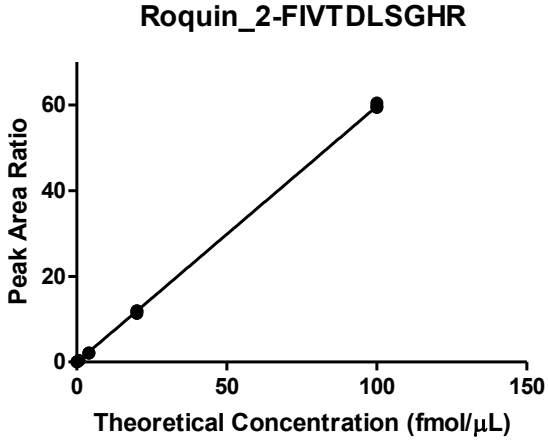
Roquin_2-FIVTDLSGHR
Peak Area Ratio
0
20
40
60
0
50
100
150
Theoretical Concentration (fmol/μL)

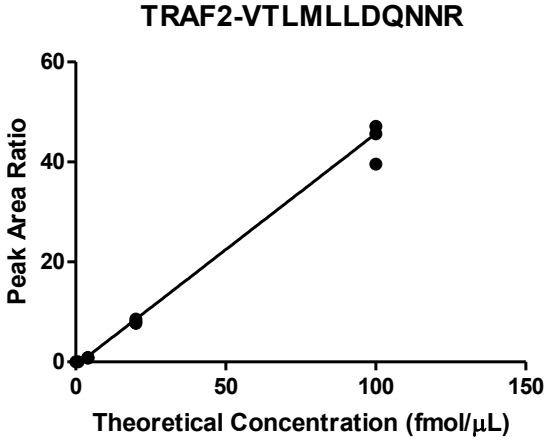
TRAF2-VTLMLLDQNNR
Peak Area Ratio
0
20
40
60
0
50
100
150
Theoretical Concentration (fmol/μL)

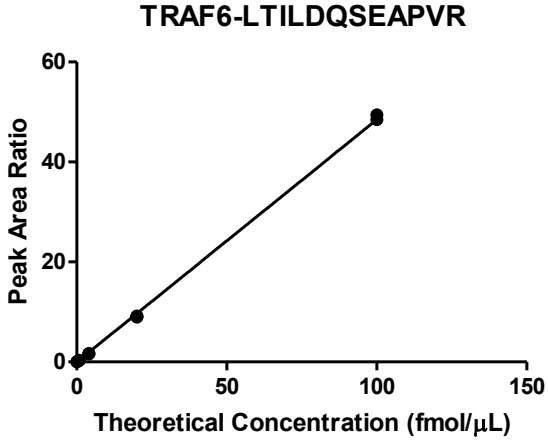
TRAF6-LTILDQSEAPVR
Peak Area Ratio
0
20
40
60
0
50
100
150
Theoretical Concentration (fmol/μL)

**Figure A-5.**

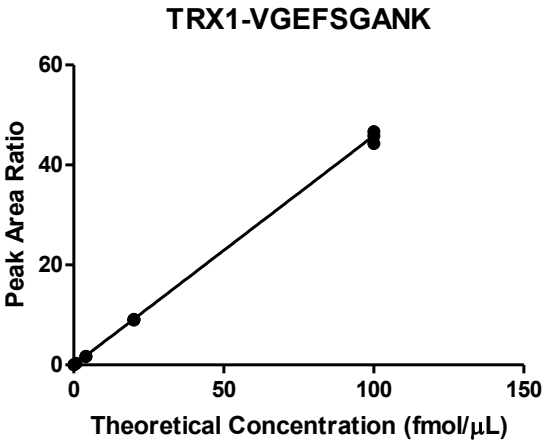
TRX1-VGEFSGANK
Peak Area Ratio
60
40
20
0
0
50
100
150
Theoretical Concentration (fmol/μL)

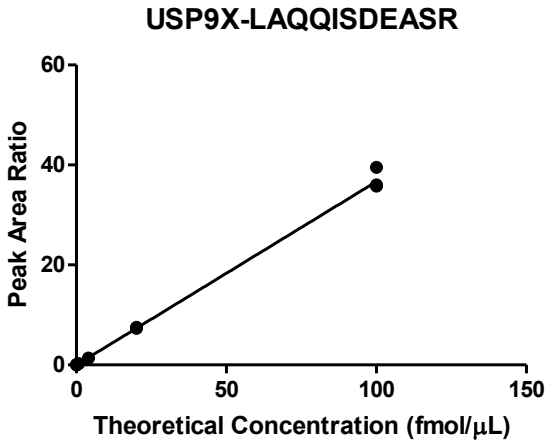
USP9X-LAQQISDEASR
Peak Area Ratio
60
40
20
0
0
50
100
150
Theoretical Concentration (fmol/μL)

**Figure A-5.**

A

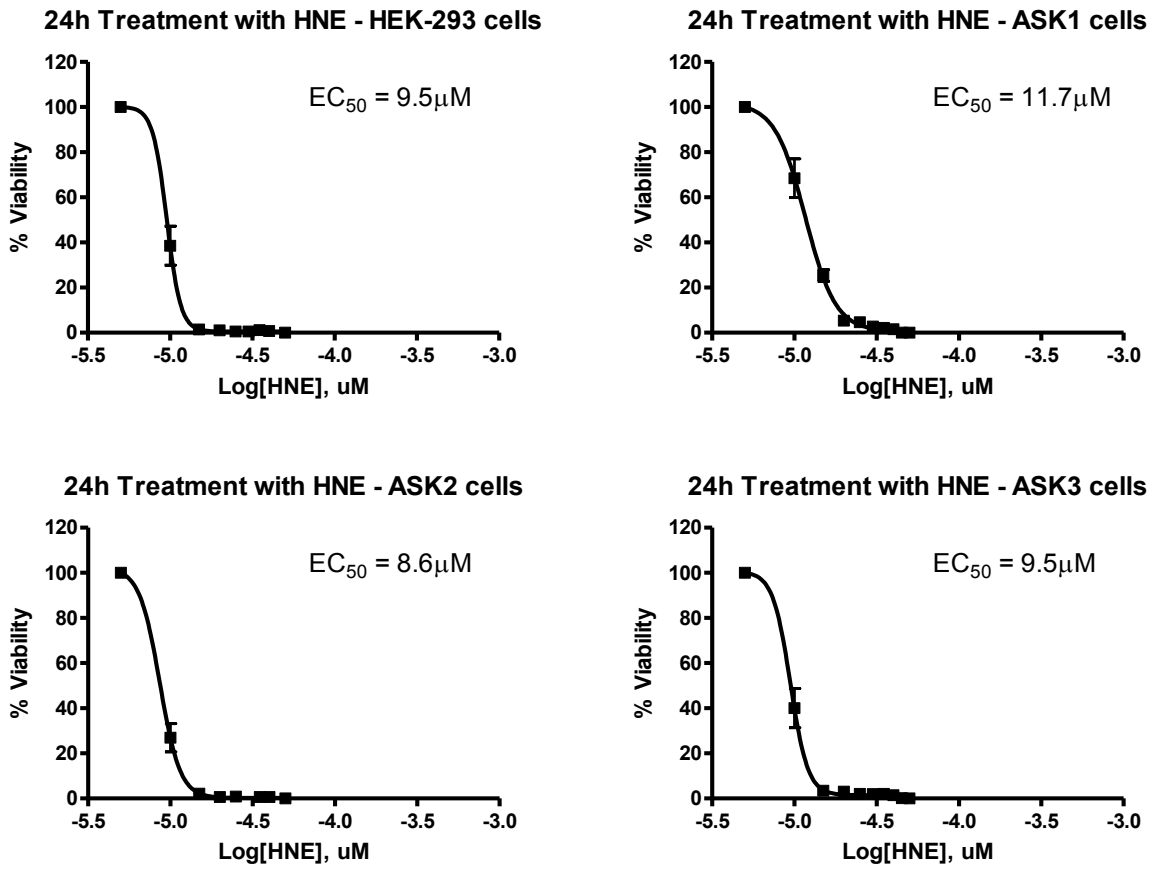


B

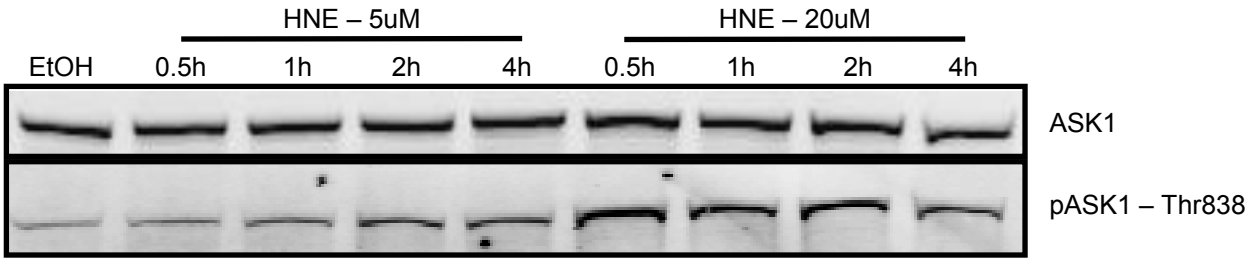


**Figure A-6**. HNE $EC_{50}$ determination. (A) $EC_{50}$ values for HNE were found for each cell line using a WST assay. (B) ASK1 activation below (5μM) and above (20μM) the $EC_{50}$ value.

**A**

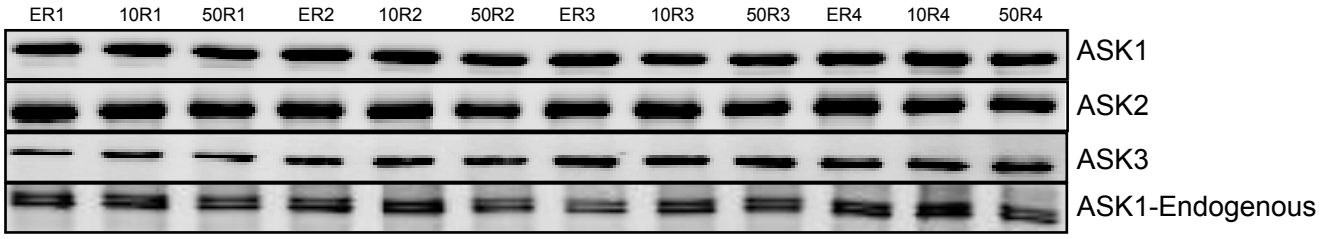


**B**

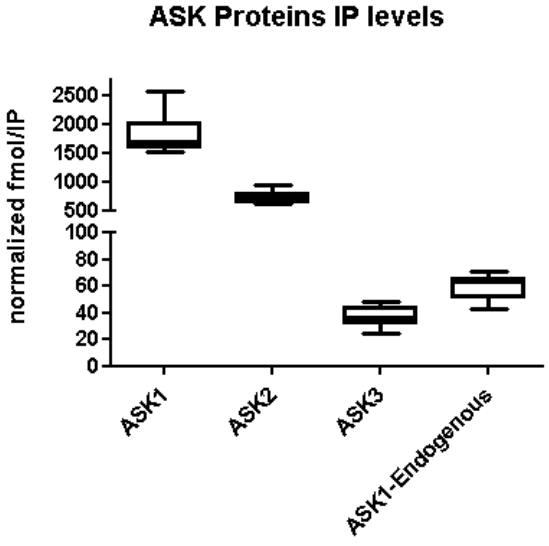


**Figure A-7**. ASK protein purification. (A) Western- and (B) PRM-based analysis of the amount of target protein purified in each cell line for the HNE concentration-response experiment.

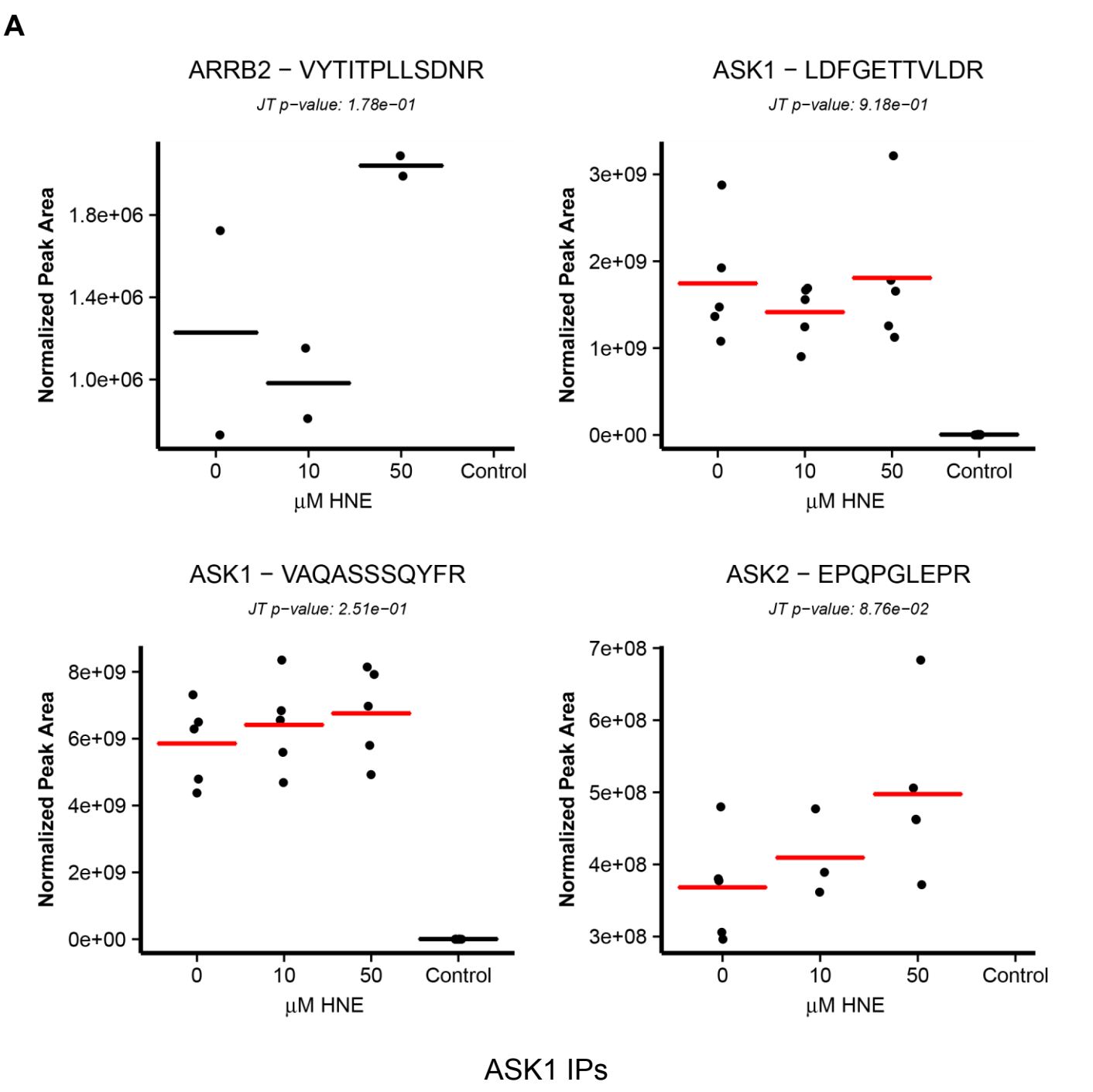


**Figure A-8.** HNE induced dynamic ASK1 complex changes. All peptides normalized by LRP for the (A) ASK1 IPs, (B) ASK2 IPs, (C) ASK3 IPs, (D) ASK1 Endogenous IPs were plotted as grouped scatter plots. The mean value for each condition is depicted as a bar. A red bar means that the peak areas for this condition were enriched over the negative control based on the Wilcoxon rank sum test with $p<0.05$ or detection in at least half of the replicates for a condition and no detection in the negative control samples. Concentration-response trends were tested in two ways: (1) the Jonckheere-Terpstra test was applied to detect an ordered trend in peak area – the results of this test are listed below the protein name and peptide sequence on each graph and (2) A Kruskal-Wallace test with post-hoc Dunn's analysis was performed – all significant pairwise comparisons are listed on the graphs with bars connecting the significantly different conditions.

A

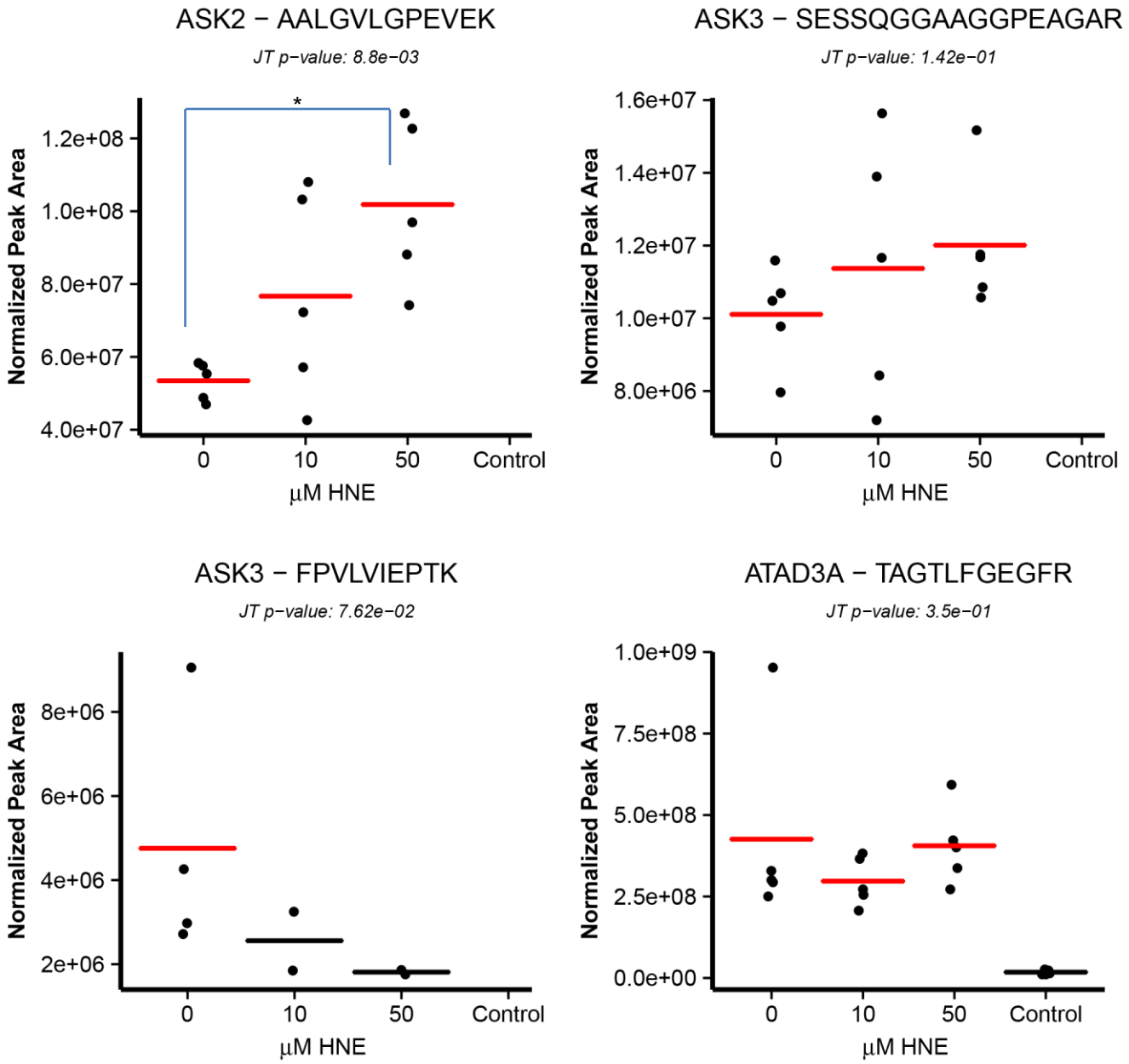


ASK1 IPs

**Figure A-8.**

**A**

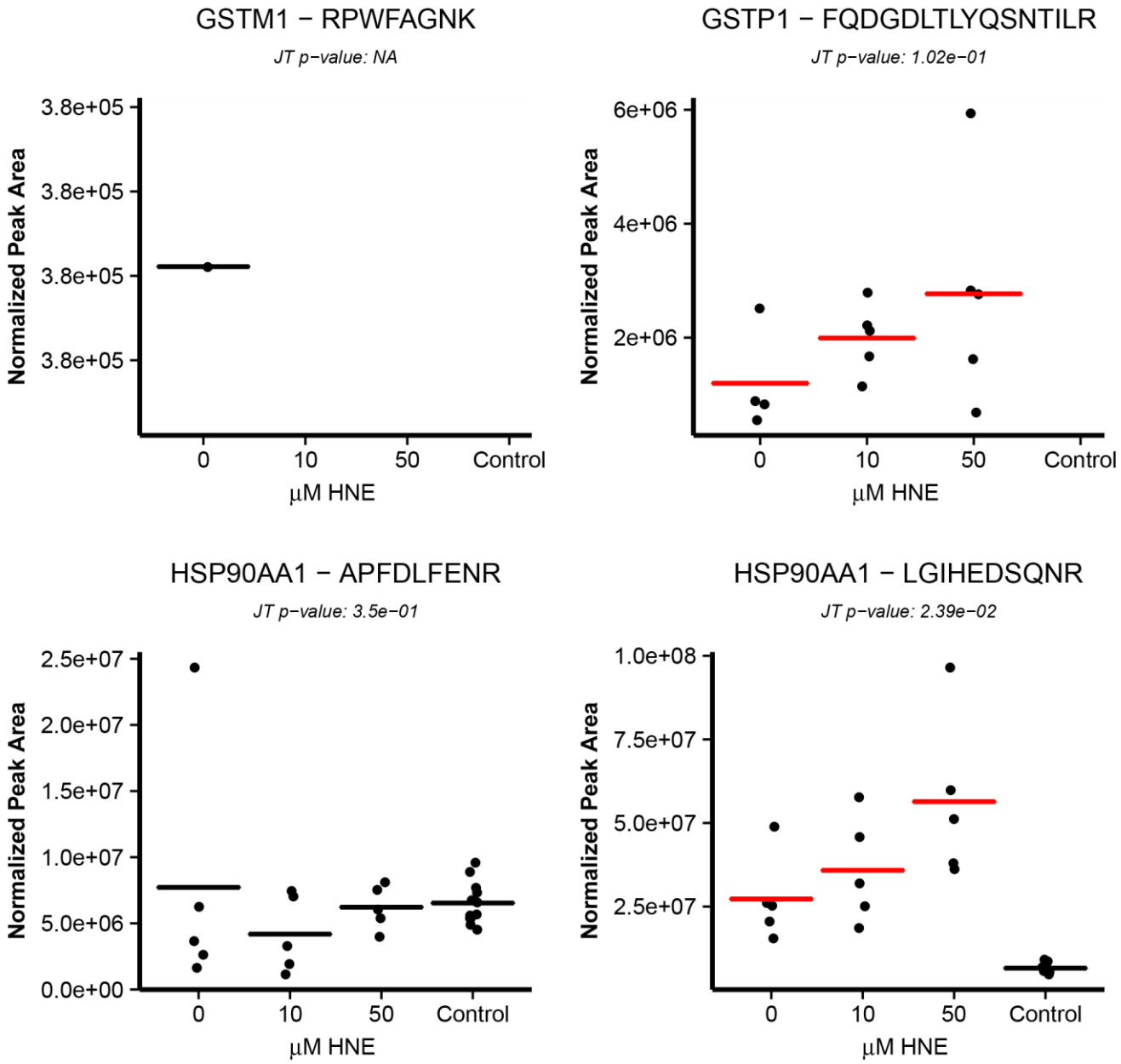


ASK1 IPs

**Figure A-8.**

**A**

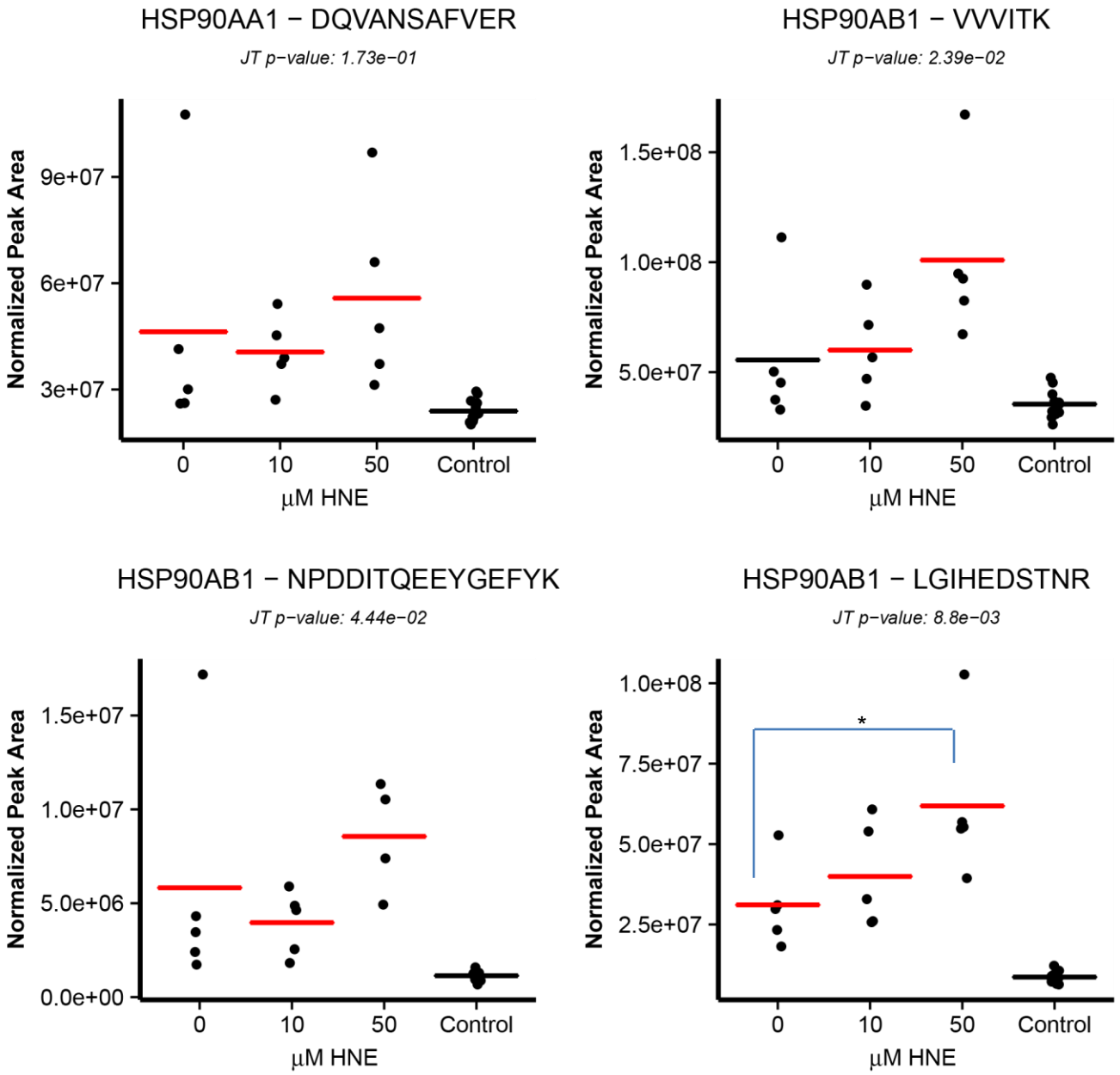


ASK1 IPs

**Figure A-8.**

**A**

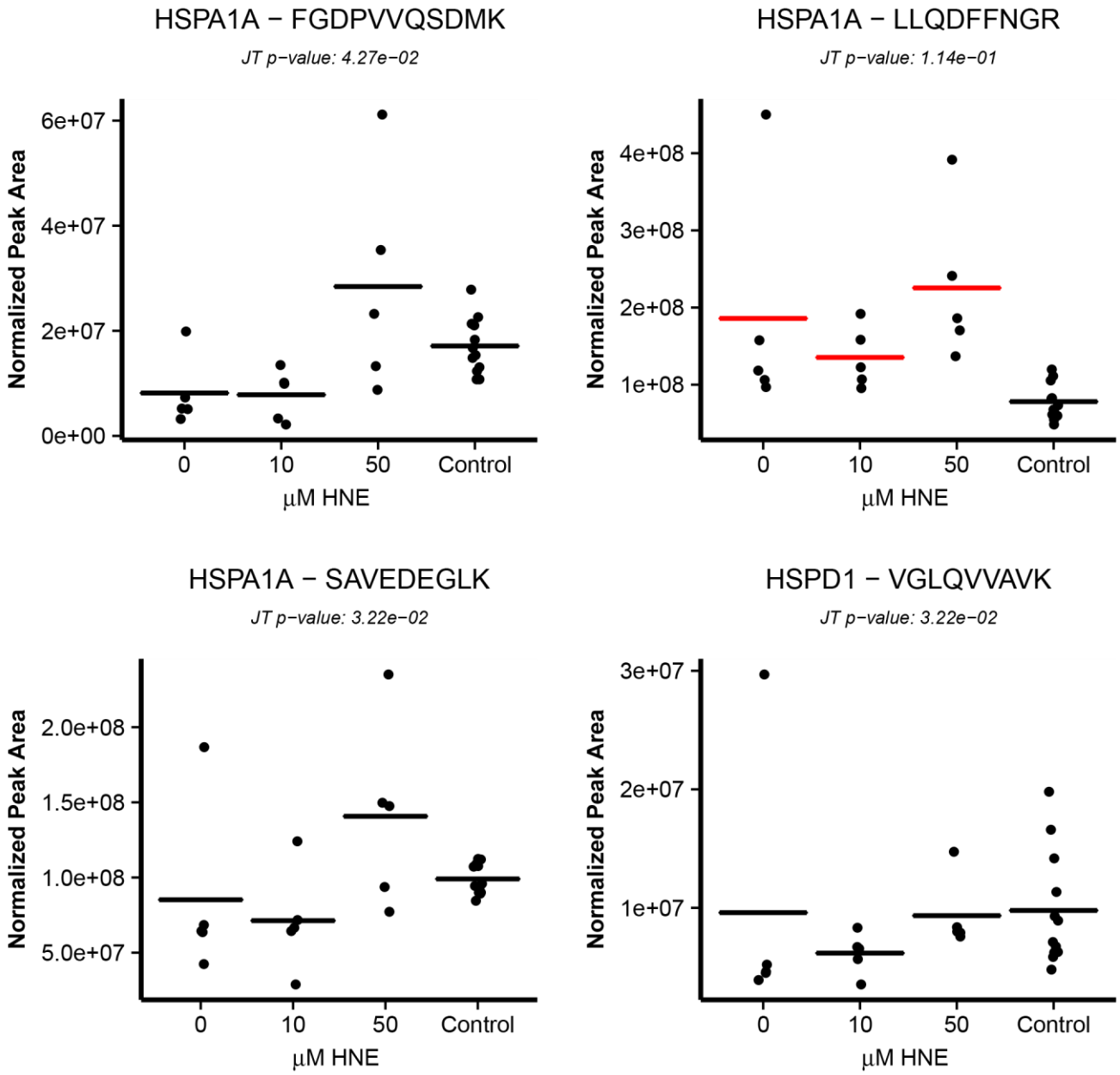


ASK1 IPs

**Figure A-8.**

**A**

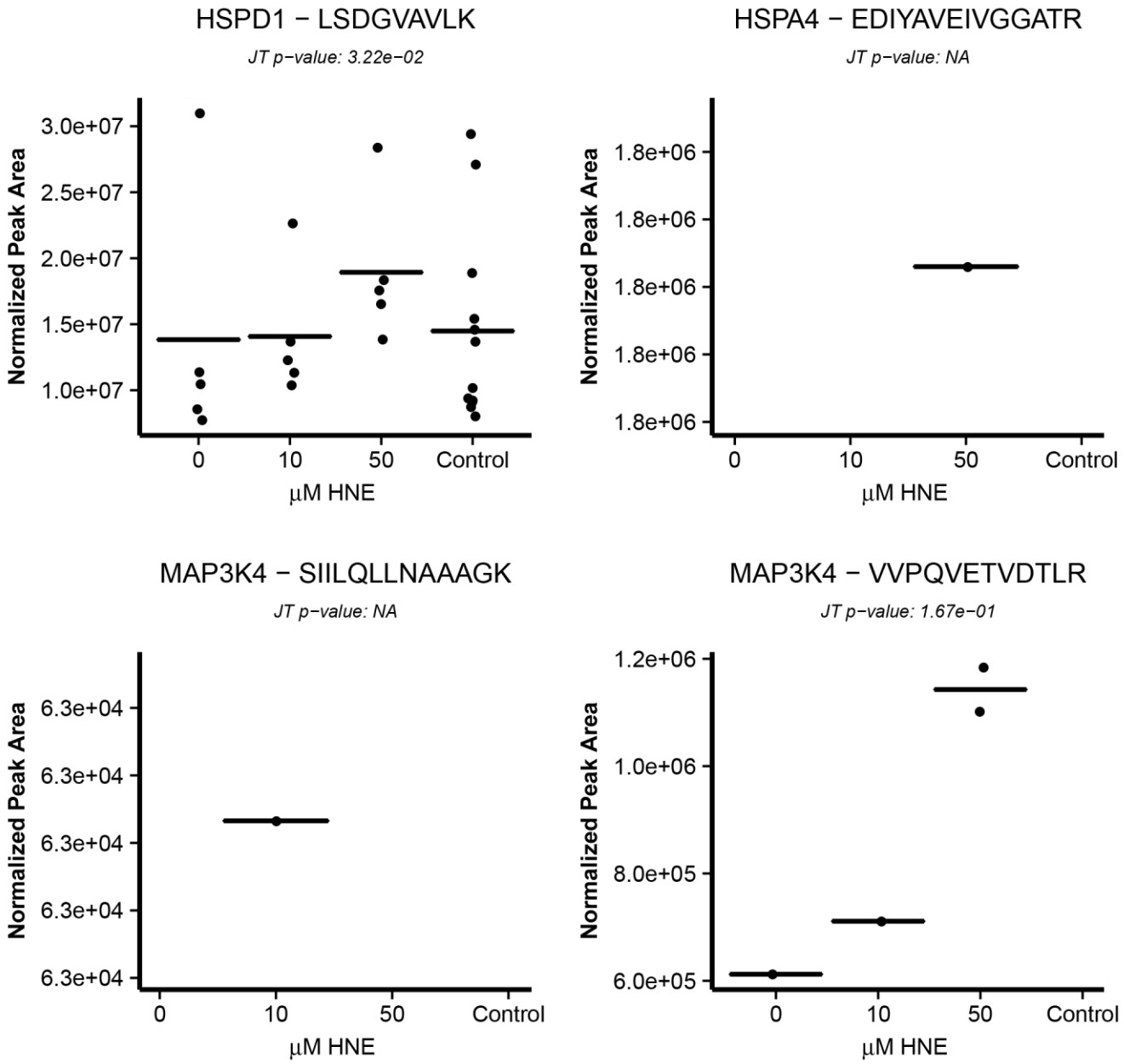


ASK1 IPs

**Figure A-8.**

**A**

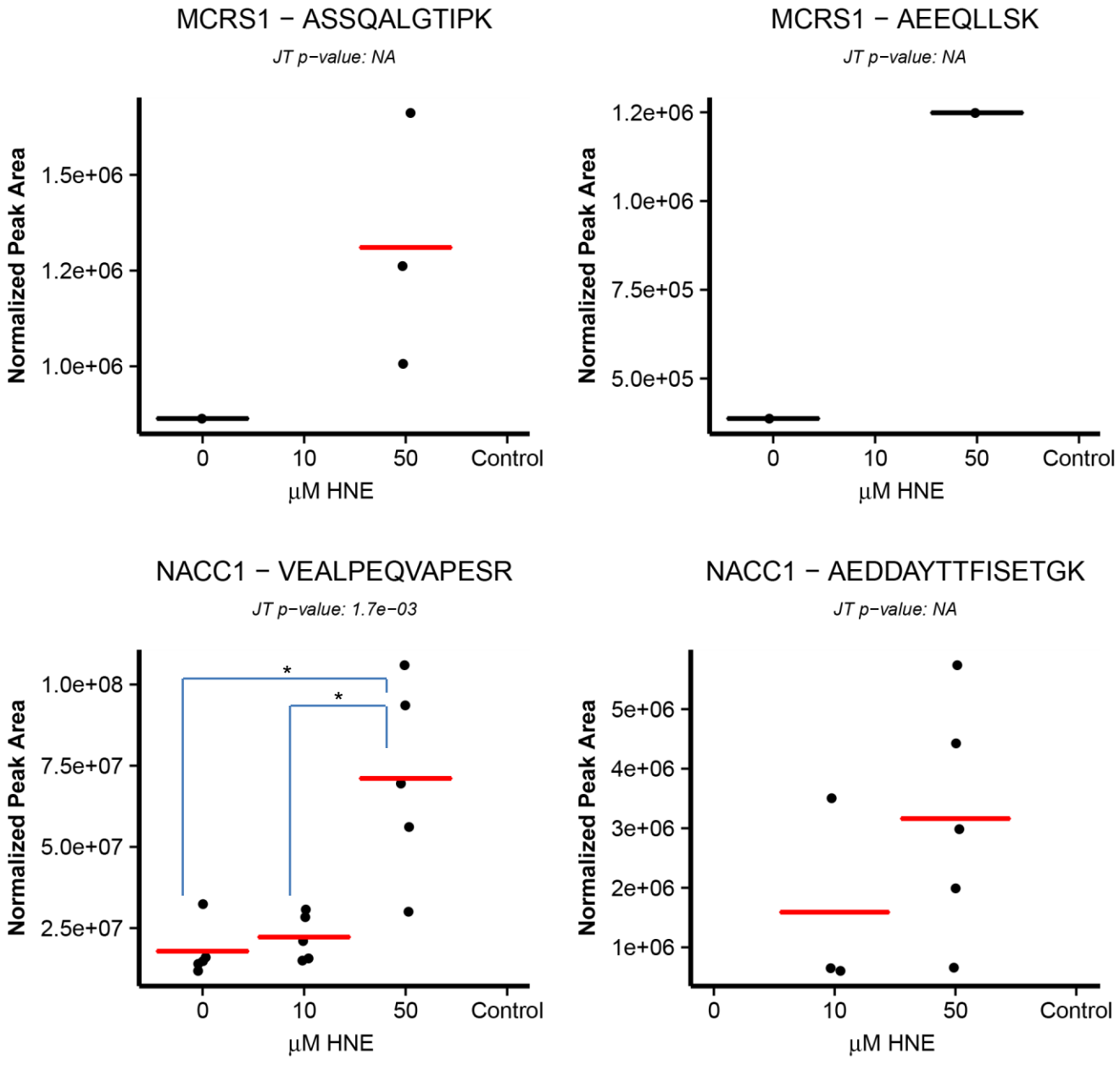


ASK1 IPs

**Figure A-8.**

**A**

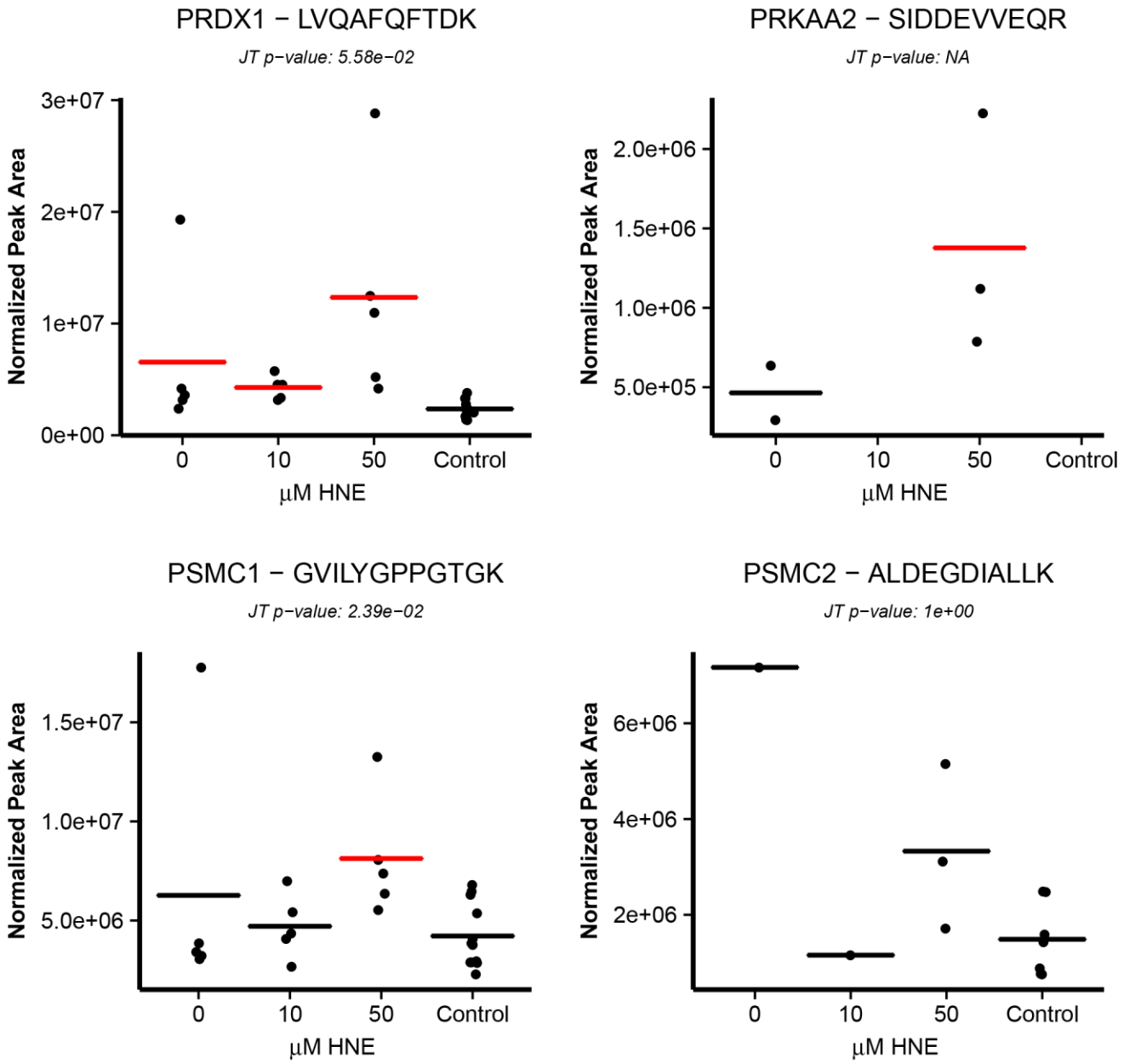


ASK1 IPs

**Figure A-8.**

A

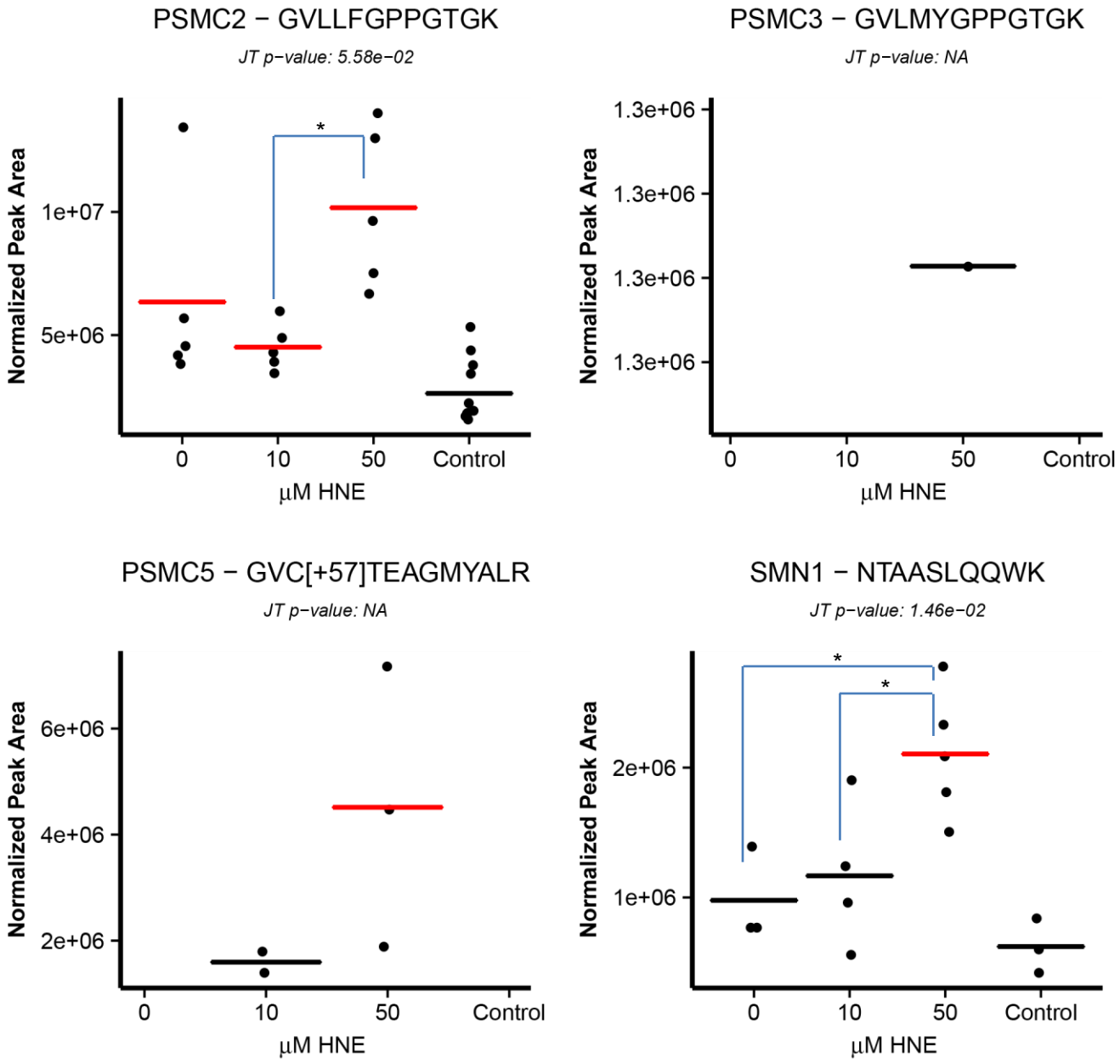


ASK1 IPs

**Figure A-8.**

A

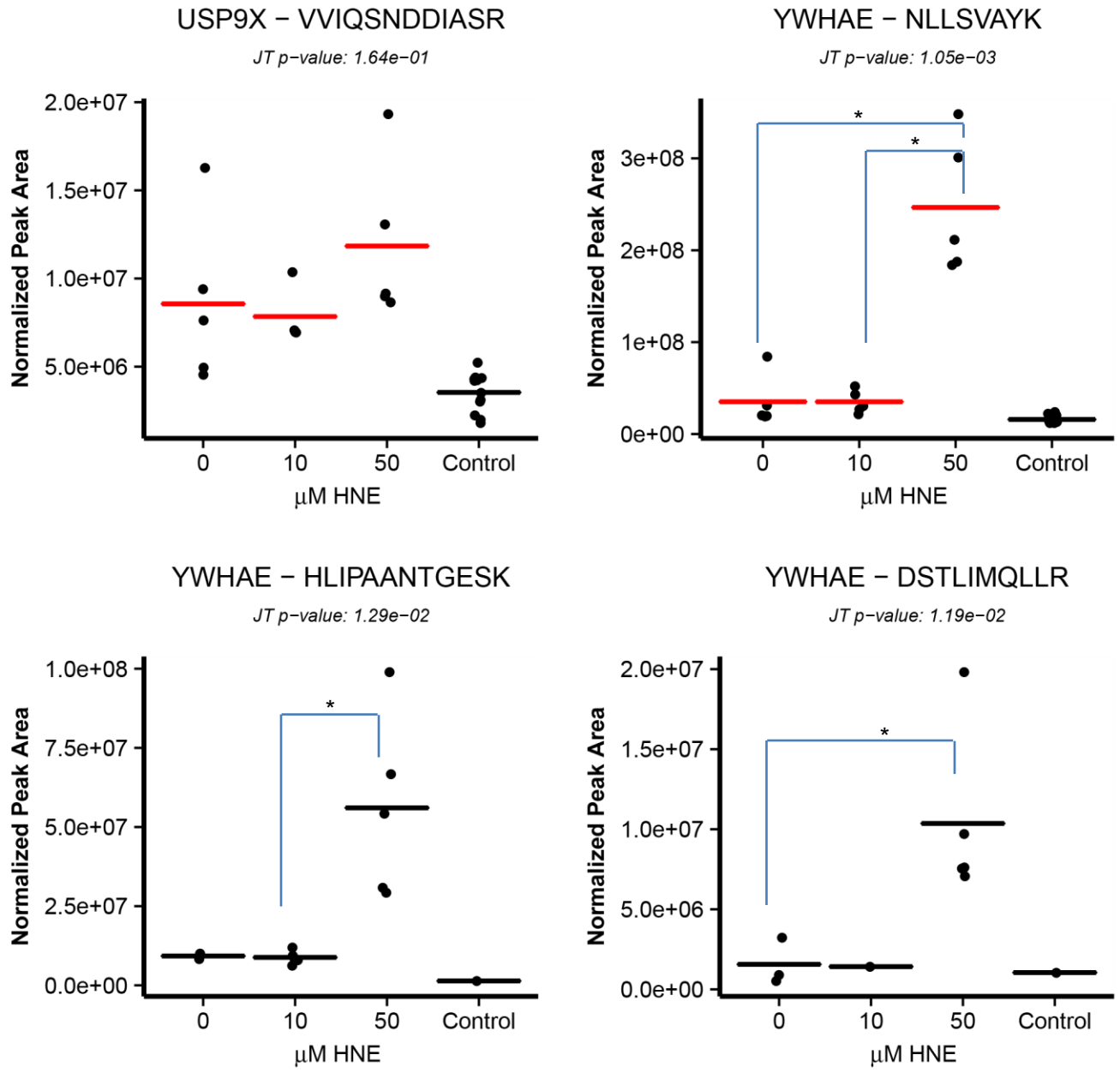


ASK1 IPs

**Figure A-8.**

**A**

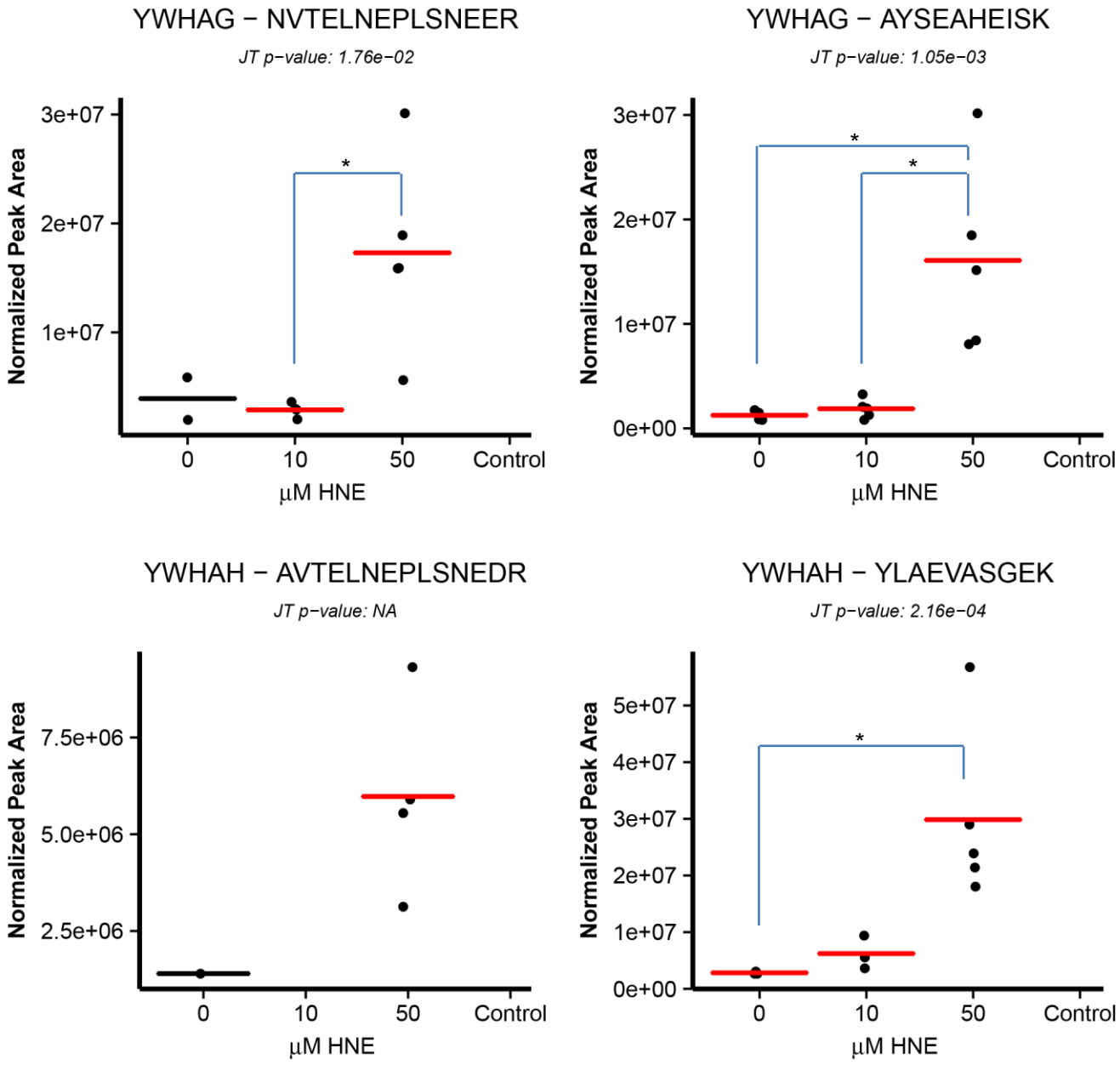


ASK1 IPs

**Figure A-8.**

**A**

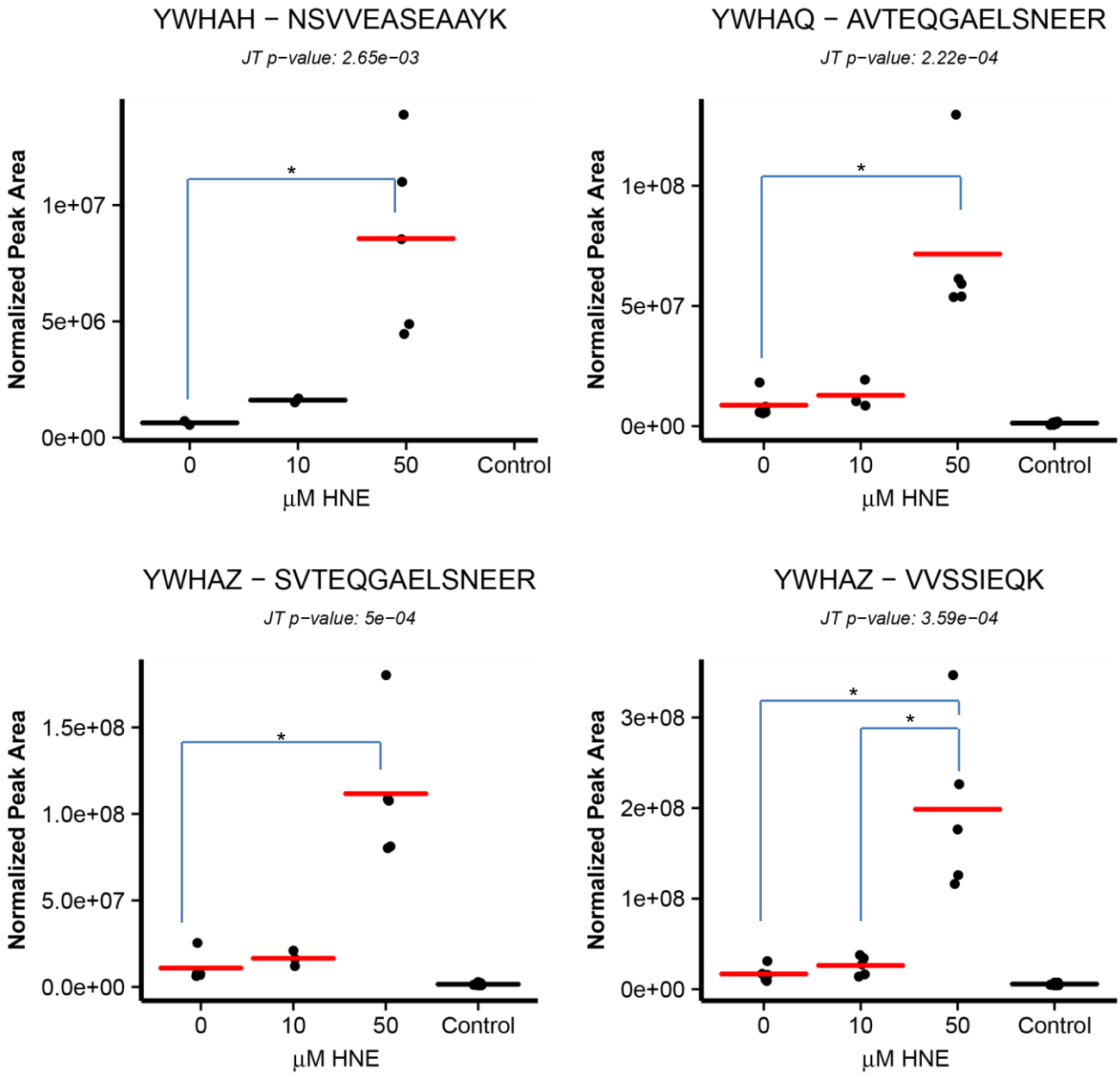
YWHAH − NSVVEASEAAYK
JT p−value: 2.65e−03
YWHAQ − AVTEQGAELSNEER
JT p−value: 2.22e−04
YWHAZ − SVTEQGAELSNEER
JT p−value: 5e−04
YWHAZ − VVSSIEQK
JT p−value: 3.59e−04
Normalized Peak Area
µM HNE
0
10
50
Control
ASK1 IPs

**Figure A-8.**

**A**

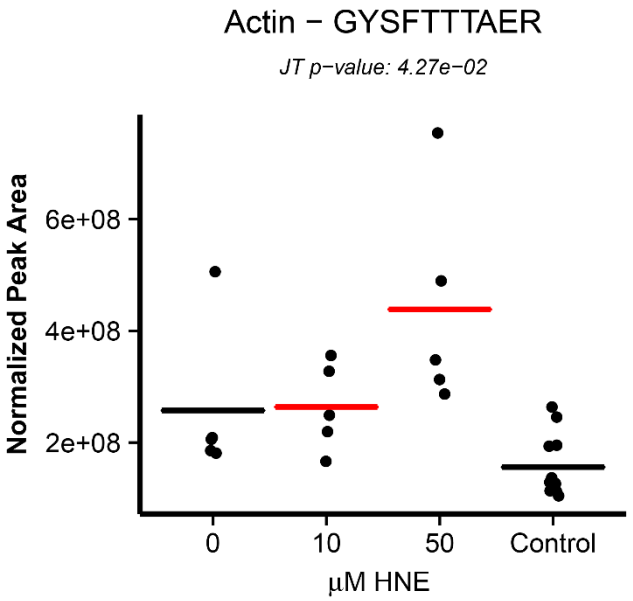


ASK1 IPs

**Figure A-8.**

**B**

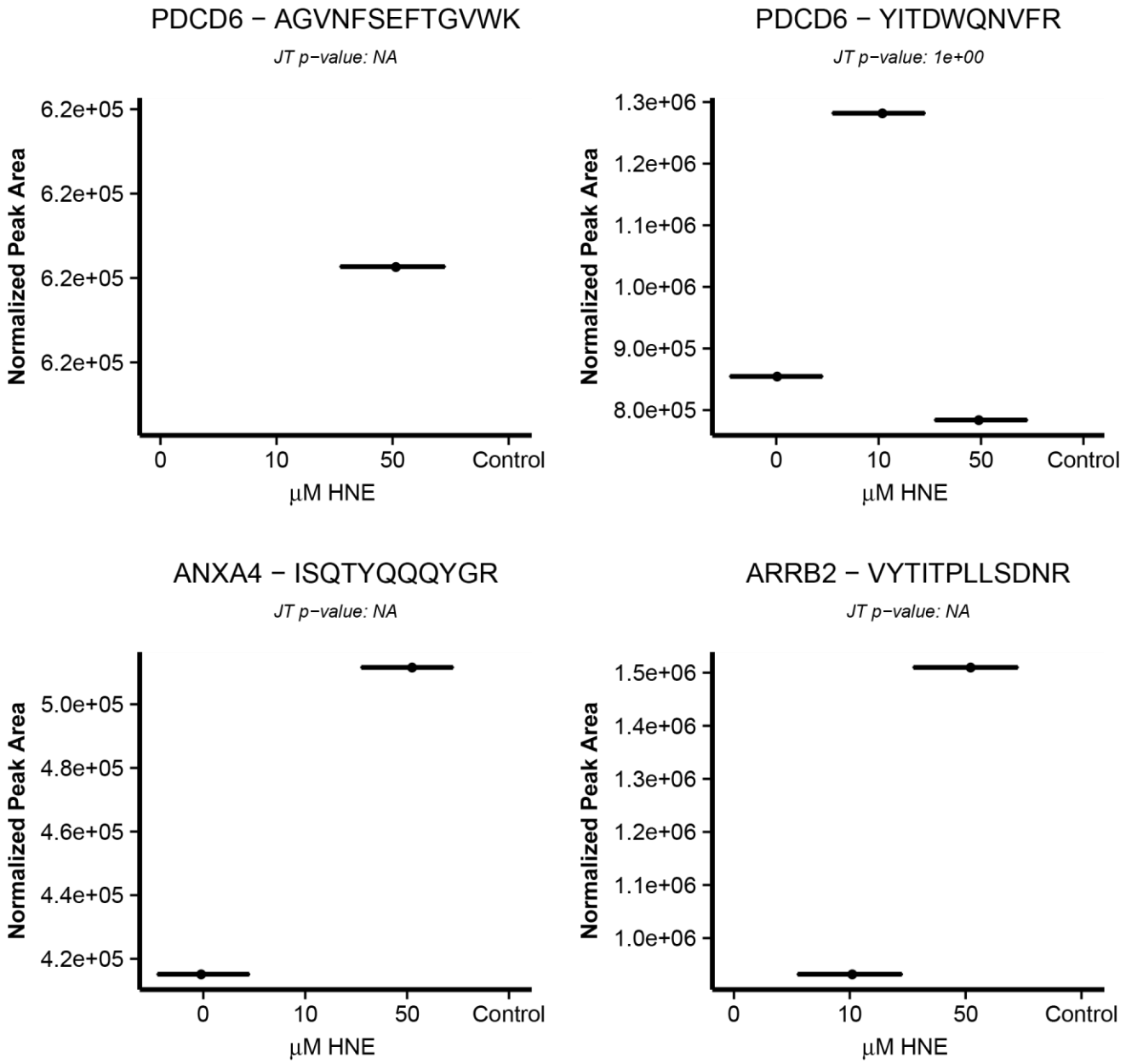


ASK2 IPs

**Figure A-8.**

**B**

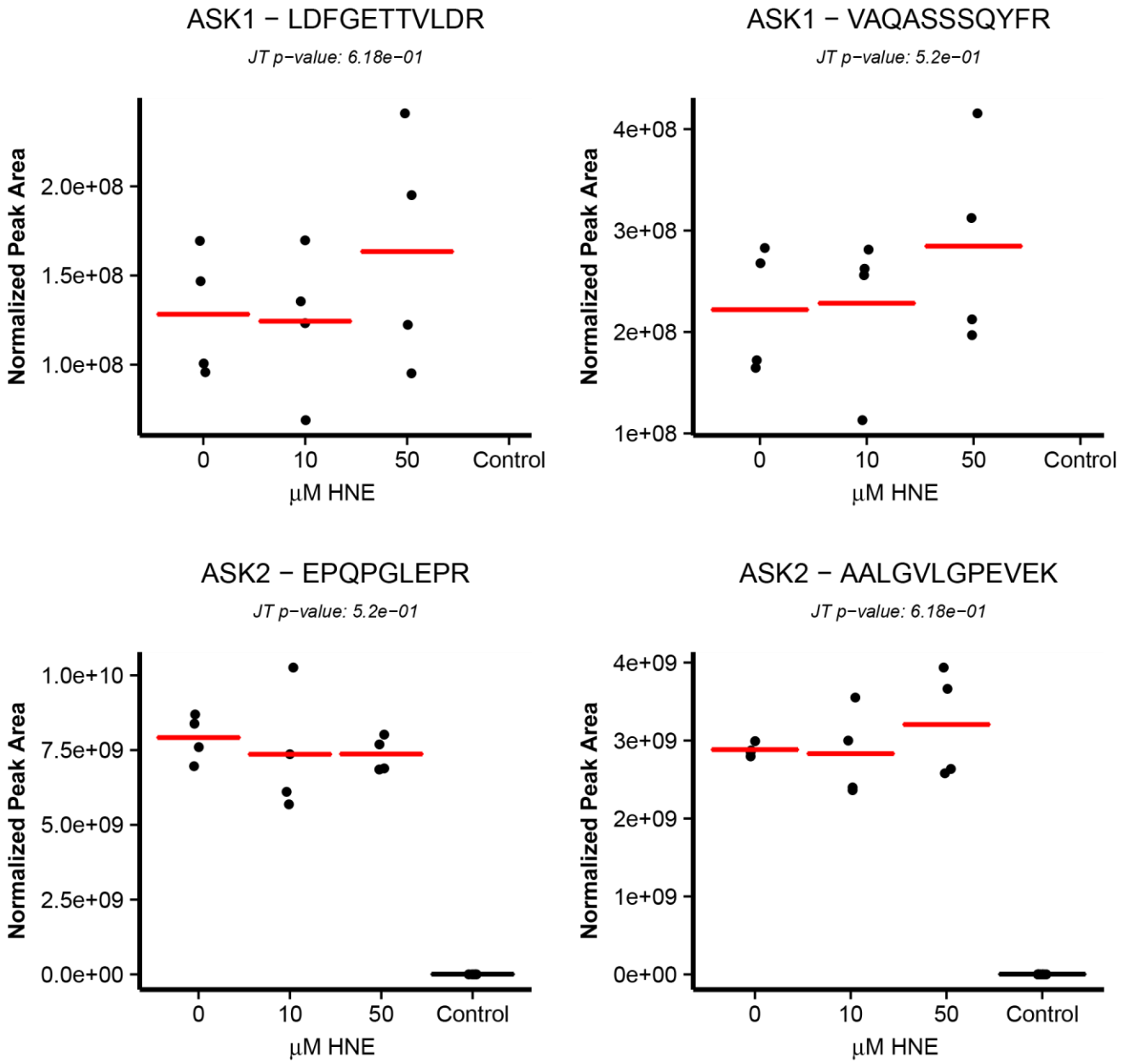


ASK2 IPs

**Figure A-8.**

**B**

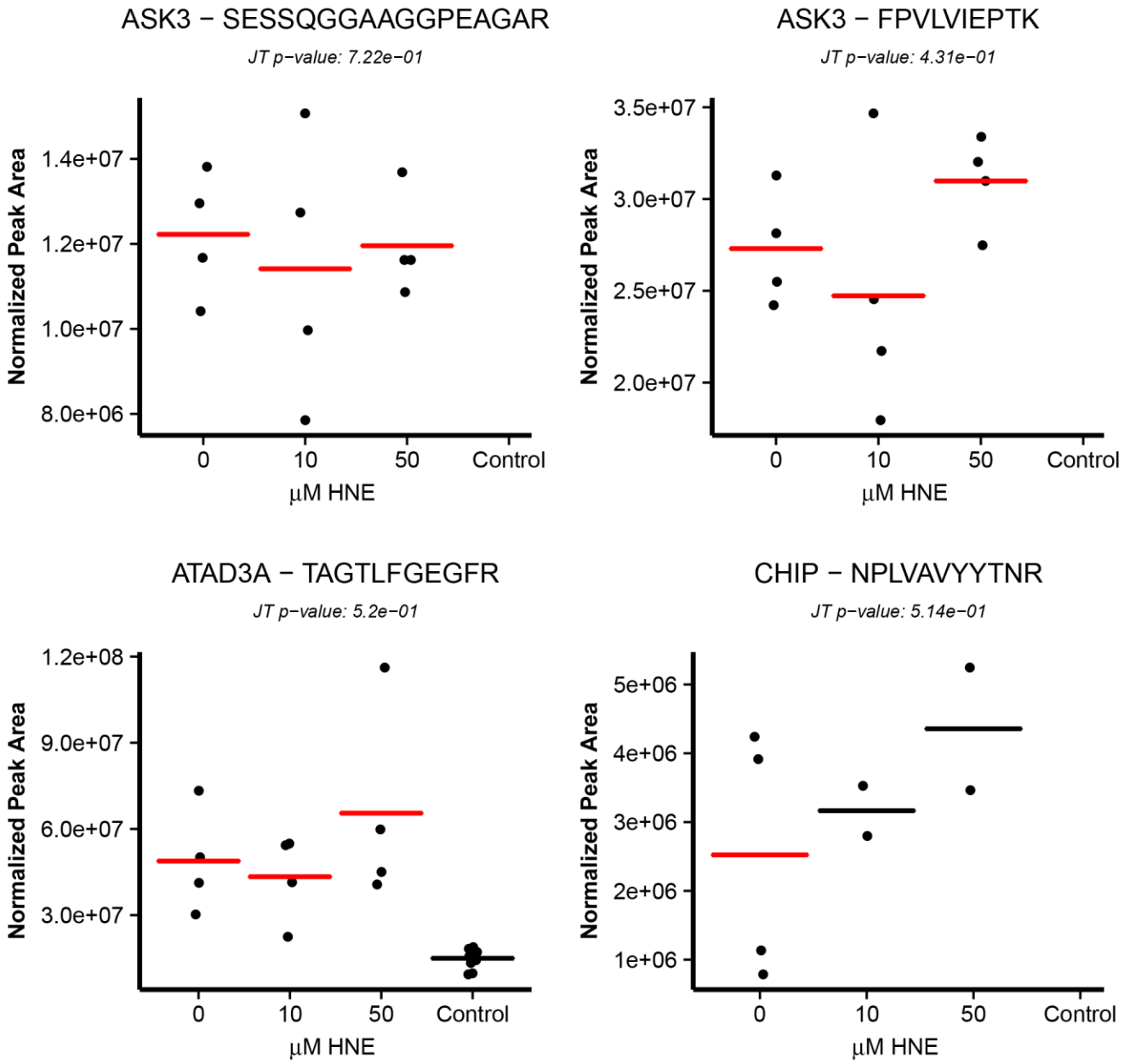


ASK2 IPs

**Figure A-8.**

**B**

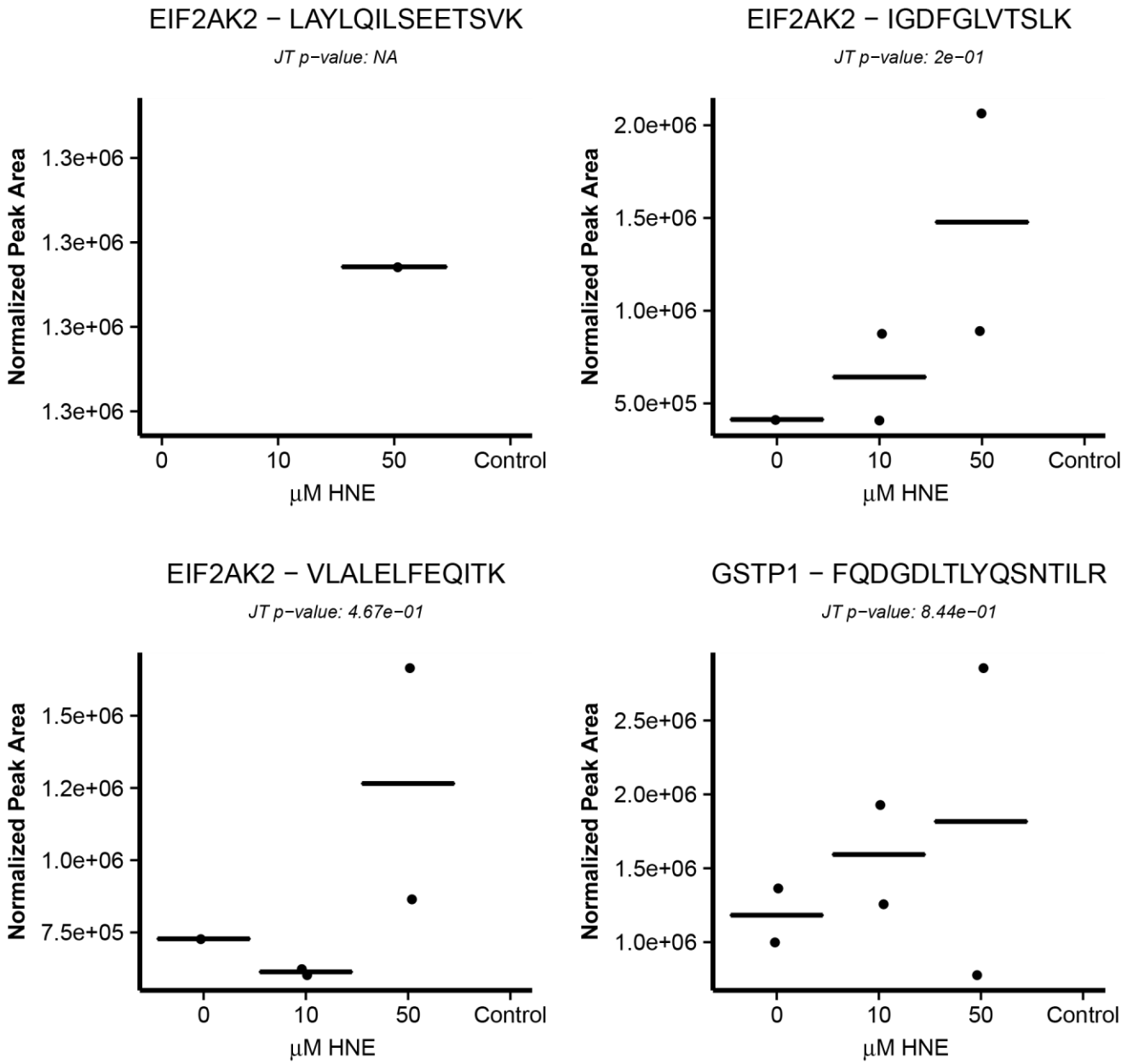
EIF2AK2 − LAYLQILSEETSVK
JT p−value: NA
EIF2AK2 − IGDFGLVTSLK
JT p−value: 2e−01
EIF2AK2 − VLALELFEQITK
JT p−value: 4.67e−01
GSTP1 − FQDGDLTLYQSNTILR
JT p−value: 8.44e−01
Normalized Peak Area
1.3e+06
2.0e+06
1.5e+06
1.0e+06
5.0e+05
1.2e+06
7.5e+05
2.5e+06
0
10
50
Control
μM HNE
ASK2 IPs

**Figure A-8.**

**B**

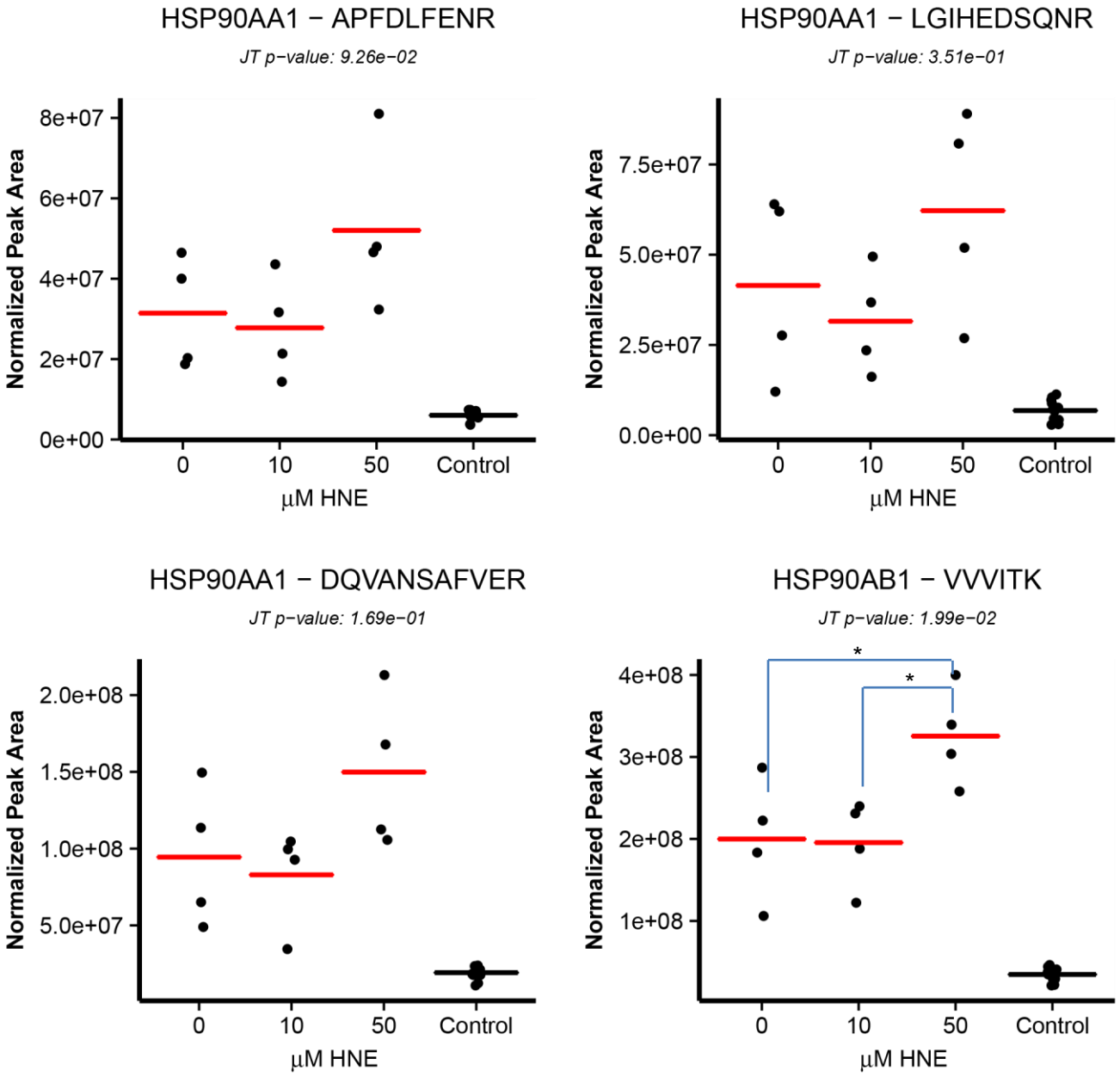
HSP90AA1 − APFDLFENR
JT p−value: 9.26e−02
HSP90AA1 − LGIHEDSQNR
JT p−value: 3.51e−01
HSP90AA1 − DQVANSAFVER
JT p−value: 1.69e−01
HSP90AB1 − VVVITK
JT p−value: 1.99e−02
Normalized Peak Area
µM HNE
0
10
50
Control
ASK2 IPs

**Figure A-8.**

**B**

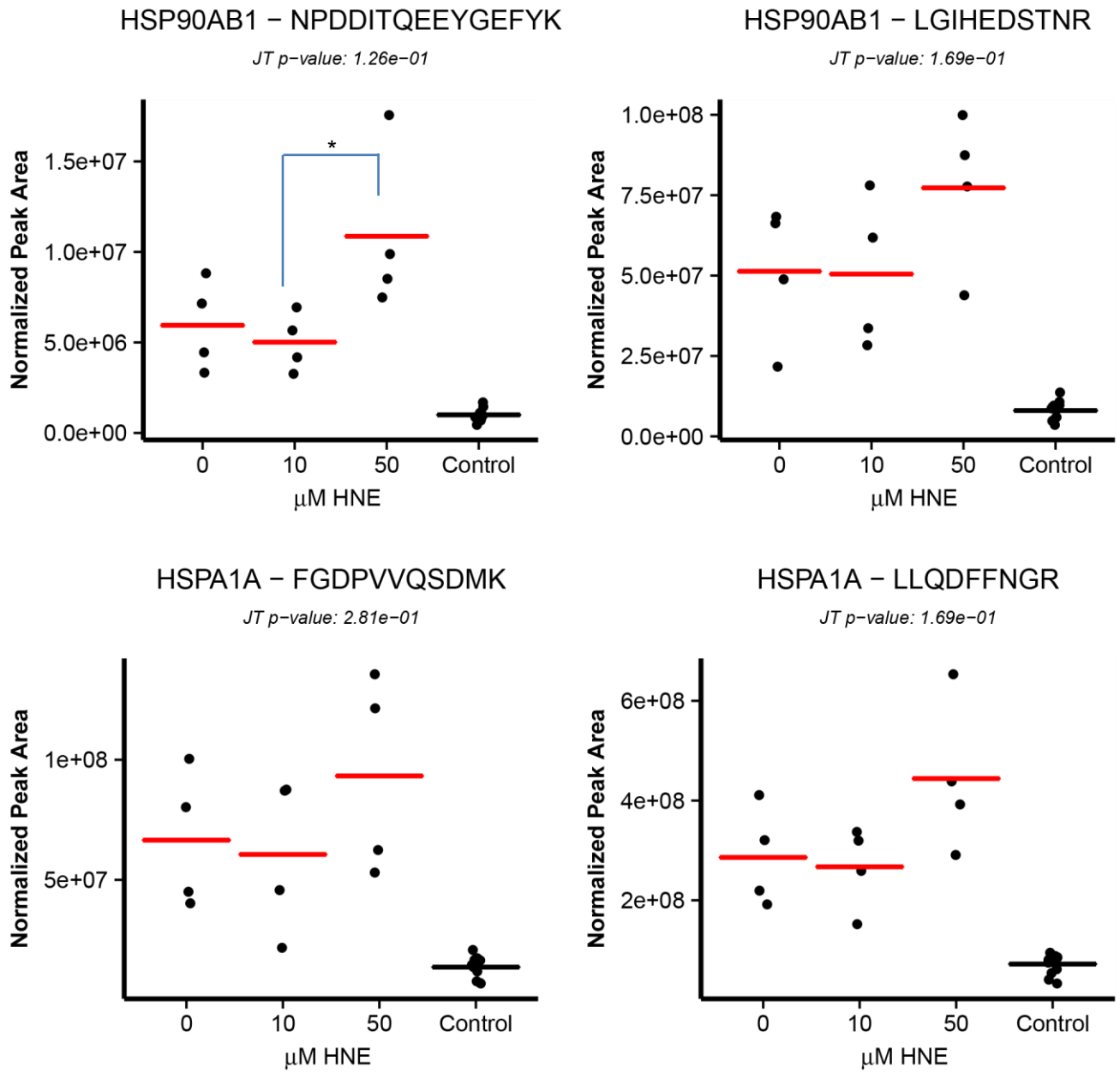
HSP90AB1 − NPDDITQEEYGEFYK
JT p−value: 1.26e−01
HSP90AB1 − LGIHEDSTNR
JT p−value: 1.69e−01
HSPA1A − FGDPVVQSDMK
JT p−value: 2.81e−01
HSPA1A − LLQDFFNGR
JT p−value: 1.69e−01
Normalized Peak Area
µM HNE
0
10
50
Control
ASK2 IPs

**Figure A-8.**

**B**

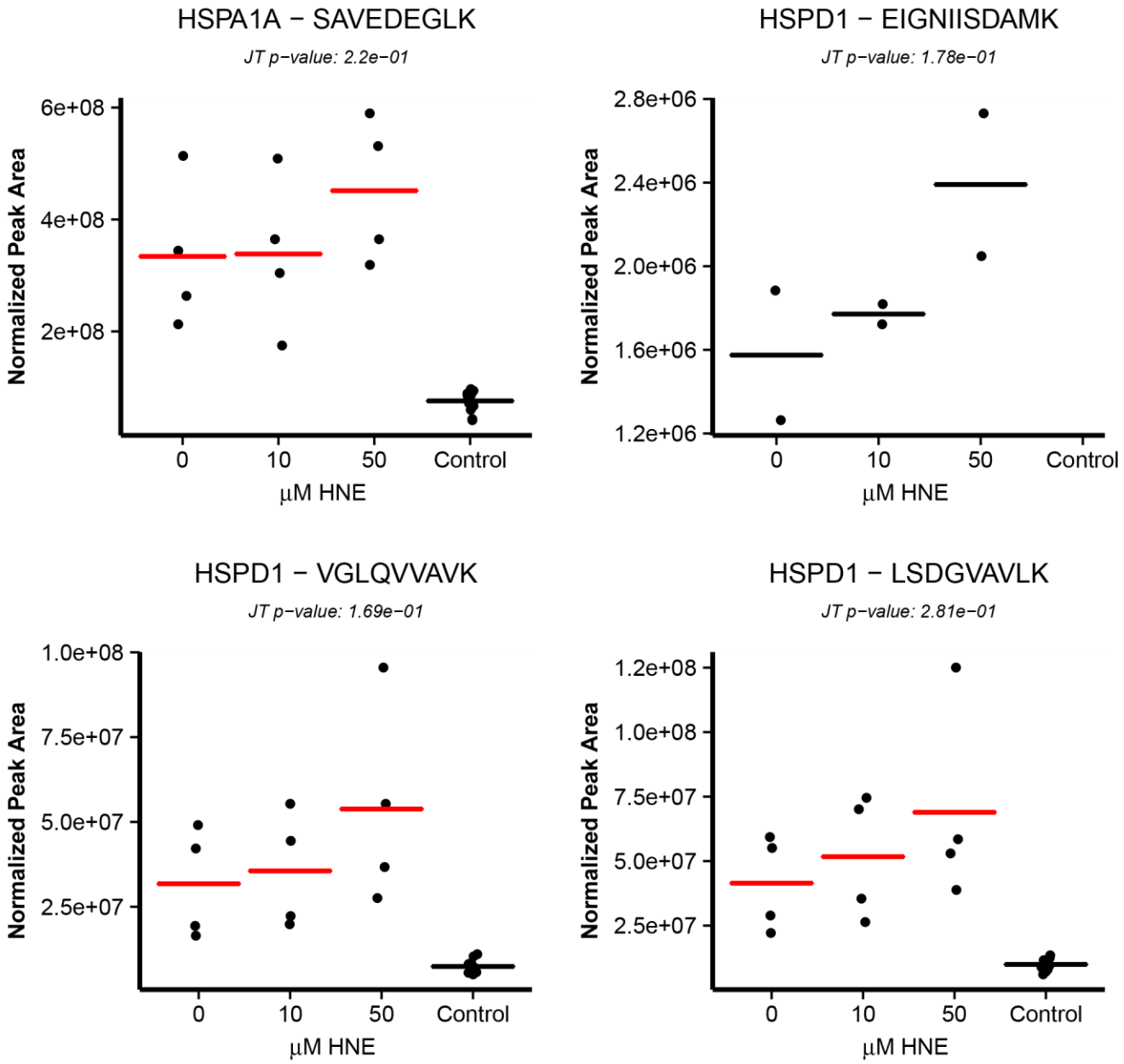


ASK2 IPs

**Figure A-8.**

**B**

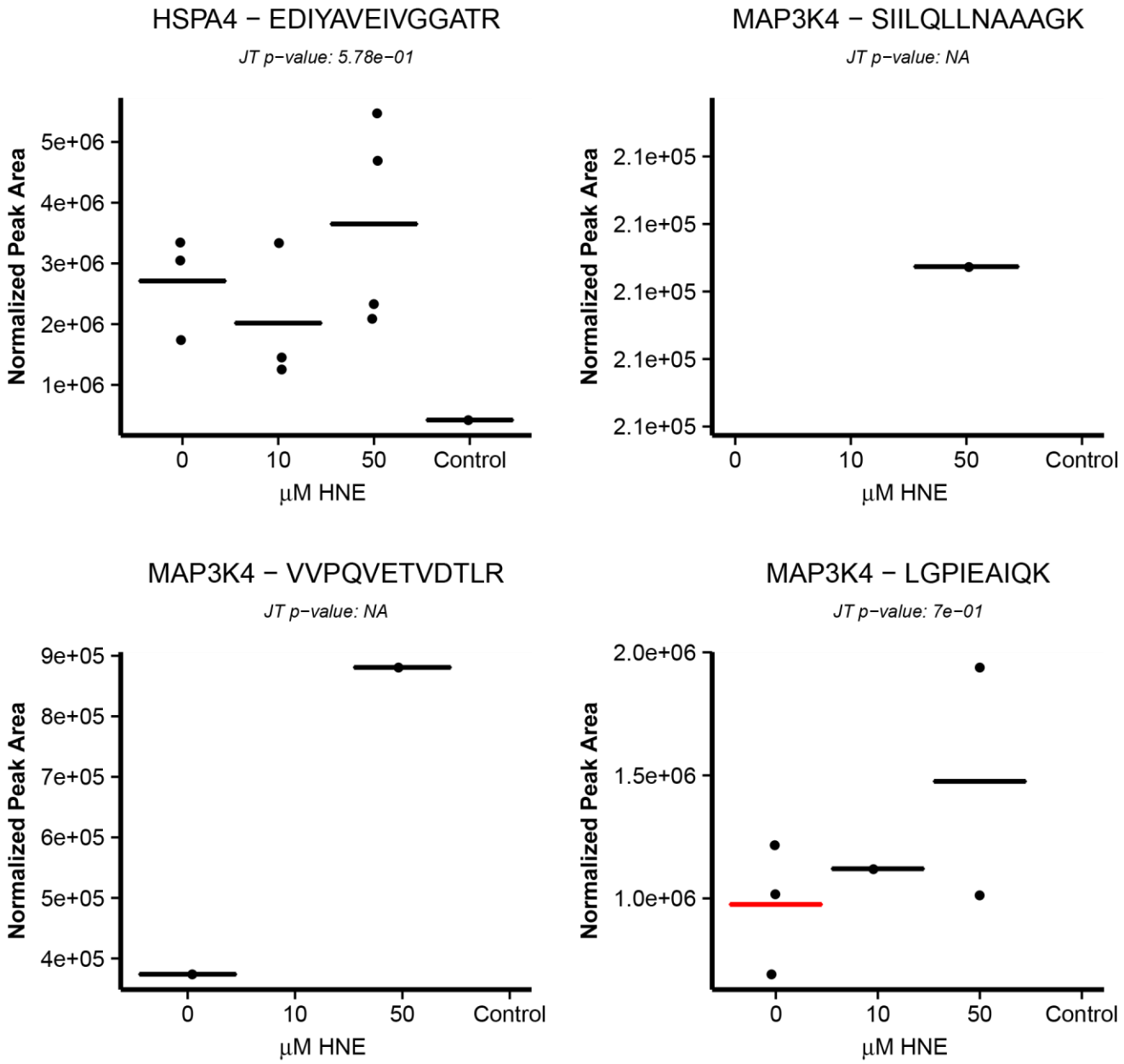


ASK2 IPs

**Figure A-8.**

**B**

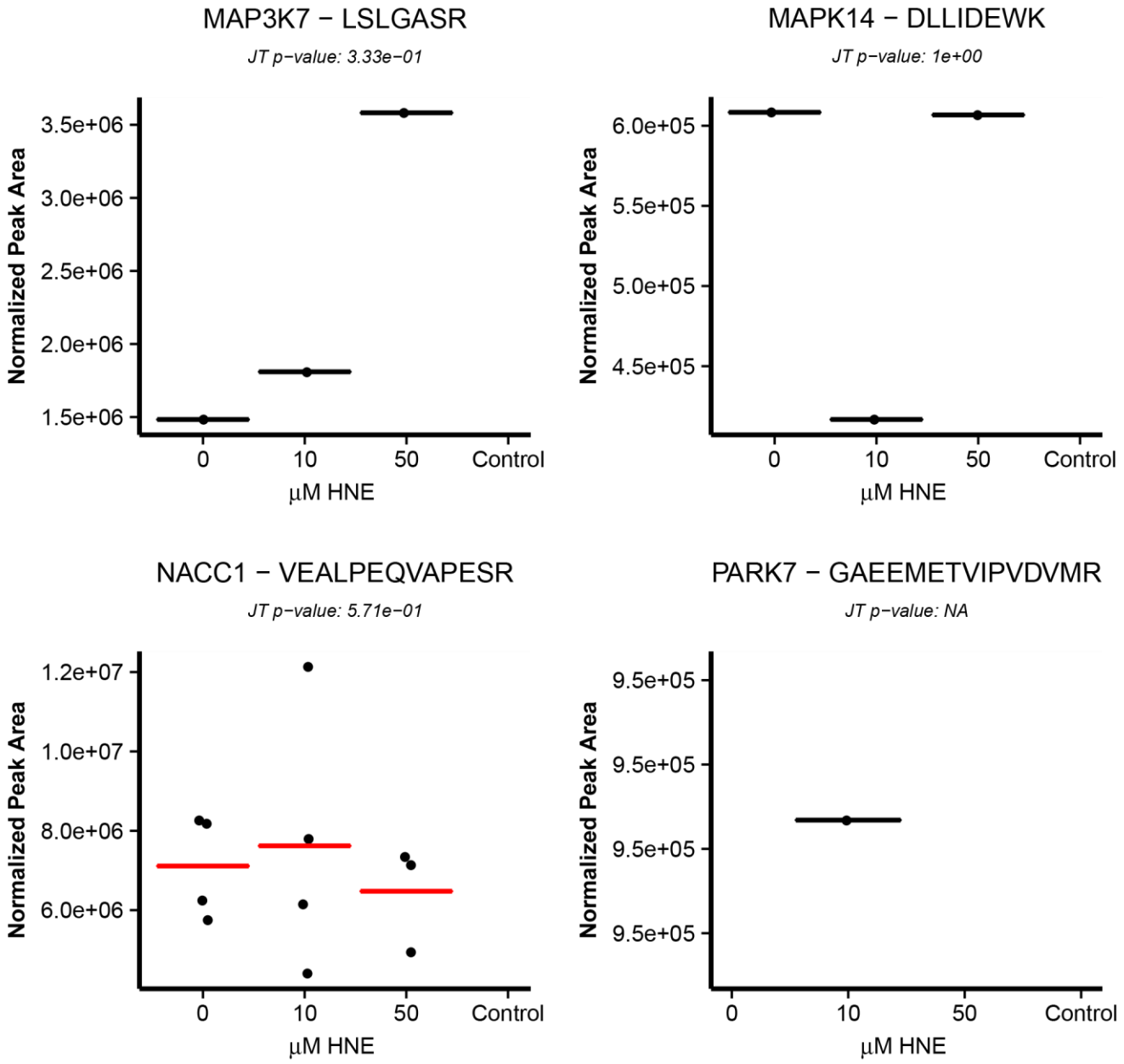


ASK2 IPs

**Figure A-8.**

**B**

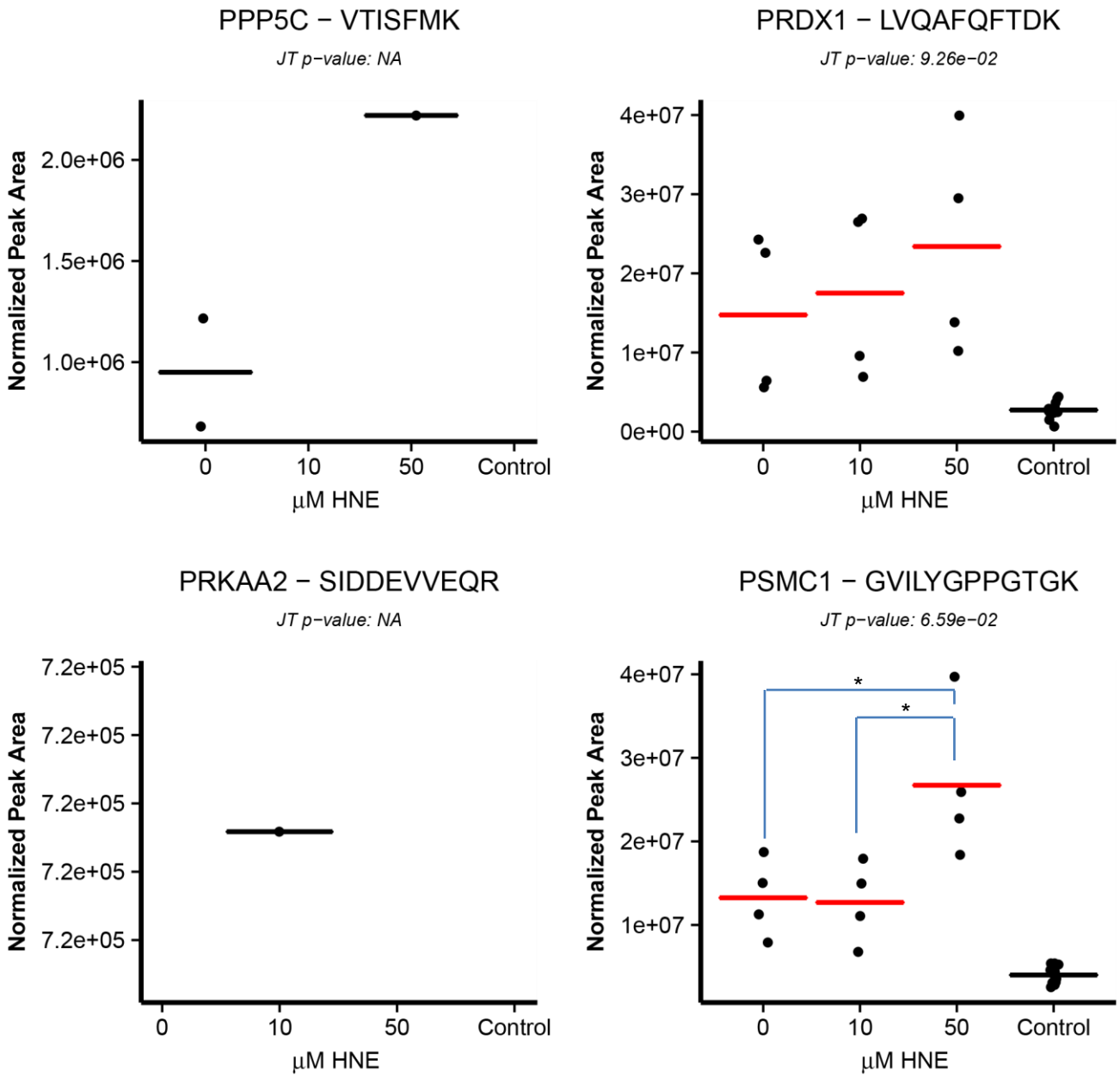


ASK2 IPs

**Figure A-8.**

**B**

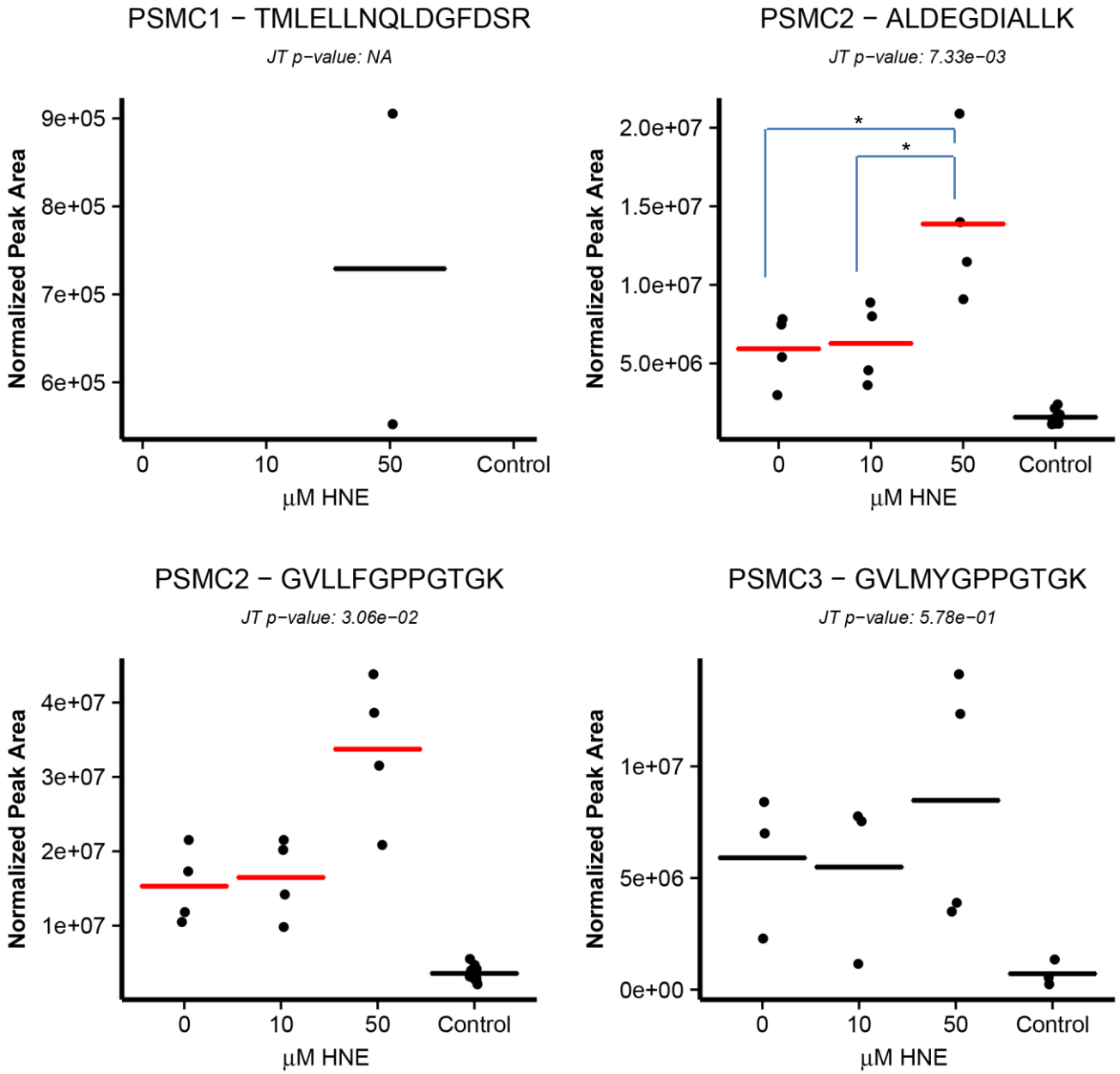
PSMC1 − TMLELLNQLDGFDSR
JT p−value: NA
PSMC2 − ALDEGDIALLK
JT p−value: 7.33e−03
PSMC2 − GVLLFGPPGTGK
JT p−value: 3.06e−02
PSMC3 − GVLMYGPPGTGK
JT p−value: 5.78e−01
Normalized Peak Area
µM HNE
0
10
50
Control
ASK2 IPs

**Figure A-8.**

**B**

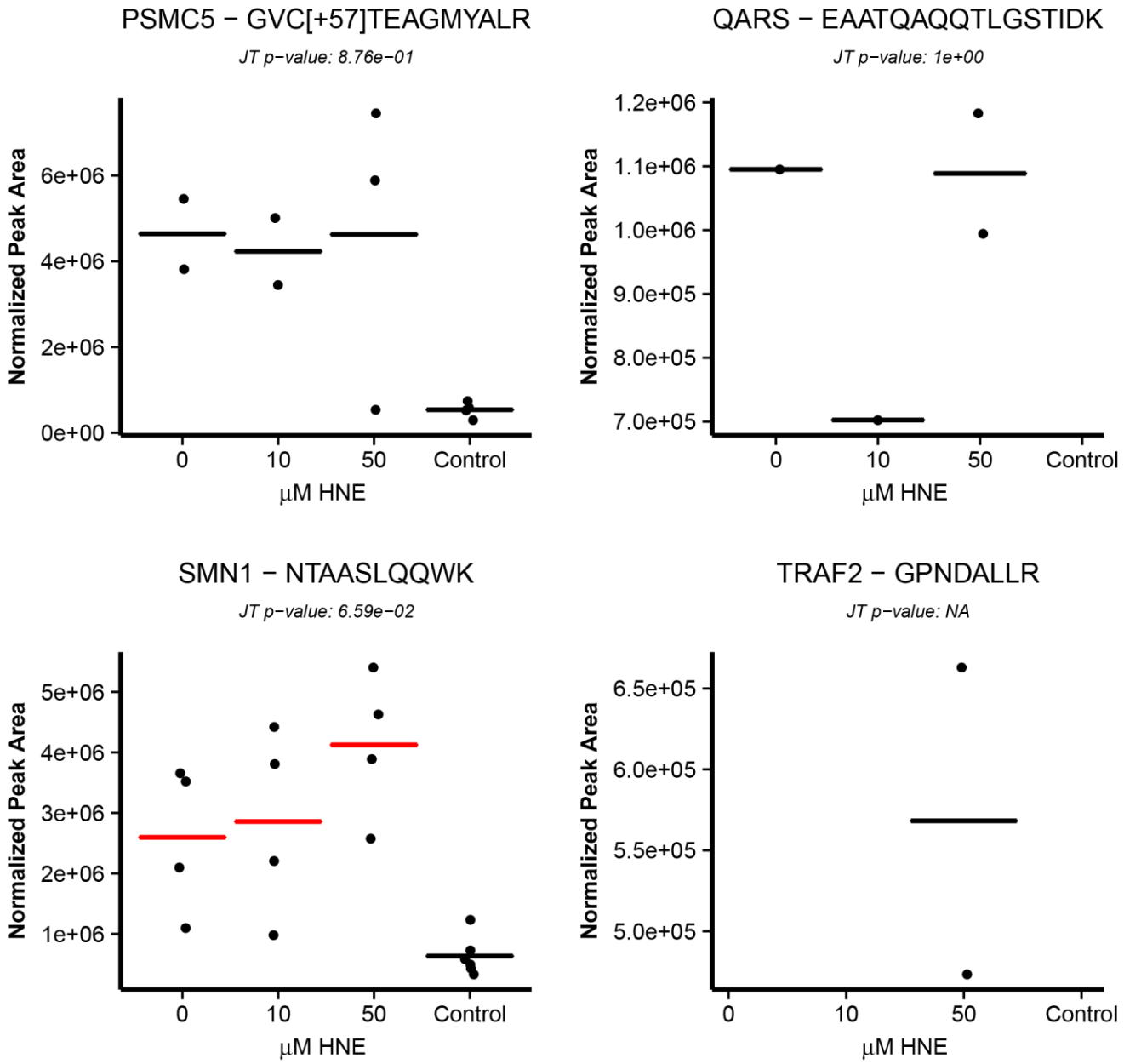
PSMC5 − GVC[+57]TEAGMYALR
JT p−value: 8.76e−01
QARS − EAATQAQQTLGSTIDK
JT p−value: 1e+00
SMN1 − NTAASLQQWK
JT p−value: 6.59e−02
TRAF2 − GPNDALLR
JT p−value: NA
Normalized Peak Area
µM HNE
0
10
50
Control
ASK2 IPs

**Figure A-8.**

**B**

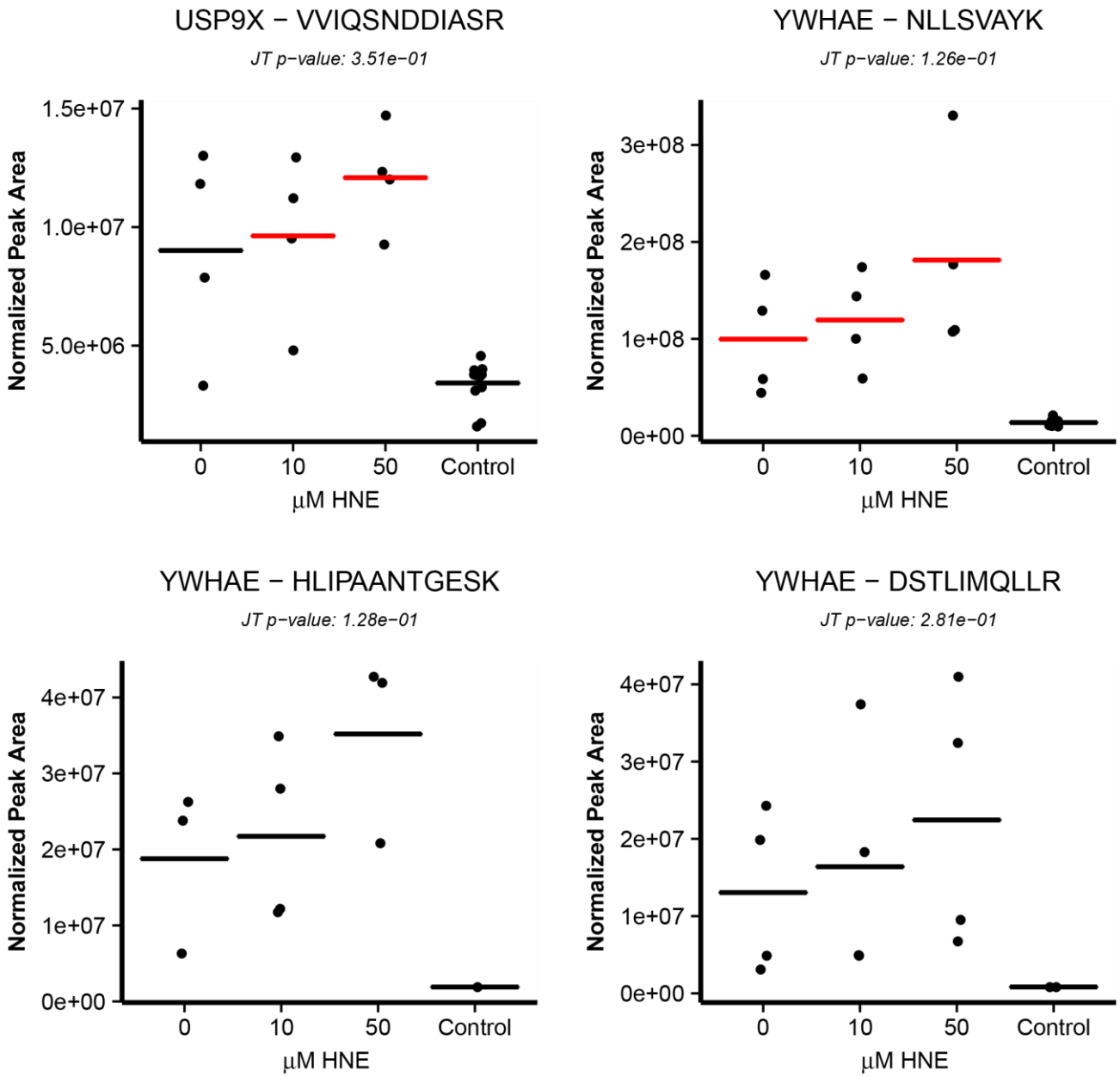
USP9X − VVIQSNDDIASR
JT p−value: 3.51e−01
YWHAE − NLLSVAYK
JT p−value: 1.26e−01
YWHAE − HLIPAANTGESK
JT p−value: 1.28e−01
YWHAE − DSTLIMQLLR
JT p−value: 2.81e−01
Normalized Peak Area
μM HNE
0
10
50
Control
ASK2 IPs

**Figure A-8.**

**B**

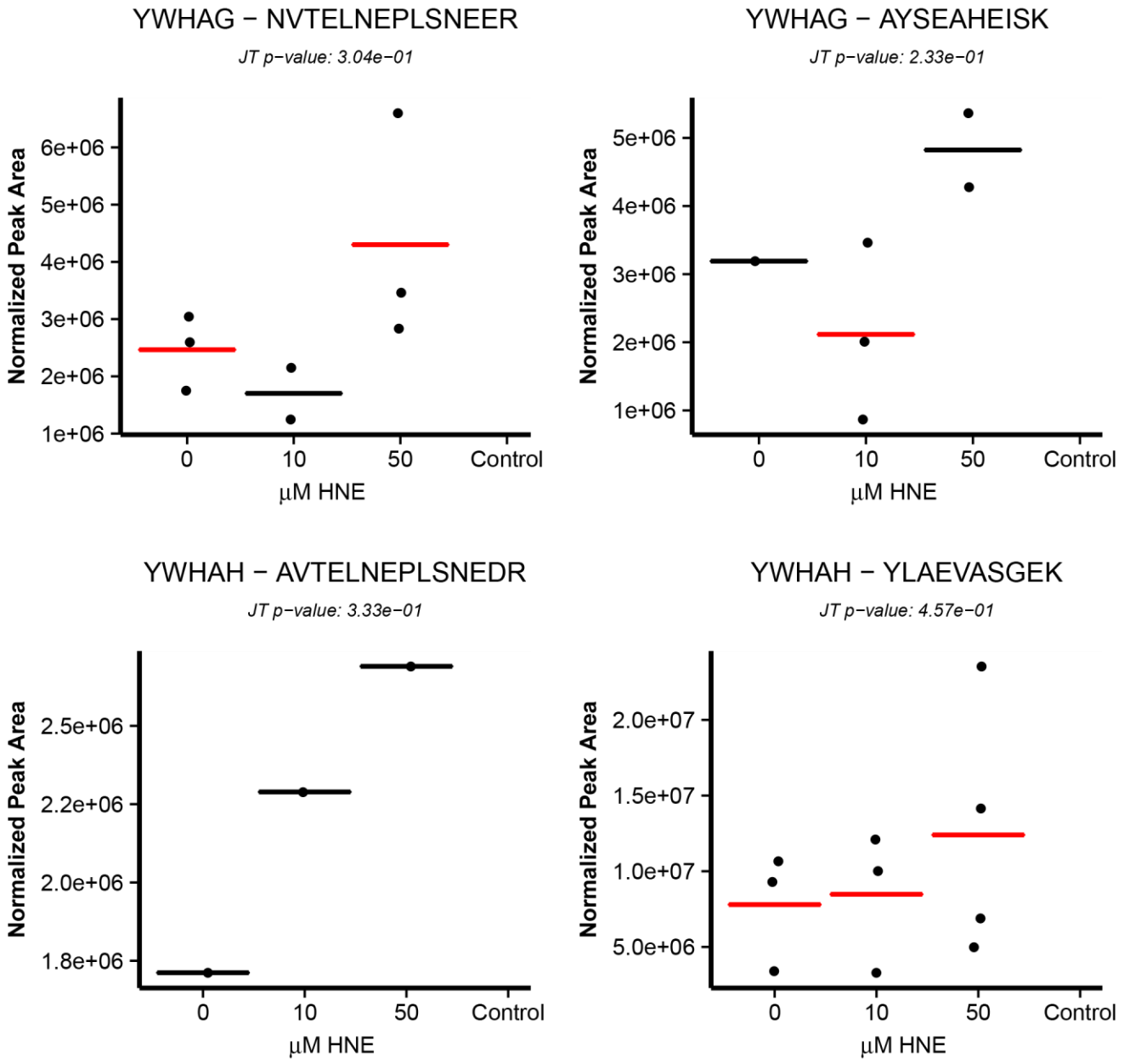
YWHAG − NVTELNEPLSNEER
JT p−value: 3.04e−01
YWHAG − AYSEAHEISK
JT p−value: 2.33e−01
YWHAH − AVTELNEPLSNEDR
JT p−value: 3.33e−01
YWHAH − YLAEVASGEK
JT p−value: 4.57e−01
Normalized Peak Area
µM HNE
0
10
50
Control
ASK2 IPs

**Figure A-8.**

**B**

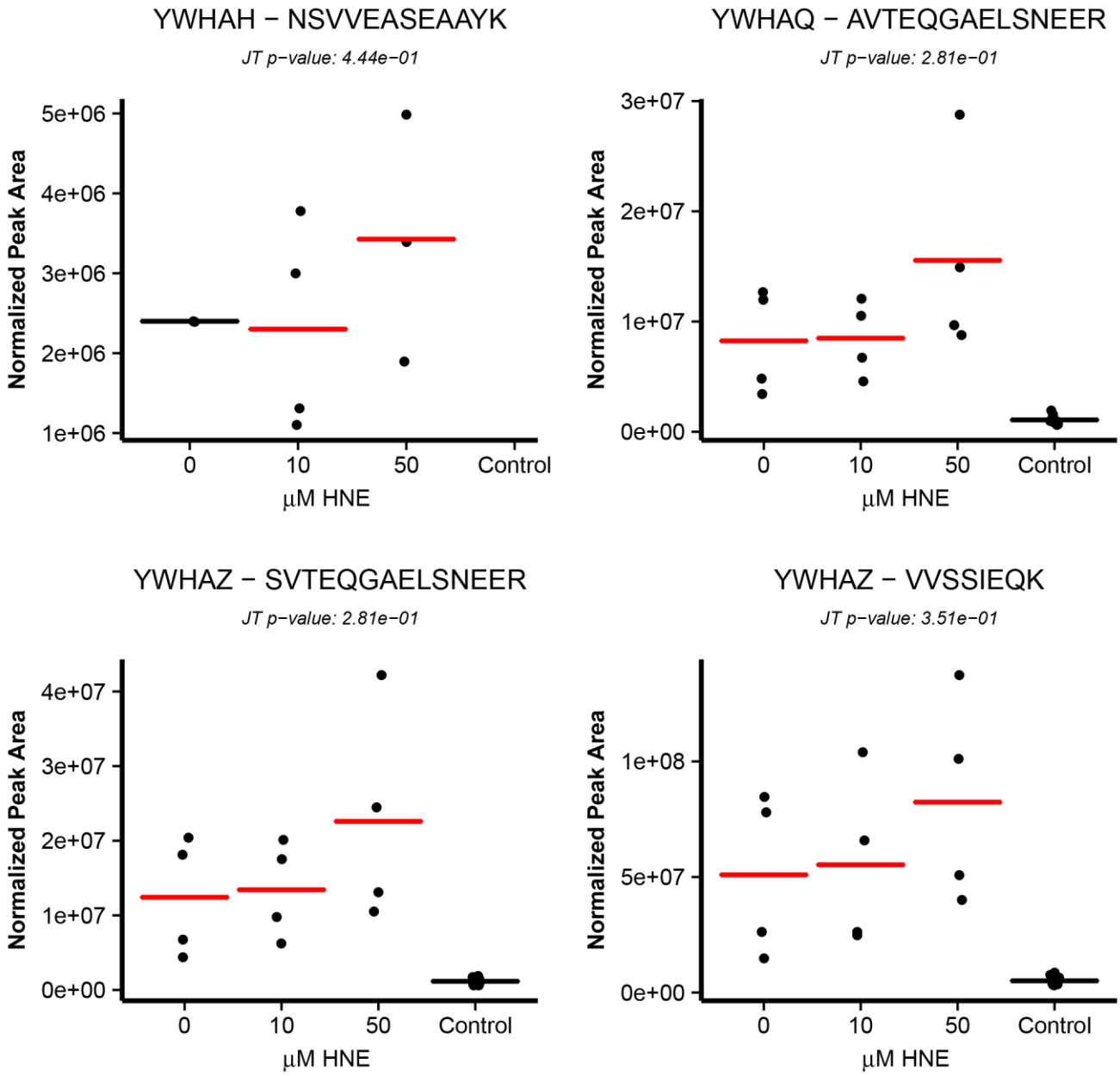
YWHAH − NSVVEASEAAYK
JT p−value: 4.44e−01
YWHAQ − AVTEQGAELSNEER
JT p−value: 2.81e−01
YWHAZ − SVTEQGAELSNEER
JT p−value: 2.81e−01
YWHAZ − VVSSIEQK
JT p−value: 3.51e−01
Normalized Peak Area
µM HNE
0
10
50
Control
ASK2 IPs

**Figure A-8.**

**B**

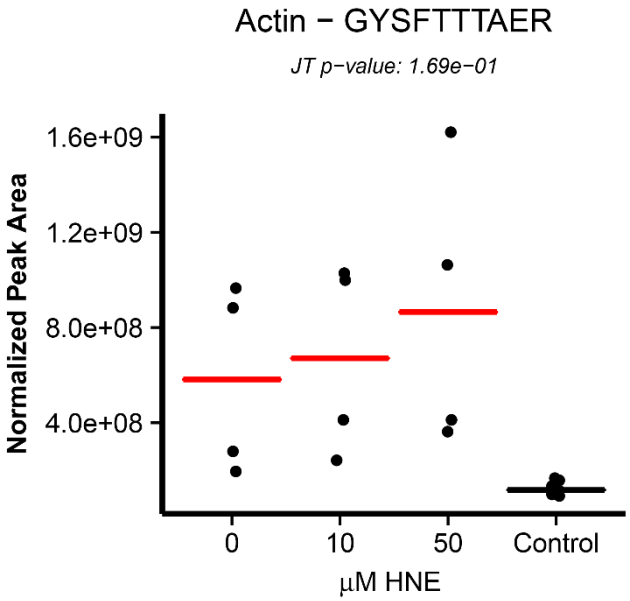


ASK2 IPs

**Figure A-8.**

C

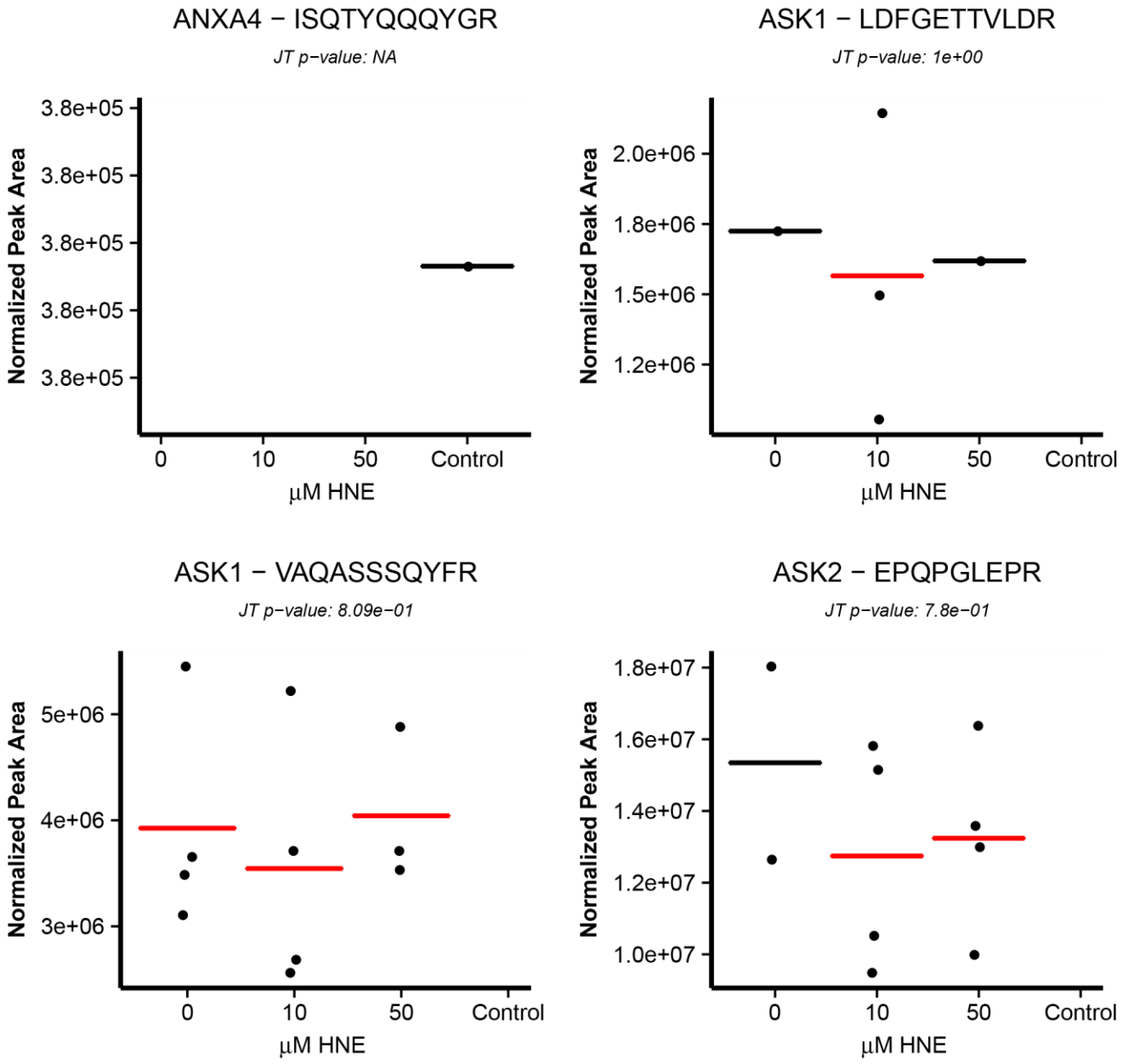


ASK3 IPs

**Figure A-8.**

C

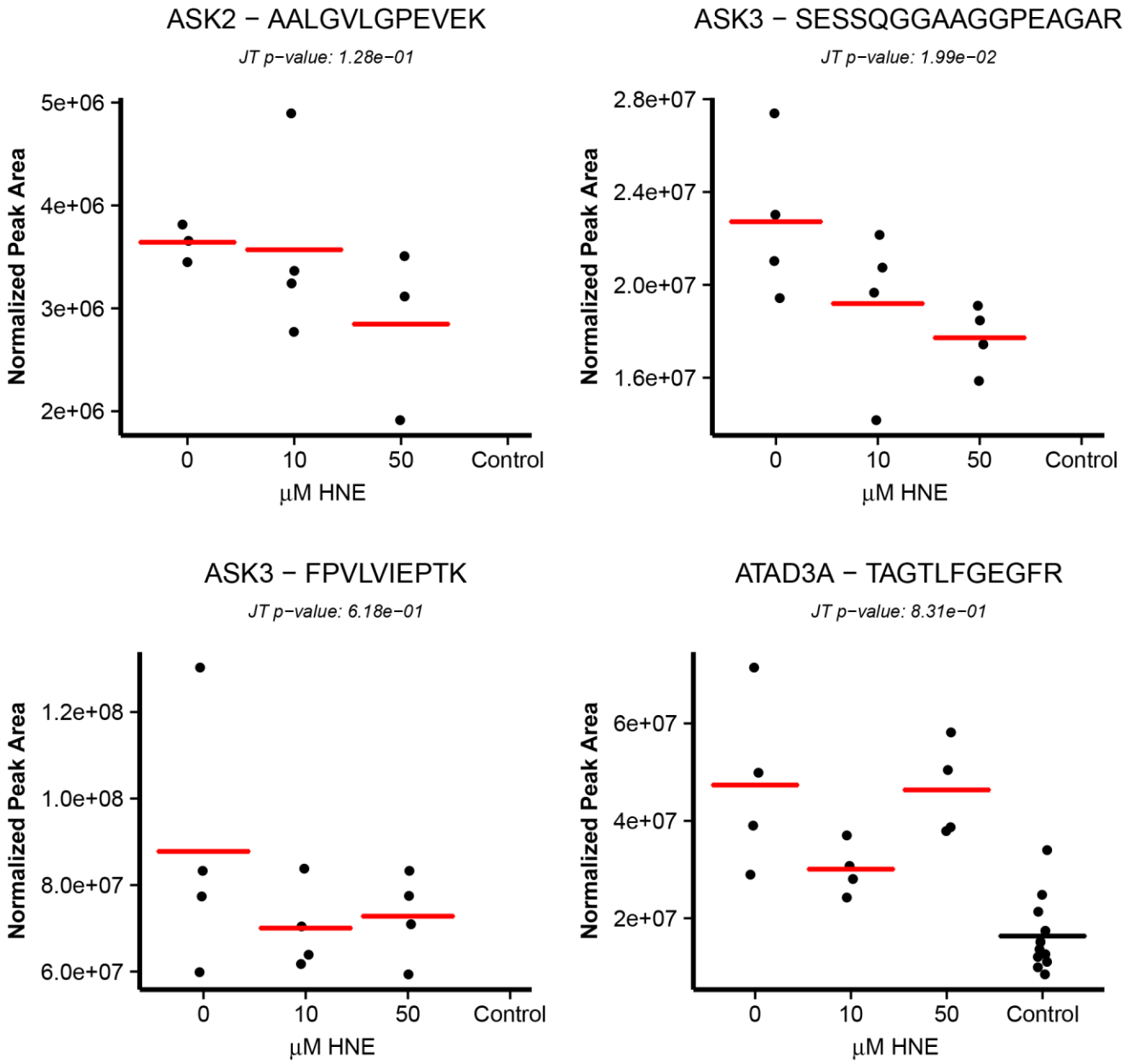


ASK3 IPs

**Figure A-8.**

C

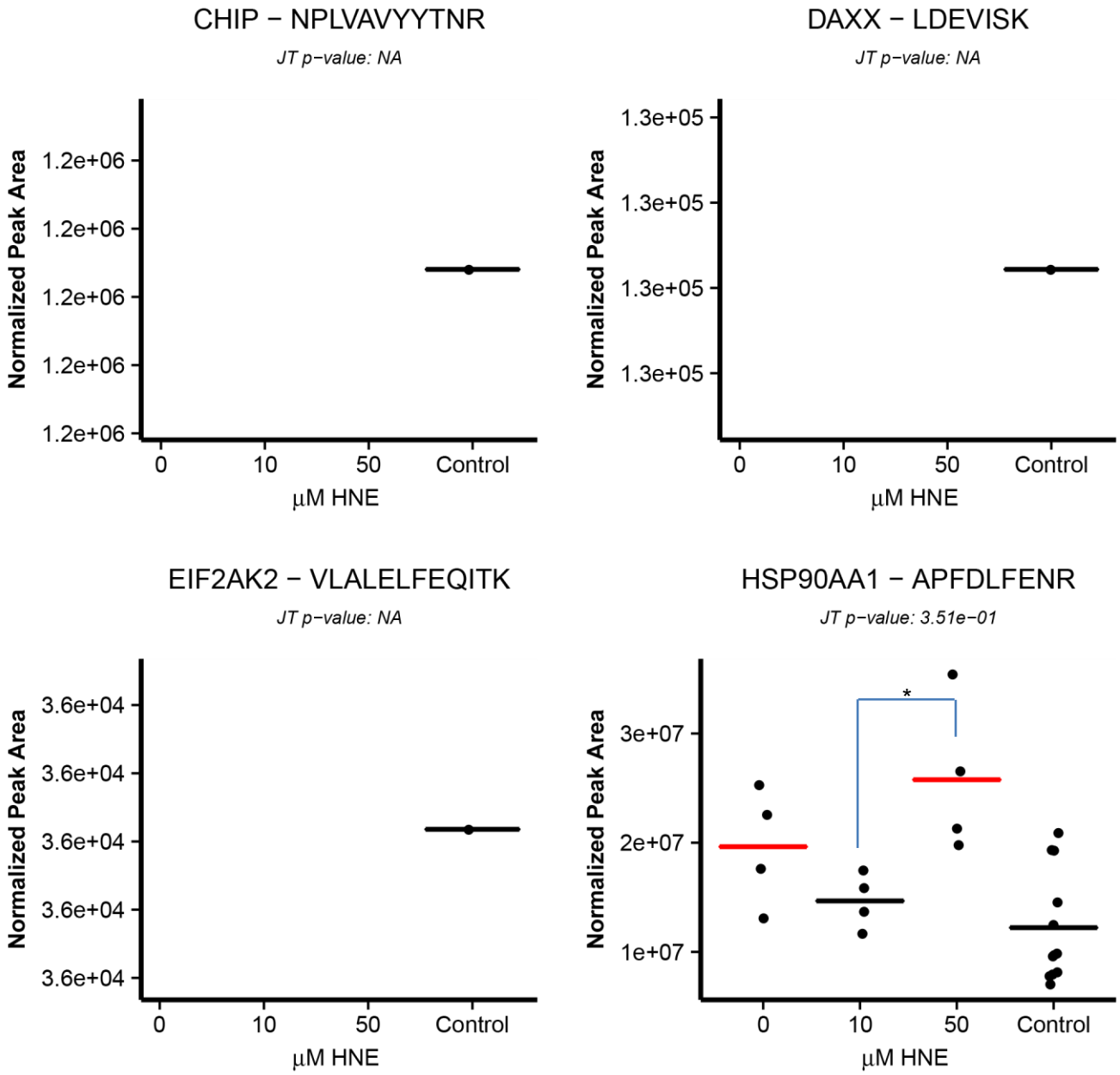


ASK3 IPs

**Figure A-8.**

C

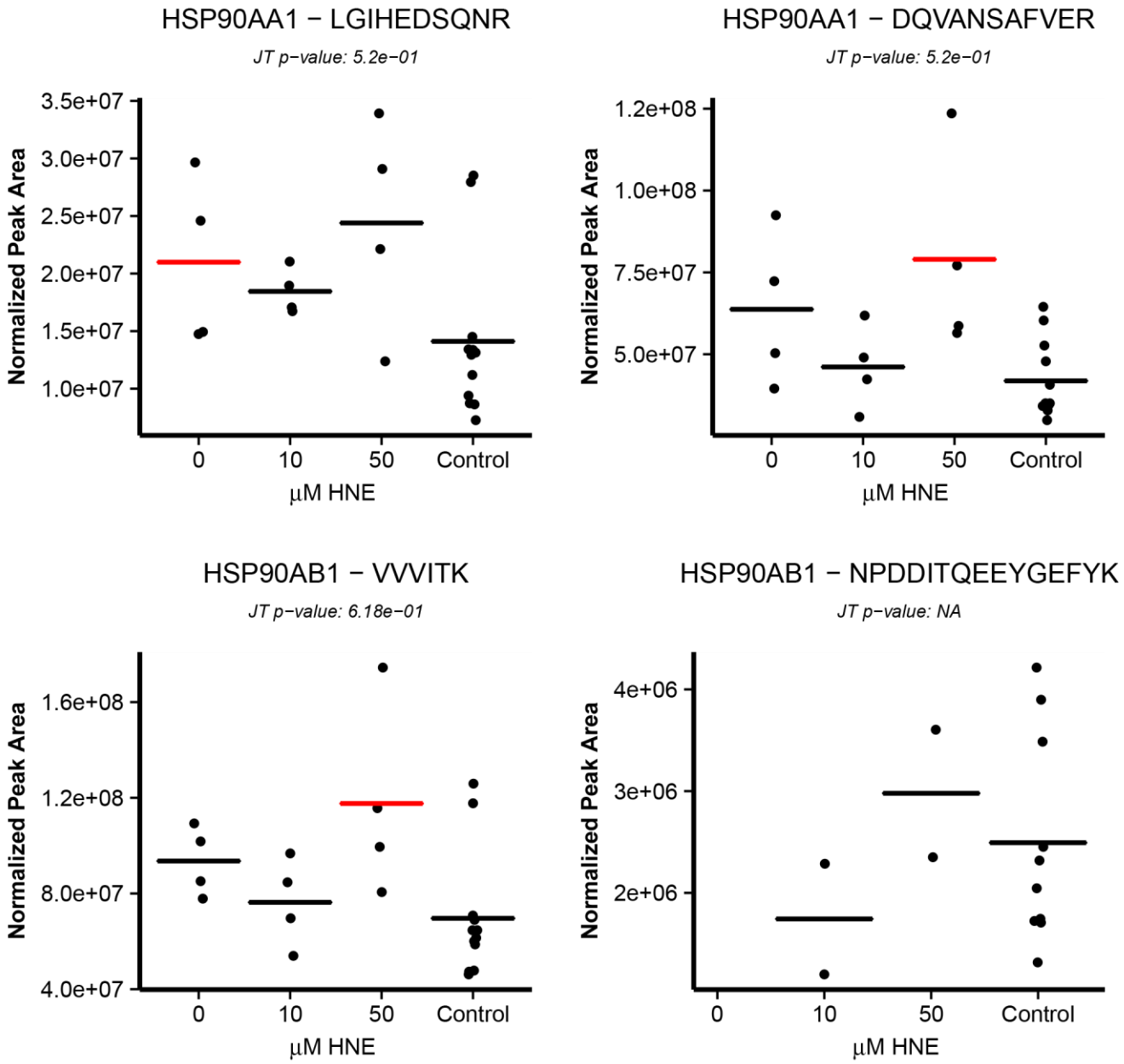


ASK3 IPs

**Figure A-8.**

C

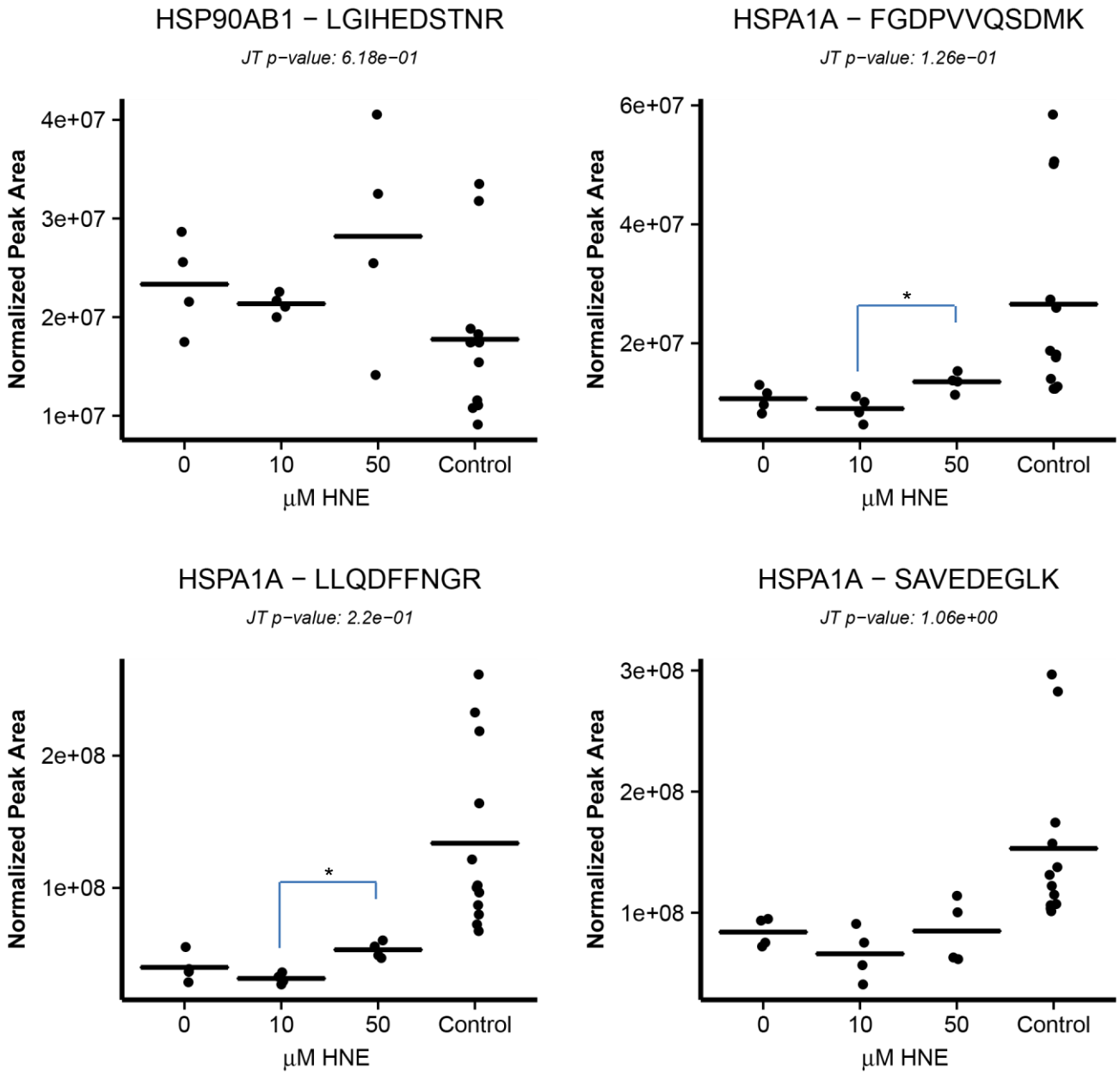
HSP90AB1 − LGIHEDSTNR
JT p−value: 6.18e−01
HSPA1A − FGDPVVQSDMK
JT p−value: 1.26e−01
HSPA1A − LLQDFFNGR
JT p−value: 2.2e−01
HSPA1A − SAVEDEGLK
JT p−value: 1.06e+00
Normalized Peak Area
µM HNE
0
10
50
Control
*
ASK3 IPs

**Figure A-8.**

C

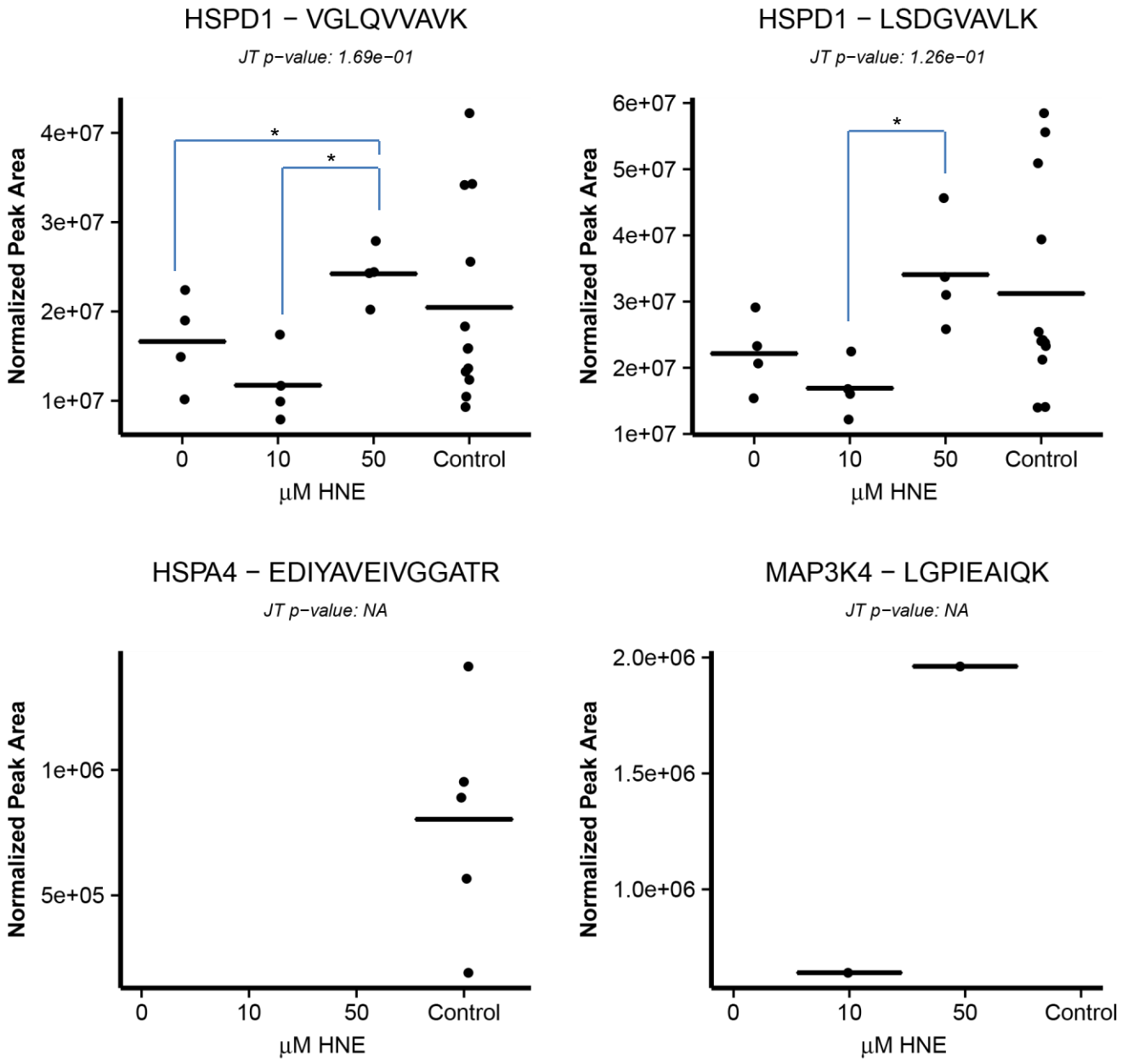
HSPD1 − VGLQVVAVK
JT p−value: 1.69e−01
HSPD1 − LSDGVAVLK
JT p−value: 1.26e−01
HSPA4 − EDIYAVEIVGGATR
JT p−value: NA
MAP3K4 − LGPIEAIQK
JT p−value: NA
Normalized Peak Area
µM HNE
0
10
50
Control
ASK3 IPs

**Figure A-8.**

C

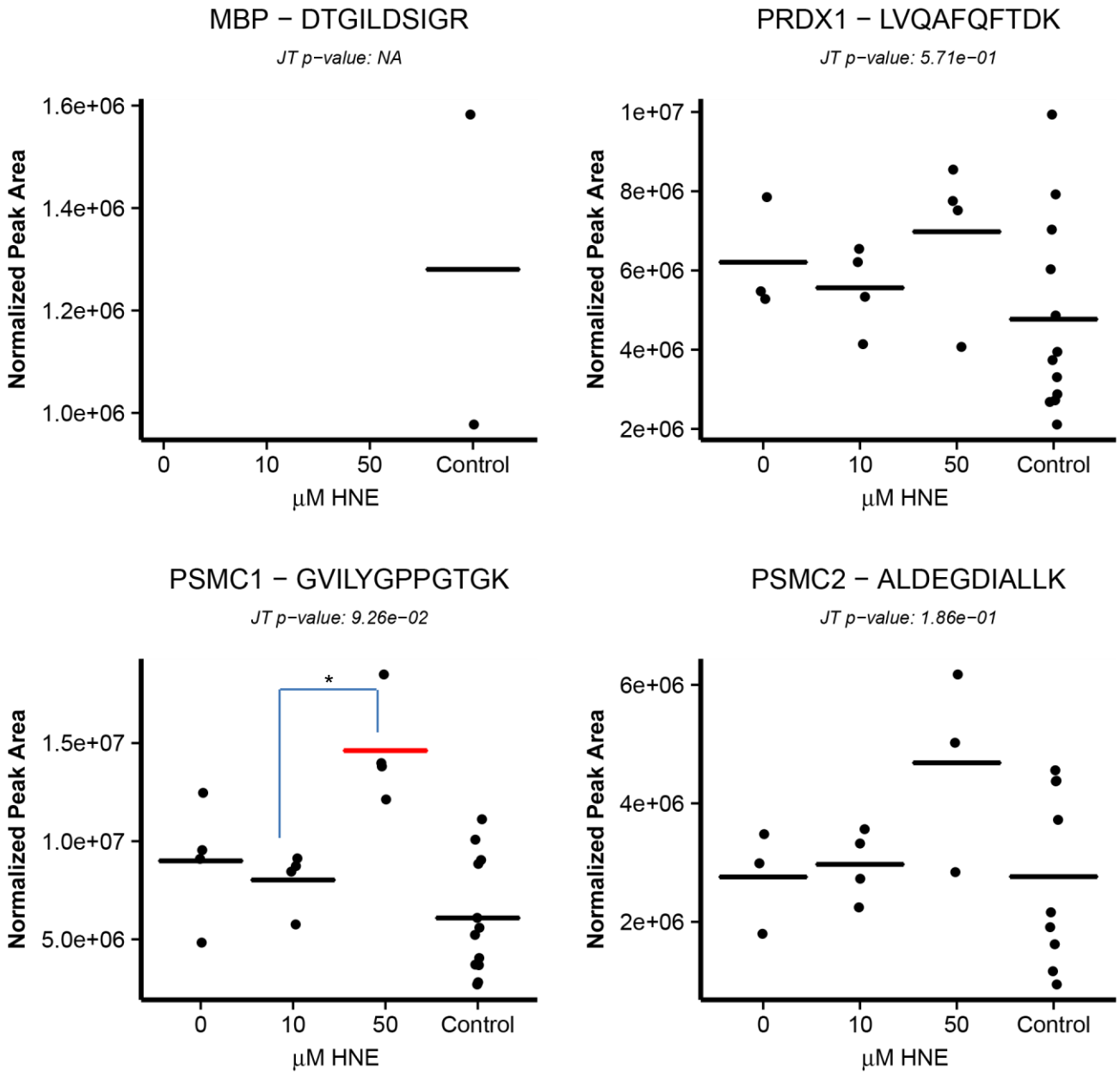
MBP − DTGILDSIGR
JT p−value: NA
PRDX1 − LVQAFQFTDK
JT p−value: 5.71e−01
PSMC1 − GVILYGPPGTGK
JT p−value: 9.26e−02
PSMC2 − ALDEGDIALLK
JT p−value: 1.86e−01
Normalized Peak Area
µM HNE
0
10
50
Control
*
ASK3 IPs

**Figure A-8.**

C

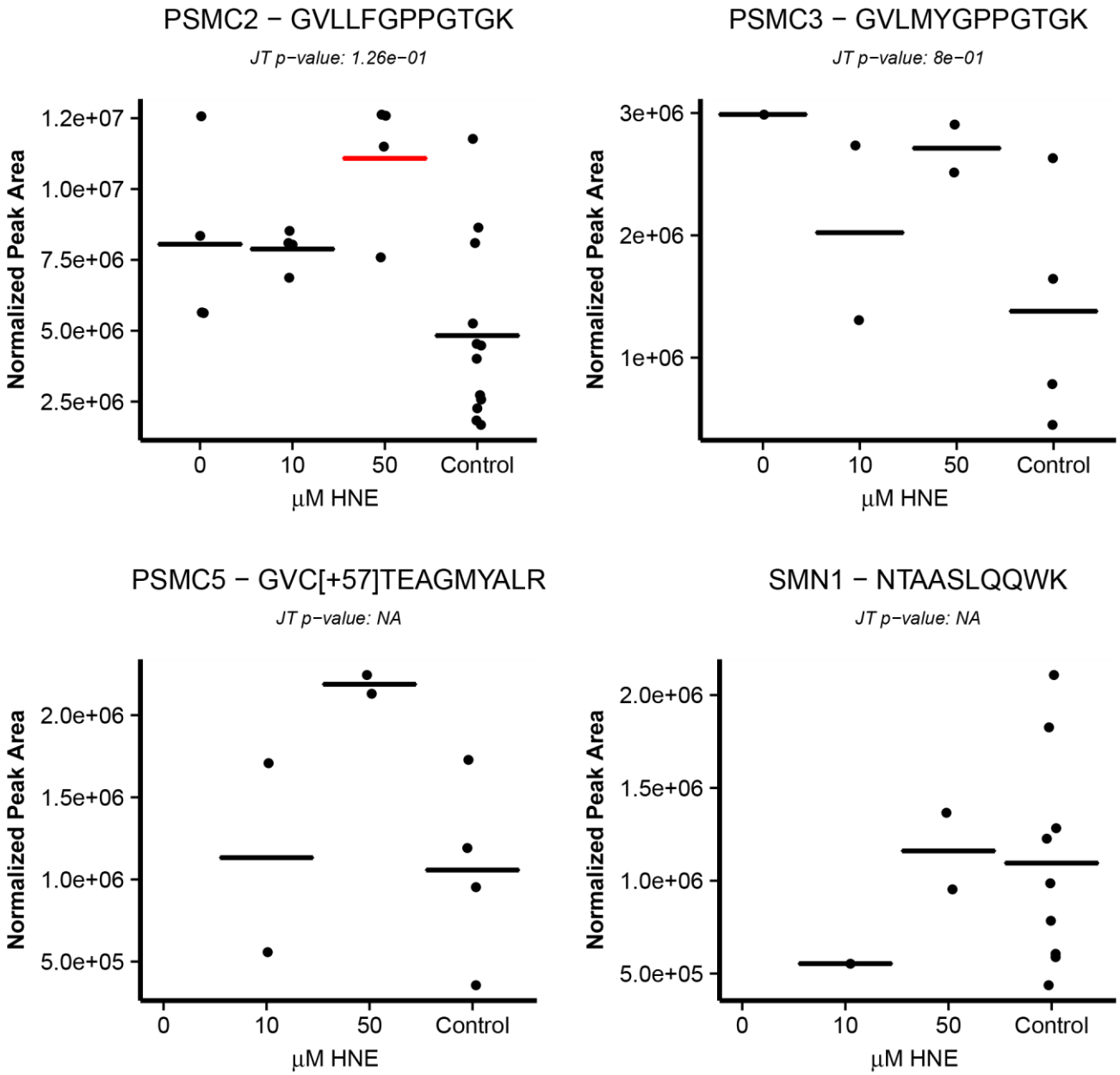
PSMC2 − GVLLFGPPGTGK
JT p−value: 1.26e−01
PSMC3 − GVLMYGPPGTGK
JT p−value: 8e−01
PSMC5 − GVC[+57]TEAGMYALR
JT p−value: NA
SMN1 − NTAASLQQWK
JT p−value: NA
Normalized Peak Area
µM HNE
0
10
50
Control
ASK3 IPs

**Figure A-8.**

C

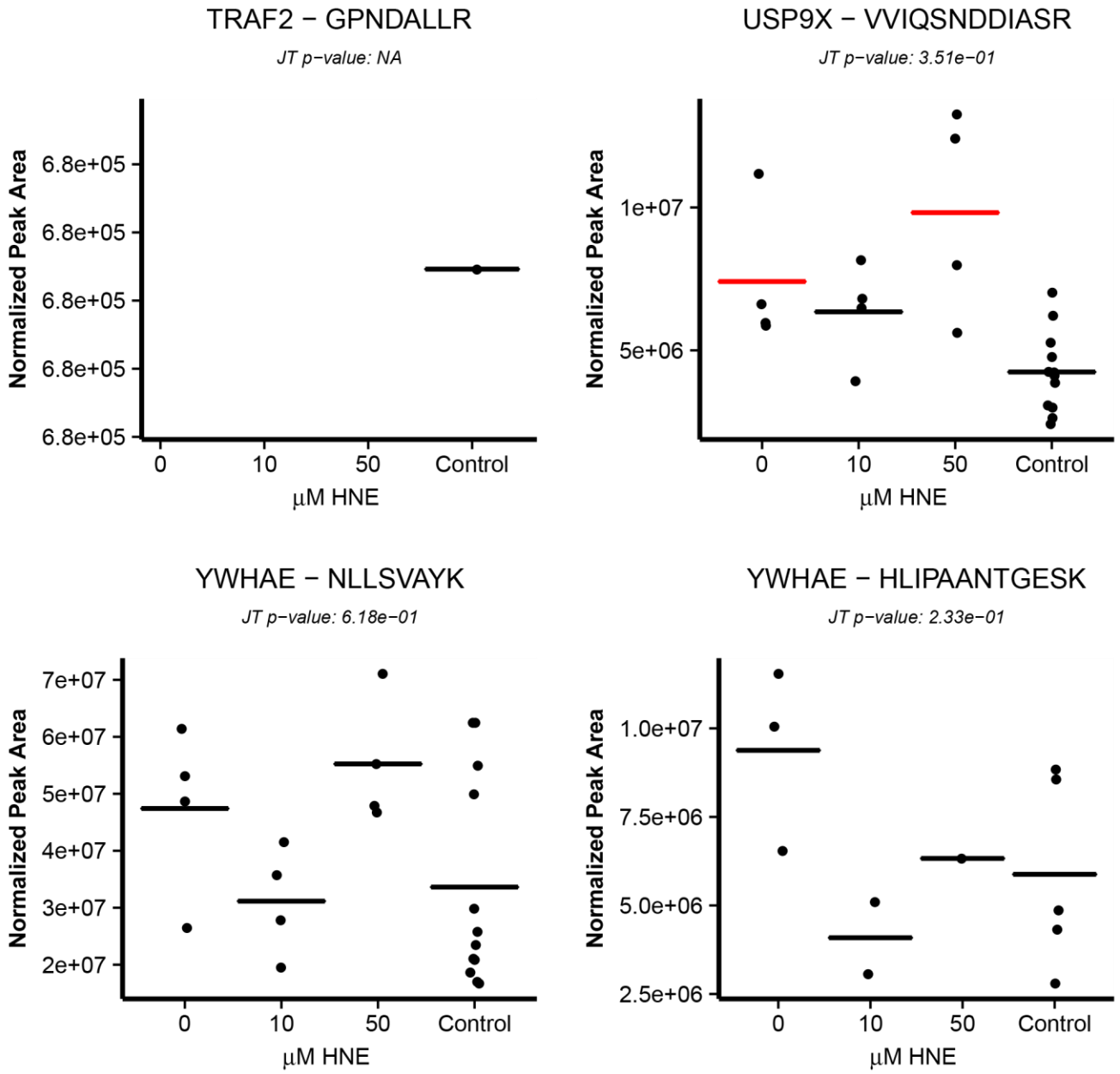


ASK3 IPs

**Figure A-8.**

C

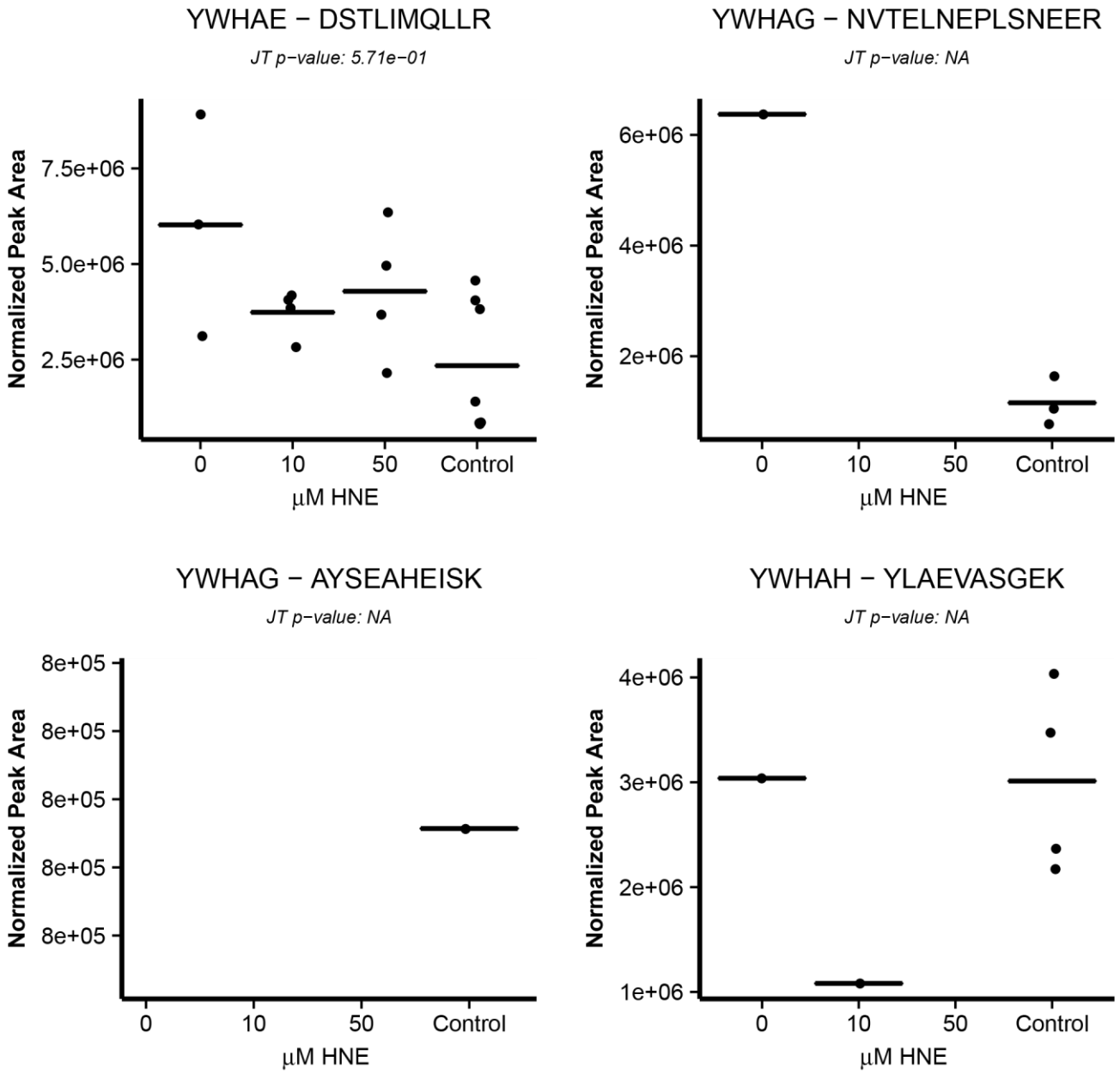


ASK3 IPs

**Figure A-8.**

C

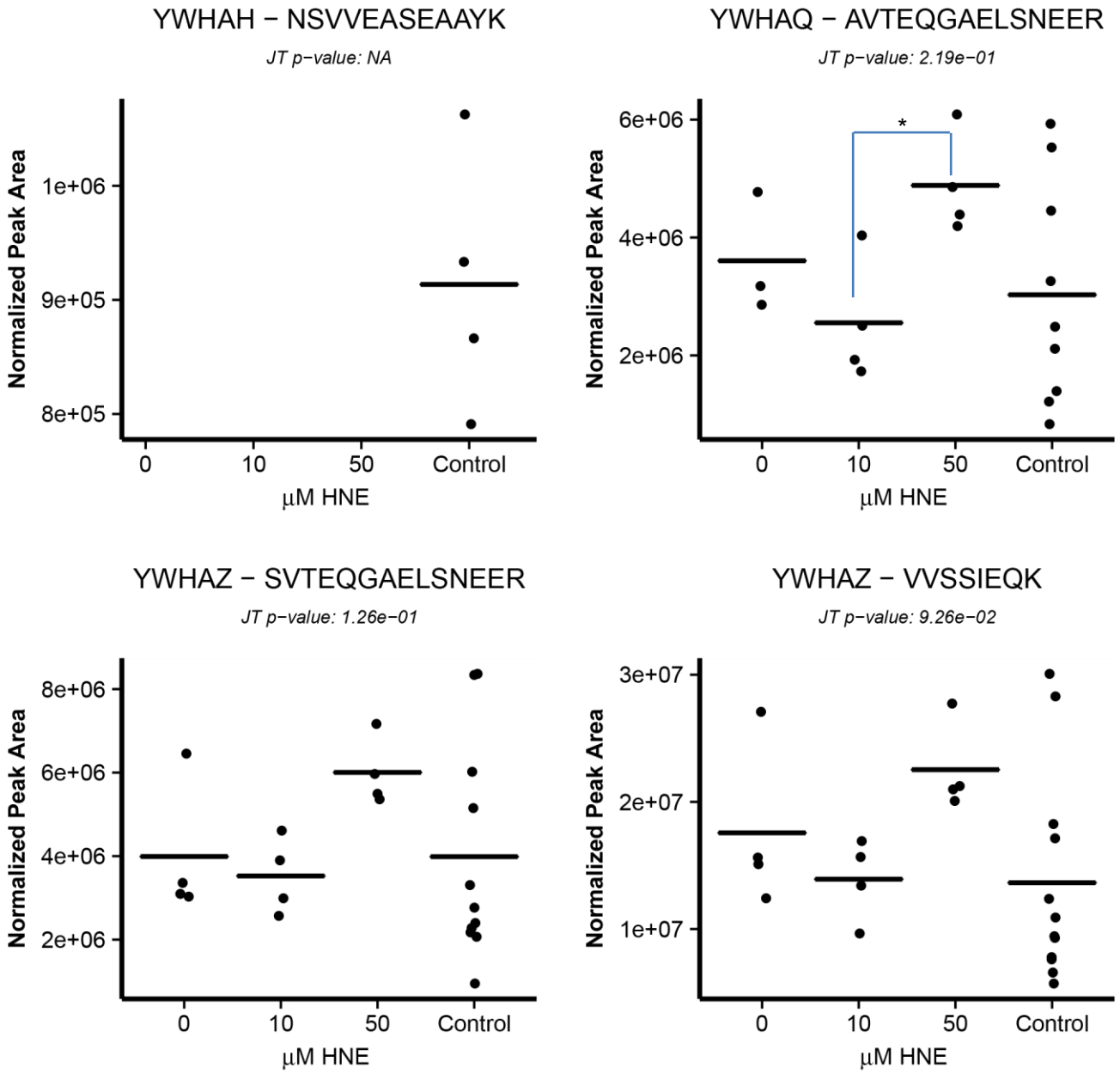
YWHAH − NSVVEASEAAYK
JT p−value: NA
YWHAQ − AVTEQGAELSNEER
JT p−value: 2.19e−01
YWHAZ − SVTEQGAELSNEER
JT p−value: 1.26e−01
YWHAZ − VVSSIEQK
JT p−value: 9.26e−02
Normalized Peak Area
µM HNE
0
10
50
Control
ASK3 IPs

**Figure A-8.**

**C**

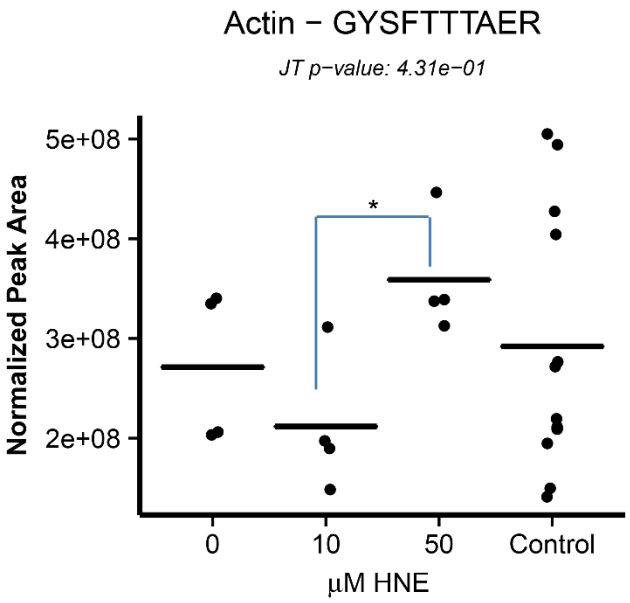


ASK3 IPs

**Figure A-8.**

**D**

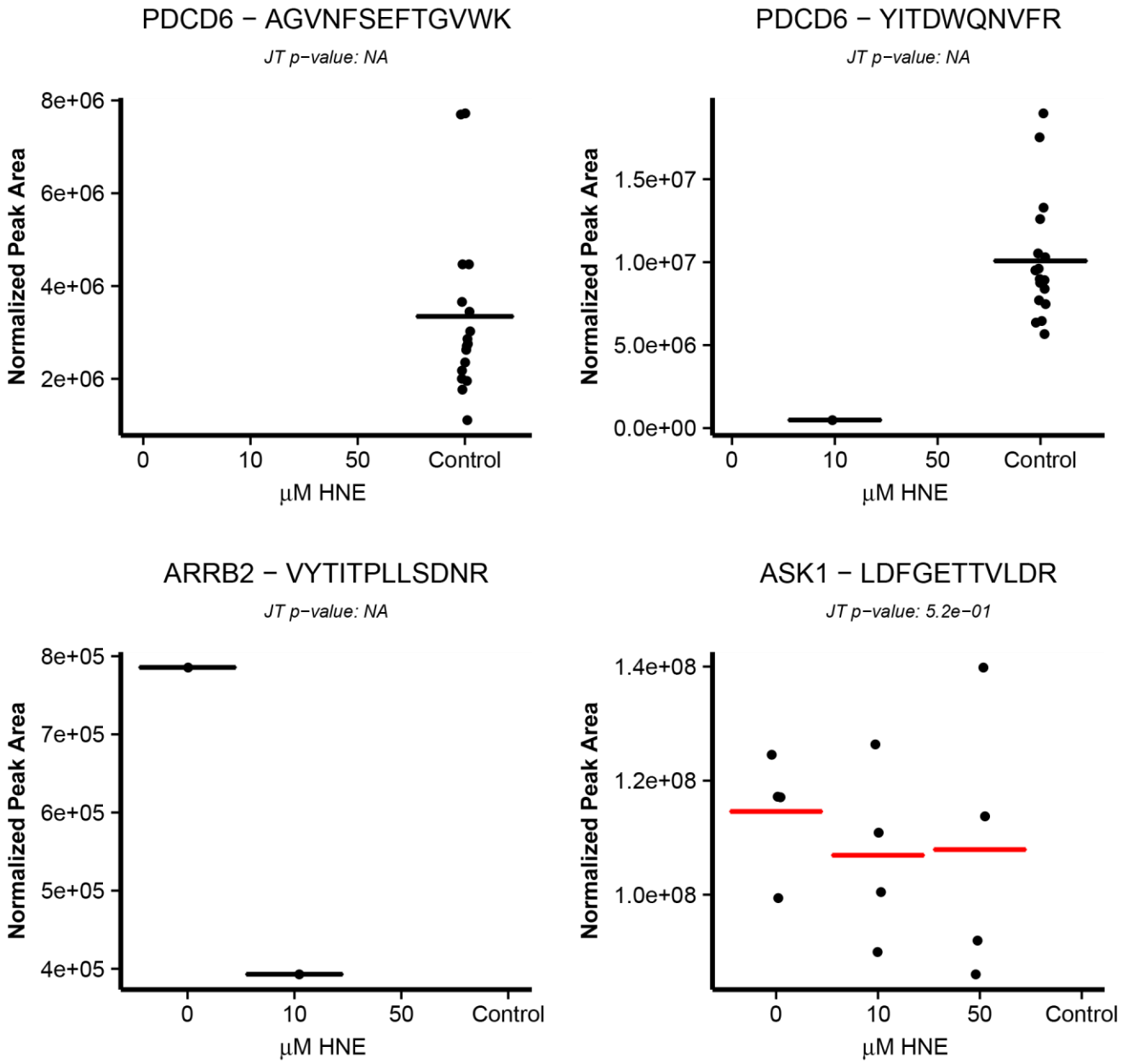


ASK1 Endogenous IPs

**Figure A-8.**

D

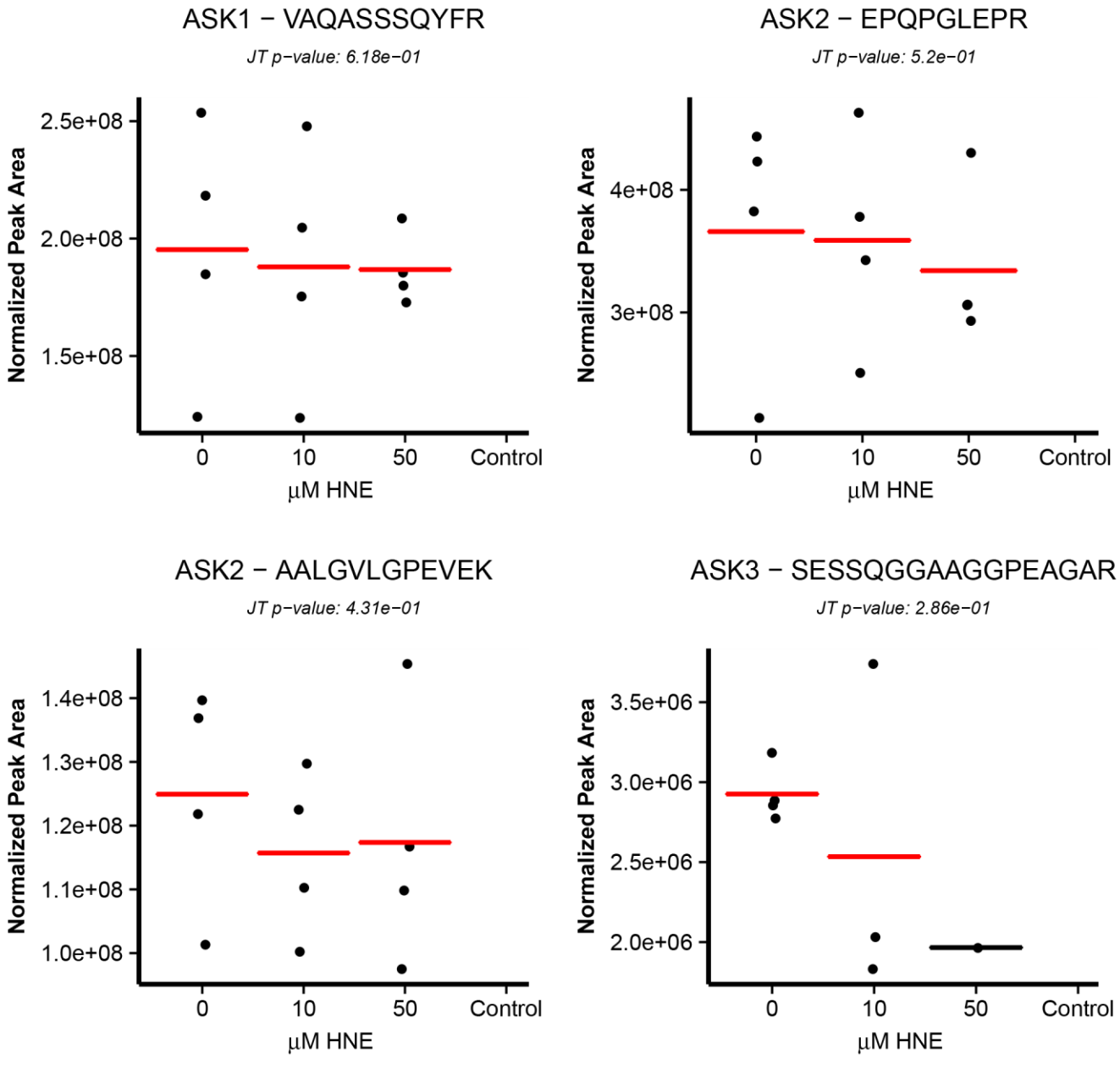


ASK1 Endogenous IPs

**Figure A-8.**

**D**

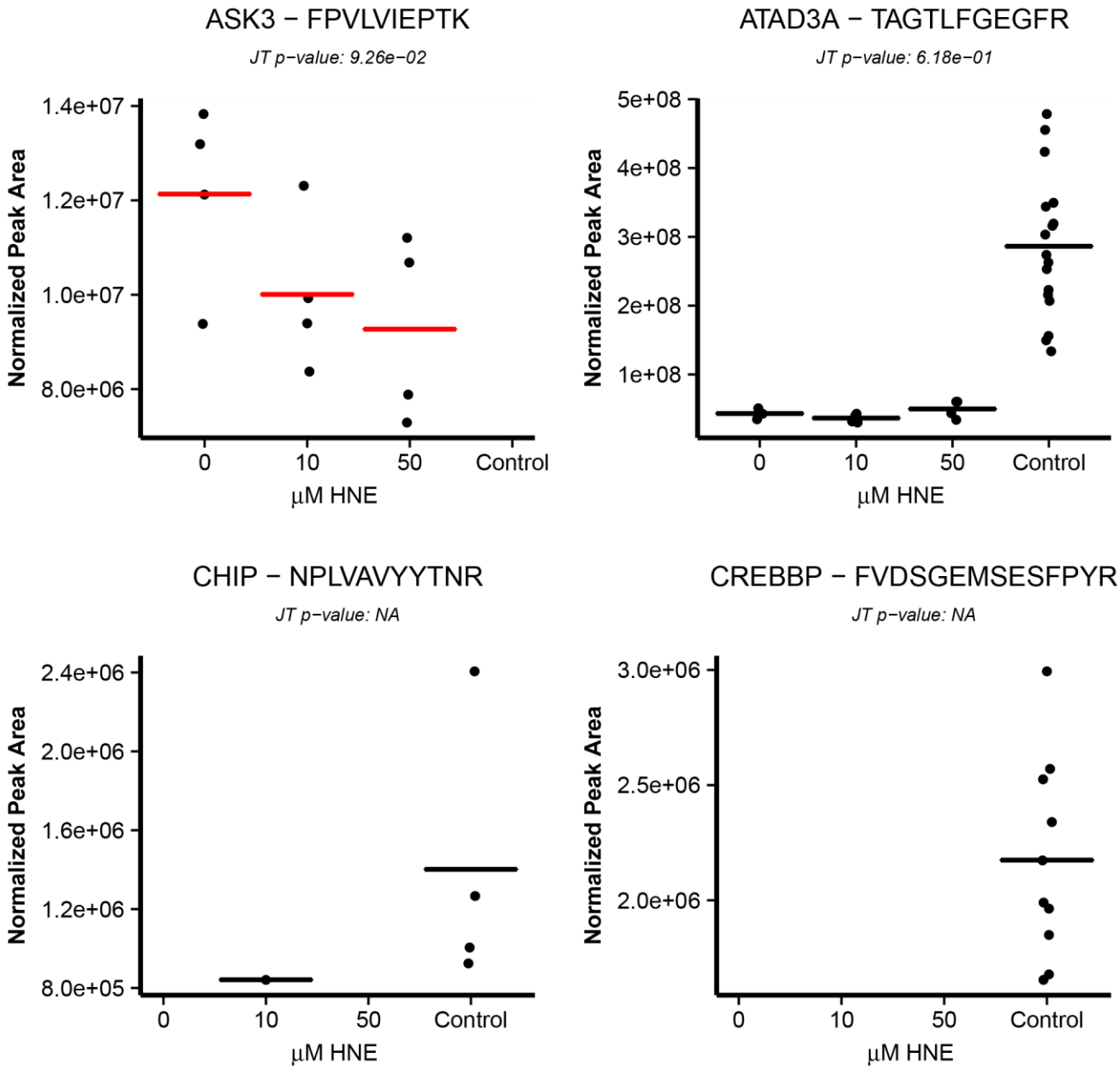
ASK3 − FPVLVIEPTK
JT p−value: 9.26e−02
ATAD3A − TAGTLFGEGFR
JT p−value: 6.18e−01
CHIP − NPLVAVYYTNR
JT p−value: NA
CREBBP − FVDSGEMSESFPYR
JT p−value: NA
Normalized Peak Area
1.4e+07
1.2e+07
1.0e+07
8.0e+06
5e+08
4e+08
3e+08
2e+08
1e+08
2.4e+06
2.0e+06
1.6e+06
1.2e+06
8.0e+05
3.0e+06
2.5e+06
2.0e+06
0
10
50
Control
µM HNE
ASK1 Endogenous IPs

**Figure A-8.**

**D**

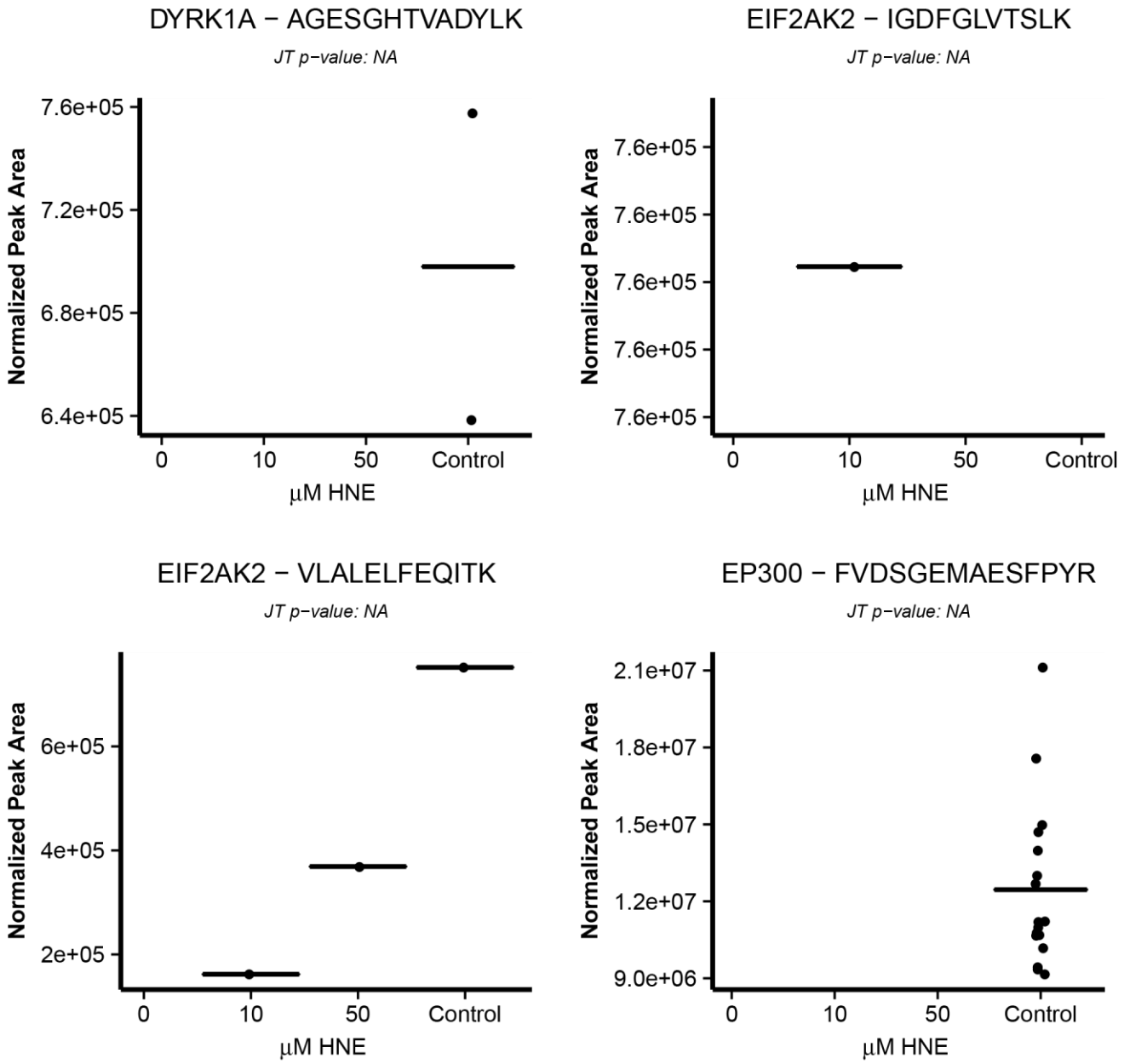


ASK1 Endogenous IPs

**Figure A-8.**

**D**

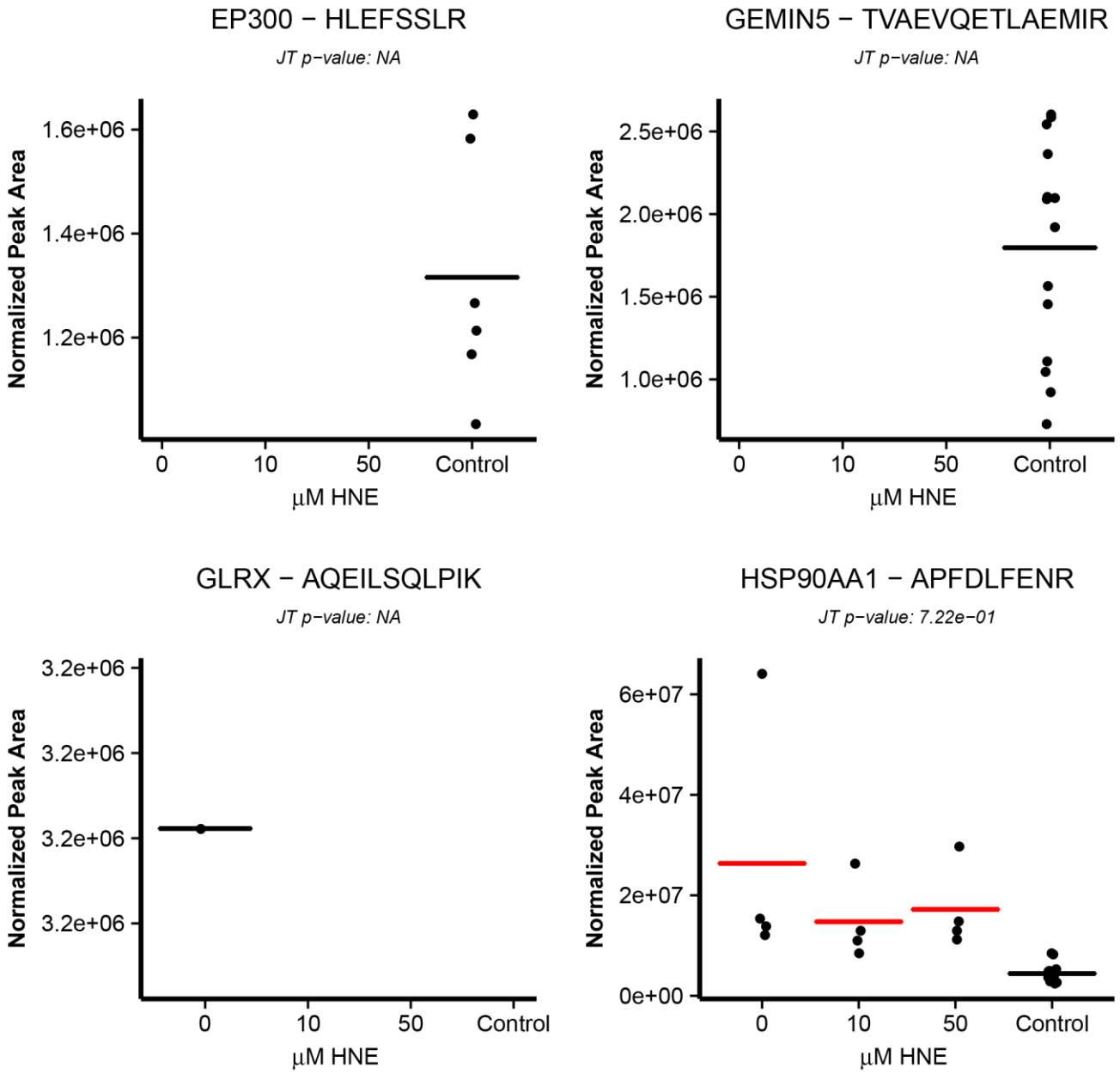


ASK1 Endogenous IPs

**Figure A-8.**

**D**

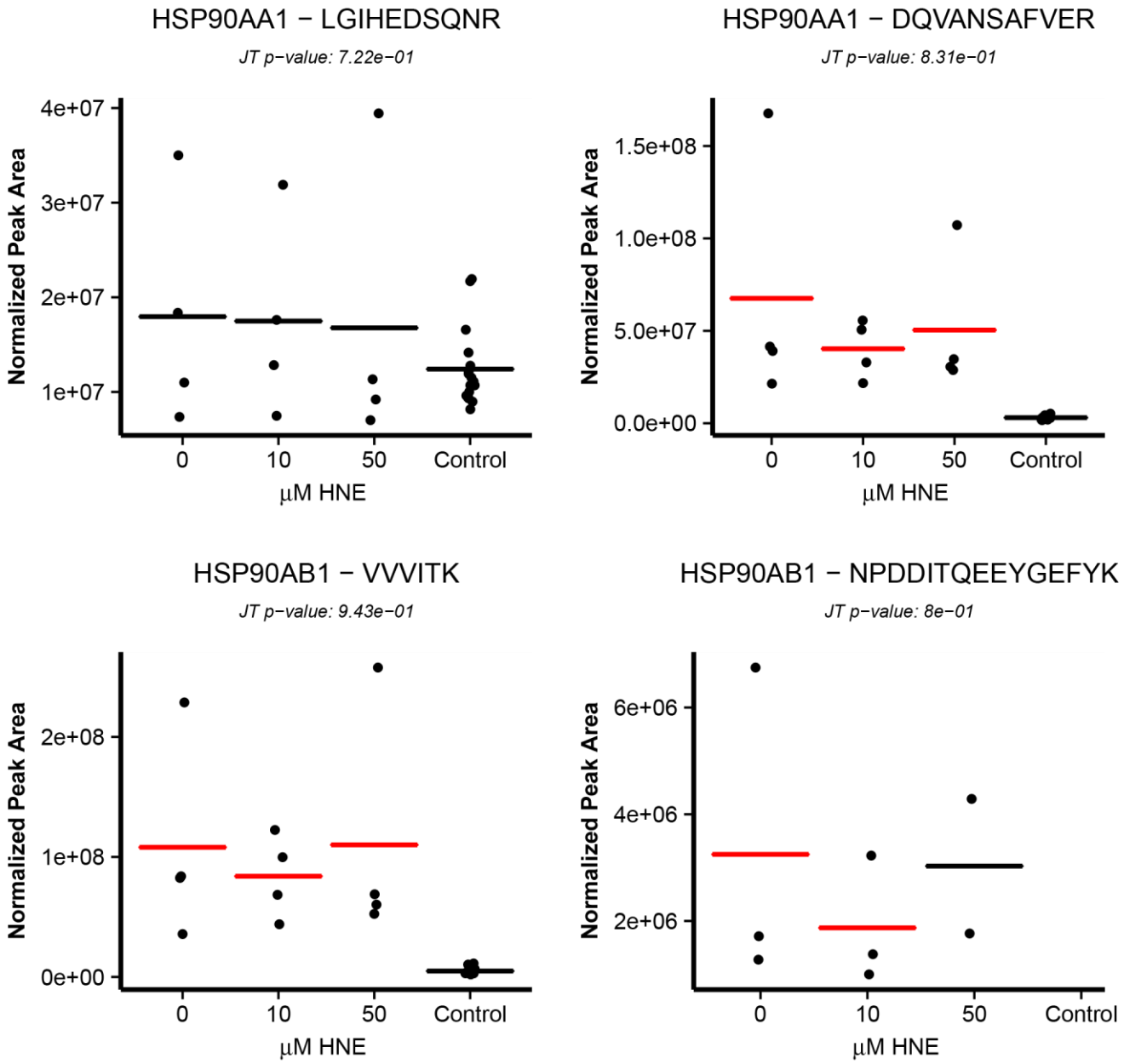


ASK1 Endogenous IPs

**Figure A-8.**

D

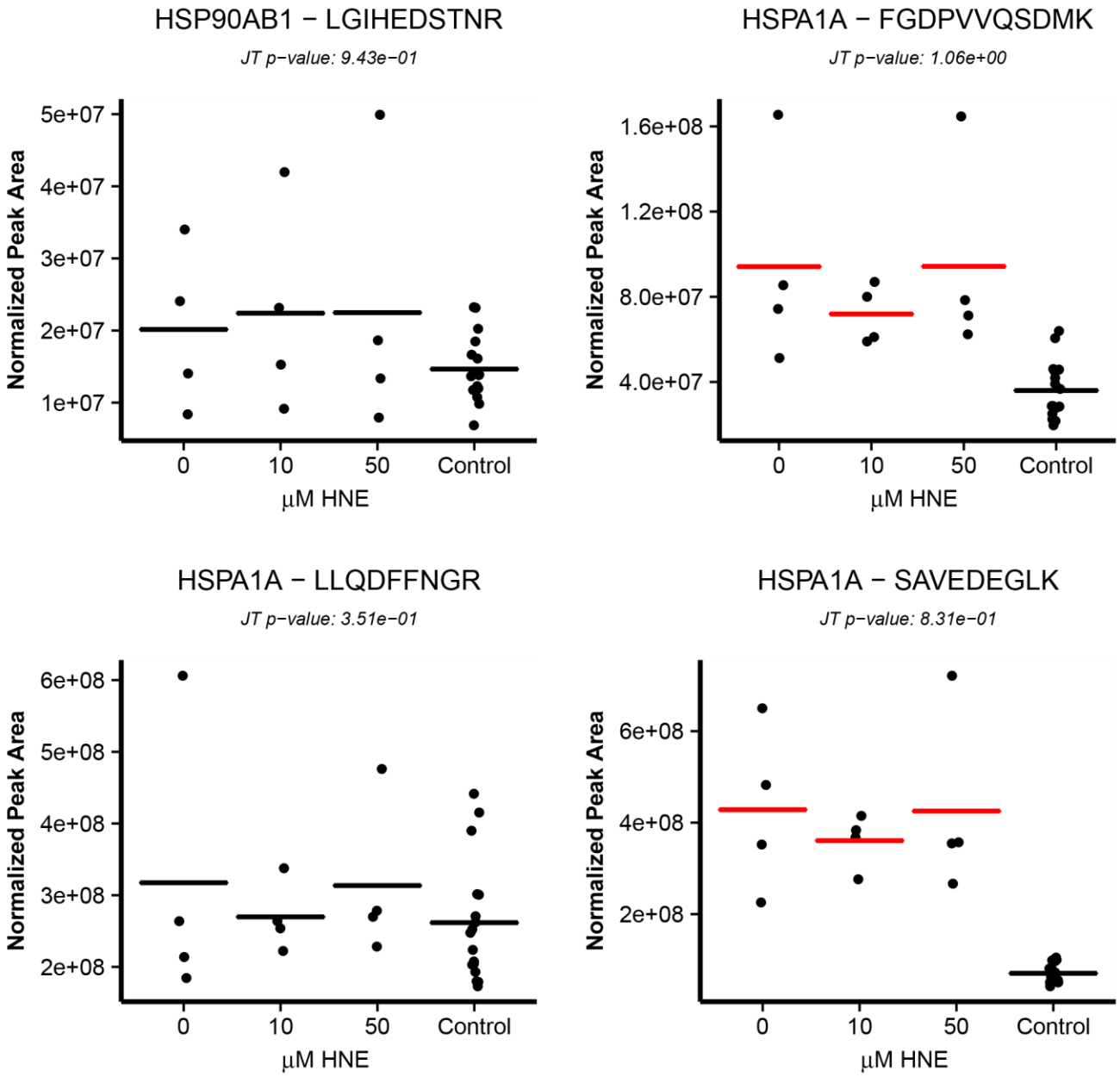
HSP90AB1 − LGIHEDSTNR
JT p−value: 9.43e−01
HSPA1A − FGDPVVQSDMK
JT p−value: 1.06e+00
HSPA1A − LLQDFFNGR
JT p−value: 3.51e−01
HSPA1A − SAVEDEGLK
JT p−value: 8.31e−01
Normalized Peak Area
µM HNE
0
10
50
Control
ASK1 Endogenous IPs

**Figure A-8.**

**D**

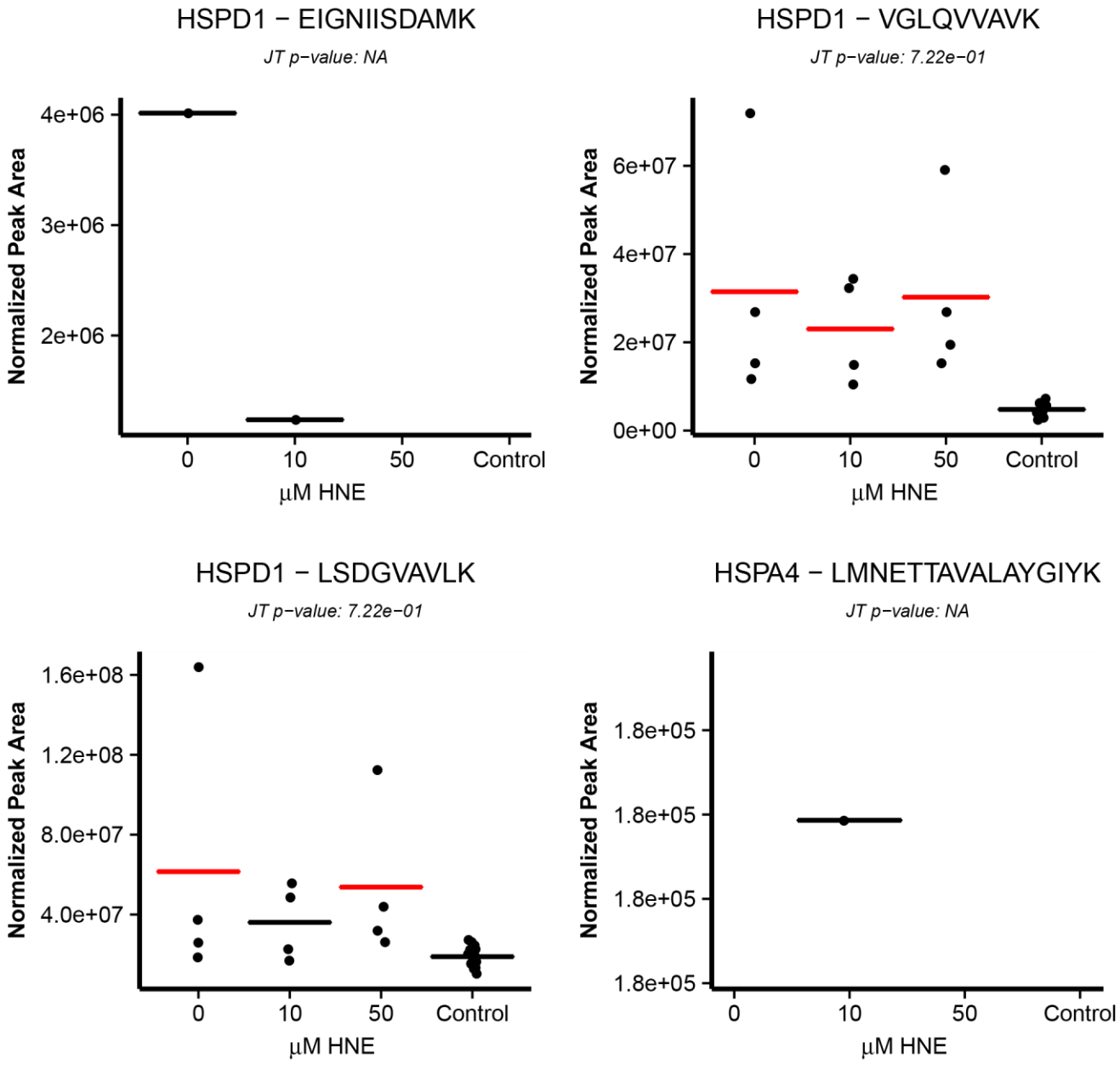


ASK1 Endogenous IPs

**Figure A-8.**

D

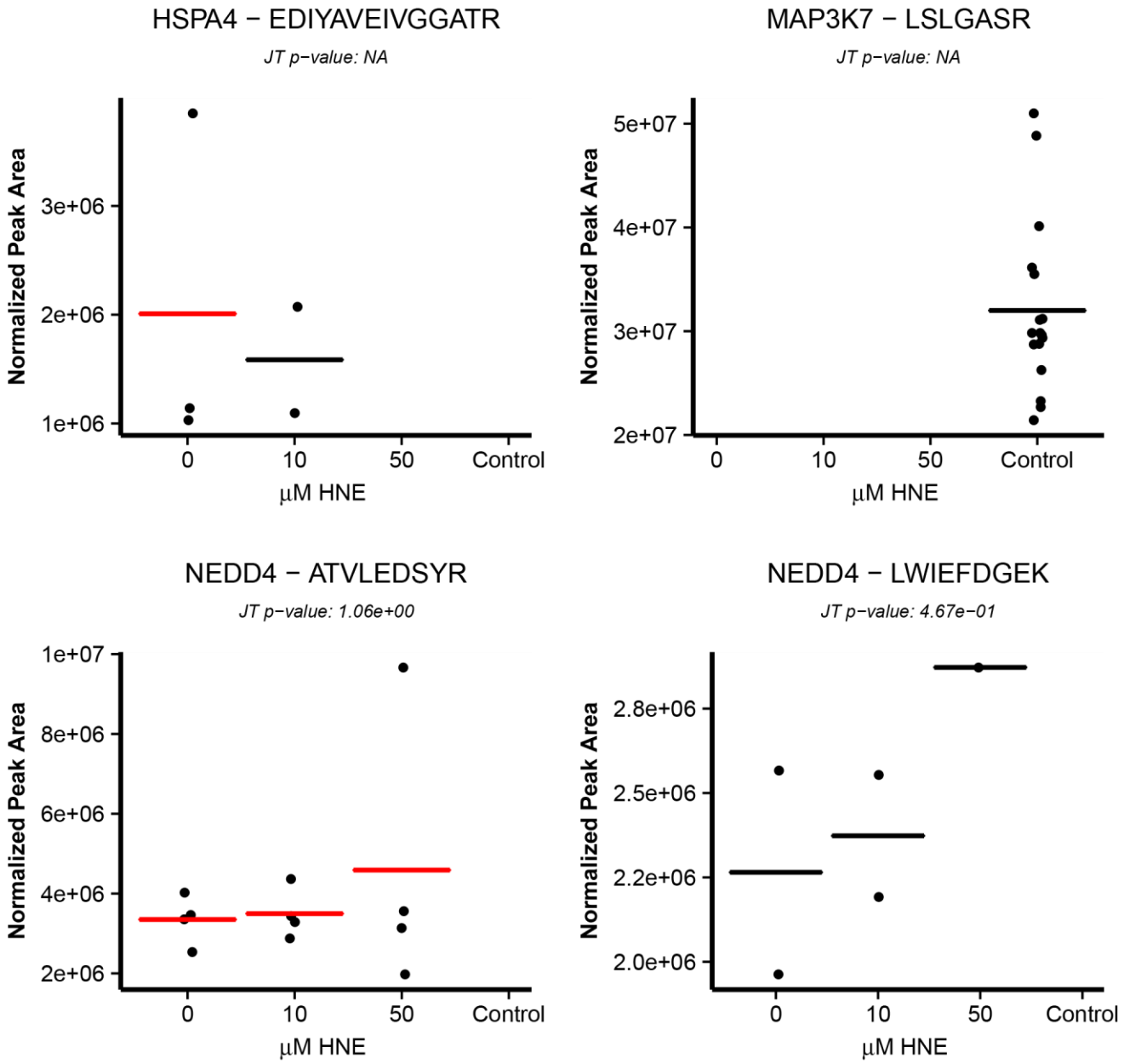


ASK1 Endogenous IPs

**Figure A-8.**

**D**

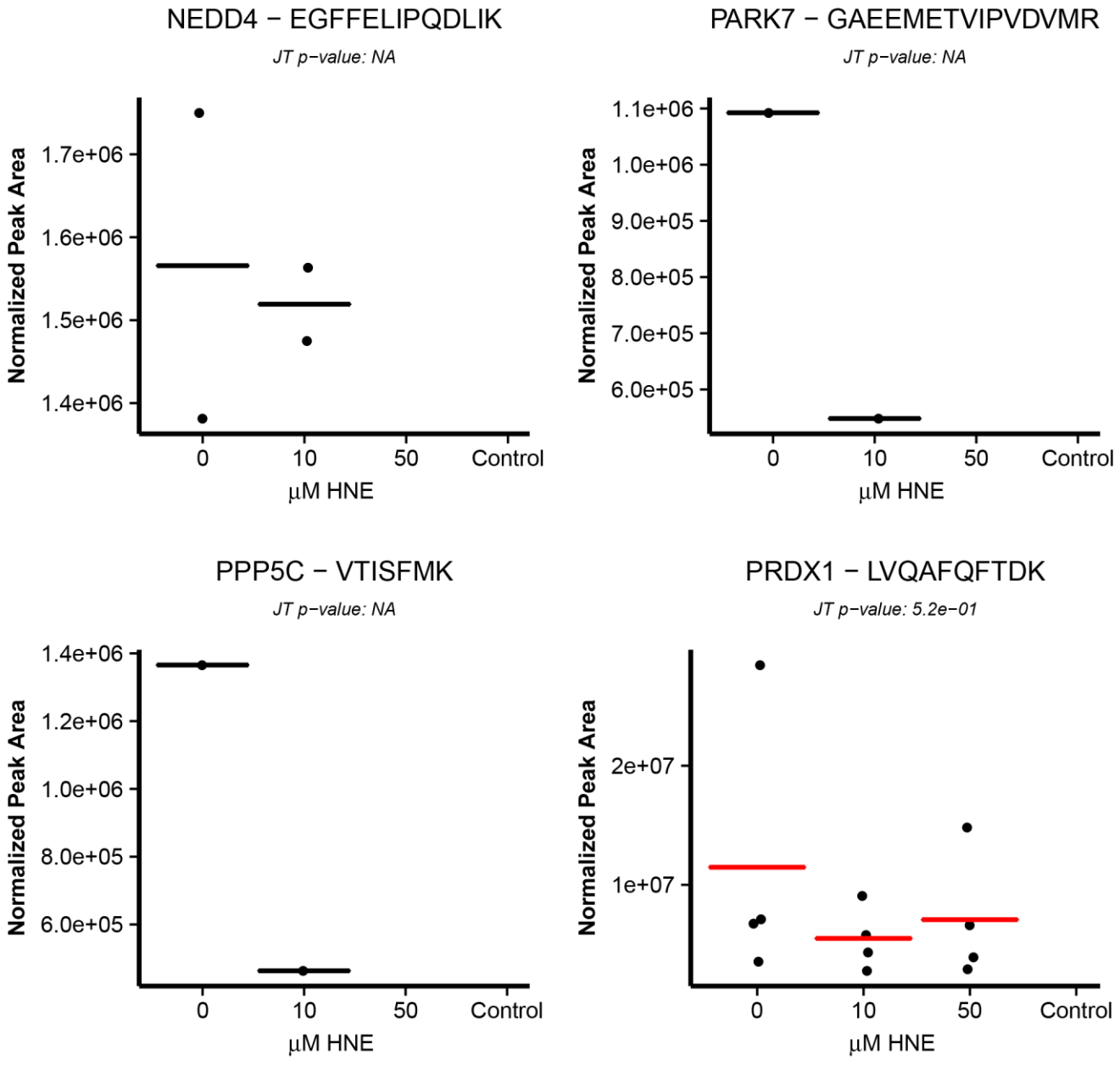


ASK1 Endogenous IPs

**Figure A-8.**

**D**

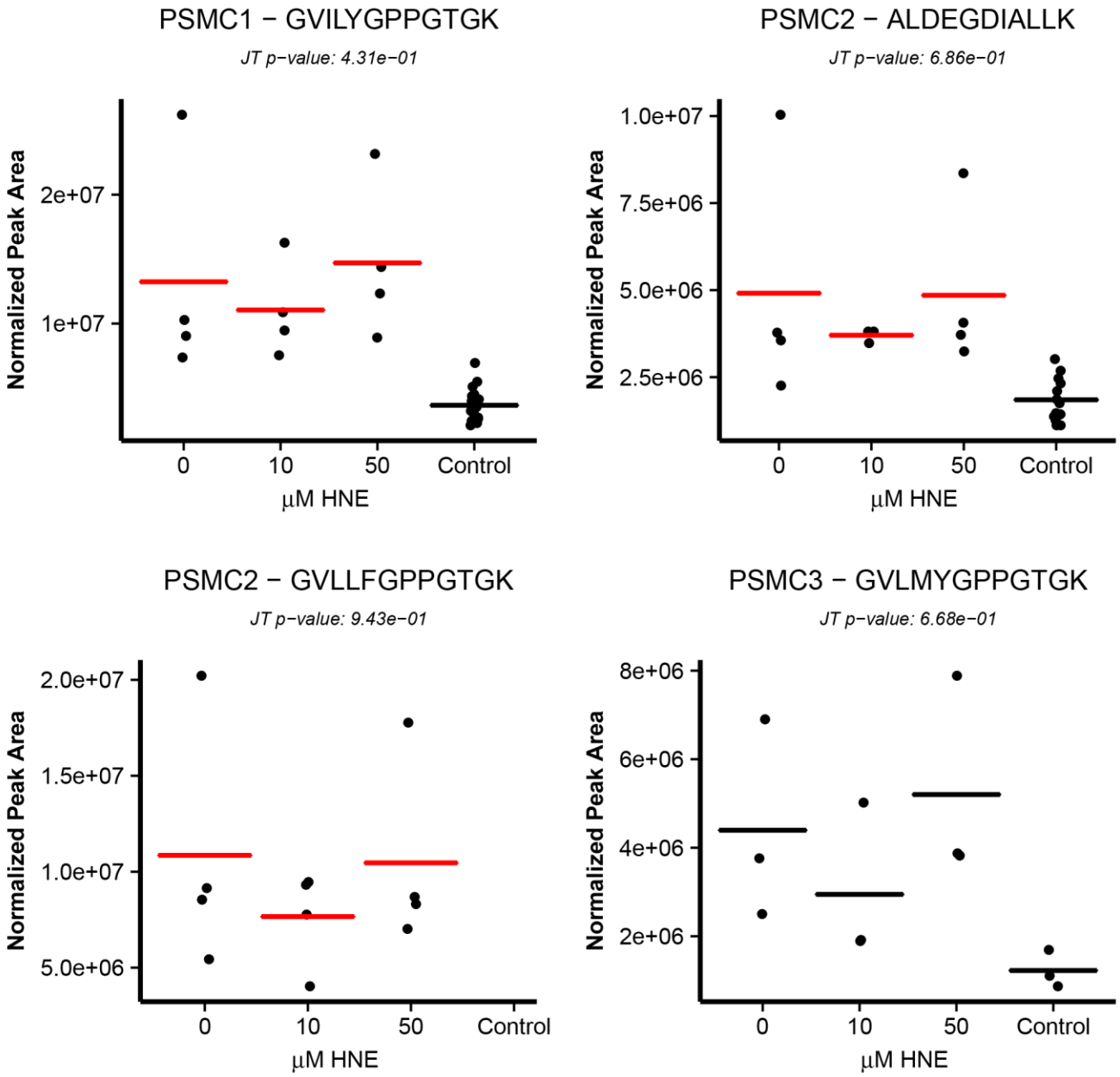


ASK1 Endogenous IPs

**Figure A-8.**

**D**

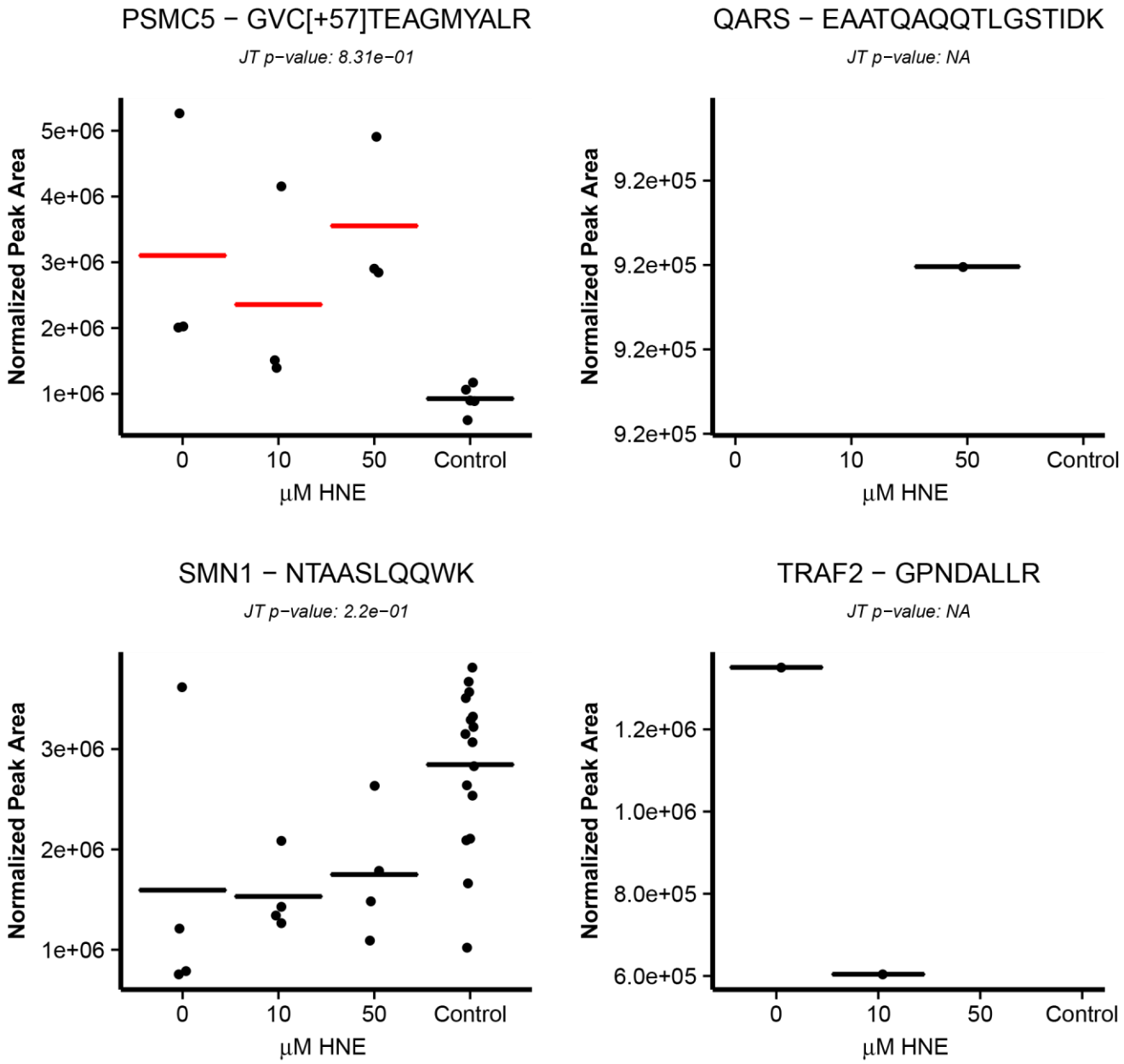
PSMC5 − GVC[+57]TEAGMYALR
JT p−value: 8.31e−01
QARS − EAATQAQQTLGSTIDK
JT p−value: NA
SMN1 − NTAASLQQWK
JT p−value: 2.2e−01
TRAF2 − GPNDALLR
JT p−value: NA
Normalized Peak Area
µM HNE
0
10
50
Control
ASK1 Endogenous IPs

**Figure A-8.**

D

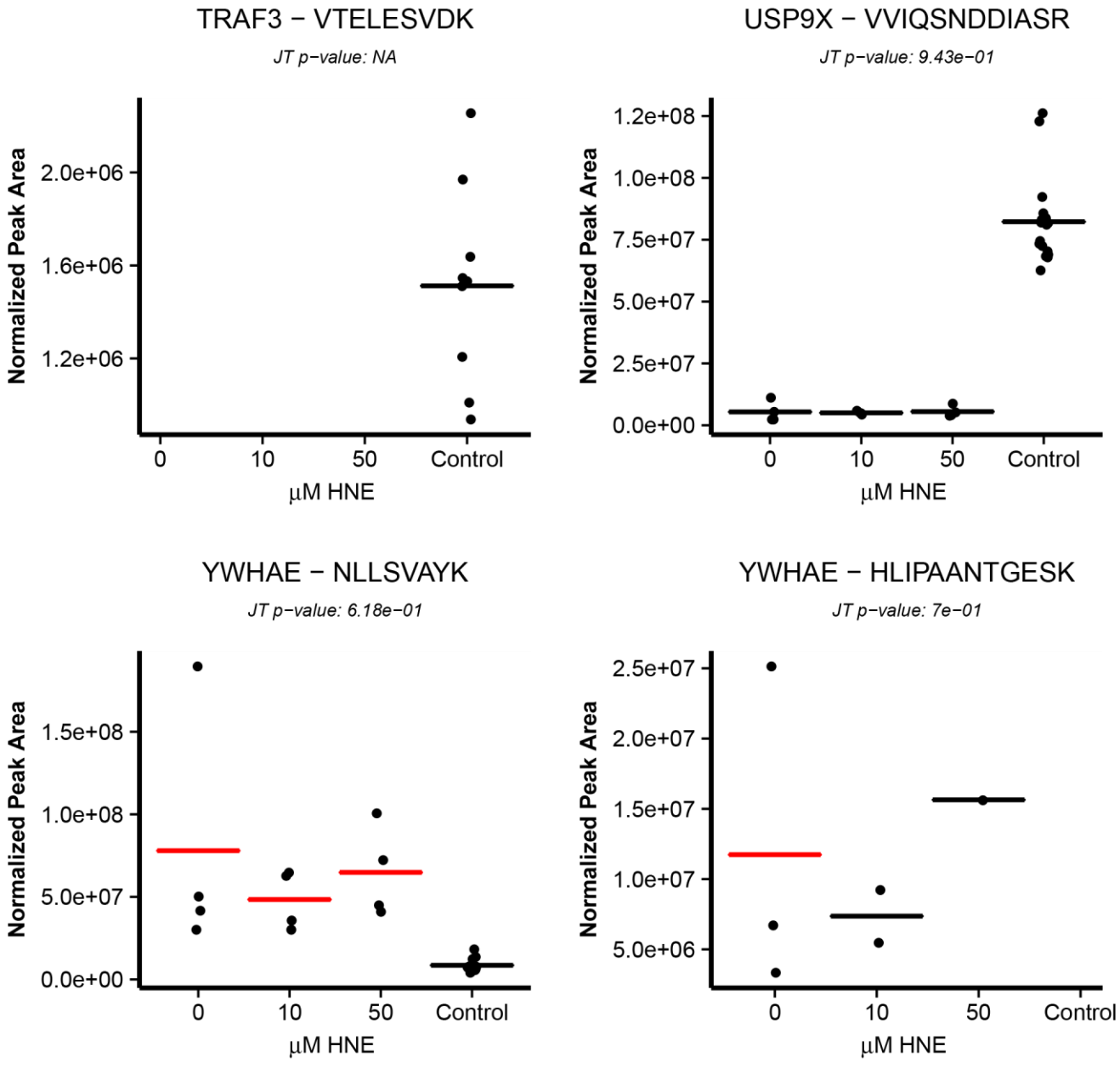
TRAF3 − VTELESVDK
JT p−value: NA
USP9X − VVIQSNDDIASR
JT p−value: 9.43e−01
YWHAE − NLLSVAYK
JT p−value: 6.18e−01
YWHAE − HLIPAANTGESK
JT p−value: 7e−01
Normalized Peak Area
μM HNE
0
10
50
Control
ASK1 Endogenous IPs

**Figure A-8.**

**D**

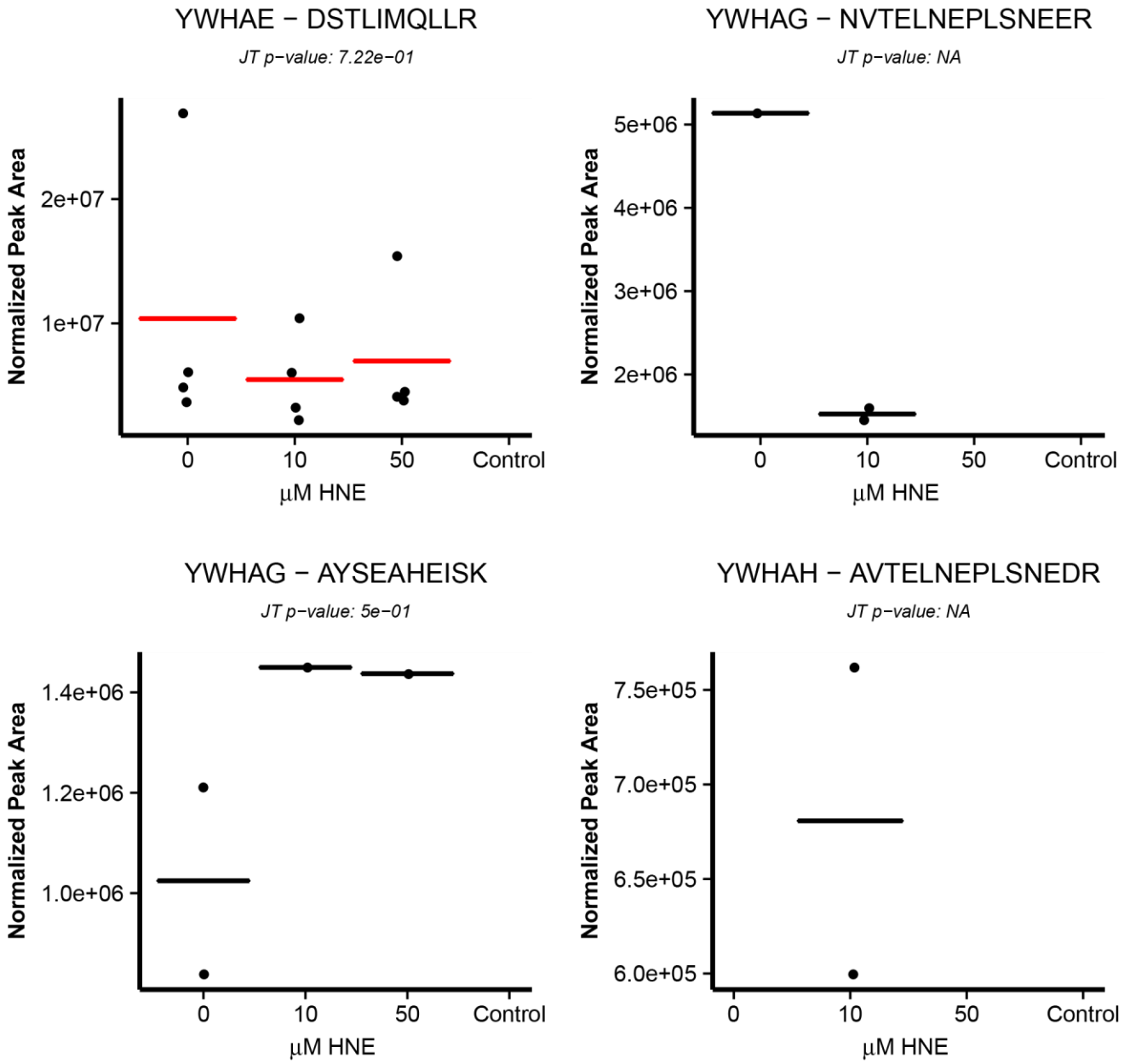
YWHAE − DSTLIMQLLR
JT p−value: 7.22e−01
YWHAG − NVTELNEPLSNEER
JT p−value: NA
YWHAG − AYSEAHEISK
JT p−value: 5e−01
YWHAH − AVTELNEPLSNEDR
JT p−value: NA
Normalized Peak Area
2e+07
1e+07
5e+06
4e+06
3e+06
2e+06
1.4e+06
1.2e+06
1.0e+06
7.5e+05
7.0e+05
6.5e+05
6.0e+05
0
10
50
Control
µM HNE
ASK1 Endogenous IPs

**Figure A-8.**

D

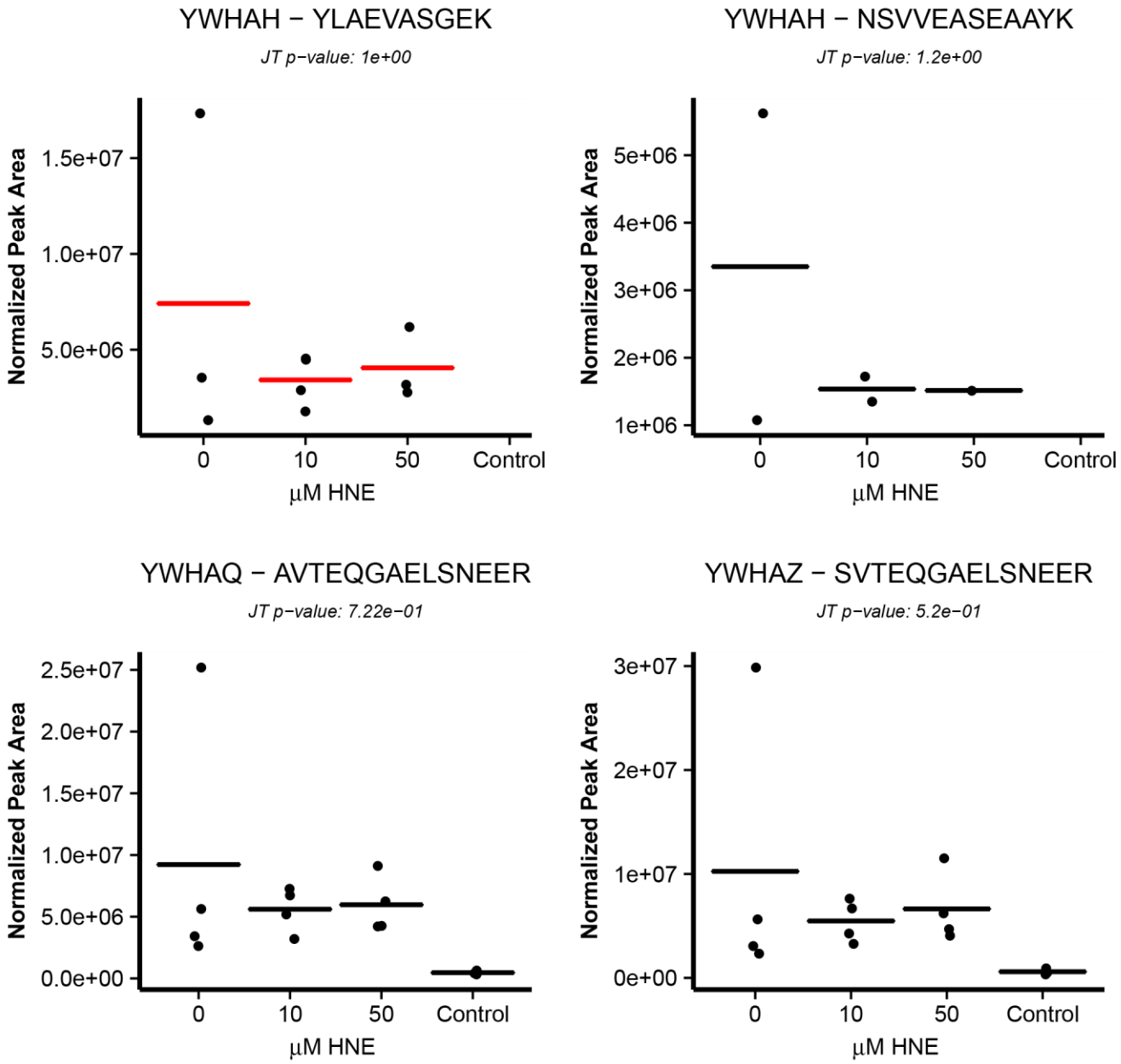


ASK1 Endogenous IPs

**Figure A-8.**

**D**

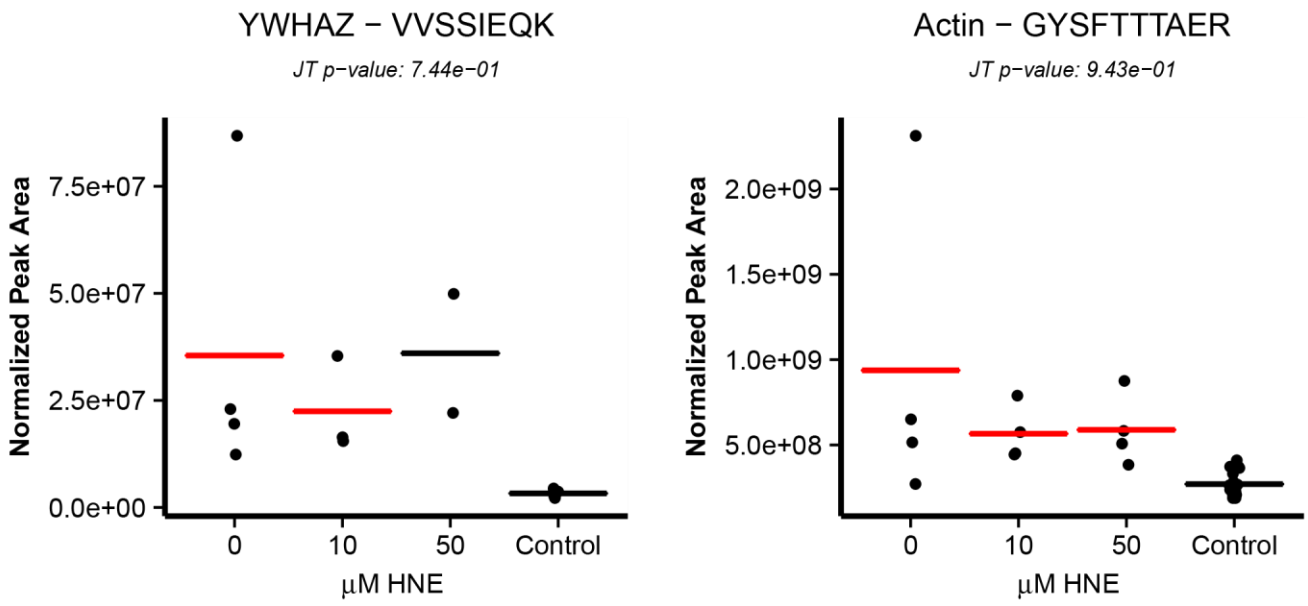


ASK1 Endogenous IPs

**Figure A-8.**

A

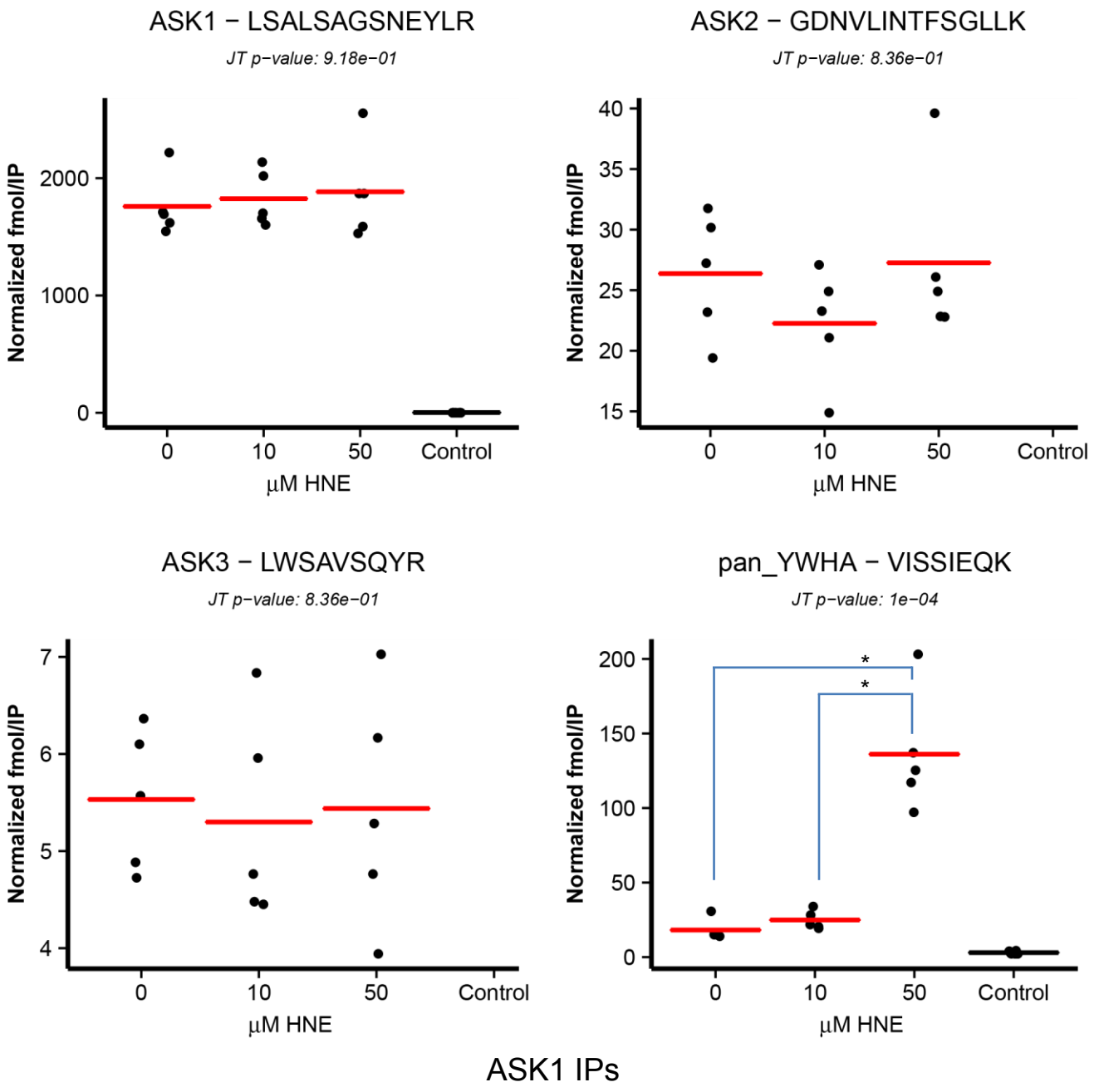


ASK1 IPs

**Figure A-9.** HNE induced dynamic ASK1 complex changes. All peptides normalized by SID for the (A) ASK1 IPs, (B) ASK2 IPs, (C) ASK3 IPs, (D) ASK1 Endogenous IPs were plotted as grouped scatter plots. The mean value for each condition is depicted as a bar. A red bar means that the peak areas for this condition were enriched over the negative control based on the Wilcoxon rank sum test with $p<0.05$ or detection in at least half of the replicates for a condition and no detection in the negative control samples. Concentration-response trends were tested in two ways: (1) the Jonckheere-Terpstra test was applied to detect an ordered trend in peak area – the results of this test are listed below the protein name and peptide sequence on each graph and (2) A Kruskal-Wallace test with post-hoc Dunn's analysis was performed – all significant pairwise comparisons are listed on the graphs with bars connecting the significantly different conditions.

**A**

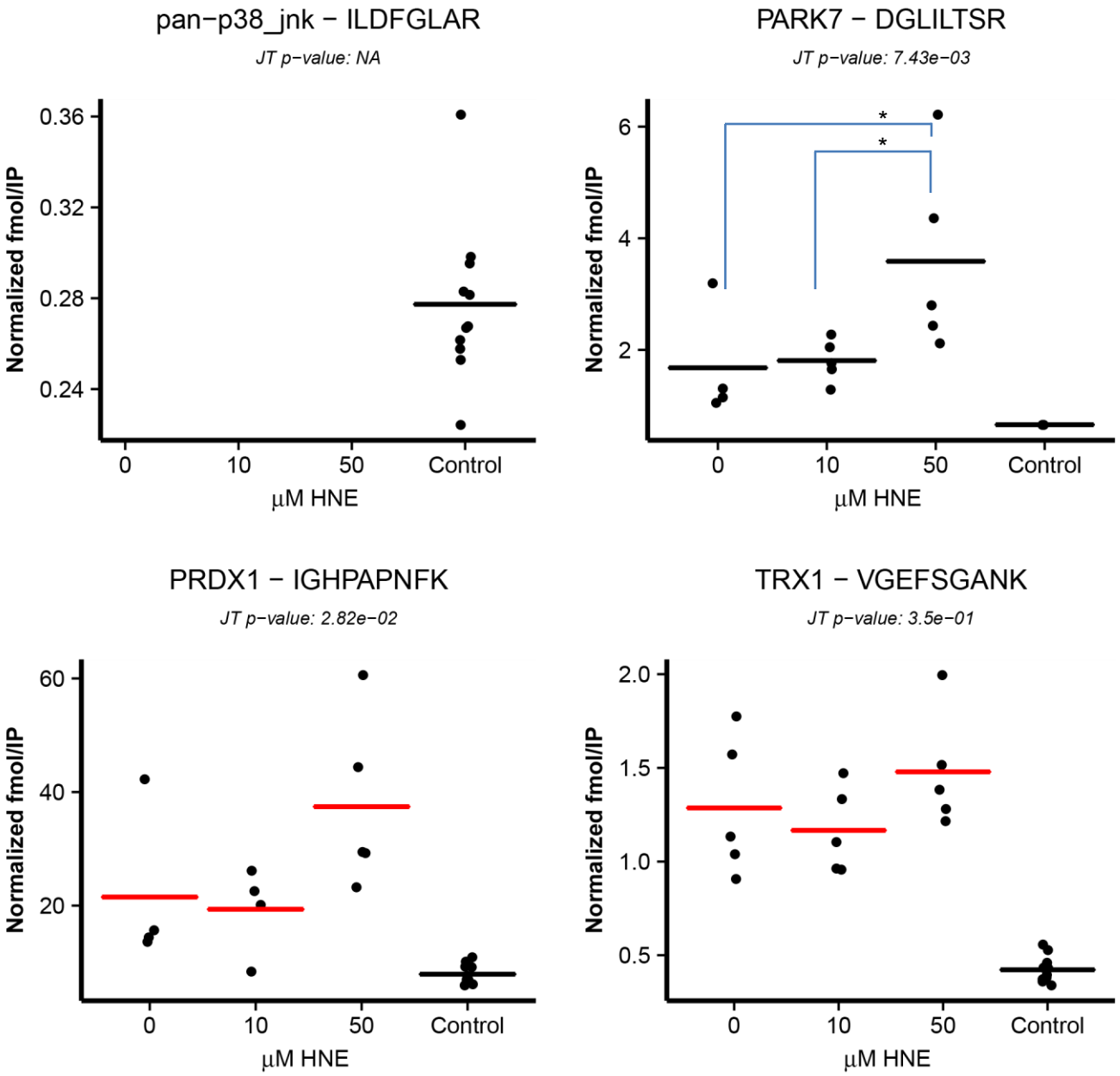
pan−p38_jnk − ILDFGLAR
JT p−value: NA
PARK7 − DGLILTSR
JT p−value: 7.43e−03
PRDX1 − IGHPAPNFK
JT p−value: 2.82e−02
TRX1 − VGEFSGANK
JT p−value: 3.5e−01
Normalized fmol/IP
µM HNE
0
10
50
Control
ASK1 IPs

**Figure A-9.**

**A**

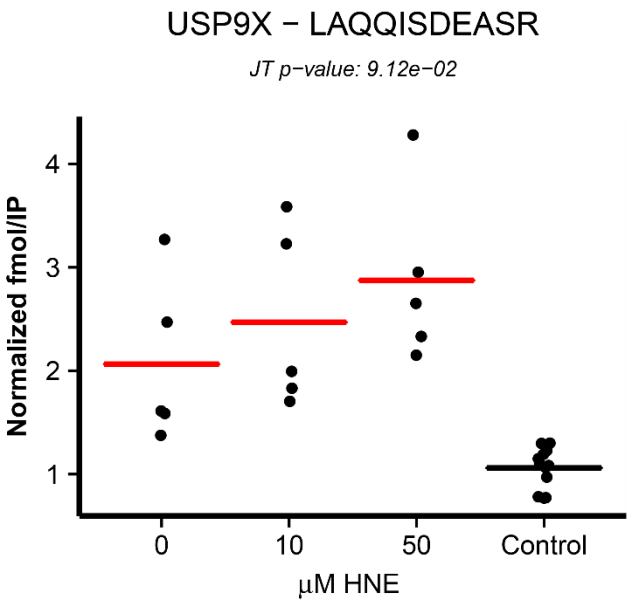


ASK1 IPs

**Figure A-9.**

**B**

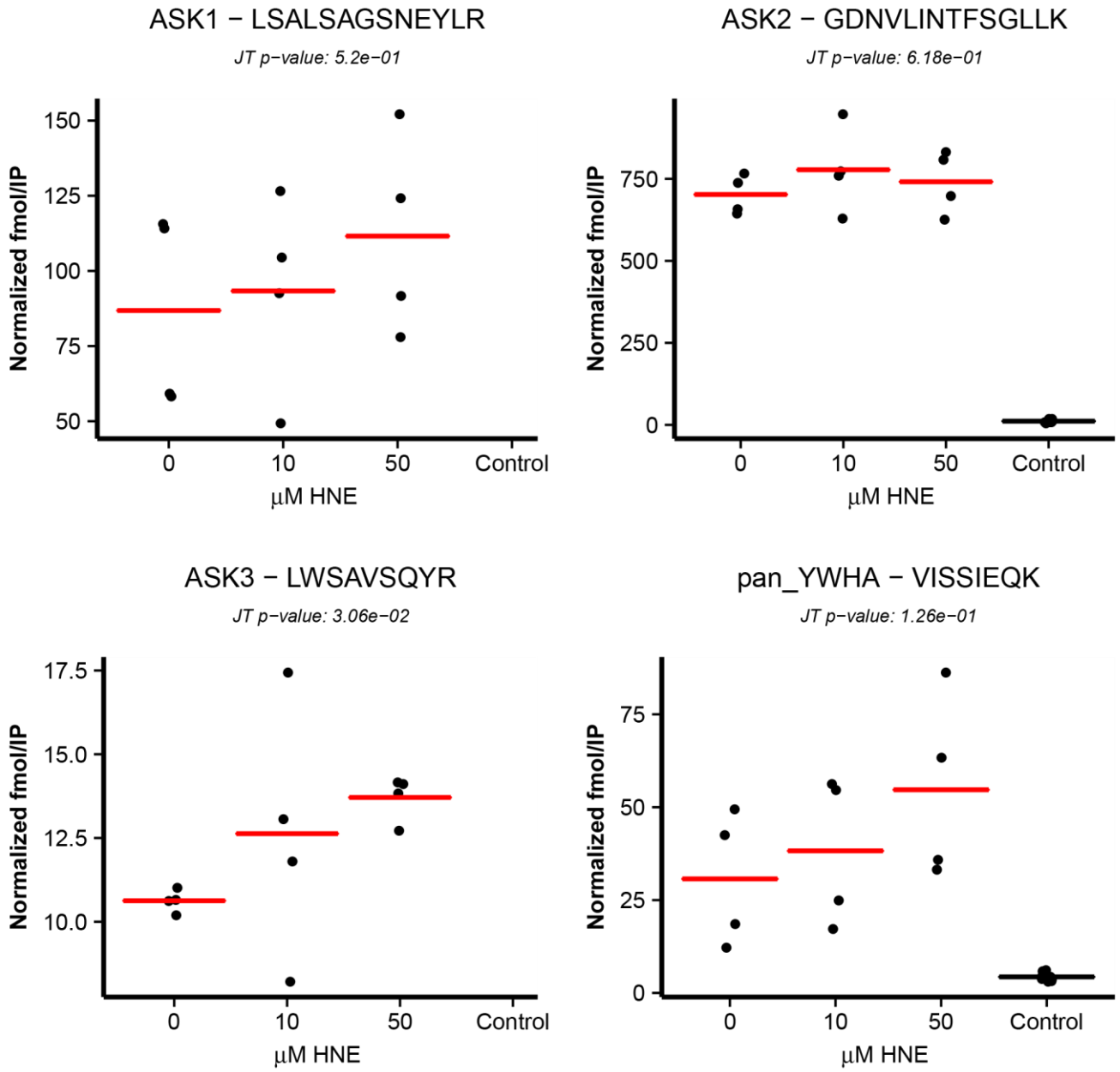


ASK2 IPs

**Figure A-9.**

**B**

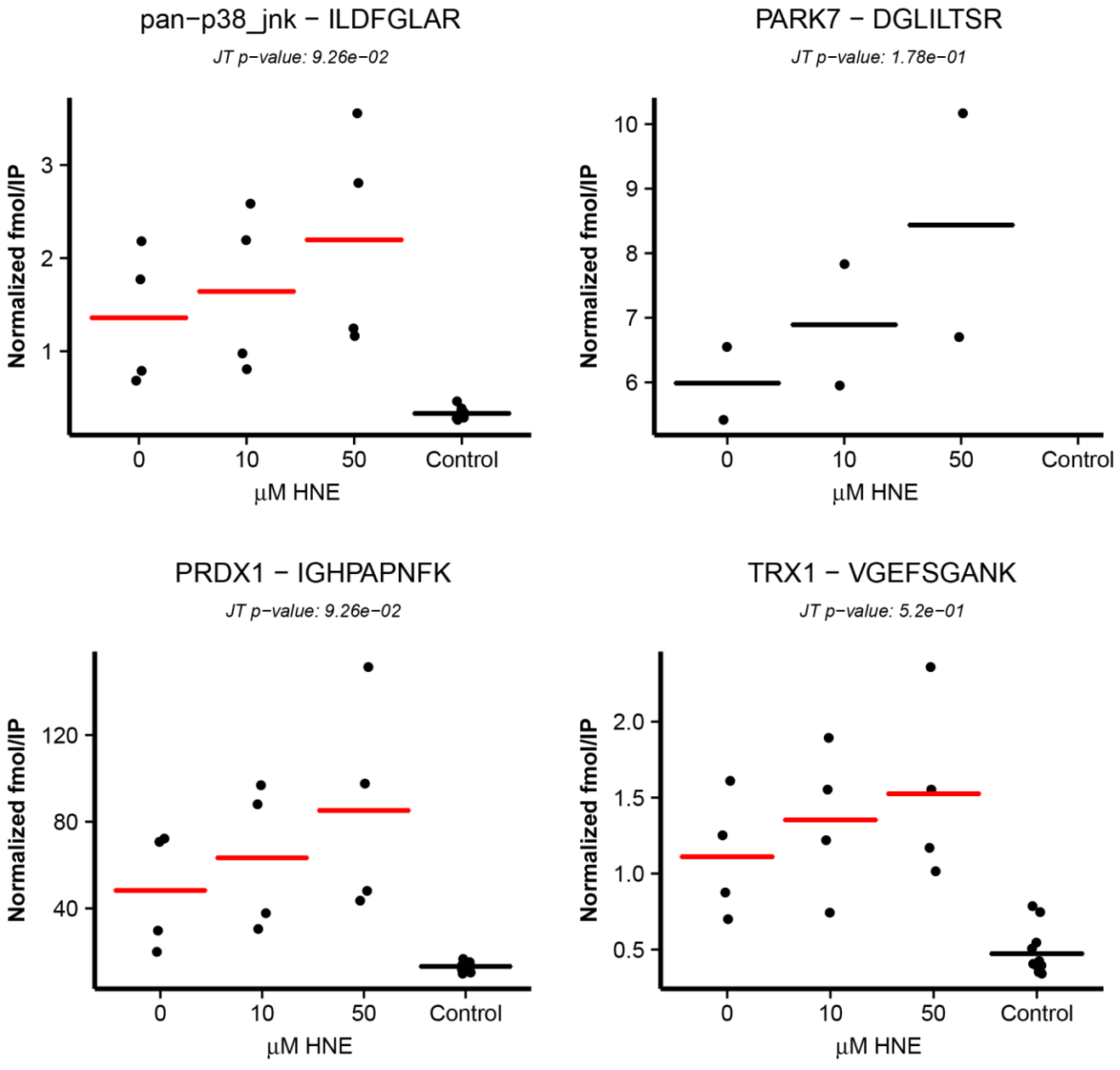
pan−p38_jnk − ILDFGLAR
JT p−value: 9.26e−02
Normalized fmol/IP
µM HNE
PARK7 − DGLILTSR
JT p−value: 1.78e−01
PRDX1 − IGHPAPNFK
JT p−value: 9.26e−02
TRX1 − VGEFSGANK
JT p−value: 5.2e−01
0
10
50
Control
ASK2 IPs

**Figure A-9.**

**B**

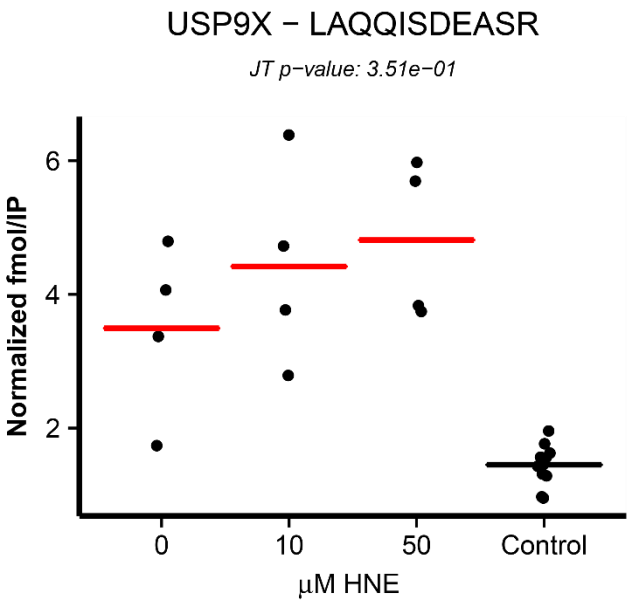


ASK2 IPs

**Figure A-9.**

C

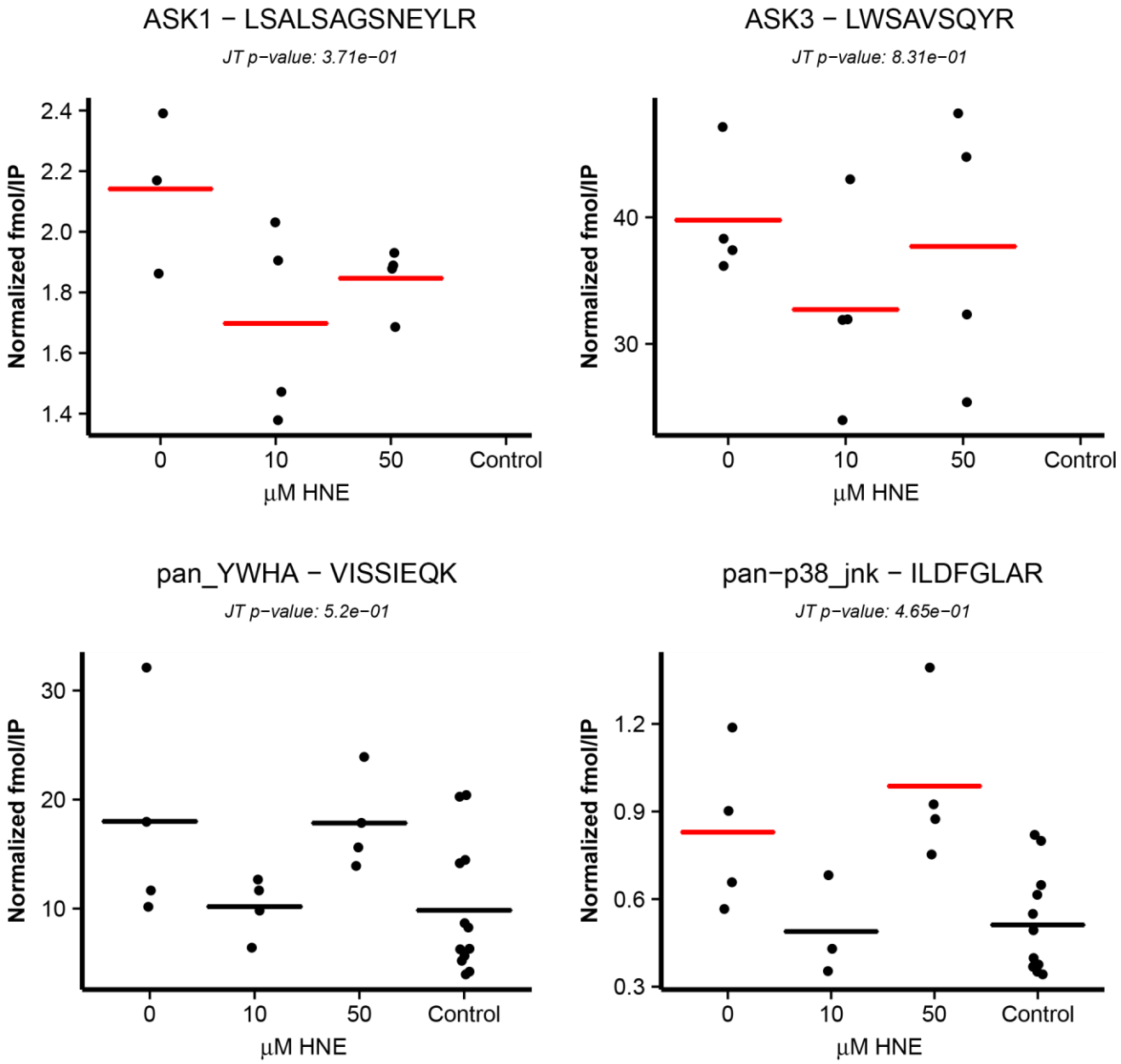


ASK3 IPs

**Figure A-9.**

C

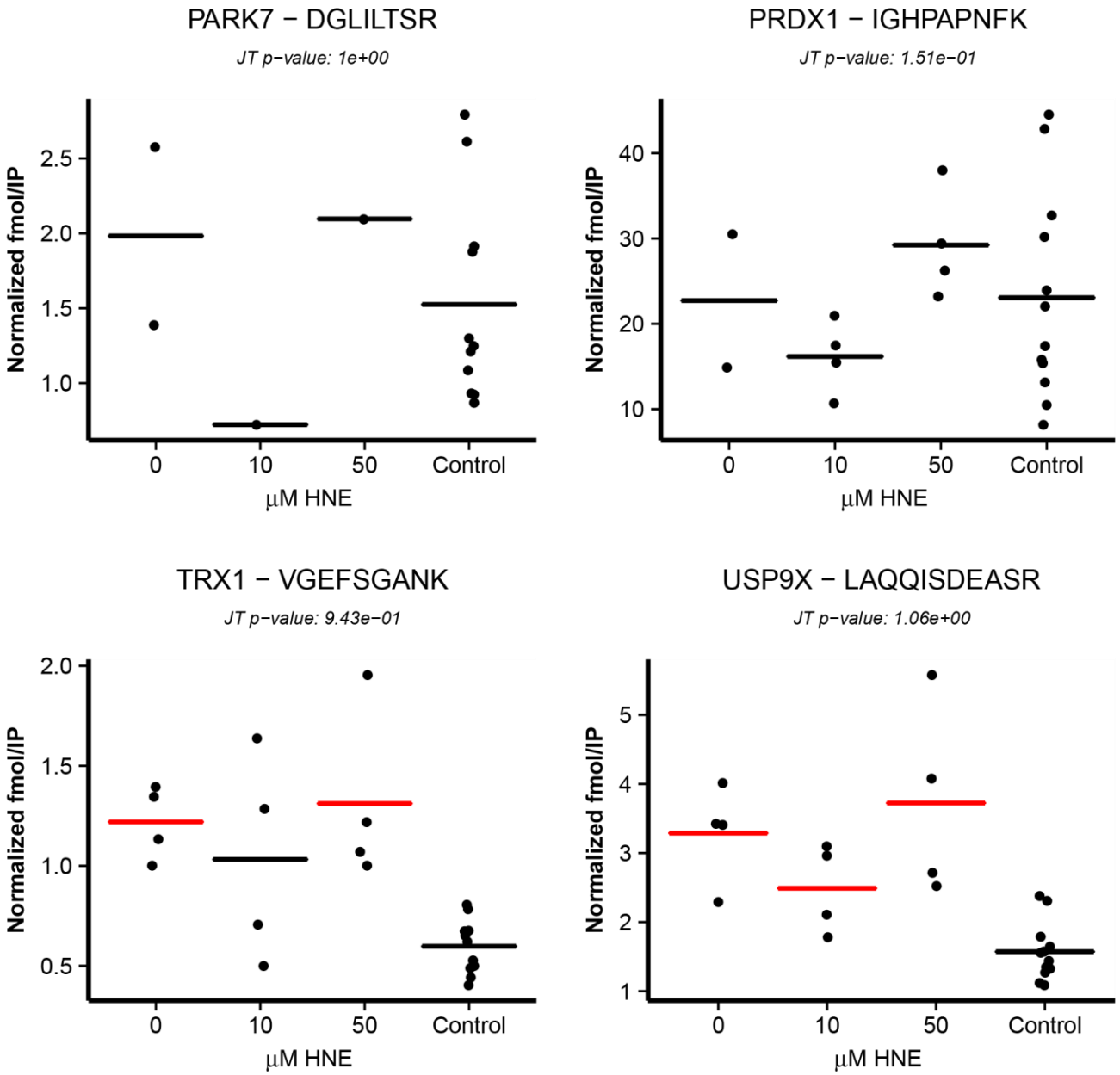
PARK7 − DGLILTSR
JT p−value: 1e+00
PRDX1 − IGHPAPNFK
JT p−value: 1.51e−01
TRX1 − VGEFSGANK
JT p−value: 9.43e−01
USP9X − LAQQISDEASR
JT p−value: 1.06e+00
Normalized fmol/IP
µM HNE
0
10
50
Control
ASK3 IPs

**Figure A-9.**

**D**

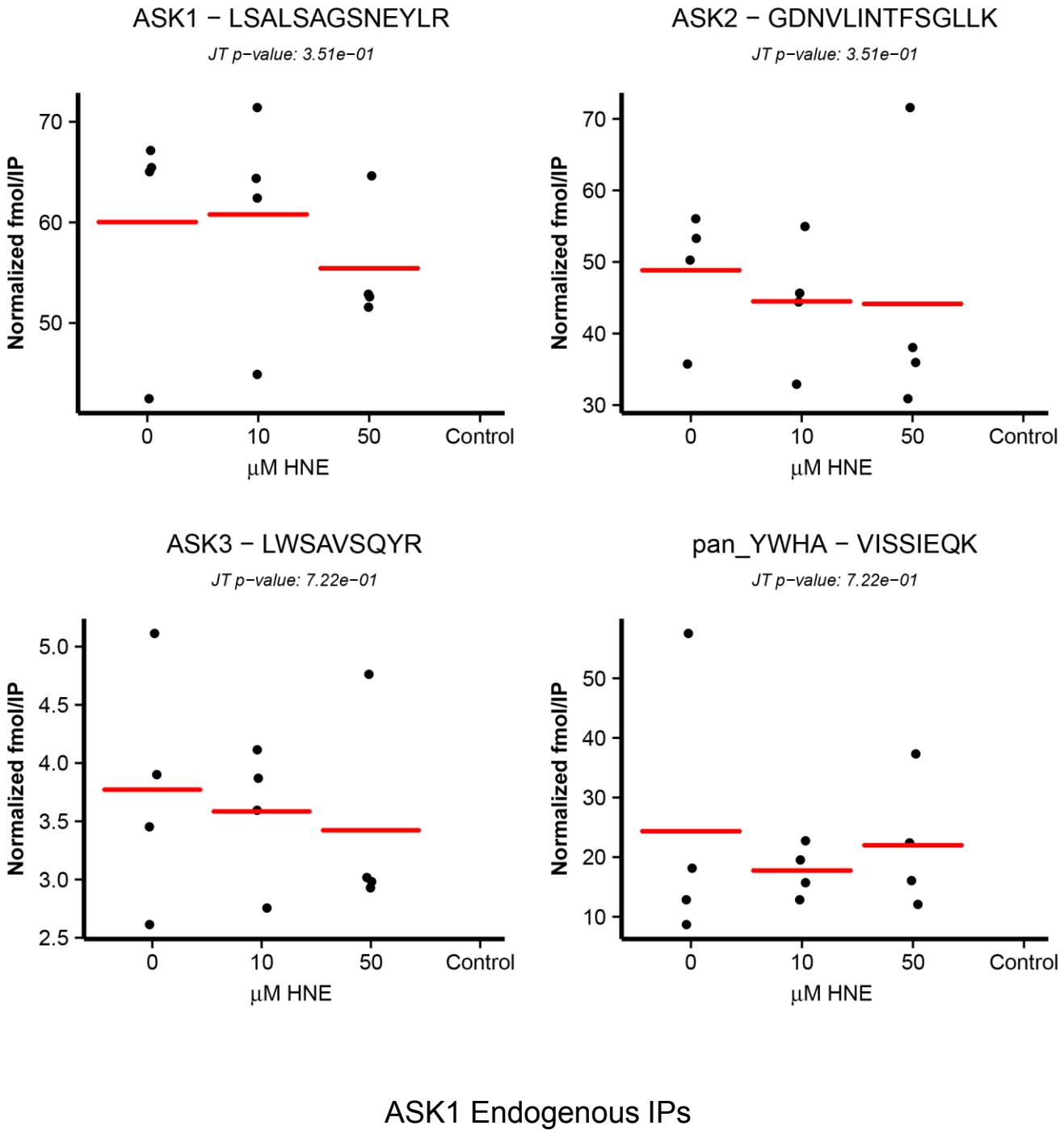
ASK1 − LSALSAGSNEYLR
JT p−value: 3.51e−01
ASK2 − GDNVLINTFSGLLK
JT p−value: 3.51e−01
ASK3 − LWSAVSQYR
JT p−value: 7.22e−01
pan_YWHA − VISSIEQK
JT p−value: 7.22e−01
Normalized fmol/IP
µM HNE
0
10
50
Control
ASK1 Endogenous IPs

**Figure A-9.**

**D**

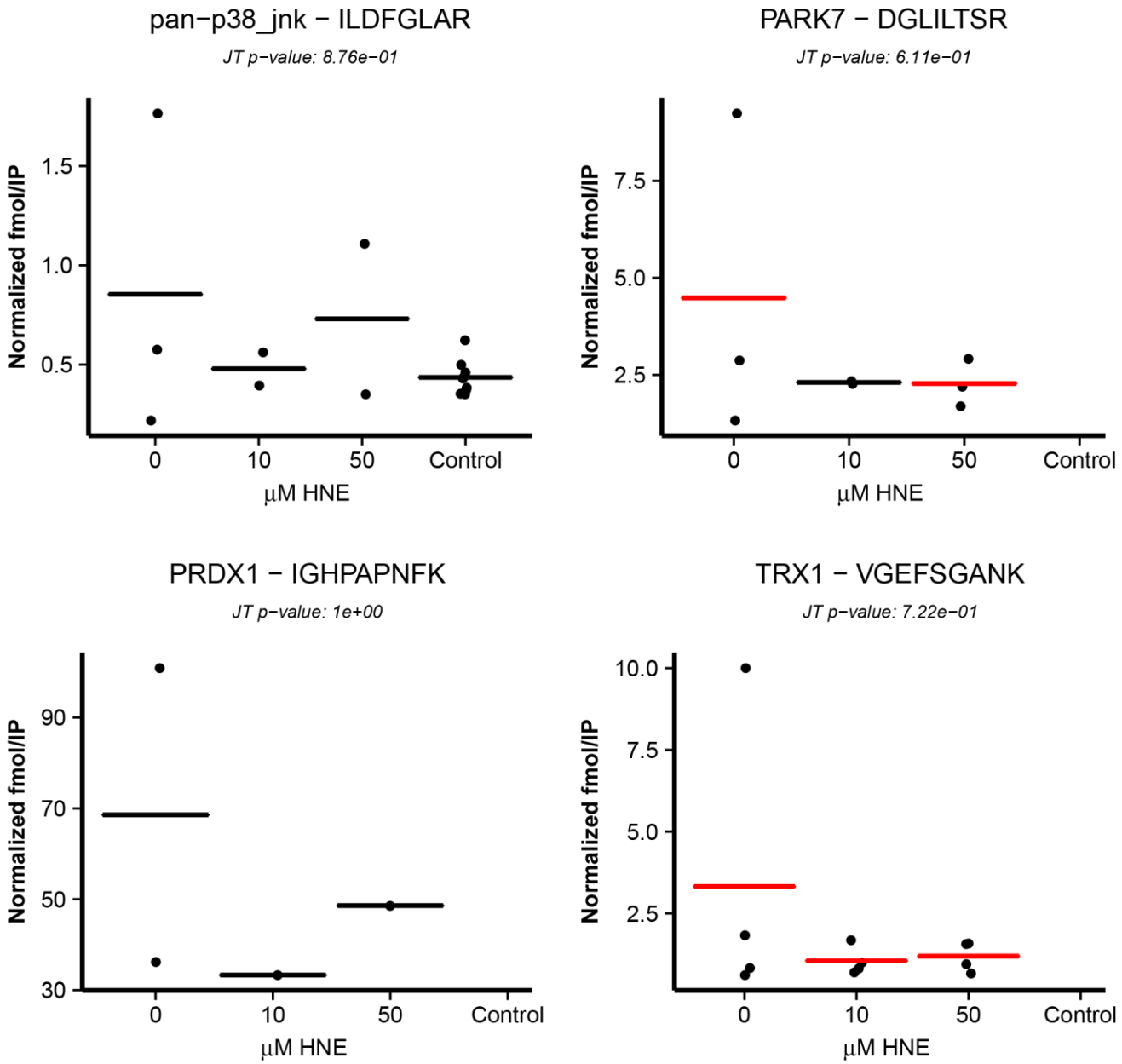
pan−p38_jnk − ILDFGLAR
JT p−value: 8.76e−01
PARK7 − DGLILTSR
JT p−value: 6.11e−01
PRDX1 − IGHPAPNFK
JT p−value: 1e+00
TRX1 − VGEFSGANK
JT p−value: 7.22e−01
Normalized fmol/IP
μM HNE
0
10
50
Control
ASK1 Endogenous IPs

**Figure A-9.**

**D**

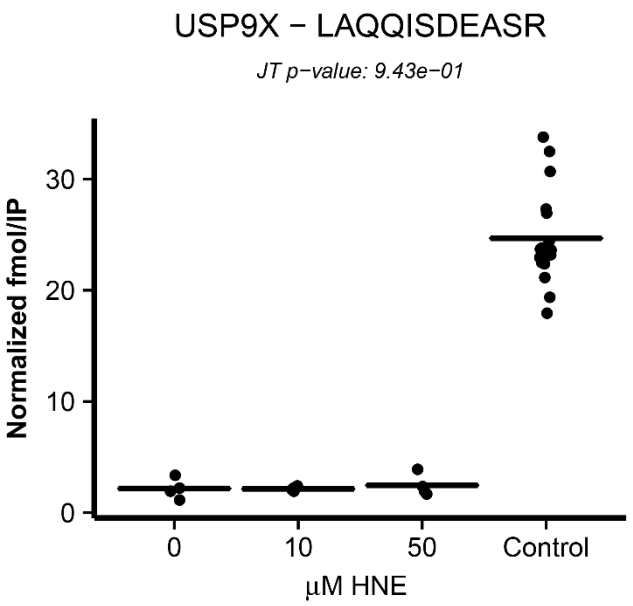


ASK1 Endogenous IPs

**Figure A-9.**

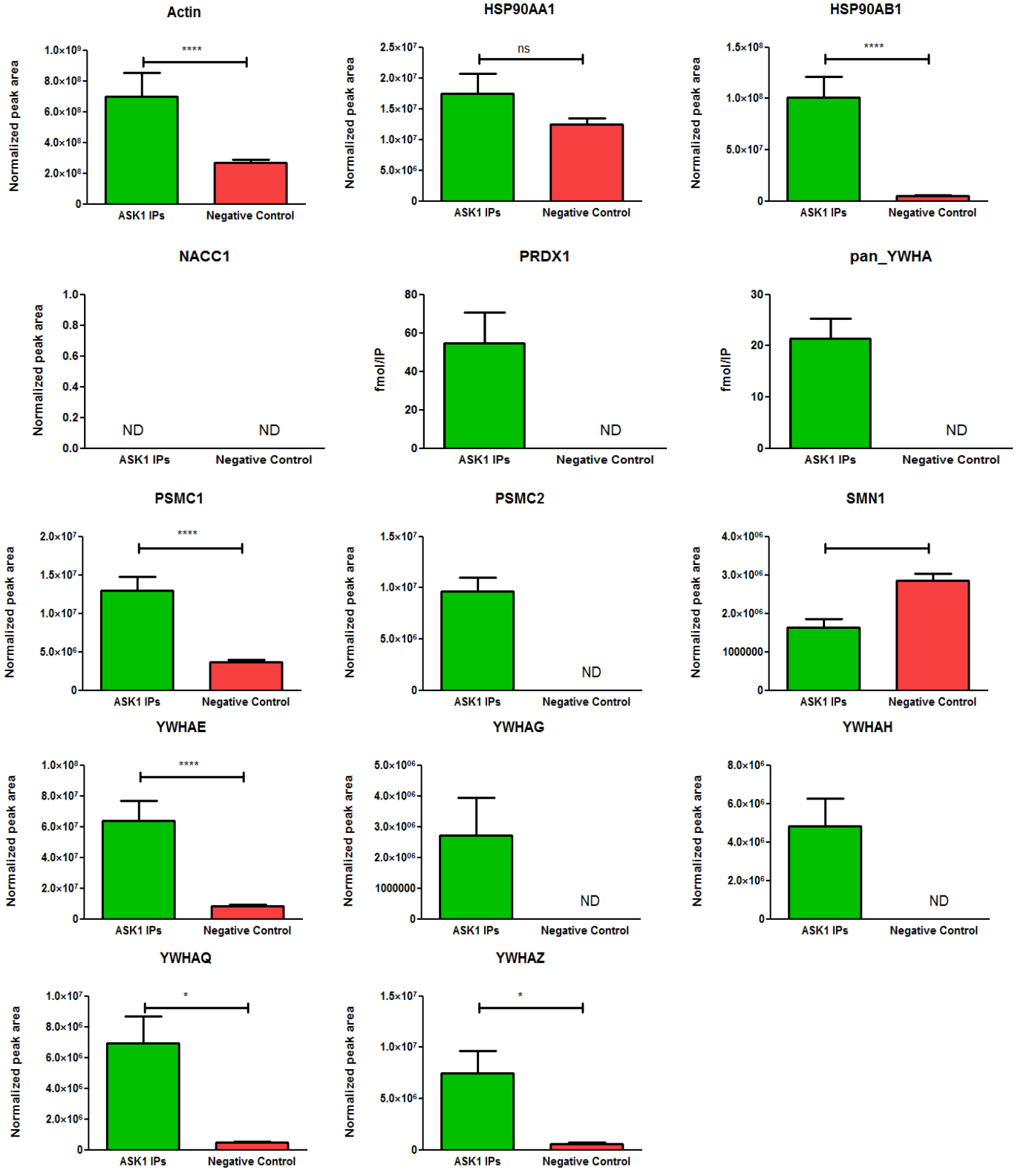


**Figure A-10.** Enrichment of dynamic ASK1-interacting proteins in HEK-293 cells. The 14 proteins that were identified as dynamic interactors in the ASK1-TAG cell line were examined in the context of ASK1 endogenous expression to determine if they were enriched in the ASK1 IPs compared to the negative control IPs. ND = not detected.

A

## Size Exclusion Chromatography methods

| | This study | Noguchi *et. al.* |
|---|---|---|
| SEC Buffer | 50mM HEPES pH 7.5<br>10mM KCl<br>150mM NaCl<br>1mM EDTA<br>1mM EGTA<br>1.5mM $MgCl_2$<br>10% glycerol<br>0.1% CHAPS<br>0.01% Brij35 | 50mM HEPES-KOH pH 7.5<br>10mM KCl<br>150mM NaCl<br>1mM EDTA<br>1mM EGTA<br>1.5mM $MgCl_2$<br>10% glycerol<br>0.1% CHAPS<br>0.01% Brij35 |
| Lysis method | $5x10^7$ cells/mL were lysed with a glass Dounce homogenizer in SEC buffer supplemented with 1mM DTT, and 1X Halt Protease & Phosphatase inhibitor. | $5x10^7$ cells/mL were lysed with a glass Dounce homogenizer in SEC buffer supplemented with 1mM DTT, 1mM phenymethylsulfonyl fluoride, and 5 ug/mL aprotinin. |
| Spin processing | The lysate was centrifuged at 20,000g for 30 minutes for clarification prior to SEC. The resulting supernatant was frozen at -80°C | The lysate was centrifuged at 10,000g for 10 minutes. The resulting supernatant was further centrifuged at 105,000g for 90 minutes. This supernatant was frozen at -135°C. |
| SEC method | The stored lysate was loaded onto a Superose6 10/300 GL column pre-equilibrated with the SEC buffer. Proteins were eluted isocratically at 0.3mL/min and collected in 0.6mL fractions. | The stored lysate was loaded onto a Superose6 10/300 GL column pre-equilibrated with the SEC buffer. Proteins were eluted isocratically at 0.3mL/min and collected in 0.5mL fractions. |
| Protein isolation | ASK signalosome complexes were isolated via immunopurification with anti-HA beads. | Each fraction was precipitated using acetone/ethanol (1:4) |
| Amount used for subsequent assays | Samples from 2 column runs were used for Western analysis. Samples from 6 column runs were used for PRM analysis. | Samples from 1 or 4 column runs were pooled and analyzed by Western |

**Figure A-11**. Size-exclusion fractionation of intact ASK1 complexes. (A) Methods comparison for the SEC assays performed in this study and Noguchi *et. al.* (B & C) Treatment of ASK1-TAG cells with ethanol (B) and 50μM HNE (C) yields similar distributions of ASK1 complexes with no shift to a higher molecular weight observed upon activation by HNE. (D) LRP-PRM analyses of ASK1, ASK2, and ASK3 in the SEC fractionated samples confirm the western results and show no change in complex localization upon activation by HNE.

**B**

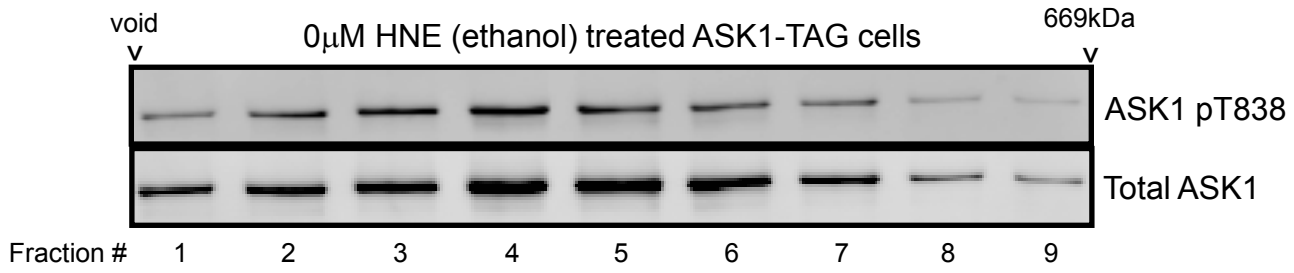


**C**

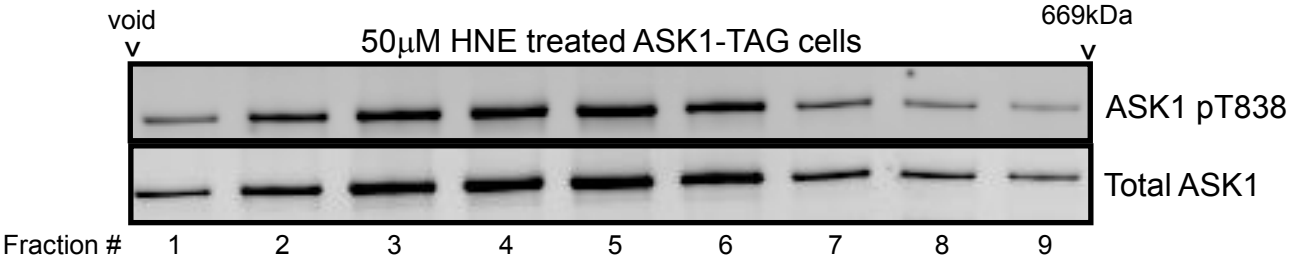


**Figure A-11.**

**D**

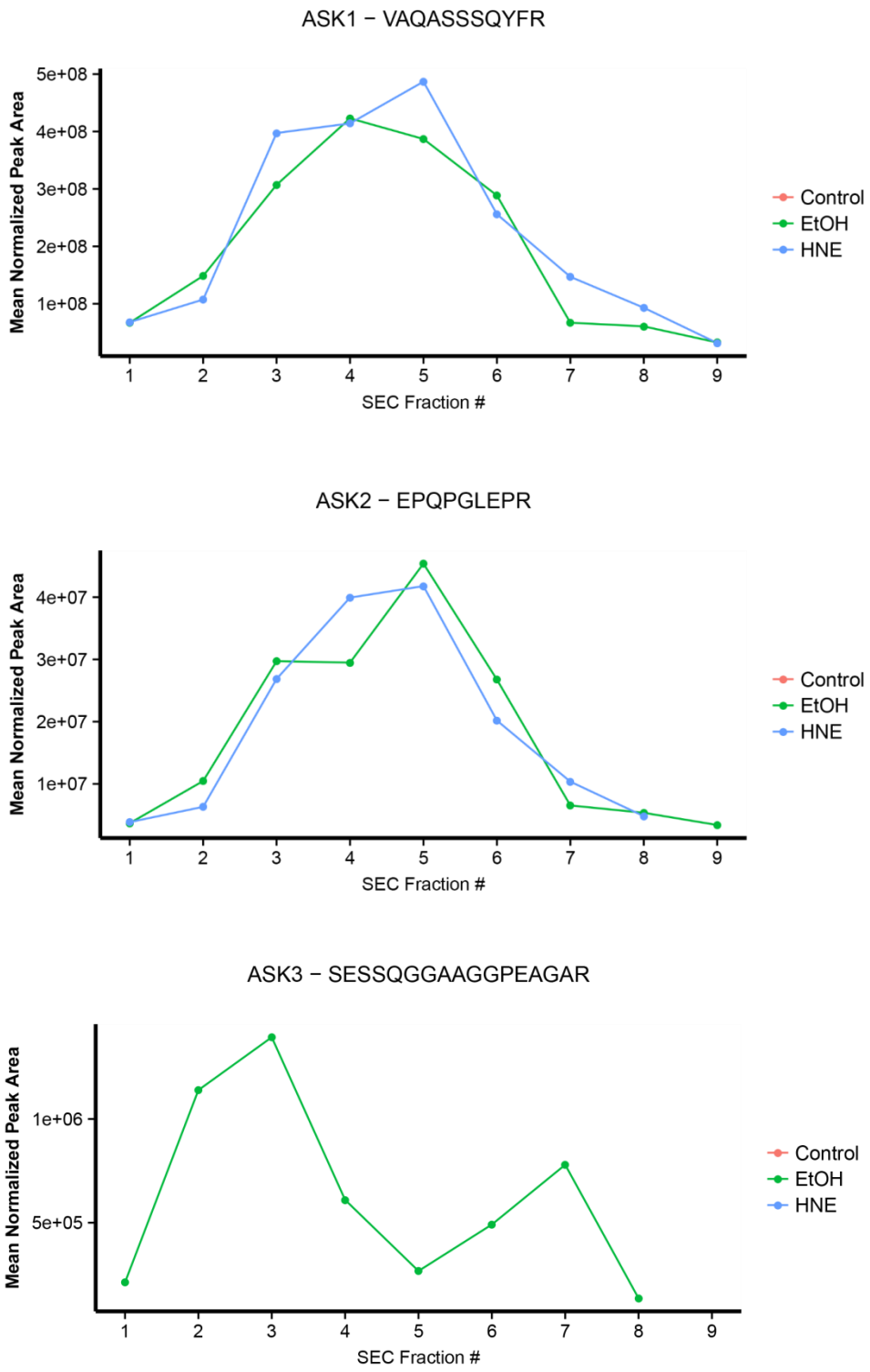
ASK1 − VAQASSSQYFR
Mean Normalized Peak Area
5e+08
4e+08
3e+08
2e+08
1e+08
1
2
3
4
5
6
7
8
9
SEC Fraction #
Control
EtOH
HNE
ASK2 − EPQPGLEPR
Mean Normalized Peak Area
4e+07
3e+07
2e+07
1e+07
SEC Fraction #
Control
EtOH
HNE
ASK3 − SESSQGGAAGGPEAGAR
Mean Normalized Peak Area
1e+06
5e+05
SEC Fraction #
Control
EtOH
HNE

**Figure A-11.**

APPENDIX B

Data to Chapter III:

# DYNAMIC PHOSPHORYLATION OF APOPTOSIS SIGNAL REGULATING KINASE 1 (ASK1) IN RESPONSE TO OXIDATION AND ELECTROPHILIC ADDUCTION

Figure B-1. Annotated MS/MS spectra for each putative phosphopeptide. Where possible, the phosphorylation was localized to a single residue. When this was not possible with the data at hand, the phosphorylation was localized to the fewest possible sites with sufficient explanatory evidence. Each page lists the peptide sequence, site(s) of modification, MS1 isolation window, precursor mass accuracy, annotated MS/MS spectrum, and a table summarizing the identified peaks for the MS/MS spectrum.

# $^{79}$GRGS[79.96633]SVGGGSR$^{89}$

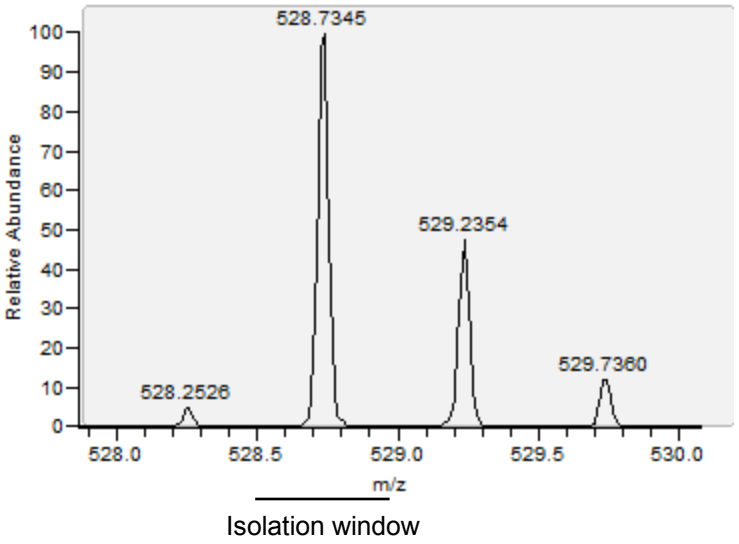


**Ser 82/83**

Precursor m/z: 528.7345
Precursor mass error: 5.20 ppm

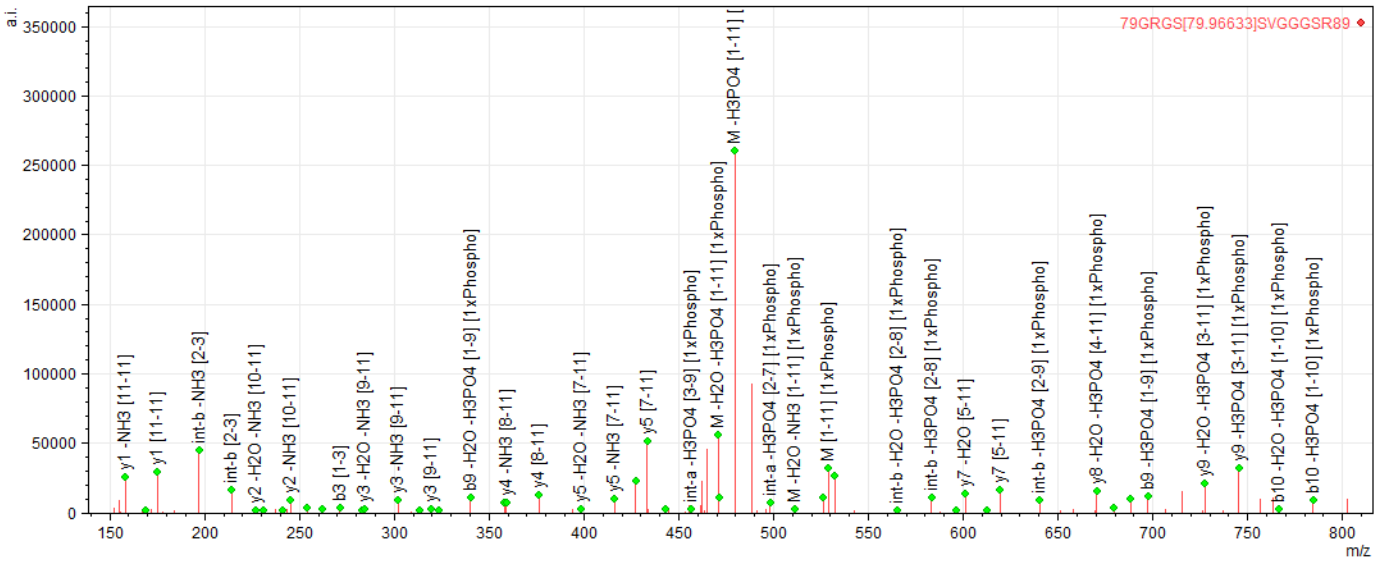


| parameter | value |
|---|---|
| Number of peaks searched | 90 |
| Number of fragments searched | 756 |
| Number of fragments matched | 63 |
| Intensity matched | 74 % |
| Sequence length | 11 |
| Ion serie matches for "b" | 2, 3 |
| Ion serie matches for "b -H2O" | |
| Ion serie matches for "b -H2O -H3PO4" | 7, 7, 9, 9, 10 |
| Ion serie matches for "b -H2O -NH3" | |
| Ion serie matches for "b -H3PO4" | 4, 5, 6, 7, 8, 9, 10 |
| Ion serie matches for "b -NH3" | 2, 3 |
| Ion serie matches for "b -NH3 -H3PO4" | 4 |
| Ion serie matches for "y" | 1, 2, 3, 4, 5, 6, 7 |
| Ion serie matches for "y -H2O" | 4, 7 |
| Ion serie matches for "y -H2O -H3PO4" | 8, 9 |
| Ion serie matches for "y -H2O -NH3" | 2, 3, 5 |
| Ion serie matches for "y -H3PO4" | 8, 9 |
| Ion serie matches for "y -NH3" | 1, 2, 3, 4, 5 |
| Ion serie matches for "y -NH3 -H3PO4" | 10 |



Figure B-1.

# $^{79}$GRGSS[79.96633]VGGGSRR$^{90}$

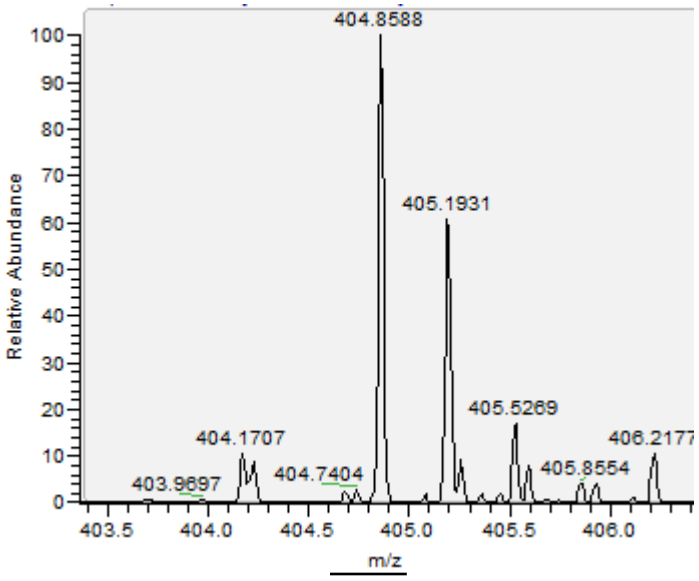


**Ser 82/83**

Precursor m/z: 404.8588
Precursor mass error: -2.06 ppm

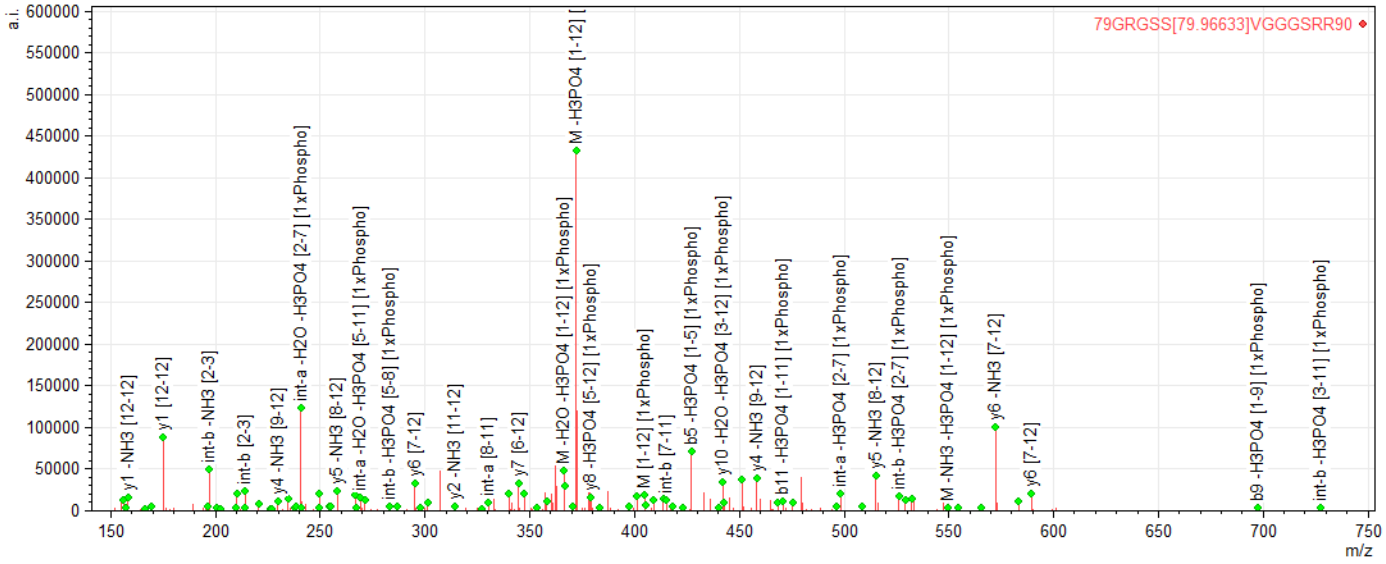


| parameter | value |
|---|---|
| Number of peaks searched | 186 |
| Number of fragments searched | 1485 |
| Number of fragments matched | 114 |
| Intensity matched | 64 % |
| Sequence length | 12 |
| Ion serie matches for "b" | 2, 3, 4 |
| Ion serie matches for "b -H2O" | 4 |
| Ion serie matches for "b -H2O -H3PO4" | 5, 6, 6, 7, 7, 9, 9 |
| Ion serie matches for "b -H2O -NH3" | |
| Ion serie matches for "b -H3PO4" | 5, 6, 7, 9, 11 |
| Ion serie matches for "b -NH3" | 2, 3, 8 |
| Ion serie matches for "b -NH3 -H3PO4" | |
| Ion serie matches for "y" | 1, 2, 3, 3, 4, 4, 5, 5, 6, 6, 7 |
| Ion serie matches for "y -H2O" | 3 |
| Ion serie matches for "y -H2O -H3PO4" | 9, 10 |
| Ion serie matches for "y -H2O -NH3" | 3, 4, 4, 5, 6, 7 |
| Ion serie matches for "y -H3PO4" | 8, 9, 10, 10, 11, 11 |
| Ion serie matches for "y -NH3" | 1, 2, 3, 4, 4, 5, 5, 6, 6 |
| Ion serie matches for "y -NH3 -H3PO4" | 8, 10, 11 |



Figure B-1.

# $^{81}$GS[79.96633]SVGGGSR$^{89}$

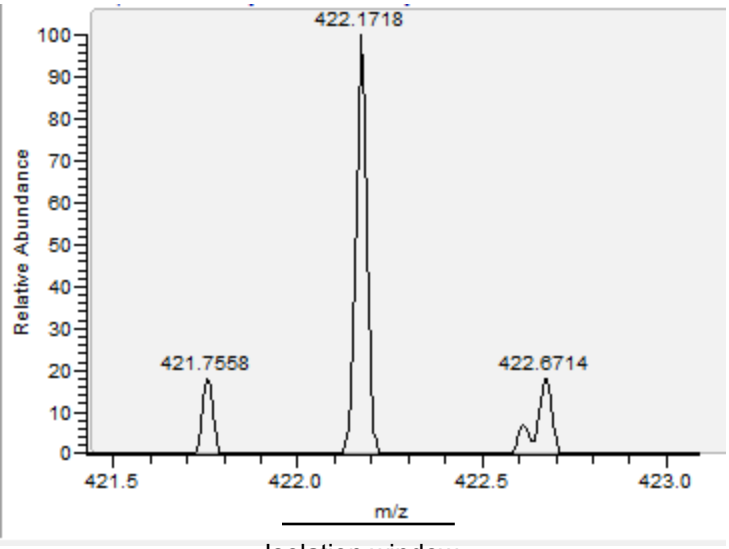


Isolation window

**Ser 82/83**

Precursor m/z: 422.1718
Precursor mass error: -0.83 ppm

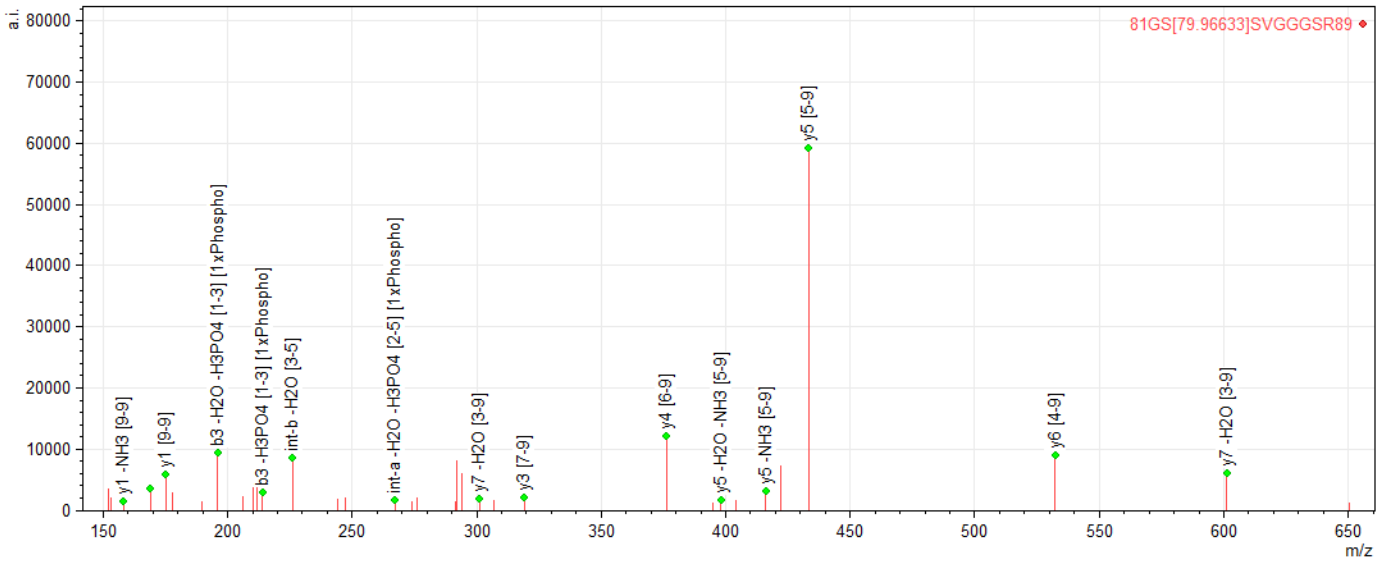


| parameter | value |
|---|---|
| Number of peaks searched | 39 |
| Number of fragments searched | 356 |
| Number of fragments matched | 16 |
| Intensity matched | 62 % |
| Sequence length | 9 |
| Ion serie matches for "b" | |
| Ion serie matches for "b -H2O" | |
| Ion serie matches for "b -H2O -H3PO4" | 3 |
| Ion serie matches for "b -H3PO4" | 3 |
| Ion serie matches for "y" | 1, 3, 4, 5, 6 |
| Ion serie matches for "y -H2O" | 3, 7, 7 |
| Ion serie matches for "y -H2O -H3PO4" | |
| Ion serie matches for "y -H2O -NH3" | 5 |
| Ion serie matches for "y -H3PO4" | |
| Ion serie matches for "y -NH3" | 1, 5 |
| Ion serie matches for "y -NH3 -H3PO4" | |



Figure B-1.

# $^{81}$GS[79.96633]SVGGGSRR$^{90}$

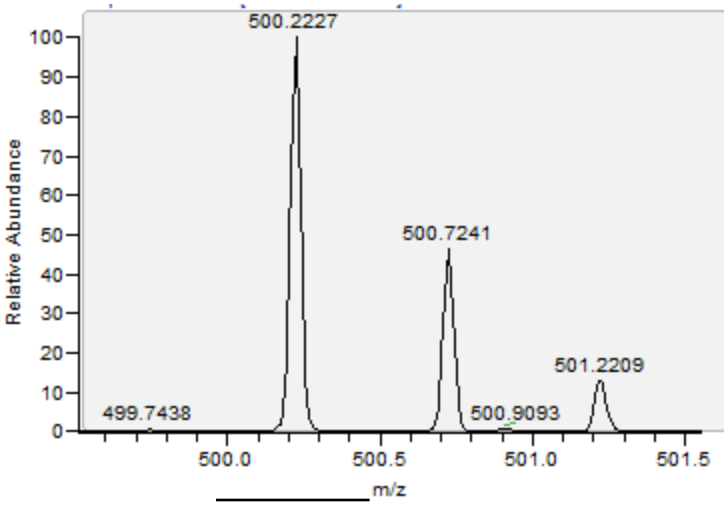


Isolation window

**Ser 82/83**

Precursor m/z: 500.2227
Precursor mass error: -1.40 ppm

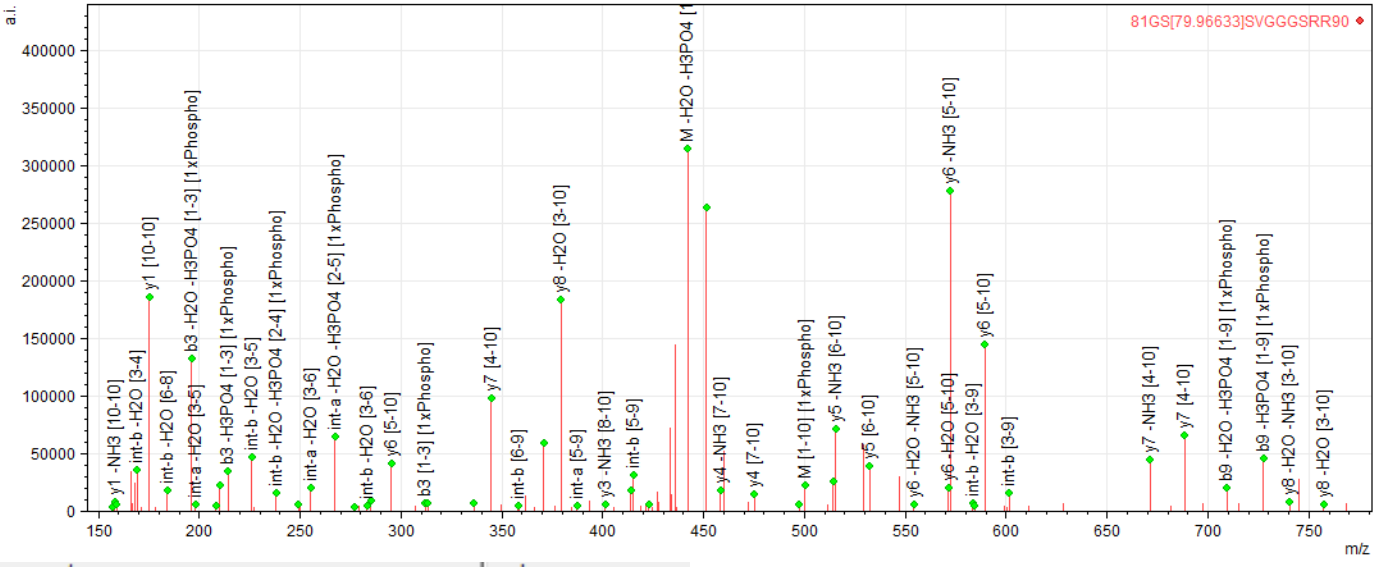


| parameter | value |
|---|---|
| Number of peaks searched | 97 |
| Number of fragments searched | 502 |
| Number of fragments matched | 58 |
| Intensity matched | 79 % |
| Sequence length | 10 |
| Ion serie matches for "b" | 3 |
| Ion serie matches for "b -H2O" | |
| Ion serie matches for "b -H2O -H3PO4" | 3, 8, 9 |
| Ion serie matches for "b -H2O -NH3" | |
| Ion serie matches for "b -H3PO4" | 3, 4, 9 |
| Ion serie matches for "b -NH3" | |
| Ion serie matches for "b -NH3 -H3PO4" | |
| Ion serie matches for "y" | 1, 4, 5, 6, 6, 7, 7 |
| Ion serie matches for "y -H2O" | 5, 6, 8, 8 |
| Ion serie matches for "y -H2O -H3PO4" | 9 |
| Ion serie matches for "y -H2O -NH3" | 5, 5, 6, 8, 8 |
| Ion serie matches for "y -H3PO4" | 9 |
| Ion serie matches for "y -NH3" | 1, 3, 4, 5, 6, 7, 7 |
| Ion serie matches for "y -NH3 -H3PO4" | |



Figure B-1.

# $^{135}$LDFGET[79.96633]TVLDR$^{145}$

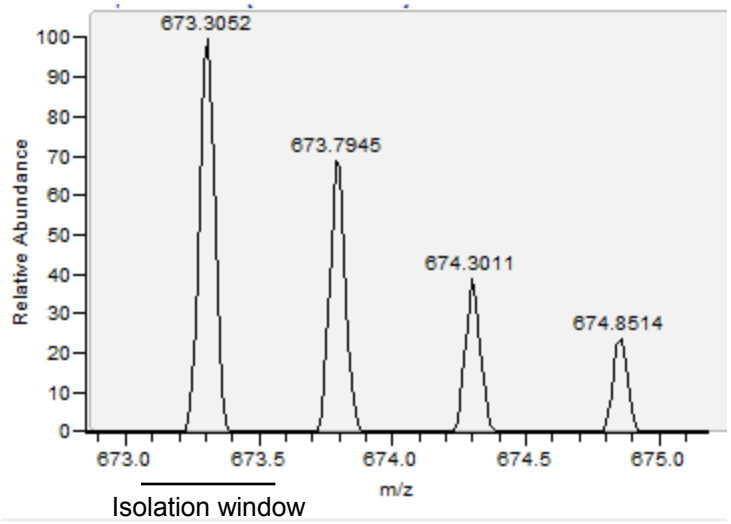


**Thr 140/141**

Precursor m/z: 673.3052
Precursor mass error: 0.30 ppm

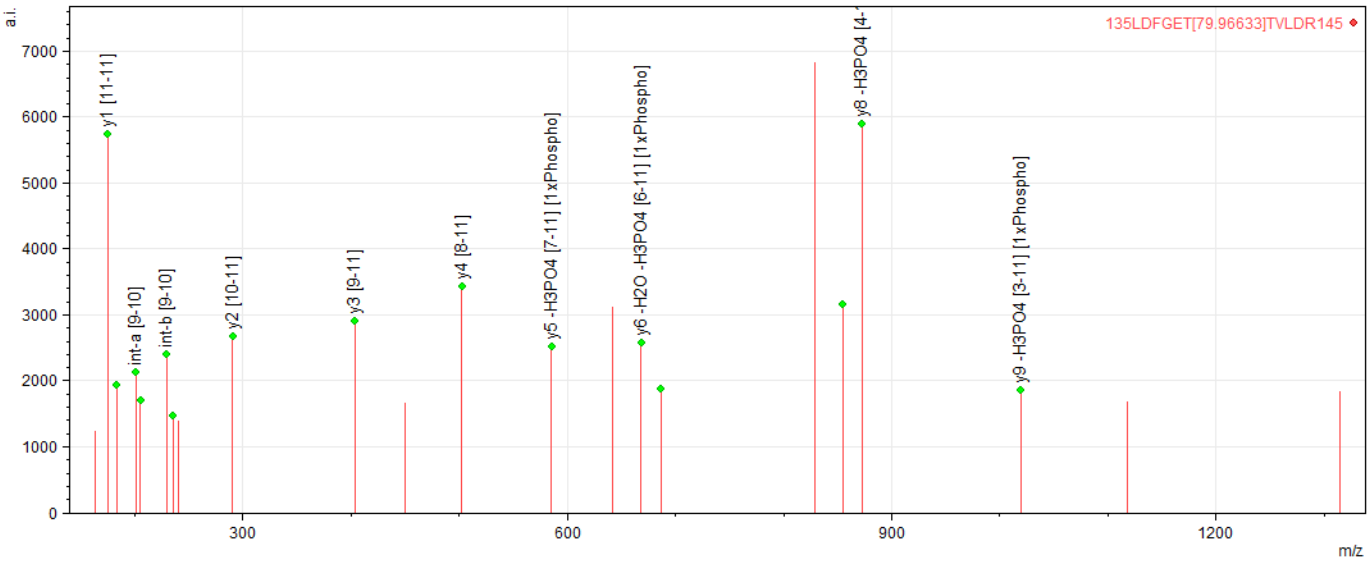


| parameter | value |
|---|---|
| Number of peaks searched | 22 |
| Number of fragments searched | 684 |
| Number of fragments matched | 19 |
| Intensity matched | 70 % |
| Sequence length | 11 |
| Ion serie matches for "b" | 2 |
| Ion serie matches for "b -H2O" | |
| Ion serie matches for "b -H2O -H3PO4" | |
| Ion serie matches for "b -H3PO4" | |
| Ion serie matches for "y" | 1, 2, 3, 4 |
| Ion serie matches for "y -H2O" | 5 |
| Ion serie matches for "y -H2O -H3PO4" | 6, 8 |
| Ion serie matches for "y -H2O -NH3" | |
| Ion serie matches for "y -H3PO4" | 6, 8, 9 |
| Ion serie matches for "y -NH3" | |
| Ion serie matches for "y -NH3 -H3PO4" | |



Figure B-1.

# $^{263}$VAQASS[79.96633]SQYFR$^{273}$

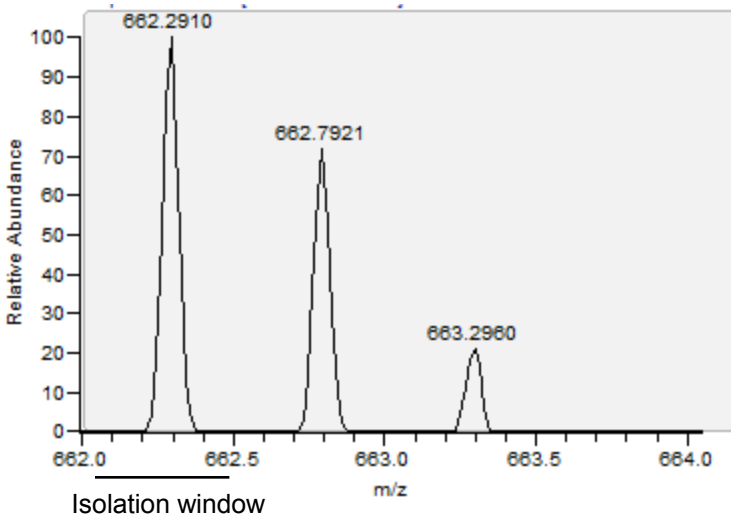


**Ser 268/269**

Precursor m/z: 662.2910
Precursor mass error: -1.36 ppm

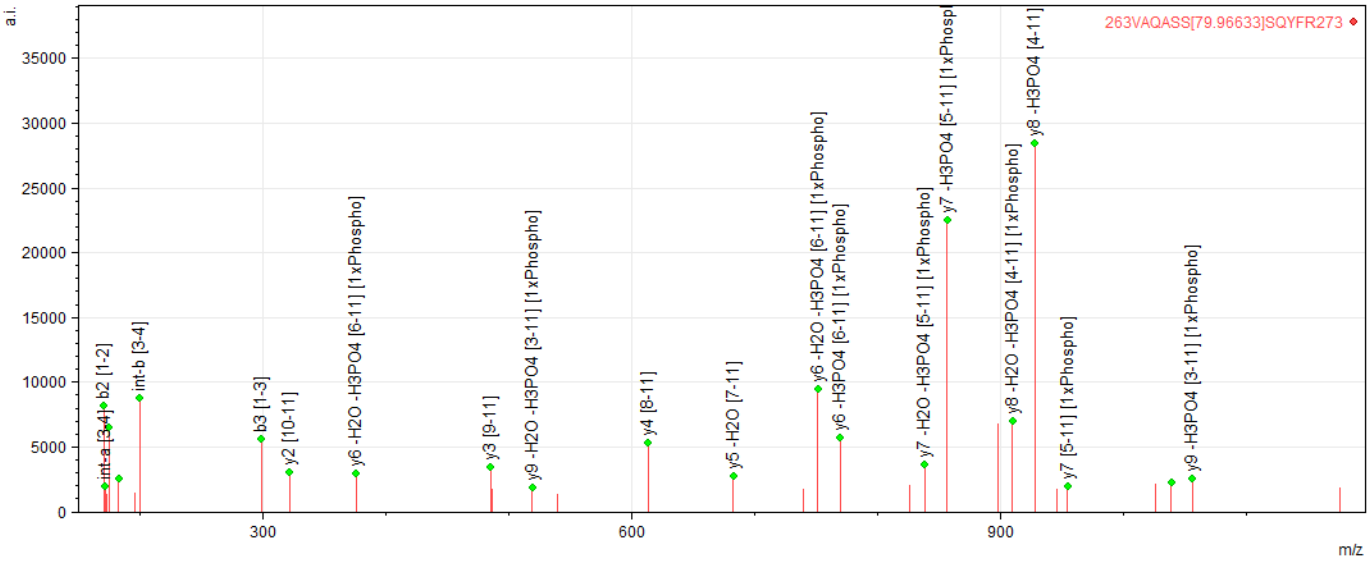


| parameter | value |
|---|---|
| Number of peaks searched | 31 |
| Number of fragments searched | 976 |
| Number of fragments matched | 27 |
| Intensity matched | 86 % |
| Sequence length | 11 |
| Ion serie matches for "b" | 2, 3 |
| Ion serie matches for "b -H2O" | |
| Ion serie matches for "b -H2O -H3PO4" | |
| Ion serie matches for "b -H2O -NH3" | |
| Ion serie matches for "b -H3PO4" | |
| Ion serie matches for "b -NH3" | |
| Ion serie matches for "b -NH3 -H3PO4" | |
| Ion serie matches for "y" | 1, 2, 3, 4, 7 |
| Ion serie matches for "y -H2O" | 5 |
| Ion serie matches for "y -H2O -H3PO4" | 6, 6, 7, 8, 9 |
| Ion serie matches for "y -H2O -NH3" | |
| Ion serie matches for "y -H3PO4" | 6, 7, 8, 9 |
| Ion serie matches for "y -NH3" | |
| Ion serie matches for "y -NH3 -H3PO4" | 9 |



Figure B-1.

# $^{353}$FHY[79.96633]AFALNR$^{361}$

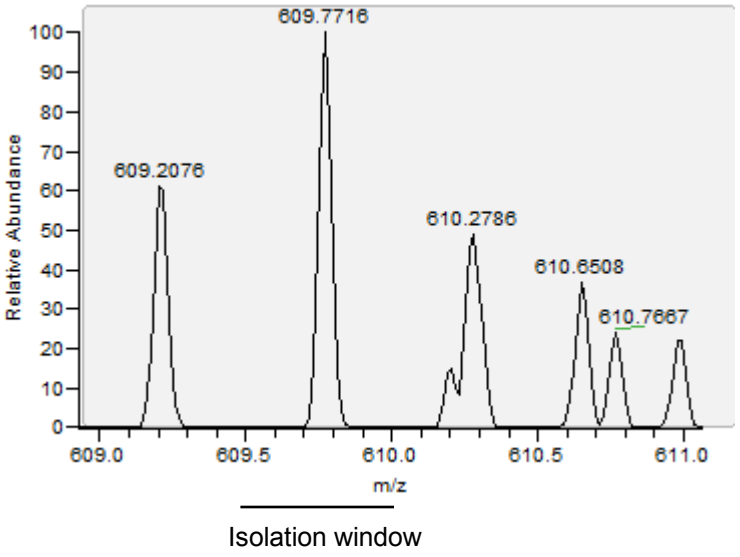


**Tyr 355**

Precursor m/z: 609.7716
Precursor mass error: 7.87 ppm

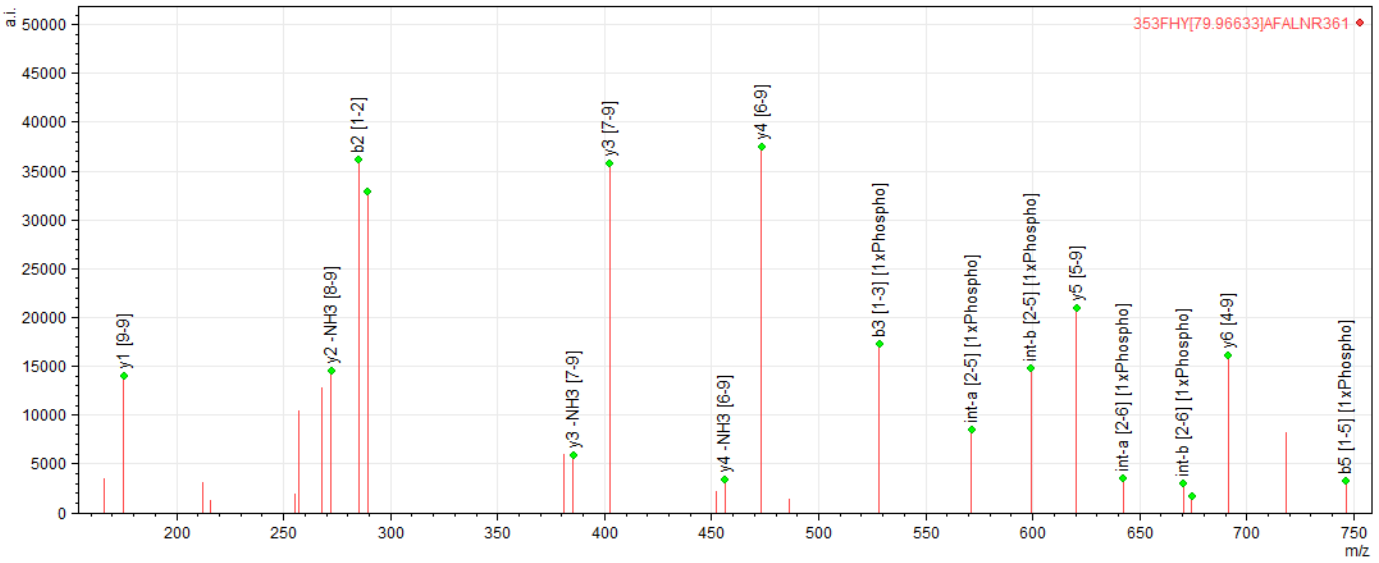


| parameter | value |
|---|---|
| Number of peaks searched | 27 |
| Number of fragments searched | 182 |
| Number of fragments matched | 18 |
| Intensity matched | 84 % |
| Sequence length | 9 |
| Ion serie matches for "b" | 2, 3, 4, 5 |
| Ion serie matches for "b -NH3" | |
| Ion serie matches for "y" | 1, 2, 3, 4, 5, 6 |
| Ion serie matches for "y -NH3" | 2, 3, 4, 6 |



Figure B-1.

# $^{944}$KKKT[79.96633]QPKLSALSAGSNEYLR$^{963}$

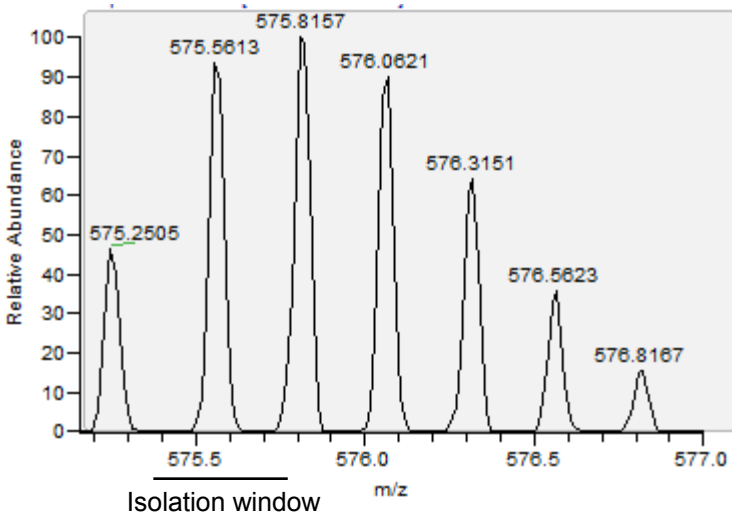


**Thr 947/S952**

Precursor m/z: 575.5613
Precursor mass error: -0.52 ppm

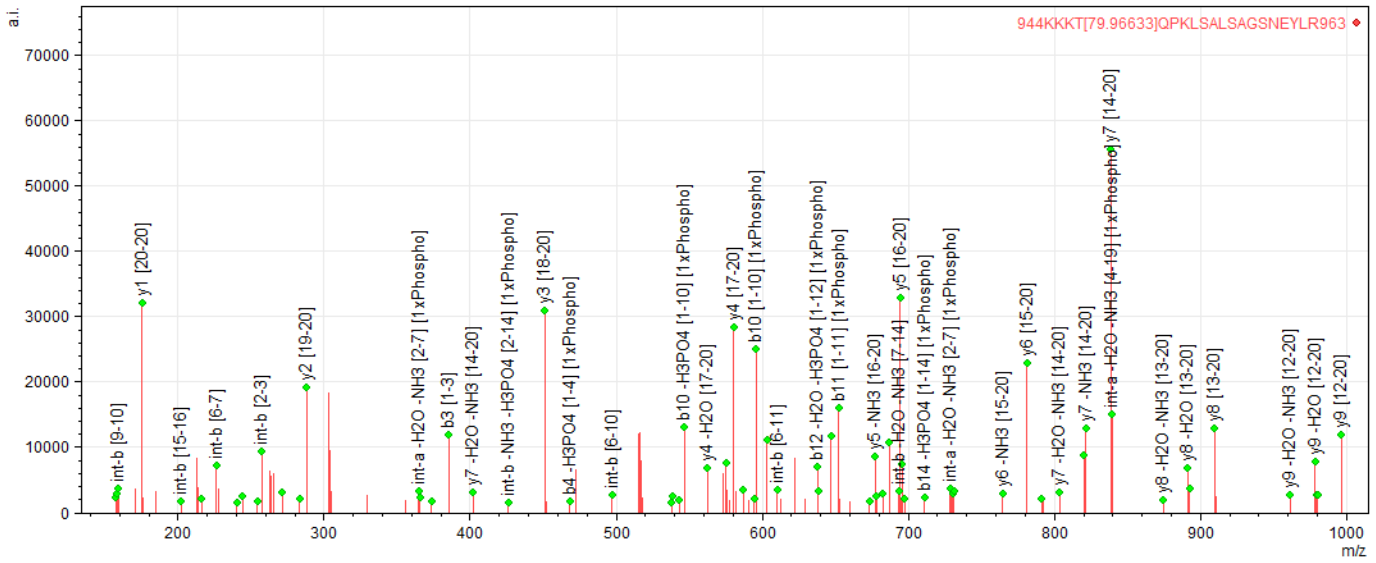


| parameter | value |
|---|---|
| Number of peaks searched | 108 |
| Number of fragments searched | 6332 |
| Number of fragments matched | 100 |
| Intensity matched | 76 % |
| Sequence length | 20 |
| Ion serie matches for "b" | 2, 3, 5, 10, 11, 12, 13 |
| Ion serie matches for "b -H2O" | 10, 12 |
| Ion serie matches for "b -H2O -H3PO4" | 10, 11, 12, 13, 15 |
| Ion serie matches for "b -H2O -NH3" | 12, 16 |
| Ion serie matches for "b -H3PO4" | 4, 10, 11, 12, 13, 14 |
| Ion serie matches for "b -NH3" | 2 |
| Ion serie matches for "b -NH3 -H3PO4" | 4, 10, 12 |
| Ion serie matches for "y" | 1, 2, 3, 4, 5, 6, 7, 8, 9 |
| Ion serie matches for "y -H2O" | 4, 7, 8, 9 |
| Ion serie matches for "y -H2O -H3PO4" | |
| Ion serie matches for "y -H2O -NH3" | 6, 7, 7, 8, 9 |
| Ion serie matches for "y -H3PO4" | |
| Ion serie matches for "y -NH3" | 1, 2, 5, 6, 7, 8, 9 |
| Ion serie matches for "y -NH3 -H3PO4" | |



Figure B-1.

# $^{945}$KKTQPKLS[79.96633]ALSAGSNEYLR$^{963}$

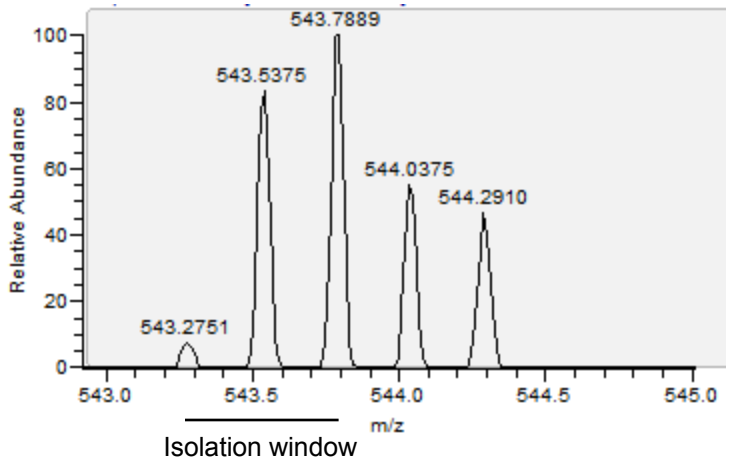


**Thr 947/S952**

Precursor m/z: 543.5375
Precursor mass error: -2.85 ppm

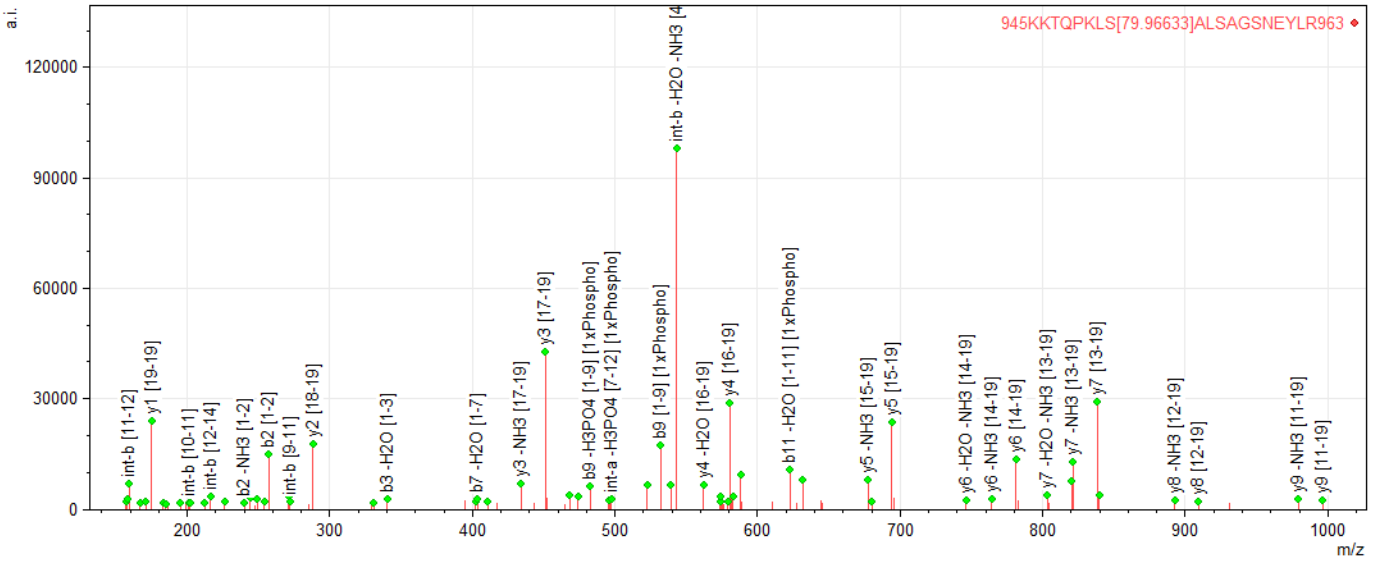


| parameter | value |
|---|---|
| Number of peaks searched | 93 |
| Number of fragments searched | 6352 |
| Number of fragments matched | 93 |
| Intensity matched | 89 % |
| Sequence length | 19 |
| Ion serie matches for "b" | 2, 8, 9, 10, 11 |
| Ion serie matches for "b -H2O" | 3, 4, 7, 9, 10, 11 |
| Ion serie matches for "b -H2O -H3PO4" | 11 |
| Ion serie matches for "b -H2O -NH3" | 4 |
| Ion serie matches for "b -H3PO4" | 9, 10, 11 |
| Ion serie matches for "b -NH3" | 2, 3 |
| Ion serie matches for "b -NH3 -H3PO4" | 9, 11 |
| Ion serie matches for "y" | 1, 2, 3, 4, 5, 6, 7, 8, 9 |
| Ion serie matches for "y -H2O" | 4, 7, 7 |
| Ion serie matches for "y -H2O -H3PO4" | |
| Ion serie matches for "y -H2O -NH3" | 6, 7, 7 |
| Ion serie matches for "y -H3PO4" | |
| Ion serie matches for "y -NH3" | 1, 2, 3, 5, 6, 7, 8, 9 |
| Ion serie matches for "y -NH3 -H3PO4" | |



Figure B-1.

# $^{951}$LSALS[79.96633]AGSNEYLR$^{963}$

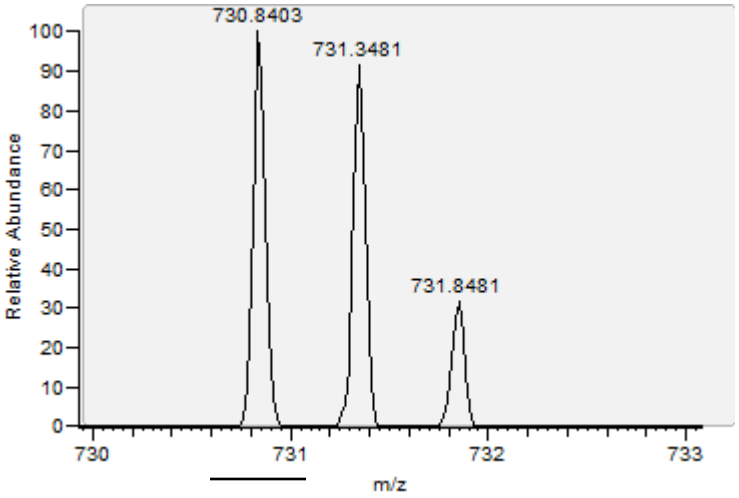


**Ser 955**

Precursor m/z: 730.8403
Precursor mass error: 3.28 ppm

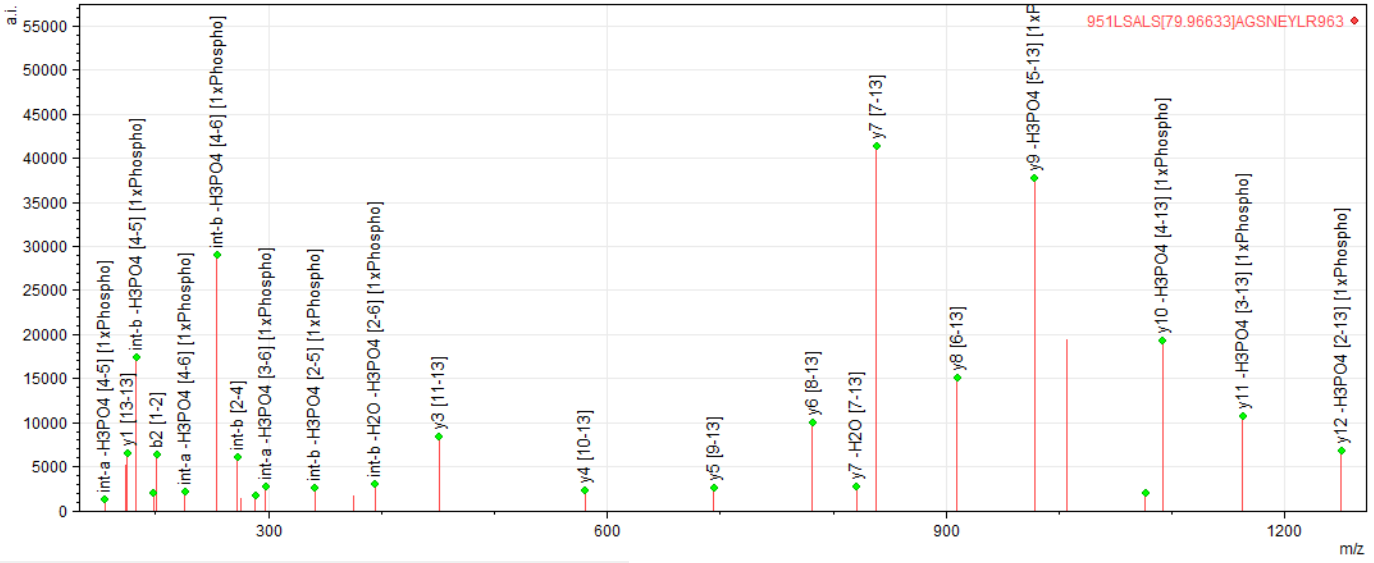


| parameter | value |
|---|---|
| Number of peaks searched | 28 |
| Number of fragments searched | 1250 |
| Number of fragments matched | 35 |
| Intensity matched | 90 % |
| Sequence length | 13 |
| Ion serie matches for "b" | 2, 3 |
| Ion serie matches for "b -H2O" | 2, 3 |
| Ion serie matches for "b -H2O -H3PO4" | 6 |
| Ion serie matches for "b -H2O -NH3" | |
| Ion serie matches for "b -H3PO4" | |
| Ion serie matches for "b -NH3" | |
| Ion serie matches for "b -NH3 -H3PO4" | |
| Ion serie matches for "y" | 1, 2, 3, 4, 5, 6, 7, 8, 9 |
| Ion serie matches for "y -H2O" | 7 |
| Ion serie matches for "y -H2O -H3PO4" | |
| Ion serie matches for "y -H2O -NH3" | |
| Ion serie matches for "y -H3PO4" | 9, 10, 11, 12 |
| Ion serie matches for "y -NH3" | |
| Ion serie matches for "y -NH3 -H3PO4" | |



Figure B-1.

# $^{951}$LSALSAGS[79.96633]NEYLR$^{963}$

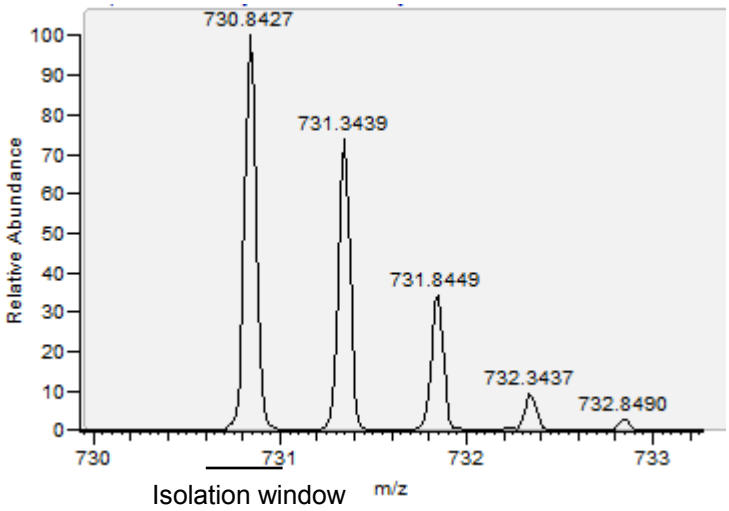


**Ser 958**

Precursor m/z: 730.8427
Precursor mass error: 0 ppm

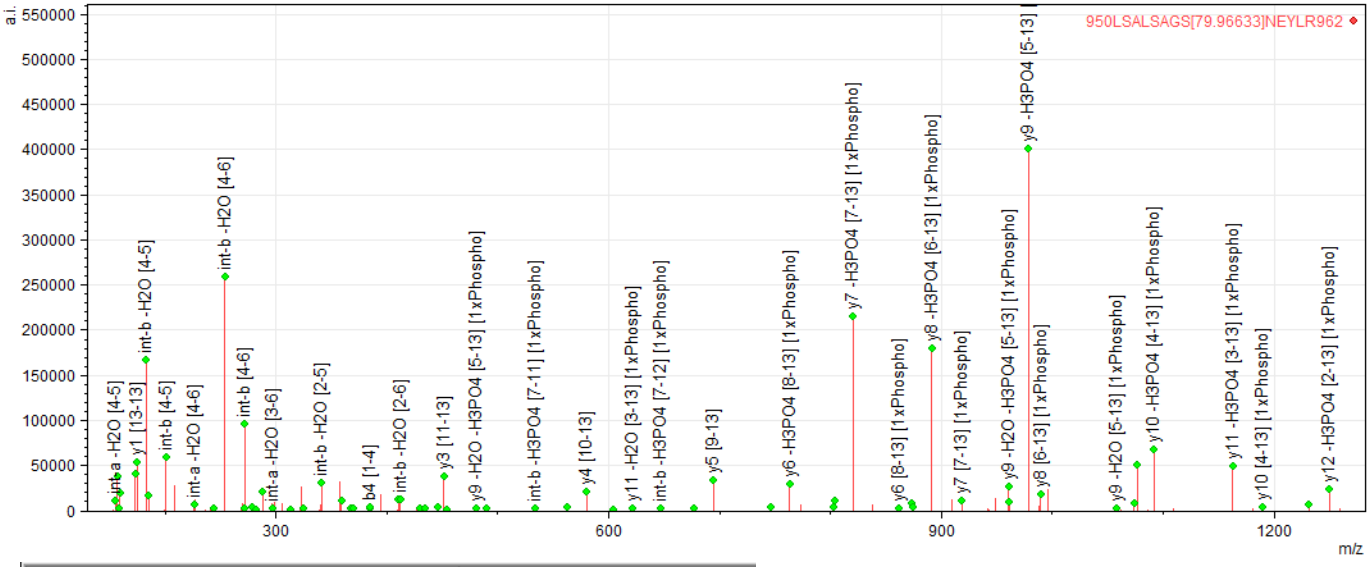


| parameter | value |
|---|---|
| Number of peaks searched | 104 |
| Number of fragments searched | 1328 |
| Number of fragments matched | 82 |
| Intensity matched | 88 % |
| Sequence length | 13 |
| Ion serie matches for "b" | 2, 3, 4, 6 |
| Ion serie matches for "b -H2O" | 2, 3, 4, 5 |
| Ion serie matches for "b -H2O -H3PO4" | |
| Ion serie matches for "b -H2O -NH3" | |
| Ion serie matches for "b -H3PO4" | |
| Ion serie matches for "b -NH3" | |
| Ion serie matches for "b -NH3 -H3PO4" | |
| Ion serie matches for "y" | 1, 2, 3, 4, 5, 6, 7, 8, 9, 10 |
| Ion serie matches for "y -H2O" | 4, 9, 11 |
| Ion serie matches for "y -H2O -H3PO4" | 7, 8, 9, 9, 10, 12 |
| Ion serie matches for "y -H2O -NH3" | |
| Ion serie matches for "y -H3PO4" | 6, 7, 7, 8, 8, 9, 9, 10, 11, 12 |
| Ion serie matches for "y -NH3" | 1, 2, 3, 4, 5 |
| Ion serie matches for "y -NH3 -H3PO4" | 6, 7, 8, 9 |



Figure B-1.

# $^{947}$TQPKLSALSAGS[79.96633]NEYLR$^{963}$

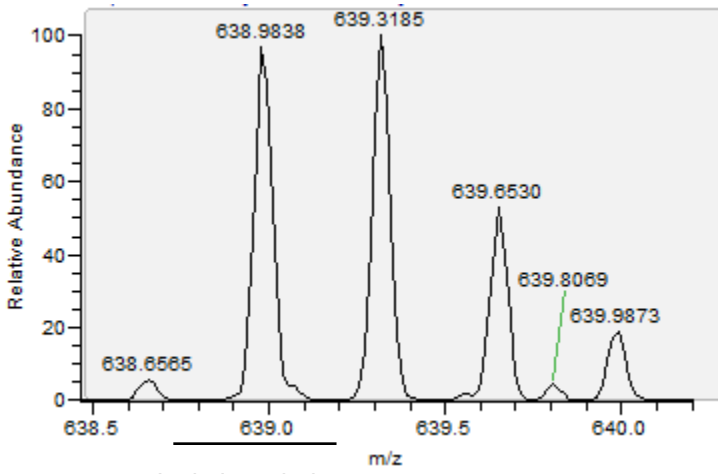


**Ser 955/958**

Precursor m/z: 638.9838
Precursor mass error: -2.50 ppm

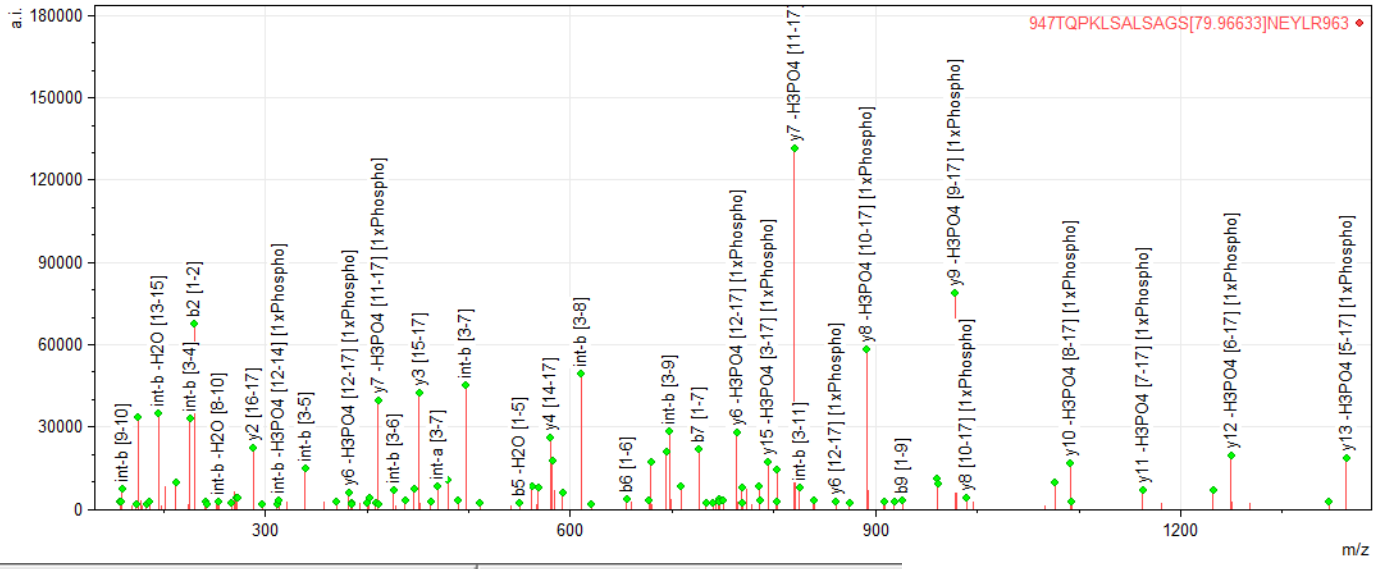


| parameter | value |
|---|---|
| Number of peaks searched | 127 |
| Number of fragments searched | 3588 |
| Number of fragments matched | 122 |
| Intensity matched | 89 % |
| Sequence length | 17 |
| Ion serie matches for "b" | 2, 5, 6, 7, 8, 9 |
| Ion serie matches for "b -H2O" | 2, 5, 7, 9 |
| Ion serie matches for "b -H2O -H3PO4" | |
| Ion serie matches for "b -H2O -NH3" | 2, 6 |
| Ion serie matches for "b -H3PO4" | |
| Ion serie matches for "b -NH3" | 12 |
| Ion serie matches for "b -NH3 -H3PO4" | |
| Ion serie matches for "y" | 1, 2, 3, 4, 5, 6, 7, 8, 9 |
| Ion serie matches for "y -H2O" | 4 |
| Ion serie matches for "y -H2O -H3PO4" | 7, 9, 11, 12, 12, 15 |
| Ion serie matches for "y -H2O -NH3" | |
| Ion serie matches for "y -H3PO4" | 6, 6, 7, 7, 8, 8, 9, 9, 10, 11, 12, 13, 14, 15 |
| Ion serie matches for "y -NH3" | 1, 2, 5 |
| Ion serie matches for "y -NH3 -H3PO4" | 6, 7, 7, 8, 8, 9, 13, 15 |



Figure B-1.

# $^{946}$KTQPKLSALSAGS[79.96633]NEYLR$^{963}$

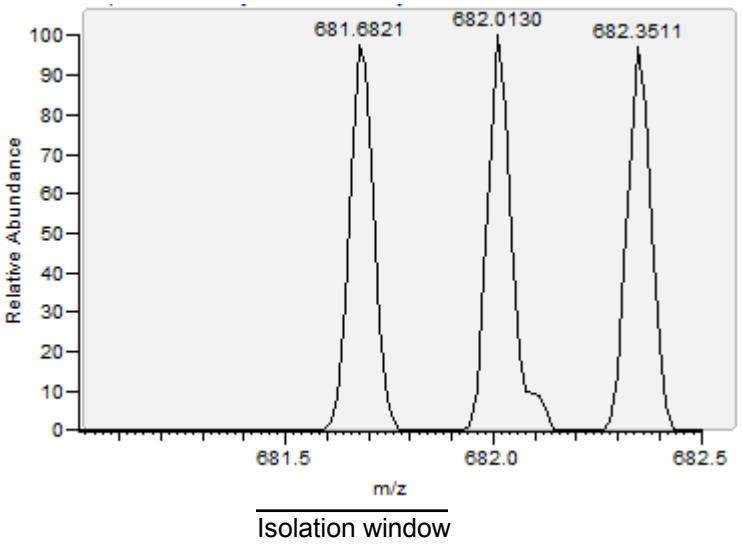


**Ser 955/958**

Precursor m/z: 681.6821
Precursor mass error: -2.30 ppm

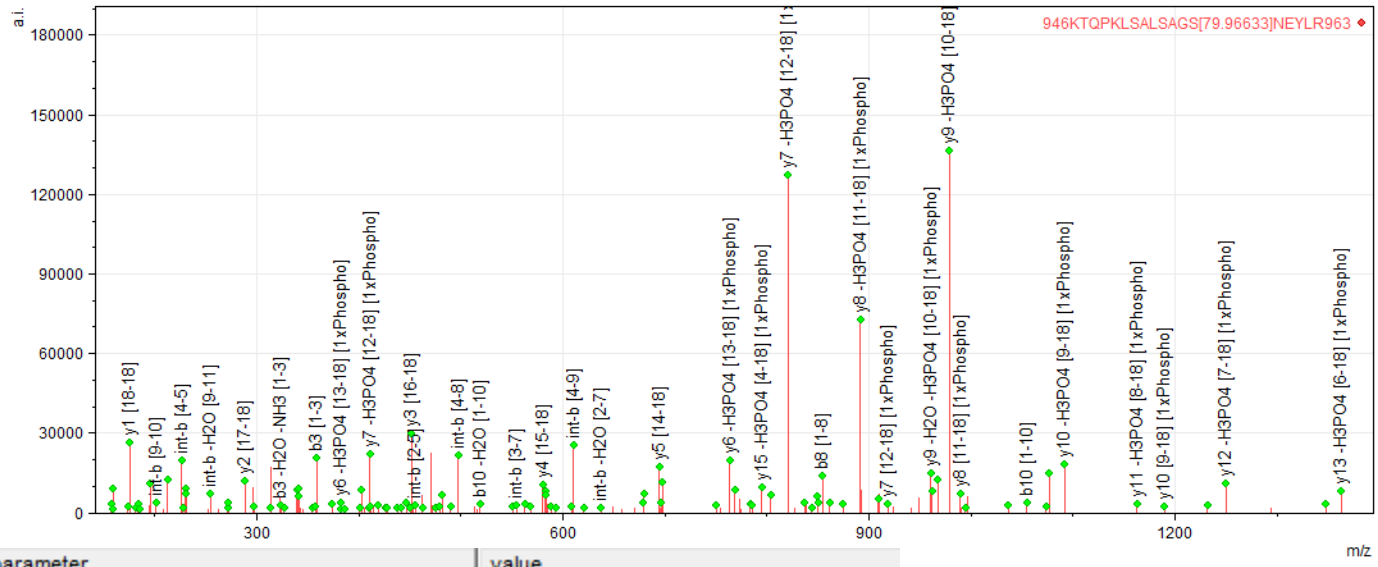


| parameter | value |
|---|---|
| Number of peaks searched | 150 |
| Number of fragments searched | 4077 |
| Number of fragments matched | 147 |
| Intensity matched | 83 % |
| Sequence length | 18 |
| Ion serie matches for "b" | 2, 3, 4, 5, 6, 7, 8, 8, 9, 10 |
| Ion serie matches for "b -H2O" | 2, 3, 6, 8, 8, 9, 10, 10, 11 |
| Ion serie matches for "b -H2O -H3PO4" | |
| Ion serie matches for "b -H2O -NH3" | 2, 3, 8 |
| Ion serie matches for "b -H3PO4" | |
| Ion serie matches for "b -NH3" | 3, 6, 6 |
| Ion serie matches for "b -NH3 -H3PO4" | |
| Ion serie matches for "y" | 1, 2, 3, 4, 5, 6, 7, 8, 9, 10, 12, 15 |
| Ion serie matches for "y -H2O" | 4 |
| Ion serie matches for "y -H2O -H3PO4" | 9, 10, 11, 12, 12, 15, 16 |
| Ion serie matches for "y -H2O -NH3" | |
| Ion serie matches for "y -H3PO4" | 6, 6, 7, 7, 8, 8, 9, 9, 10, 11, 12, 13, 15, 17 |
| Ion serie matches for "y -NH3" | 1, 2 |
| Ion serie matches for "y -NH3 -H3PO4" | 6, 7, 7, 8, 8, 9, 9, 16 |



Figure B-1.

# $^{951}$LSALSAGS[79.96633]NEYLR$^{963}$

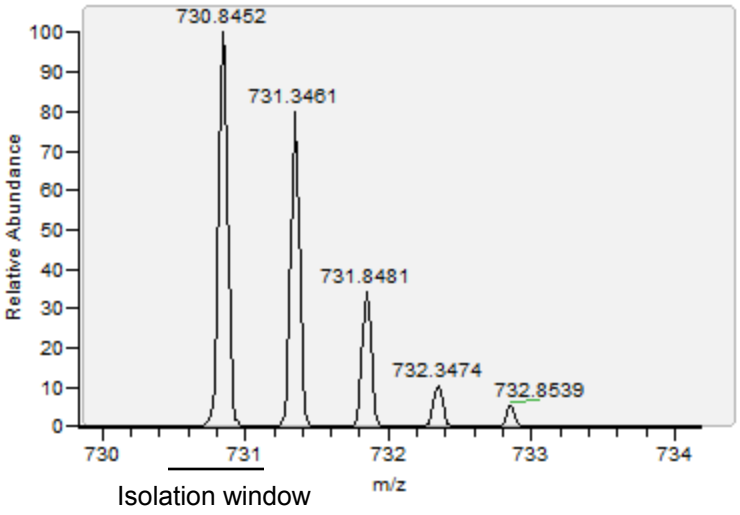


**Ser 955/958**

Precursor m/z: 730.8452
Precursor mass error: -3.42 ppm

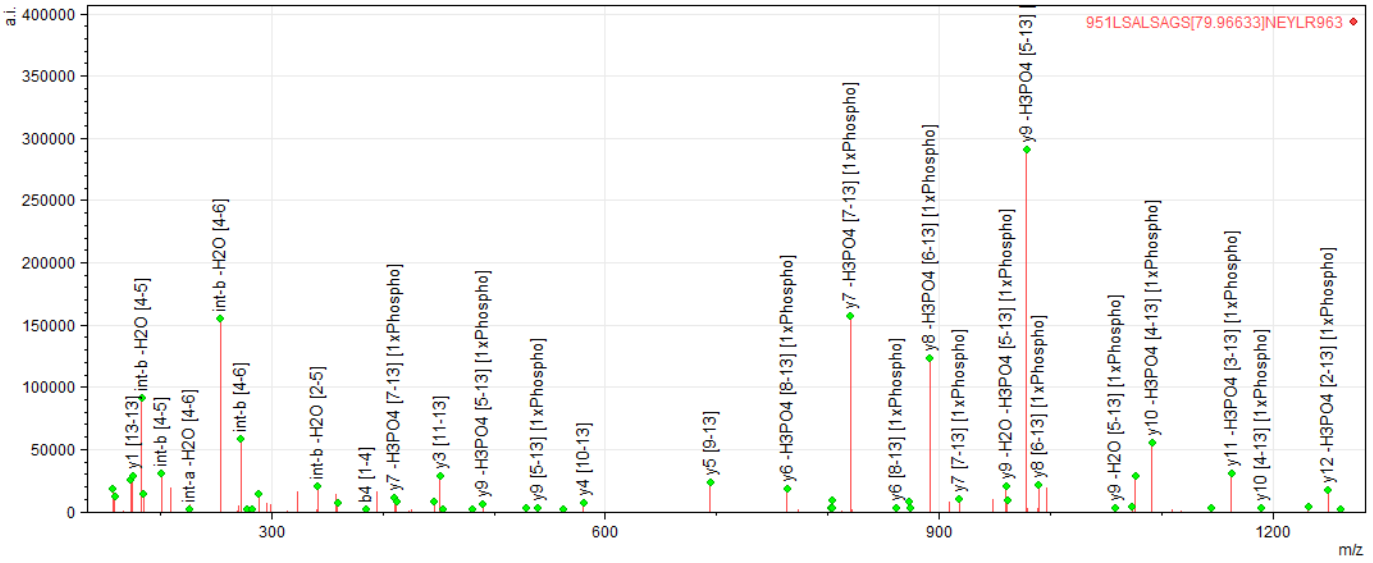


| parameter | value |
|---|---|
| Number of peaks searched | 78 |
| Number of fragments searched | 1328 |
| Number of fragments matched | 66 |
| Intensity matched | 89 % |
| Sequence length | 13 |
| Ion serie matches for "b" | 2, 3, 4, 6 |
| Ion serie matches for "b -H2O" | 2, 3, 5 |
| Ion serie matches for "b -H2O -H3PO4" | |
| Ion serie matches for "b -H2O -NH3" | |
| Ion serie matches for "b -H3PO4" | |
| Ion serie matches for "b -NH3" | |
| Ion serie matches for "b -NH3 -H3PO4" | |
| Ion serie matches for "y" | 1, 2, 3, 4, 5, 6, 7, 8, 9, 9, 10, 11 |
| Ion serie matches for "y -H2O" | 4, 9 |
| Ion serie matches for "y -H2O -H3PO4" | 7, 8, 9, 9, 10, 11, 12 |
| Ion serie matches for "y -H2O -NH3" | |
| Ion serie matches for "y -H3PO4" | 6, 7, 7, 8, 8, 9, 9, 10, 11, 12 |
| Ion serie matches for "y -NH3" | 4 |
| Ion serie matches for "y -NH3 -H3PO4" | 7, 8, 9 |



Figure B-1.

# [1000]TRAKS[79.96633]C[57.02146]GERDVK[1011]

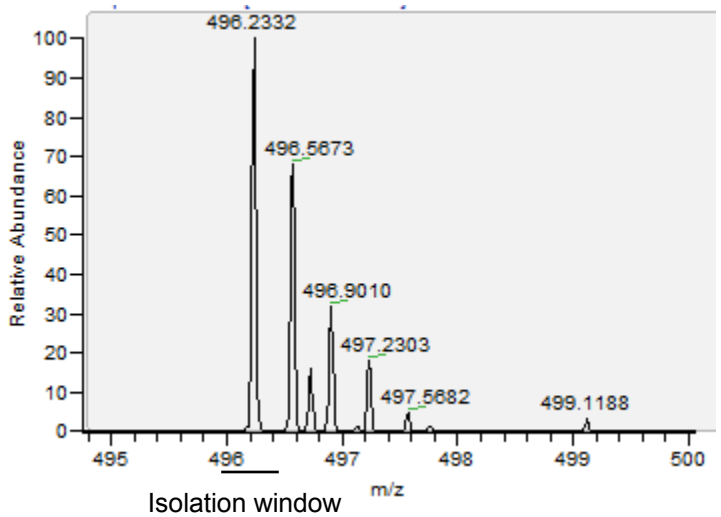


**Thr 1000/S1004**

Precursor m/z: 496.2332
Precursor mass error: -1.21 ppm

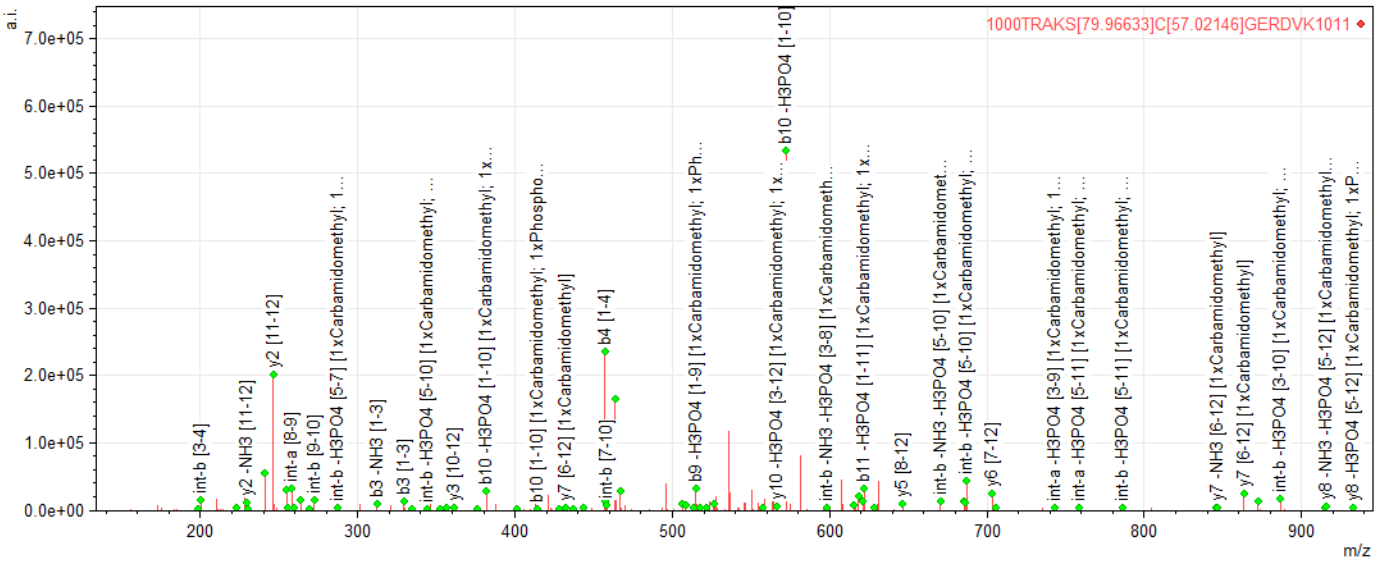


| parameter | value |
|---|---|
| Number of peaks searched | 170 |
| Number of fragments searched | 1845 |
| Number of fragments matched | 84 |
| Intensity matched | 62 % |
| Sequence length | 12 |
| Ion serie matches for "b" | 2, 3, 4, 10, 10 |
| Ion serie matches for "b -H2O" | |
| Ion serie matches for "b -H2O -H3PO4" | 5, 5, 6, 8, 10 |
| Ion serie matches for "b -H2O -NH3" | 2 |
| Ion serie matches for "b -H3PO4" | 5, 5, 6, 7, 8, 8, 9, 10, 10, 11 |
| Ion serie matches for "b -NH3" | 2, 3 |
| Ion serie matches for "b -NH3 -H3PO4" | 9, 10, 10 |
| Ion serie matches for "y" | 2, 3, 4, 4, 5, 6, 6, 7, 7 |
| Ion serie matches for "y -H2O" | 5, 6, 7 |
| Ion serie matches for "y -H2O -H3PO4" | 8, 9, 10 |
| Ion serie matches for "y -H2O -NH3" | 6 |
| Ion serie matches for "y -H3PO4" | 8, 8, 10 |
| Ion serie matches for "y -NH3" | 2, 6, 7 |
| Ion serie matches for "y -NH3 -H3PO4" | 8, 8 |



Figure B-1.

# $^{1000}$TRAKS[79.96633]C[57.02146]GERDVKGIR$^{1014}$

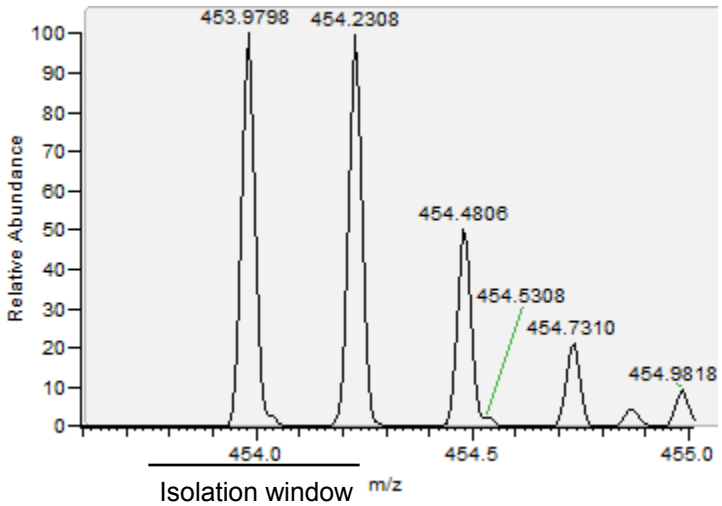


**Thr 1000/S1004**

Precursor m/z: 453.9788
Precursor mass error: -1.93 ppm

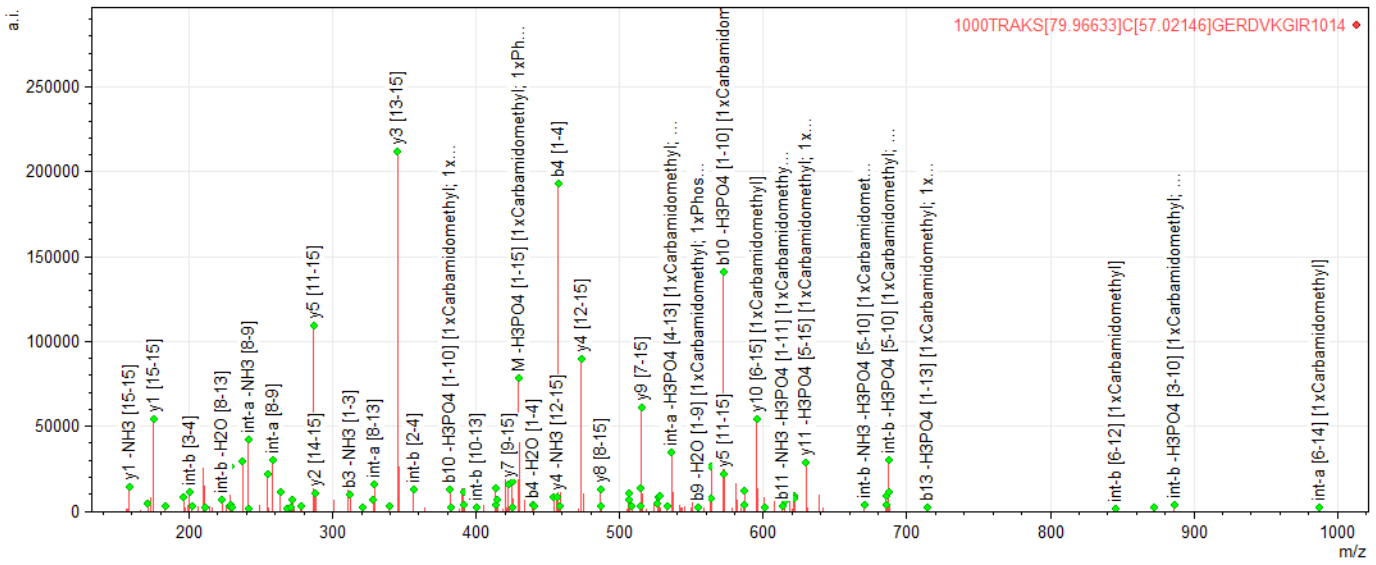


| parameter | value |
|---|---|
| Number of peaks searched | 168 |
| Number of fragments searched | 3824 |
| Number of fragments matched | 103 |
| Intensity matched | 77 % |
| Sequence length | 15 |
| Ion serie matches for "b" | 2, 3, 4, 4, 9, 13 |
| Ion serie matches for "b -H2O" | 4, 9 |
| Ion serie matches for "b -H2O -H3PO4" | 5, 5, 10 |
| Ion serie matches for "b -H2O -NH3" | 2 |
| Ion serie matches for "b -H3PO4" | 5, 5, 8, 9, 10, 10, 11, 12, 13, 14 |
| Ion serie matches for "b -NH3" | 2, 3, 4 |
| Ion serie matches for "b -NH3 -H3PO4" | 9, 10, 11 |
| Ion serie matches for "y" | 1, 2, 3, 4, 4, 5, 5, 6, 7, 8, 9, 10 |
| Ion serie matches for "y -H2O" | 7, 10, 10 |
| Ion serie matches for "y -H2O -H3PO4" | |
| Ion serie matches for "y -H2O -NH3" | |
| Ion serie matches for "y -H3PO4" | 11, 11, 13 |
| Ion serie matches for "y -NH3" | 1, 2, 3, 4, 4, 5, 7, 9, 10, 10 |
| Ion serie matches for "y -NH3 -H3PO4" | 11, 11, 12, 14 |



Figure B-1.

# $^{1002}$AKS[79.96633]C[57.02146]GERDVK$^{1011}$

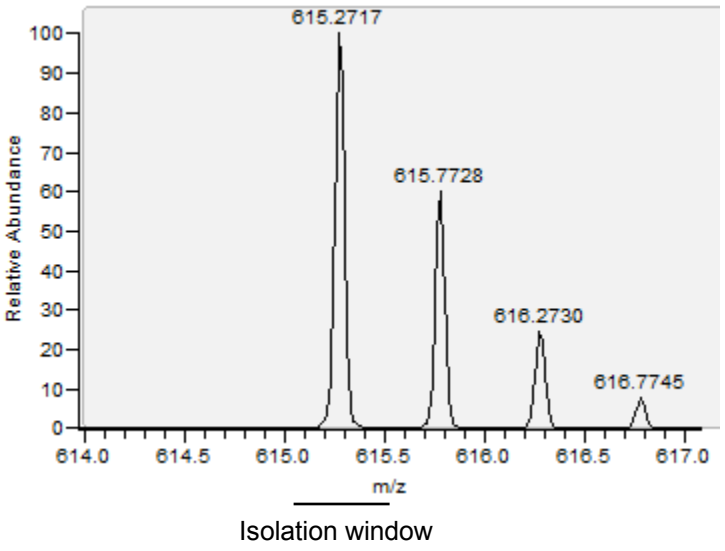


**Ser 1004**

Precursor m/z: 615.2717
Precursor mass error: -1.38 ppm

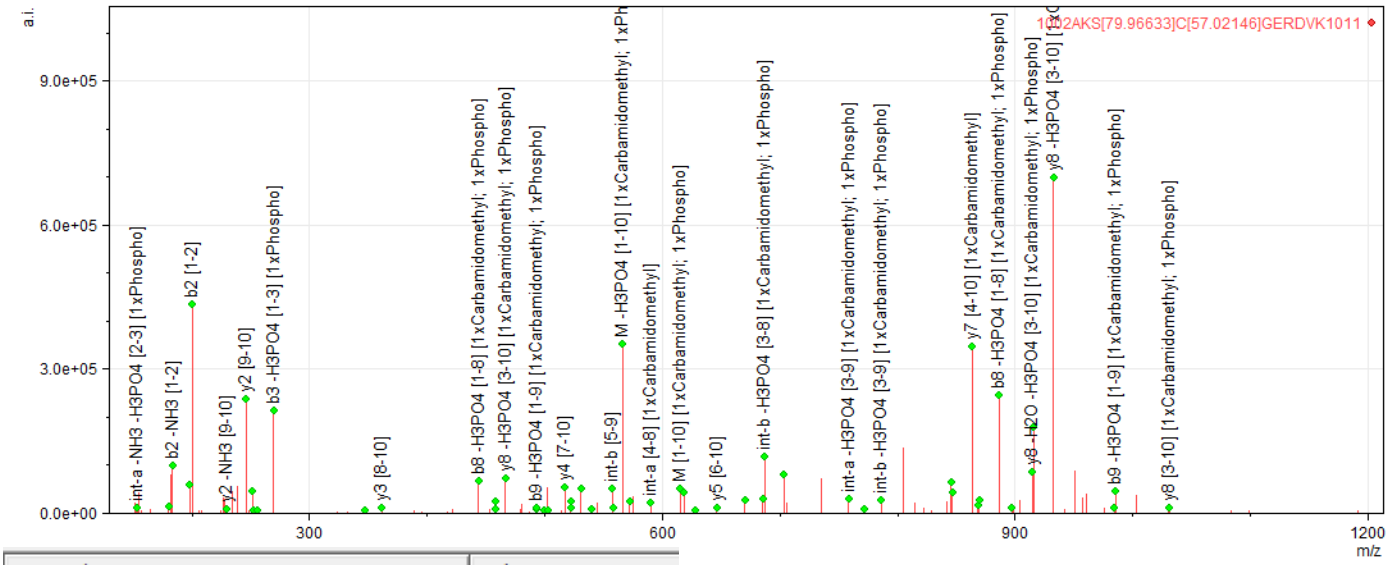


| parameter | value |
|---|---|
| Number of peaks searched | 106 |
| Number of fragments searched | 758 |
| Number of fragments matched | 60 |
| Intensity matched | 78 % |
| Sequence length | 10 |
| Ion serie matches for "b" | 2, 8, 8 |
| Ion serie matches for "b -H2O" | |
| Ion serie matches for "b -H2O -H3PO4" | 3, 8 |
| Ion serie matches for "b -H2O -NH3" | |
| Ion serie matches for "b -H3PO4" | 3, 7, 8, 8, 9, 9 |
| Ion serie matches for "b -NH3" | 2 |
| Ion serie matches for "b -NH3 -H3PO4" | 3, 8 |
| Ion serie matches for "y" | 2, 3, 4, 5, 6, 7, 8 |
| Ion serie matches for "y -H2O" | 4, 5, 6, 7 |
| Ion serie matches for "y -H2O -H3PO4" | 8, 8, 9 |
| Ion serie matches for "y -H2O -NH3" | |
| Ion serie matches for "y -H3PO4" | 8, 8, 9 |
| Ion serie matches for "y -NH3" | 2, 7 |
| Ion serie matches for "y -NH3 -H3PO4" | 8, 8, 9 |



Figure B-1.

# $^{1057}$ILT[79.96633]EDQDKIVR$^{1067}$

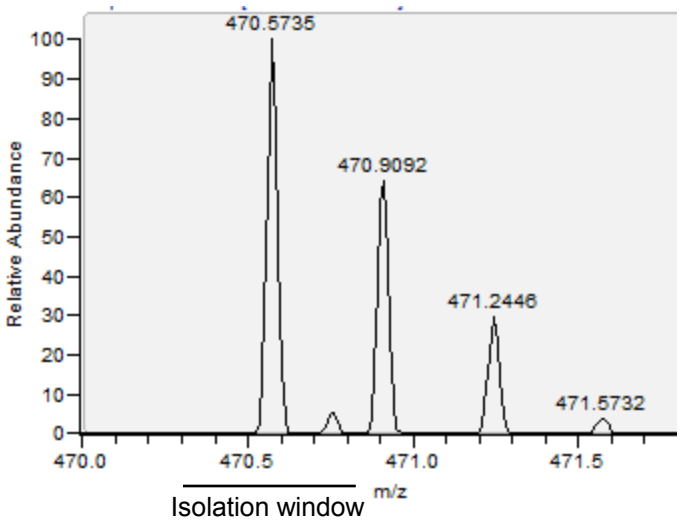


**Thr 1059**

Precursor m/z: 470.5735
Precursor mass error: -1.70 ppm

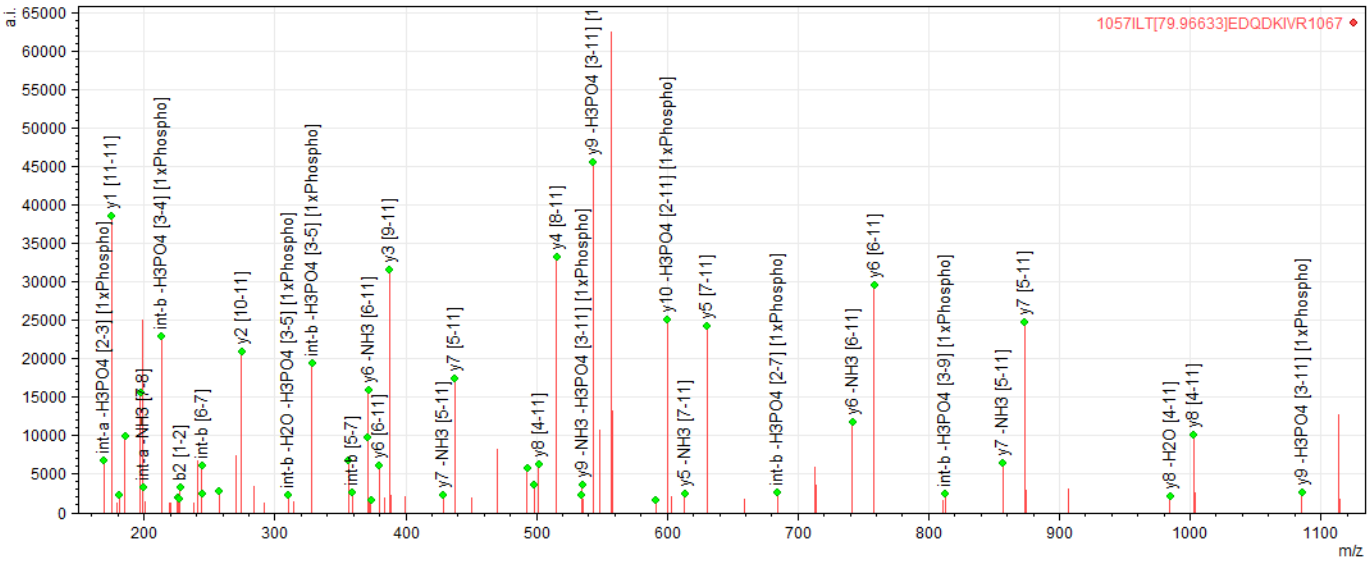


| parameter | value |
|---|---|
| Number of peaks searched | 81 |
| Number of fragments searched | 1326 |
| Number of fragments matched | 51 |
| Intensity matched | 69 % |
| Sequence length | 11 |
| Ion serie matches for "b" | 2 |
| Ion serie matches for "b -H2O" | |
| Ion serie matches for "b -H2O -H3PO4" | |
| Ion serie matches for "b -H2O -NH3" | |
| Ion serie matches for "b -H3PO4" | |
| Ion serie matches for "b -NH3" | |
| Ion serie matches for "b -NH3 -H3PO4" | |
| Ion serie matches for "y" | 1, 2, 3, 4, 5, 6, 6, 7, 7, 8, 8 |
| Ion serie matches for "y -H2O" | 6, 8, 8 |
| Ion serie matches for "y -H2O -H3PO4" | 9 |
| Ion serie matches for "y -H2O -NH3" | |
| Ion serie matches for "y -H3PO4" | 9, 9, 10 |
| Ion serie matches for "y -NH3" | 2, 4, 5, 6, 6, 7, 7 |
| Ion serie matches for "y -NH3 -H3PO4" | 9, 10 |



Figure B-1.

# $^{1240}$S[79.96633]LNVQLGR$^{1247}$

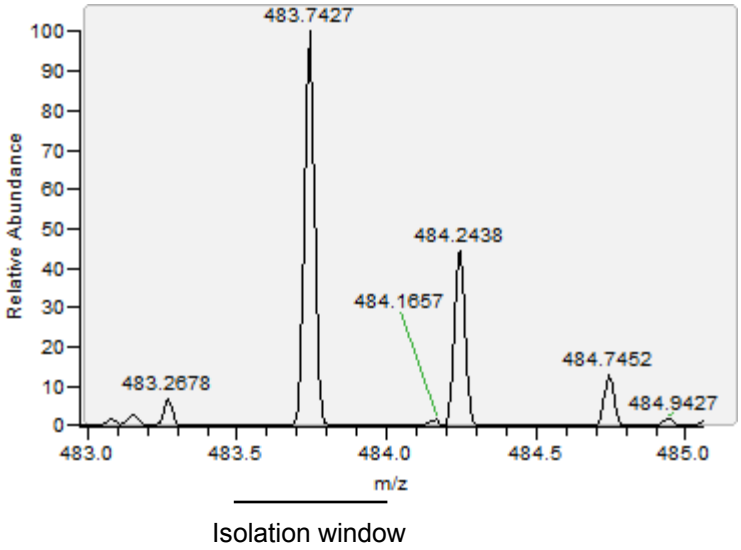


**Ser 1240**

Precursor m/z: 483.7427
Precursor mass error: -1.34 ppm

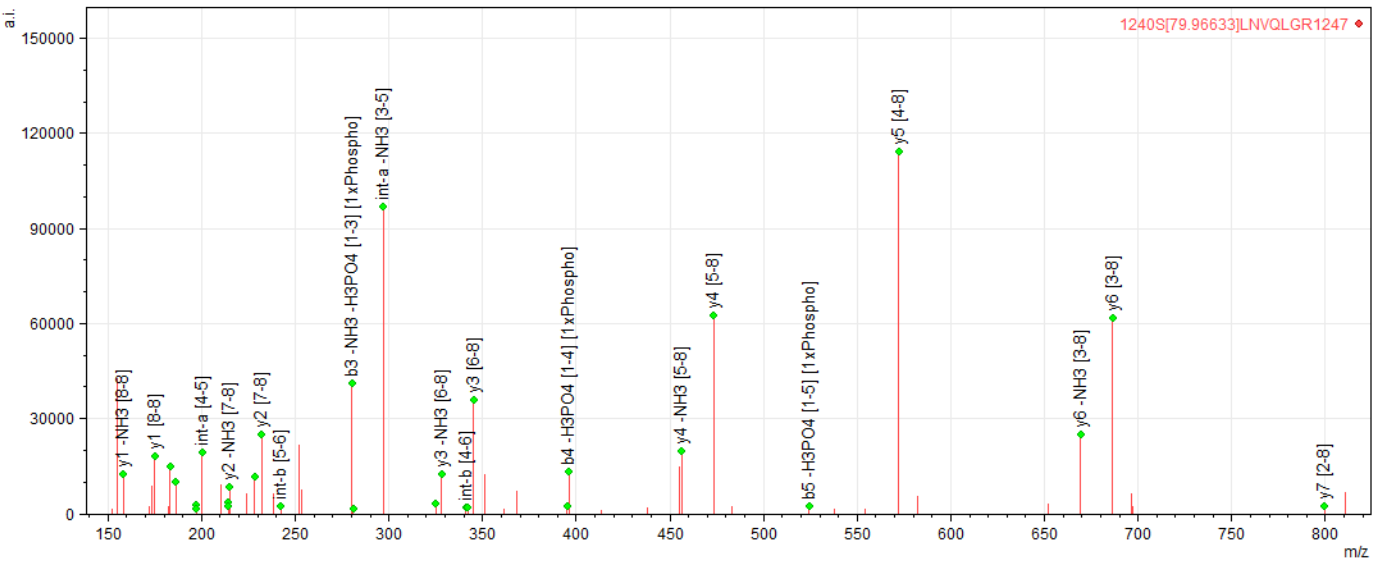


| parameter | value |
|---|---|
| Number of peaks searched | 55 |
| Number of fragments searched | 262 |
| Number of fragments matched | 37 |
| Intensity matched | 77 % |
| Sequence length | 8 |
| Ion serie matches for "b" | 2, 3 |
| Ion serie matches for "b -H2O" | |
| Ion serie matches for "b -H2O -H3PO4" | |
| Ion serie matches for "b -H2O -NH3" | |
| Ion serie matches for "b -H3PO4" | 2, 3, 4, 5 |
| Ion serie matches for "b -NH3" | |
| Ion serie matches for "b -NH3 -H3PO4" | 3 |
| Ion serie matches for "y" | 1, 2, 3, 4, 5, 6, 7 |
| Ion serie matches for "y -NH3" | 1, 2, 3, 4, 6 |



Figure B-1.

Figure B-2. Graphs of all detected and quantified ASK1 phosphopeptides in the HNE treated cells. For each concentration point (10 and 50 μM) the peptide peak are was compared against the peptide peak area for the control sample (0 μM). Graphs are shown for (A) Ser 83 (B) Thr 947|Ser 952 (C) Ser 955|Ser 958 (D) Thr 1000|Ser 1004 (E) Ser 1059 (F) Ser 1240.

A

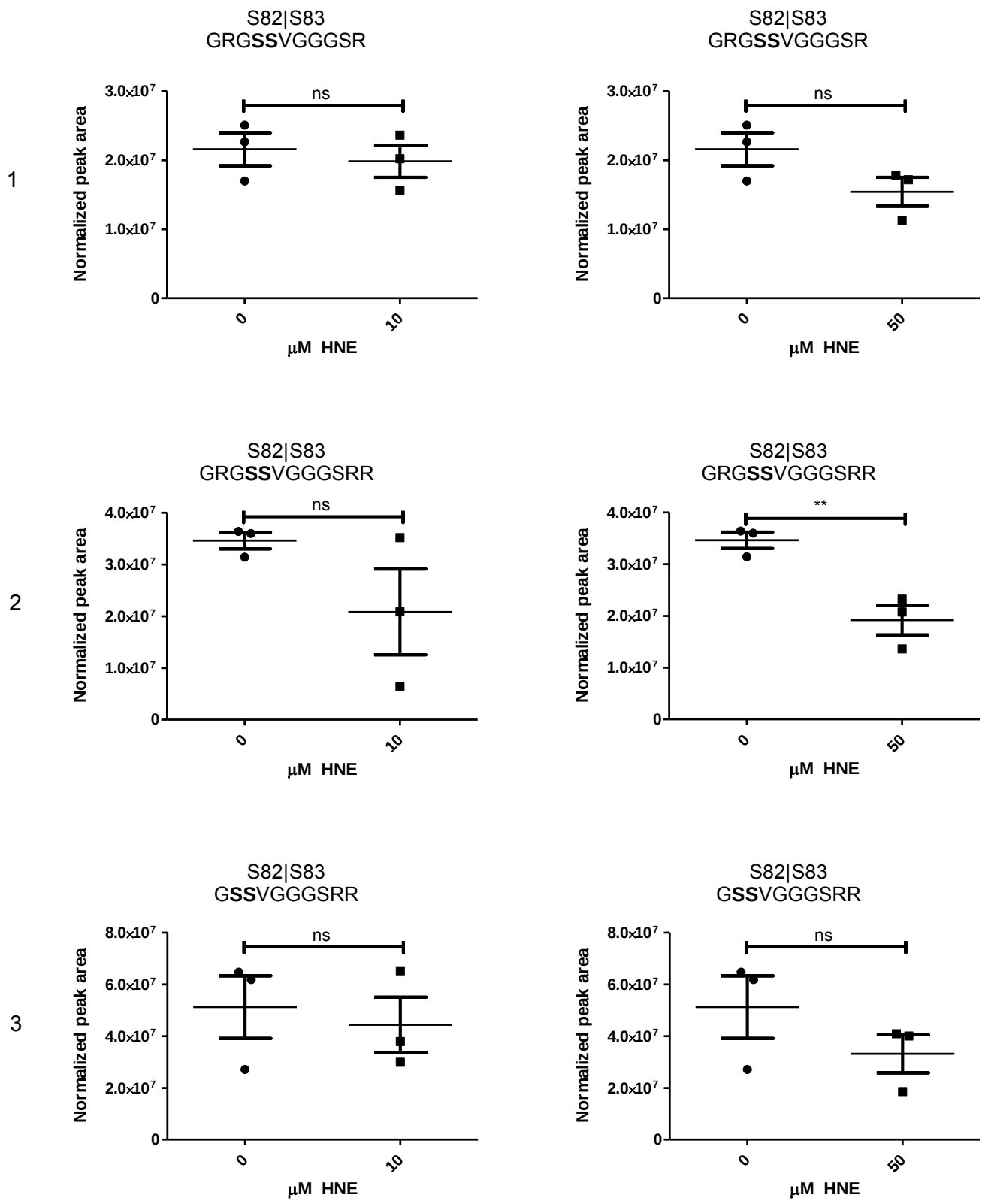
1
S82|S83
GRGSSVGGGSR
Normalized peak area
3.0x10^7
2.0x10^7
1.0x10^7
0
ns
0
10
µM HNE
S82|S83
GRGSSVGGGSR
Normalized peak area
3.0x10^7
2.0x10^7
1.0x10^7
0
ns
0
50
µM HNE
2
S82|S83
GRGSSVGGGSRR
Normalized peak area
4.0x10^7
3.0x10^7
2.0x10^7
1.0x10^7
0
ns
0
10
µM HNE
S82|S83
GRGSSVGGGSRR
Normalized peak area
4.0x10^7
3.0x10^7
2.0x10^7
1.0x10^7
0
**
0
50
µM HNE
3
S82|S83
GSSVGGGSRR
Normalized peak area
8.0x10^7
6.0x10^7
4.0x10^7
2.0x10^7
0
ns
0
10
µM HNE
S82|S83
GSSVGGGSRR
Normalized peak area
8.0x10^7
6.0x10^7
4.0x10^7
2.0x10^7
0
ns
0
50
µM HNE



Figure B-2.

B

1

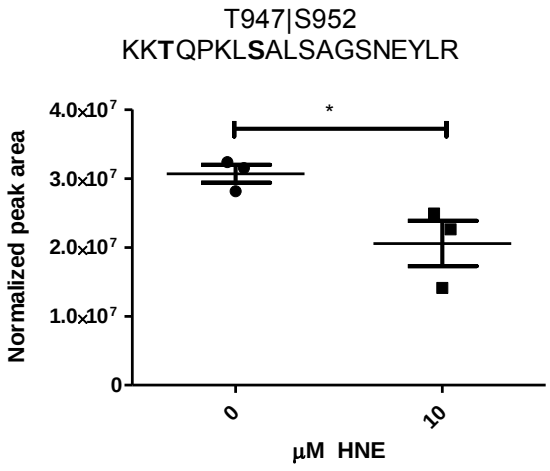


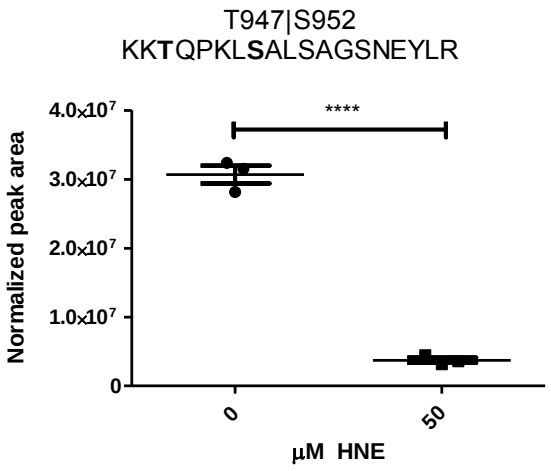


2

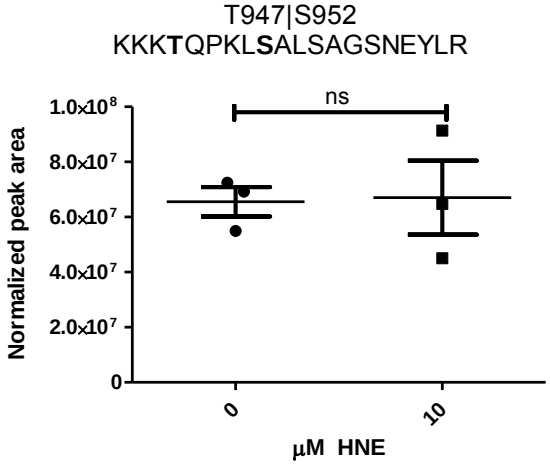


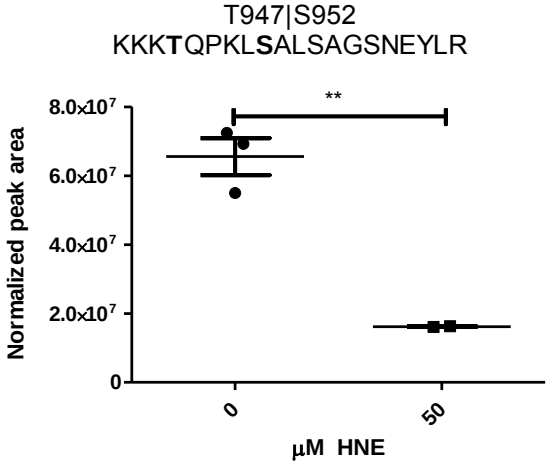


C

1

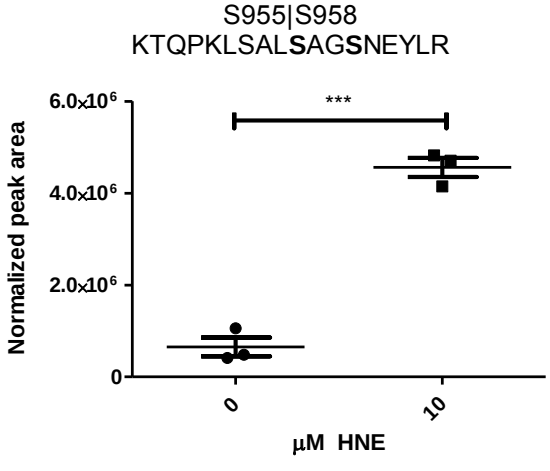


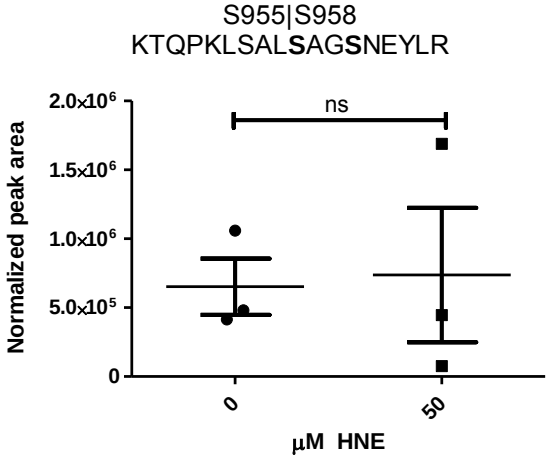




Figure B-2.

C

2

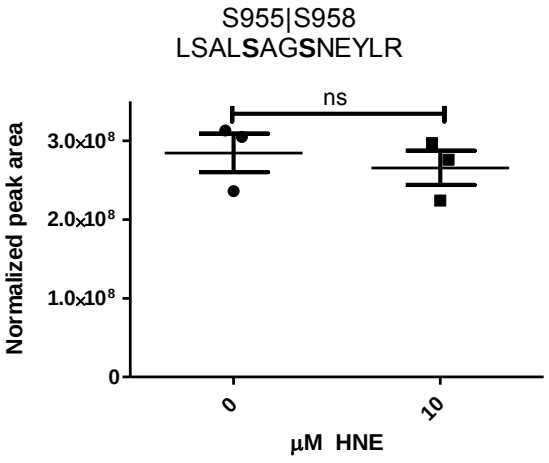


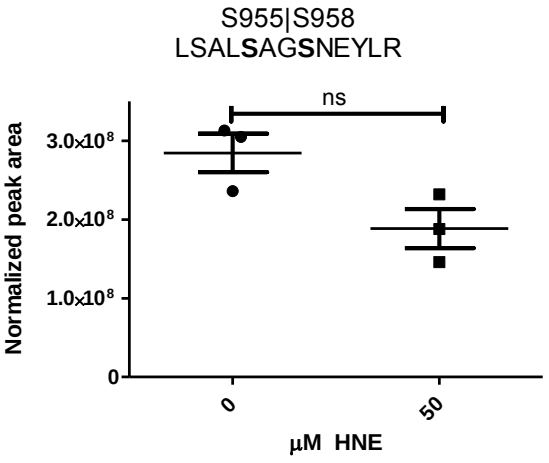


3

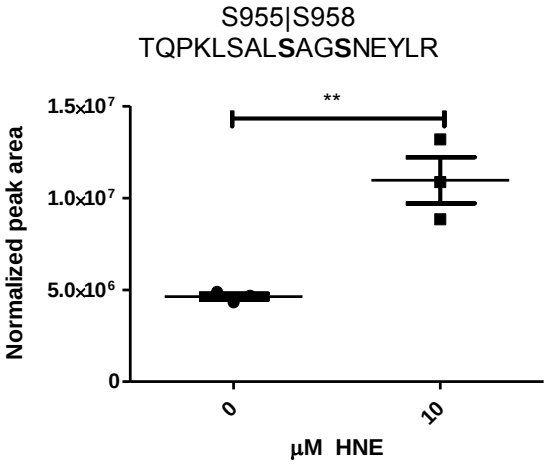


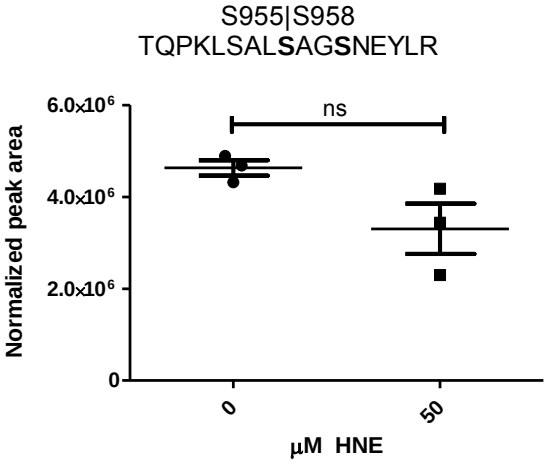


D

1

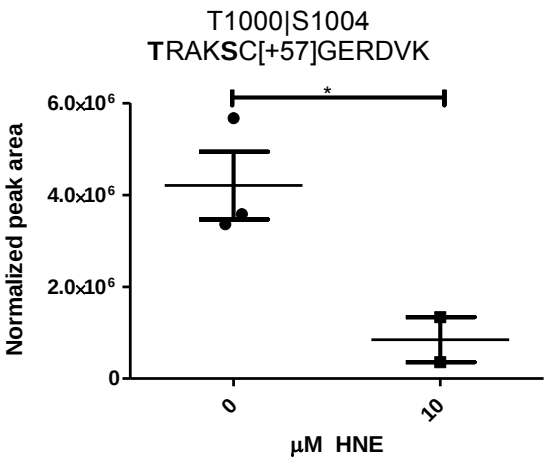


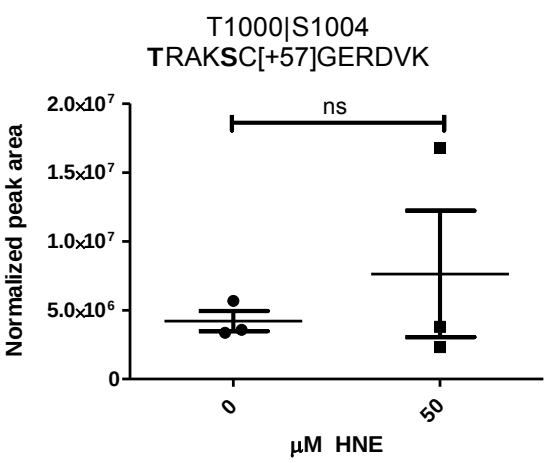




Figure B-2.

D

2

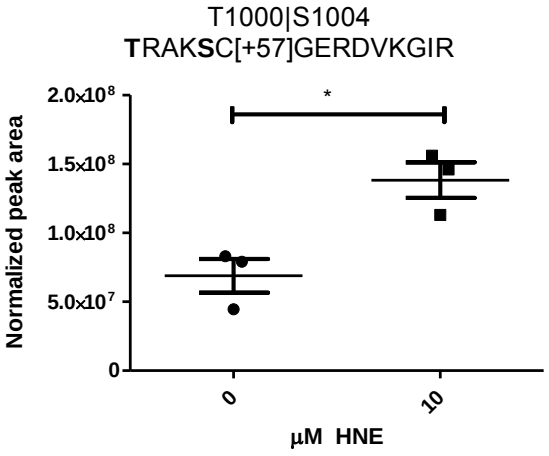


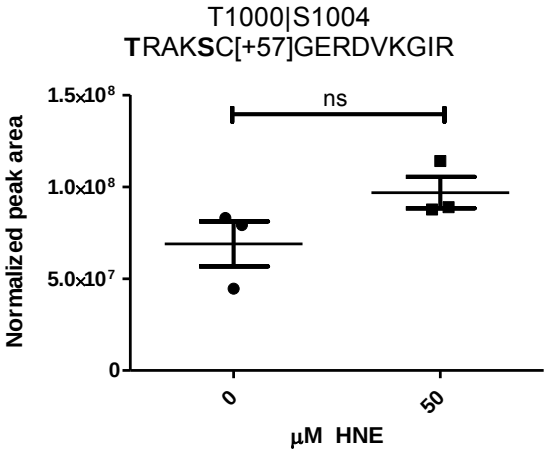


3

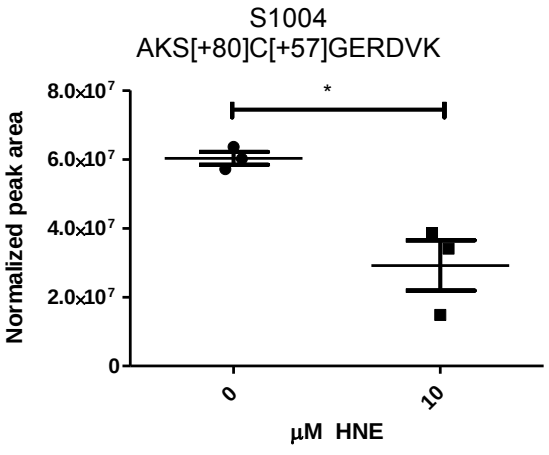


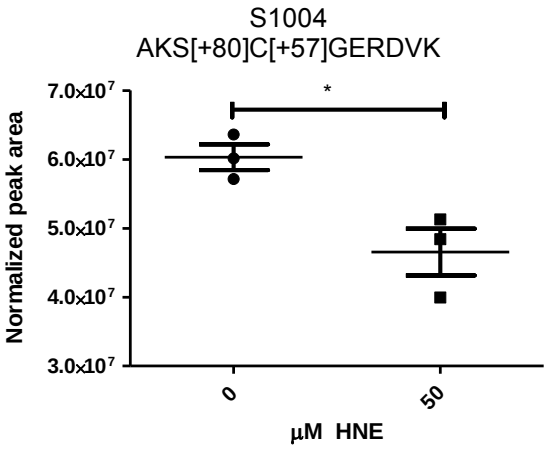


E

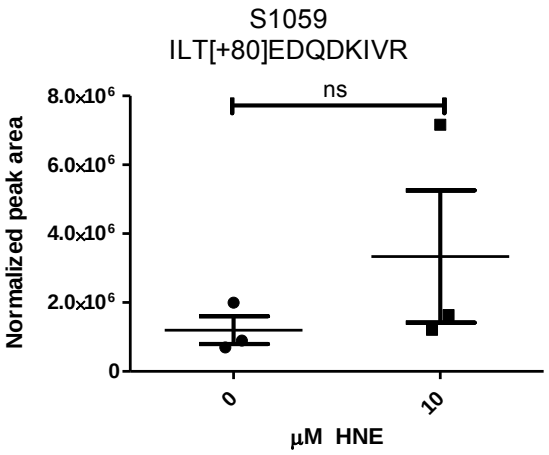


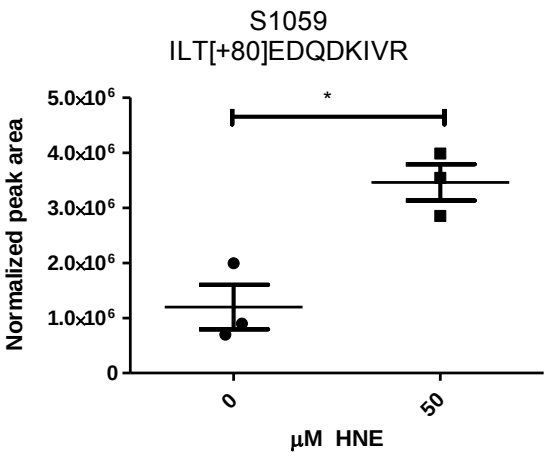




Figure B-2.

F

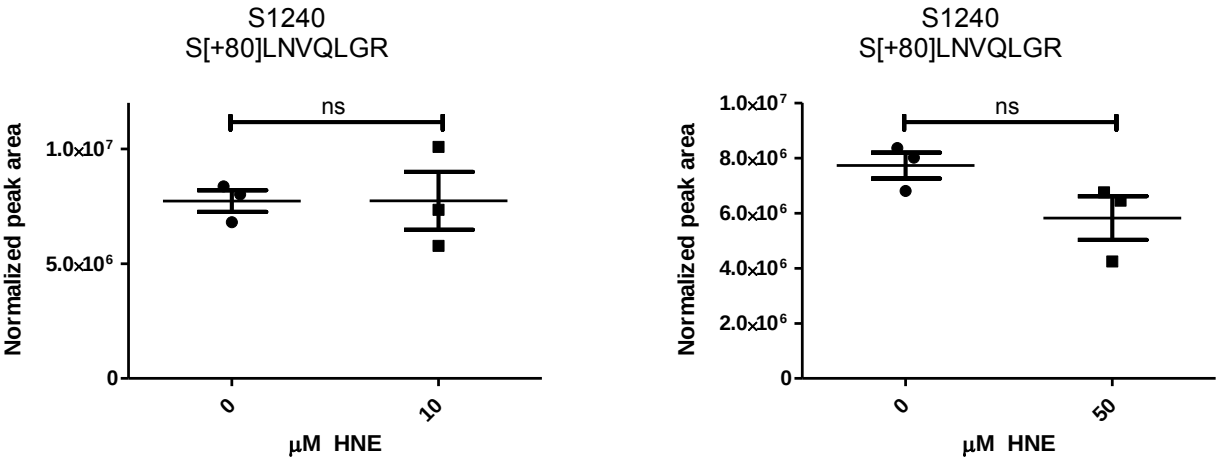
S1240
S[+80]LNVQLGR
ns
Normalized peak area
1.0x10^7
5.0x10^6
0
0
10
µM HNE
S1240
S[+80]LNVQLGR
ns
Normalized peak area
1.0x10^7
8.0x10^6
6.0x10^6
4.0x10^6
2.0x10^6
0
0
50
µM HNE



Figure B-2.

Figure B-3. Graphs of all detected and quantified ASK1 phosphopeptides in the $H_2O_2$ treated cells. For each concentration point (500 and 5000 μM) the peptide peak are was compared against the peptide peak area for the control sample (0 μM). Graphs are shown for (A) Ser 83 (B) The 140|Thr 141 (C) Ser 268|Ser 269 (D) Tyr 355 (E) Thr 947|Ser 952 (F) Ser 955 (G) Ser 958 (H) Ser 1004 (I) Ser 1240.

A

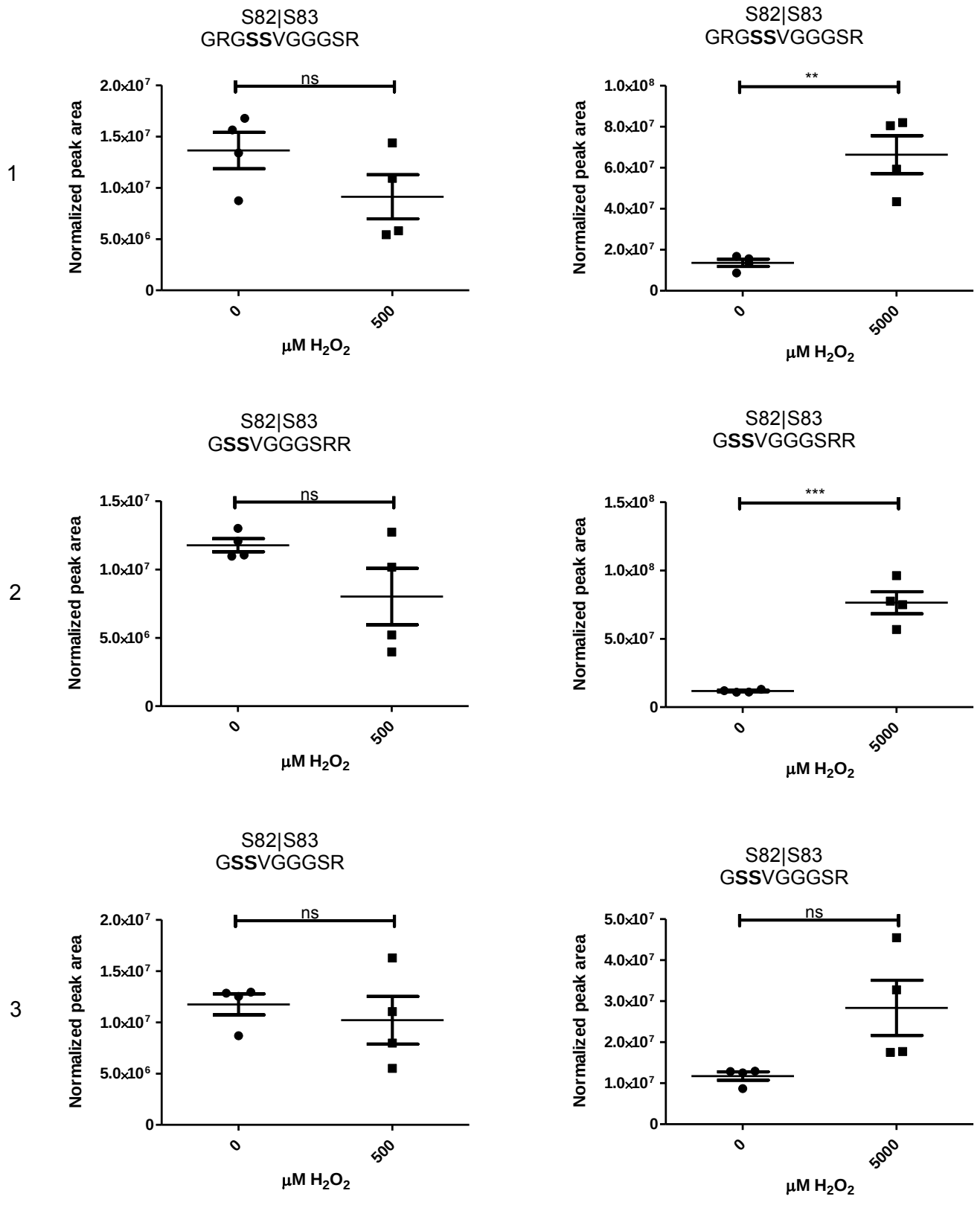
1
S82|S83
GRGSSVGGGSR
ns
Normalized peak area
2.0x10^7
1.5x10^7
1.0x10^7
5.0x10^6
0
0
500
μM H2O2
S82|S83
GRGSSVGGGSR
**
Normalized peak area
1.0x10^8
8.0x10^7
6.0x10^7
4.0x10^7
2.0x10^7
0
0
5000
μM H2O2
2
S82|S83
GSSVGGGSRR
ns
Normalized peak area
1.5x10^7
1.0x10^7
5.0x10^6
0
0
500
μM H2O2
S82|S83
GSSVGGGSRR
***
Normalized peak area
1.5x10^8
1.0x10^8
5.0x10^7
0
0
5000
μM H2O2
3
S82|S83
GSSVGGGSR
ns
Normalized peak area
2.0x10^7
1.5x10^7
1.0x10^7
5.0x10^6
0
0
500
μM H2O2
S82|S83
GSSVGGGSR
ns
Normalized peak area
5.0x10^7
4.0x10^7
3.0x10^7
2.0x10^7
1.0x10^7
0
0
5000
μM H2O2



Figure B-3.

A

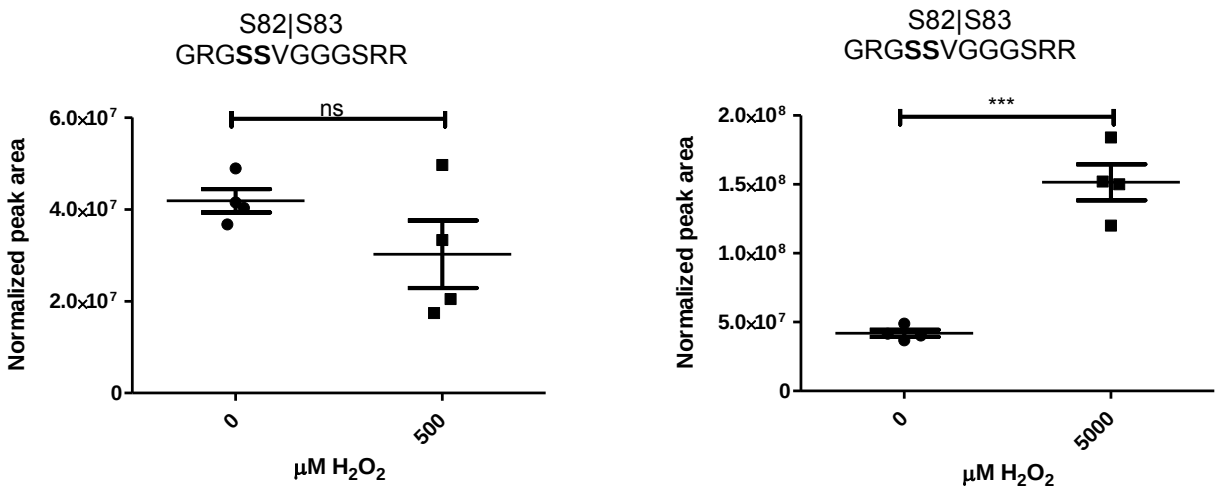


B

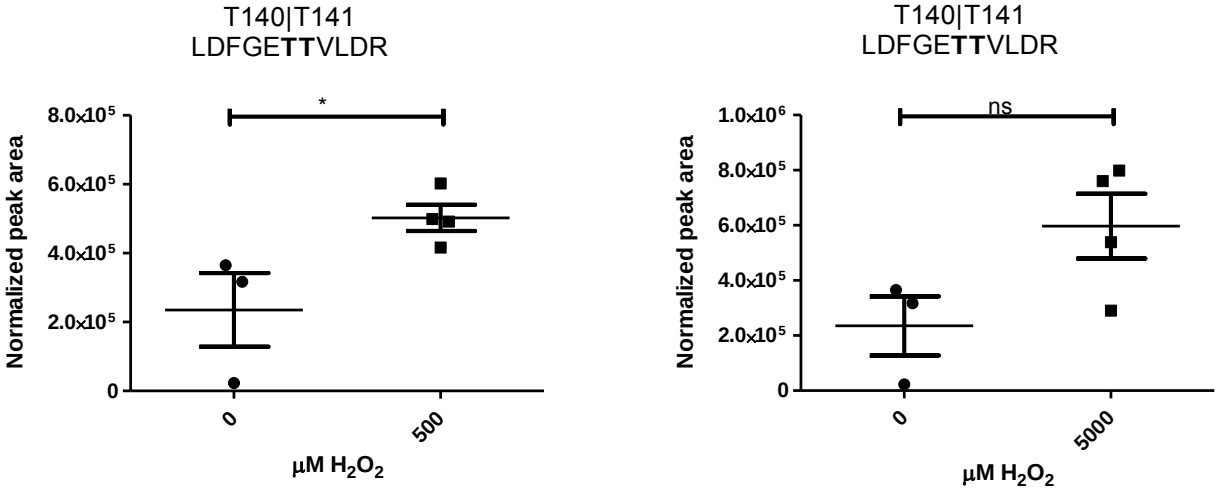


C

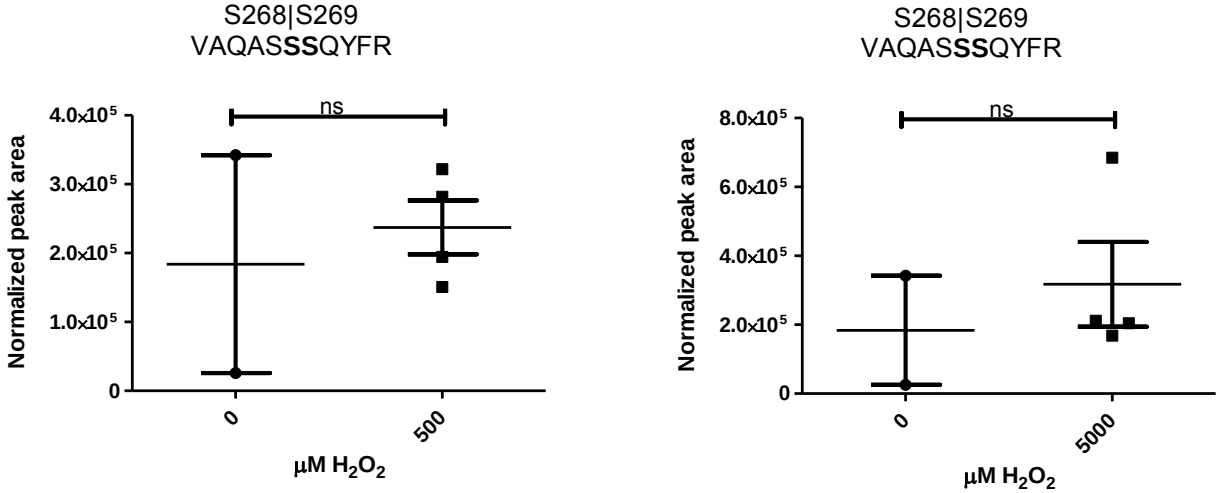




Figure B-3.

D

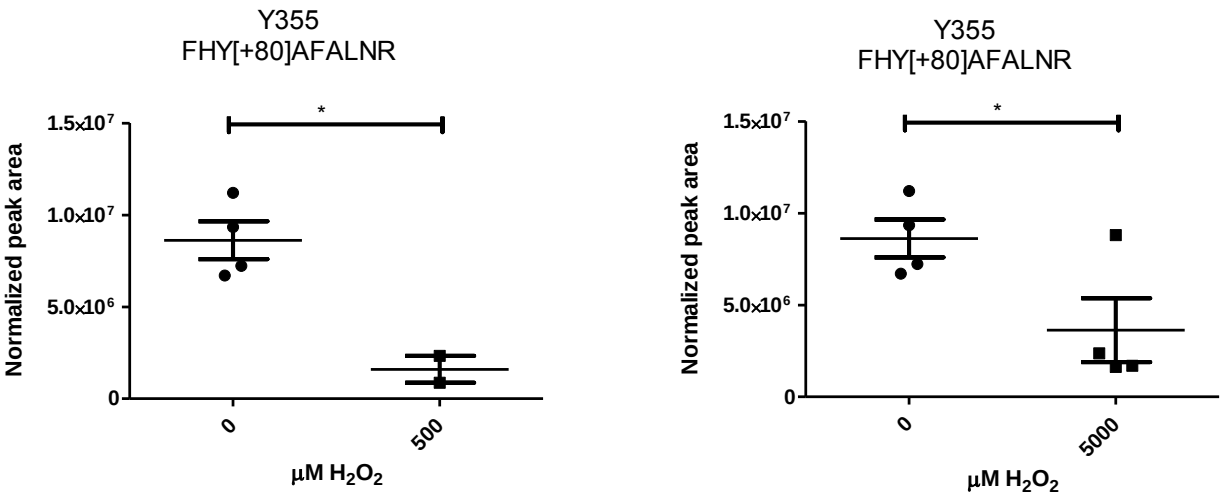


E

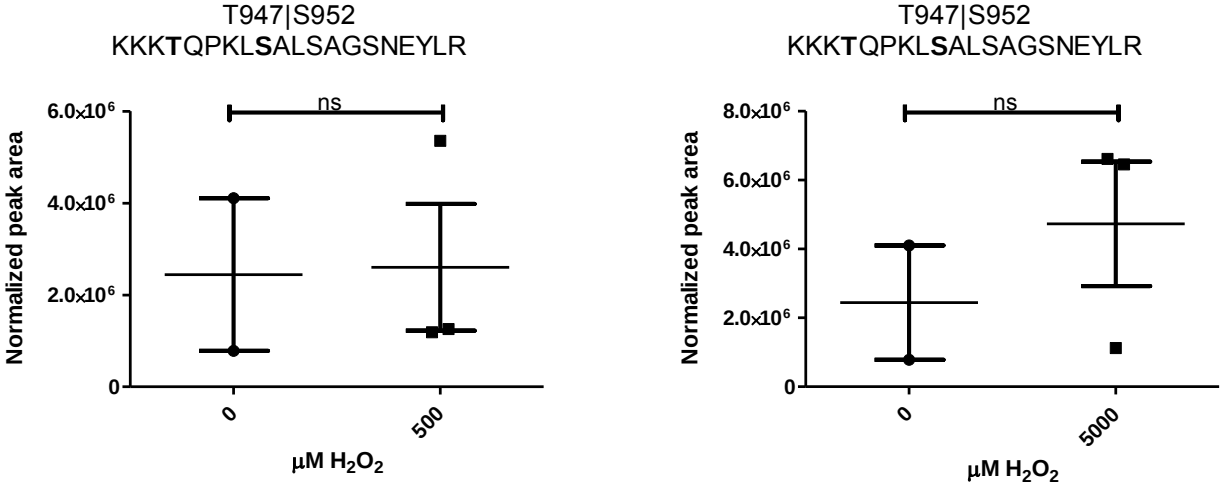


F

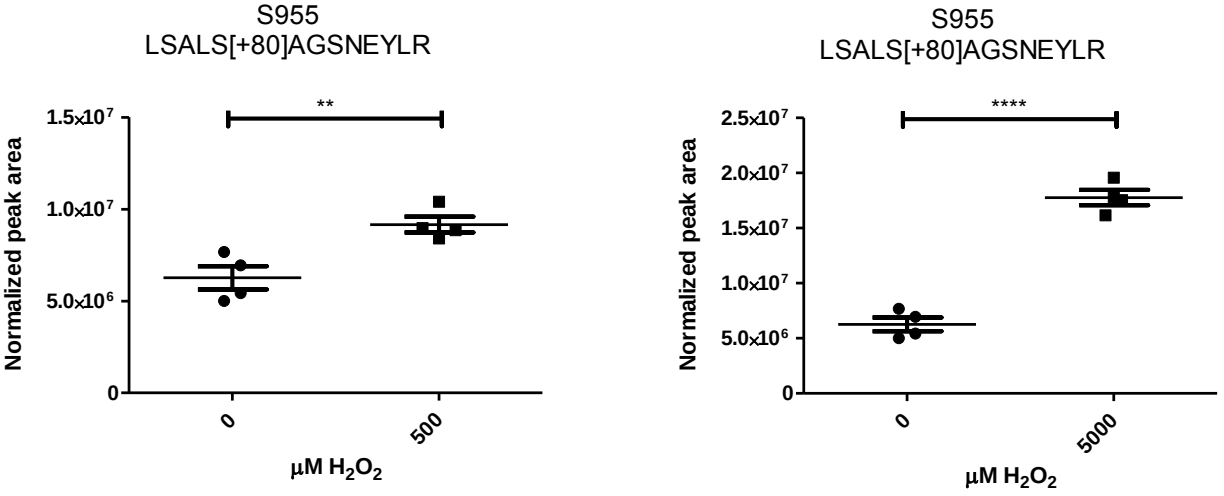




Figure B-3.

G

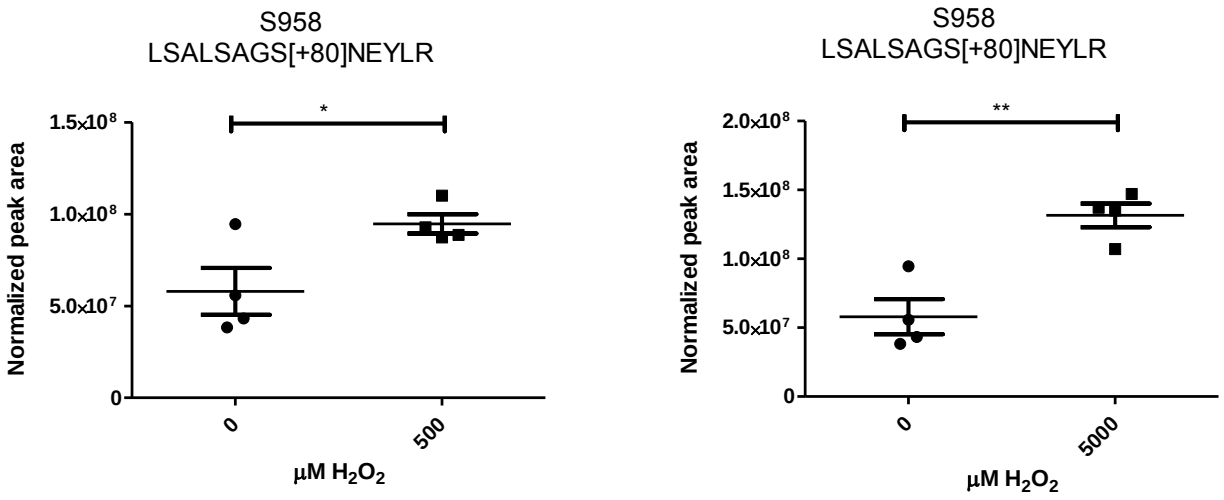


H

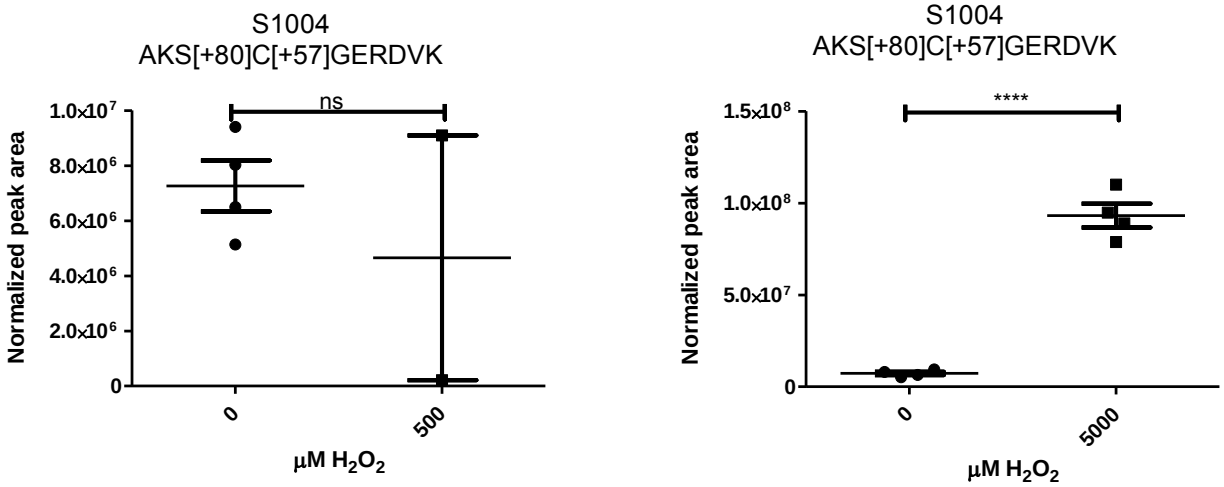


I

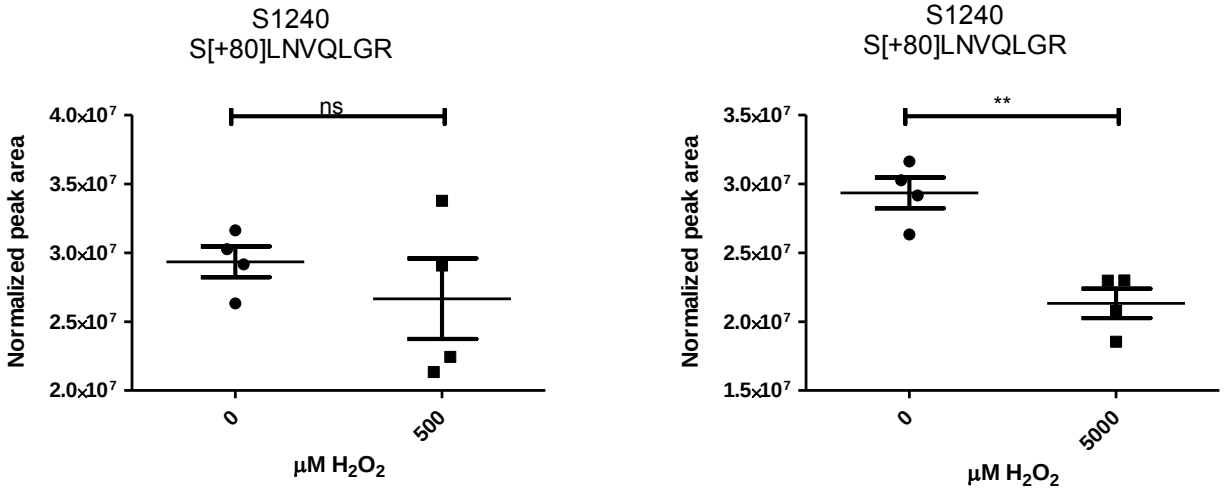




Figure B-3.

Figure B-4. Annotated MS/MS spectra for each putative HNE adducted ASK1 peptide. Each page lists the peptide sequence, site of modification, MS1 isolation window, precursor mass accuracy, annotated MS/MS spectrum, and a table summarizing the identified peaks for the MS/MS spectrum.

# $^{927}$AC[158.13068]ANDLLVDEFLK$^{939}$

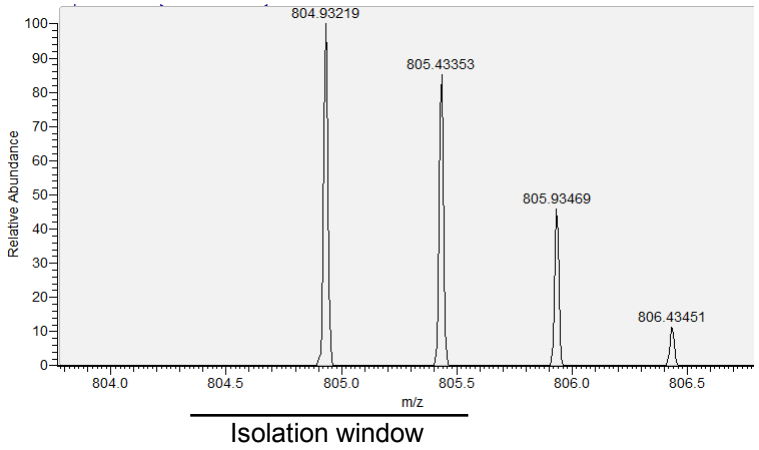


**Cys 928**

Precursor m/z: 804.93219
Precursor mass error: 1.14ppm

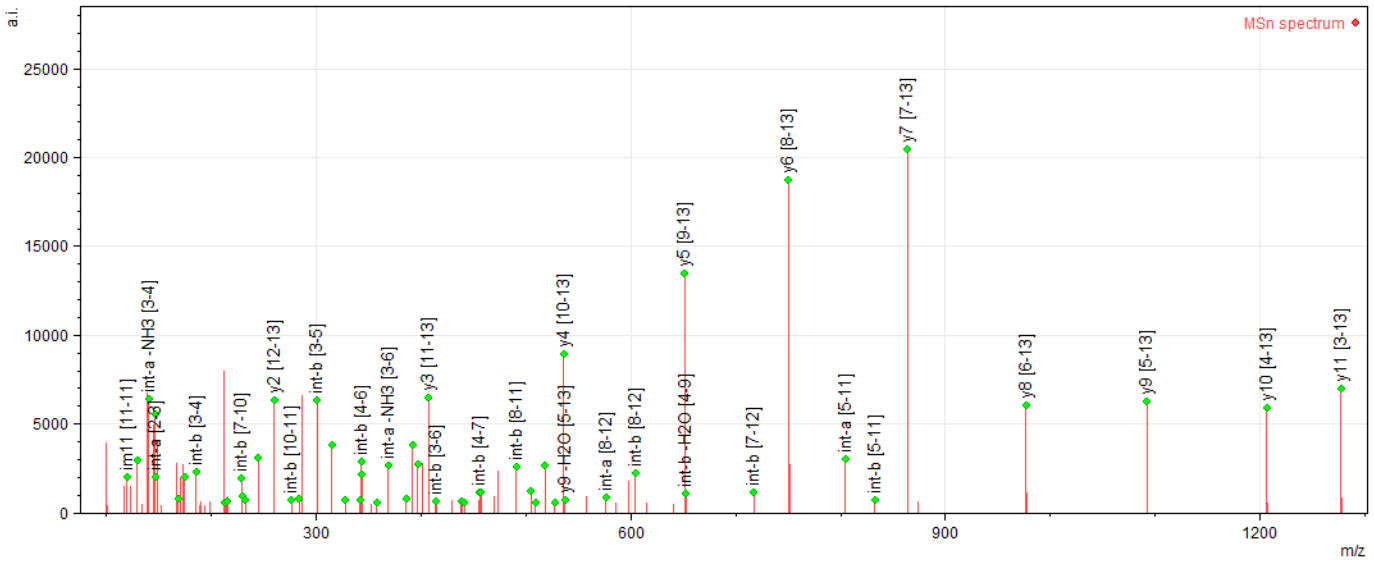


| parameter | value |
|---|---|
| Number of peaks searched | 99 |
| Number of fragments searched | 812 |
| Number of fragments matched | 63 |
| Intensity matched | 69 % |
| Sequence length | 13 |
| Ion serie matches for "b" | 2 |
| Ion serie matches for "b -H2O" | |
| Ion serie matches for "b -H2O -NH3" | |
| Ion serie matches for "b -NH3" | |
| Ion serie matches for "y" | 1, 2, 3, 4, 5, 6, 7, 8, 9, 10, 11 |
| Ion serie matches for "y -H2O" | 4, 9 |
| Ion serie matches for "y -H2O -NH3" | |
| Ion serie matches for "y -NH3" | 1 |



Figure B-4.

# $^{1004}$SC[158.13068]GERDVK$^{1011}$

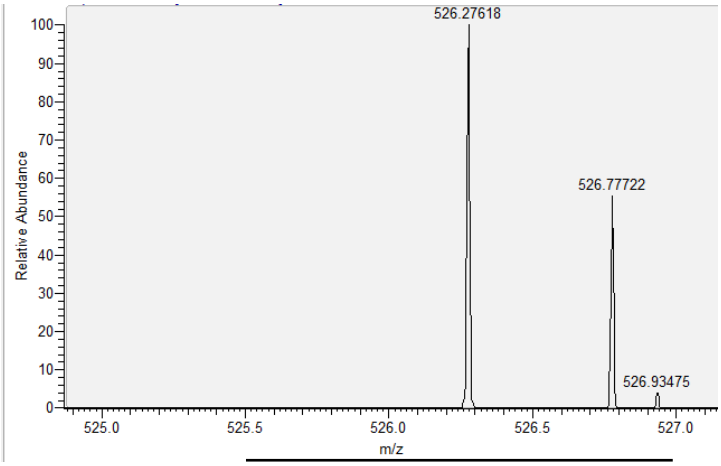


**Cys 1005**

Precursor m/z: 526.27618
Precursor mass error: -0.60ppm

Isolation window

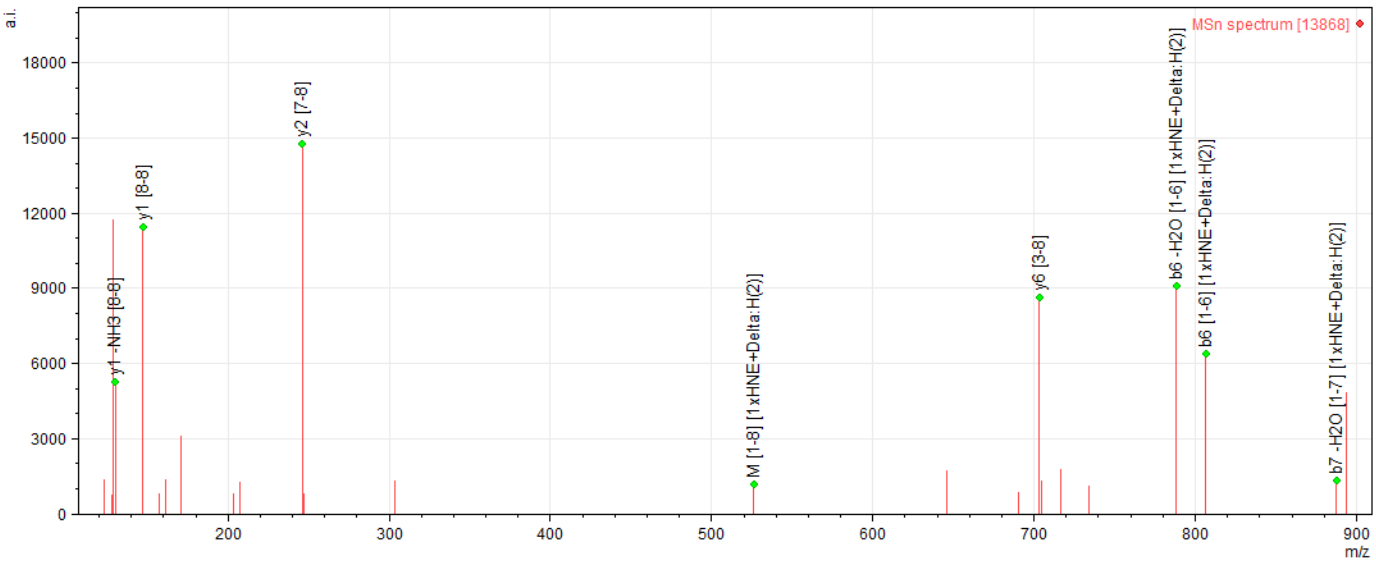


| parameter | value |
|---|---|
| Number of peaks searched | 24 |
| Number of fragments searched | 322 |
| Number of fragments matched | 8 |
| Intensity matched | 62 % |
| Sequence length | 8 |
| Ion serie matches for "b" | 6 |
| Ion serie matches for "b -H2O" | 6, 7 |
| Ion serie matches for "b -H2O -NH3" | |
| Ion serie matches for "b -NH3" | |
| Ion serie matches for "y" | 1, 2, 6 |
| Ion serie matches for "y -H2O" | |
| Ion serie matches for "y -H2O -NH3" | |
| Ion serie matches for "y -NH3" | 1 |



Figure B-4.